

**Bioconjugation and Cross-Linkage of Diene-Modified  
Oligodeoxyribonucleotides *via* the *Diels-Alder* Reaction**

Inauguraldissertation  
der Philosophisch-naturwissenschaftlichen Fakultät  
der Universität Bern

vorgelegt von

**Rolf Tona**

von Vernate TI

Leiter der Arbeit

Prof. Dr. R. Häner

Departement für Chemie und Biochemie  
der Universität Bern



**Bioconjugation and Cross-Linkage of Diene-Modified  
Oligodeoxyribonucleotides *via* the *Diels-Alder* Reaction**

Inauguraldissertation  
der Philosophisch-naturwissenschaftlichen Fakultät  
der Universität Bern

vorgelegt von

**Rolf Tona**

von Vernate TI

Leiter der Arbeit

Prof. Dr. R. Häner

Departement für Chemie und Biochemie  
der Universität Bern

Von der Philosophisch-naturwissenschaftlichen Fakultät angenommen.

Bern,

Der Dekan:

Prof. Dr. P. Messerli

*Für meine Eltern.*

---

## CONTENTS

ABSTRACT.....	VI
SUMMARY.....	VII
<b>1 INTRODUCTION.....</b>	<b>1</b>
1.1 History of DNA and RNA.....	1
1.2 Modified DNA and RNA.....	3
1.2.1 Antigene and Antisense.....	3
1.2.2 RNA Interference.....	7
1.2.3 Locked Nucleic Acid.....	8
1.2.4 Peptide Nucleic Acids .....	8
1.2.5 Molecular Beacons.....	9
1.2.6 Probing and Mapping of RNA .....	11
1.2.7 Labelling.....	11
1.3 DNA and RNA Architecture .....	12
1.3.1 Branched DNA.....	12
1.3.2 Triplex DNA.....	14
1.3.3 Quadruplex DNA.....	15
1.3.4 Cross-Linked DNA.....	17
1.4 Templated, Non-Enzymatic Reactions with Oligonucleotides.....	18
1.5 The Diels-Alder Reaction.....	24
1.6 Bioconjugation.....	29
1.7 Aim of this Work.....	32
<b>2 EXPERIMENTAL PART.....</b>	<b>37</b>
2.1 Definitions.....	37
2.1.1 Absorbance.....	37
2.1.2 Automated Oligonucleotide Synthesis.....	37
2.1.3 Circular Dichroism.....	39
2.1.4 Extinction Coefficient .....	39

2.1.5	Hyperchromicity.....	39
2.1.6	Lambert-Beer Law.....	40
2.1.7	Loading Capacity.....	41
2.1.8	Melting Temperature.....	41
2.1.9	Optical Density.....	42
2.1.10	Transmittance.....	42
2.2	Abbreviations.....	43
2.2.1	Solvents.....	43
2.2.2	Conditions.....	43
2.2.3	Chemicals and Groups.....	43
2.2.4	Various Abbreviations.....	44
2.3	Instrumentation and Methods.....	45
2.3.1	NMR spectrometry.....	45
2.3.2	UV spectrometry.....	45
2.3.3	IR spectrometry.....	46
2.3.4	ESI Mass Spectrometry.....	46
2.3.5	Melting Points.....	46
2.3.6	Melting Curves of Oligonucleotides.....	46
2.3.7	Automated DNA-Synthesis.....	47
2.3.8	Analytical TLC.....	47
2.3.9	Preparative Polumn Chromatography.....	48
2.3.10	HPLC.....	48
2.3.11	Oligonucleotide Desalting.....	49
2.3.12	PAGE.....	50
2.4	General Aspects.....	51
2.4.1	Chemicals.....	51
2.4.2	General Methods .....	51
2.5	Diene Phosphoramidites.....	55
2.5.1	Synthesis of 7.....	55
2.5.2	Synthesis of 15.....	62
2.5.3	Synthesis of 18.....	70
2.5.4	Synthesis of 21.....	73

---

2.5.5	Synthesis of 25.....	77
2.5.6	Synthesis of 29.....	81
2.5.7	Synthesis of 32.....	85
2.5.8	Synthesis of 35.....	88
2.6	Ene Phosphoramidites.....	91
2.6.1	Synthesis of 39.....	91
2.6.2	Synthesis of 43.....	95
2.6.3	Synthesis of 47.....	99
2.6.4	Synthesis of 49.....	103
2.6.5	Synthesis of 51.....	105
2.6.6	Synthesis of 53.....	107
2.6.7	Synthesis of 56.....	109
2.7	Dimaleimides.....	112
2.7.1	Synthesis of 57.....	112
2.7.2	Synthesis of 59.....	113
2.7.3	Synthesis of 60.....	115
2.7.4	Synthesis of 61.....	116
2.7.5	Synthesis of 62.....	117
2.7.6	Synthesis of 63.....	118
2.7.7	Synthesis of 64.....	119
2.7.8	Synthesis of 65.....	120
2.8	Maleimides.....	121
2.8.1	Synthesis of 66.....	121
2.8.2	Synthesis of 67.....	122
2.8.3	Synthesis of 68.....	123
2.8.4	Synthesis of 70.....	124
2.9	Trimaleimide.....	126
2.9.1	Synthesis of 71.....	126
2.10	Oligodeoxyribonucleotide Synthesis.....	127
2.10.1	Oligodeoxyribonucleotides for Ene-Diene Cross-Linkage.....	128
2.10.2	Hairpin and Hairpin-Mimic Oligodeoxyribonucleotides containing a Diene Moiety.....	130

---

2.11 Cross-Linkage and Bioconjugation of Oligodeoxyribonucleotides.....	133
2.11.1 Ene-Diene Oligodeoxyribonucleotide Cross-Linkage.....	133
2.11.2 Bioconjugation of Oligodeoxyribonucleotides with Maleimides and Linkage with Dimaleimides.....	134
<b>3 RESULTS AND DISCUSSION.....</b>	<b>139</b>
3.1 Synthesis of the Building Blocks and the Modified Oligonucleotides.....	139
3.1.1 Synthesis of Phosphoramidites.....	139
3.1.2 Synthesis of Dimaleimides.....	141
3.1.3 Synthesis of Maleimides.....	143
3.1.4 Trimaleimide Synthesis.....	144
3.2 Oligodeoxyribonucleotide Synthesis.....	144
3.3 Cross-Linkage of Ene- and Diene-Modified Oligodeoxyribonucleotides.....	146
3.3.1 First Experiments Towards the Direct Cross-Linking of Two Hybridised Strands.....	146
3.3.2 Cross-Linking Experiments of GC-rich Oligodeoxyribonucleotides Containing Electron-Rich Ene- and Diene-Modifications.....	152
3.4 Cross-Linkage of Diene-Modified Oligodeoxyribonucleotides.....	162
3.4.1 Interstrand Cross-Linkage with Di-Functional Maleimides.....	162
3.4.2 Experiments Towards the Cross-Linking of Non-complementary DNAs with Dimaleimide Reagents.....	181
3.5 Bioconjugation of Diene-Modified Oligodeoxyribonucleotides.....	185
3.5.1 Hairpin Mimics containing Diene-Building Blocks as Loop Replacements.....	185
3.5.2 Bioconjugation of Diene-Modified Hairpin Mimics.....	193
3.5.3 Fluorescein Bioconjugation of Diene-Modified Oligodeoxyribonucleotides.....	200
3.6 Conclusions .....	208
3.7 Outlook .....	208
<b>4 REFERENCES.....</b>	<b>215</b>

---



<b>5 APPENDIX.....</b>	<b>225</b>
5.1 Proposal 2003.....	225
5.2 Poster - SCS Fall Meeting 2003.....	238
5.3 Poster - SCS Fall Meeting 2004.....	239
5.4 Curriculum Vitae.....	240

---

## ABSTRACT

The synthesis of *diene* containing phosphoramidites and their successful integration into oligodeoxyribonucleotides is reported. Further bioconjugation with various maleimide dienophiles, carrying different pendant groups, and cross-linkage of *diene*-modified oligodeoxyribonucleotides with different dimaleimides *via* the *Diels-Alder* Reaction are described.

---

## SUMMARY

Synthetic oligonucleotides are valuable tools for disciplines like gene therapy, disease diagnostics and DNA-architecture. Within this context, reactions with modified oligonucleotides contain a large promise of novel applications.

The *Diels-Alder* reaction is very specific and water, the biologically most relevant solvent, is known to be an exceptionally good medium for these [2+4]-cycloadditions. These two important properties and the fact that not much was reported on *Diels-Alder* reactions in the context of oligonucleotides, solicited our interest for the studies described here.

To achieve cross-linkage between two complementary strands *via* the *Diels-Alder* reaction, phosphoramidites with electron-poor *ene* and electron-rich *diene* moieties were synthesized and inserted into oligodeoxyribonucleotides. The phosphoramidites of the first generation were 1,4-anthracene dicarboxylic acid, 2,3-anthracene dicarboxylic acid, fumaric acid and maleic acid. They all contained 3-amino-1-propanol spacers, linked *via* amide bonds. Maleic acid building blocks and, especially, oligodeoxyribonucleotides of 2,3-anthracene and maleic acid derivatives were not stable because of intramolecular maleimide formation. The electron-poor fumaric acid building block turned out to be too reactive towards oxidation during automated DNA synthesis. Melting experiments of a duplex bearing the 1,4-anthracene building block in one strand and the oxidized fumaric acid derivative in the complementary strand showed a destabilisation of 3 °C compared to the unmodified duplex.

To avoid oxidation of the electron-poor double bond during oligonucleotide synthesis, phosphoramidites of different electron-rich *enes* were synthesized and integrated into oligodeoxyribonucleotides. Oligodeoxyribonucleotides bearing 1,4-anthracene and 2,3-naphthalene building blocks were synthesized. Melting experiments of the duplexes between these *diene*- and *ene*-modified strands showed destabilization of about 7 °C in case of the 1,4-anthracene derivative and about 5 °C with the 2,3-naphthalene derivative. Because of the low reactivity of the electron rich *ene*-moieties, however, it was not possible to directly cross-link the *ene*- and *diene*-modified duplexes. Partial degradation of the oligodeoxyribonucleotides was observed during incubation at up to 100 °C.

Hairpin mimics containing different *diene*-building blocks, serving as loop replacements, were compared in melting experiments with unmodified hairpins containing a T<sub>4</sub>- or an A<sub>4</sub>-loop. The hairpin mimic with the 1,4-anthracene derivative shows a stabilization of 6.5 °C compared to a T<sub>4</sub>-loop. The new 2,4-hexadiene building blocks, with ethyleneglycol,

---

propanediol and butanediol spacers, increase the melting points of the hairpin mimics by 6 °C to 9 °C compared to the unmodified hairpins. All *dienes* lead to hairpin mimics that are more stable than the respective unmodified hairpins and at the same time have the benefit of an additional reactive group.

Hairpin mimics and single strands containing the different *diene* building blocks were bioconjugated with a maleimide derivative of fluoresceine. Modifications placed in a duplex or the stem part of a hairpin result in destabilisation of the structure. The negative effect was most pronounced by bioconjugation with the bulky fluoresceine maleimide. Bioconjugation of hairpin mimics containing the *diene*-modification in the loop led to various degrees of destabilisation, depending on the bulk of the substituent.

To explore the possibilities of bioconjugation, a hairpin mimic of the 2,4-hexadiene building block with a propane diol spacer, was conjugated to various maleimides. Maleimides attached to simple functional groups, such as aromates, fluorophores, metal ligands and to a second maleimide were used. The hairpin mimic was almost 9 °C more stable than the respective unmodified hairpin. The bioconjugates behaved different in the melting experiments. Some were as stable as the *diene* hairpin mimic while others were destabilized by 7 °C to 9 °C.

Since the integration of intact electron poor *ene*-moieties into oligodeoxyribonucleotides was not possible, we investigated the possibility to cross-link complementary *diene*-modified oligodeoxyribonucleotides *via* a dimaleimide. Dimaleimides with linkers of different length and others with an aromatic core were synthesized for that reason. Cross-linkage of duplexes with different 2,4-hexadiene modifications *via* different dimaleimides, in aqueous media was successful and resulted in highly stable, cross.linked duplexes ( $\Delta T_m$  up to +53°C).

Very importantly, cross-linkage of non-complementary *diene*-modified oligodeoxyribonucleotides, under the same conditions and with the same dimaleimides did not occur. Oligodeoxyribonucleotides conjugated to a dimaleimide were isolated, but no further linkage to a second *diene*-modified Oligodeoxyribonucleotide was observed without the use of a template.

# 1 INTRODUCTION

## 1.1 History of DNA and RNA – From Miescher to HUGO

*Friedrich Miescher* discovered nucleic acid in **1869** at the time of the Franco-Prussian War. In treating wounded soldiers, the 22 year old Swiss physician obtained a ready supply of white blood cells from the pus on the soldier's bandages. By digestion and extraction of the pus he obtained a preparation of cell nuclei - the first subcellular fractionation. He called this substance *nuclein*.

In **1879** *A. Kossel*, a German biochemist, isolated nuclein from starch. He found that nucleic acids consist of nitrogen-containing bases, such as thymine, cytosine, and uracil.

*Friedrich Miescher* isolated a pure sample of the material from the sperm of salmon and in **1889** his pupil, *Richard Altmann*, named it "nucleic acid". This substance was found to exist only in the chromosomes.

In **1902** *E. Fischer* received the Nobel Prize for basic research on sugars, purines, uric acid, enzymes, nitric acid and ammonia.

By **1908** all four bases of DNA had been characterised and it was found that they occur in roughly equal amounts.

During the following years *Levene and Jacob* identified the sugar components of RNA (**1909**) and DNA (**1930**) as D-ribose and D-deoxy-ribose.

**1931**: The book *Nucleic Acids* was published by *Levine*. He proved that the sugar components are connected via phosphodiesteres. In the same year *Griffith* discovers "transformation".

In **1944**, *Oswald Avery, Colin MacLeod, and Maclyn McCarty* published the first experiment demonstrating that DNA was the genetic material.

**1952** *R. Signer* provides a sample of very pure DNA which gave x-ray diffractions of high quality.

In **1953** the molecular biologists *J. D. Watson*, an American, and *F. H. Crick*, an Englishman, proposed that the two DNA strands were coiled in a double helix. In this model each nucleotide subunit along one strand is bound to a nucleotide subunit on the other strand by hydrogen bonds between the base portions of the nucleotides. The fact that adenine bonds only with thymine (A—T) and guanine bonds only with cytosine (G—C) determines that the

## 1 INTRODUCTION

---

strands will be complementary, i.e., that for every adenine on one strand there will be a thymine on the other strand. It is the property of complementarity between two strands that ensures that DNA can be replicated.

**1955:** *Chargaff & Davidson* published a set of three volumes on "The Nucleic Acids", describing in great detail their physical properties and characterisation.

**1956:** Genetic experiments supporting the hypothesis that genetic messages of DNA are conveyed by its sequence of base pairs.

**1958:** *Messelson and Stahl* demonstrated that DNA replicates semi-conservatively.

**1959:** Discovery of RNA polymerase.

In **1961** *Jacob and Monod* proved that messenger RNA transfers the genetic information.

**1961:** The triplet nature of the genetic code is discovered.

**1970:** Isolation of the first restriction enzyme. *Temin and Baltimore* report the discovery of reverse transcriptase in retroviruses.

**1972:** Use of ligase to link together restriction fragments. The first recombinant molecules generated.

**1973:** Eukaryotic genes were cloned in bacterial plasmids.

**1977:** DNA sequencing was discovered.

**1979:** *Khorana* synthesized the first artificial gene (126 bp).

**1981:** Catalytic activity of RNA was discovered.

**1983:** The first version of "GenBank" was created for storage of DNA sequences.

**1989:** First use of the Polymerase Chain Reaction (PCR) technique.

**1990:** Start of the Human Genome Project with the goal to *identify* all the approximately 30,000 genes in human DNA, to *determine* the sequences of the 3 billion chemical base pairs that make up the human DNA and to *store* this information in databases within 15 years.

**1995:** The first bacterial genomes were completely sequenced (*Haemophilus influenzae* and *Mycoplasma genitalium*).

**1996:** The first eukaryotic genome was completely sequenced (*Saccharomyces cerevisiae*, 13,000,000 bp on 16 chromosomes).

**1997:** *Dolly*, a sheep, was cloned successfully; The *E.coli* genome was sequenced.

The Human Genome Project ends in **2003** with the completion of the human genetic sequence.

## 1.2 Modified DNA and RNA

The field of altered nucleic acids can be divided in two major disciplines. In the first, the existing genome of an organism is changed through insertion, deletion or modification of genes. The goal of these alterations is the generation of new geno- and phenotypes. In this case, the modification is a change of the sequence in the genome. Since just the natural nucleosides are used, this genome can still be replicated, transcribed and translated.

In contrast to that, many chemical modifications of the backbone exist, the sugars and the bases which can't be replicated, transcribed nor translated. Chemical modifications like methylation and oxidation are observed in nature. For these damages nature even developed various types of repair mechanisms. But in addition to this, bioorganic chemists have synthesized modified building blocks for use in automated oligonucleotide synthesis. These modifications can serve as tools for diagnostics, therapy, structure determination or other applications in basic research.

### 1.2.1 Antisense and Antisense

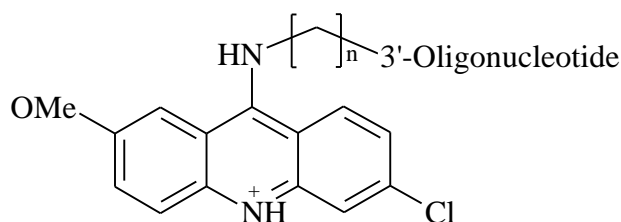
Antisense and antisense therapy have a common goal, which is called *gene silencing*.<sup>1-3</sup> By the addition of an oligonucleotide-like molecule, which interacts sequence-specifically with DNA or mRNA, inhibition of transcription or translation is sought. Such sequence-specific recognition of nucleic acids is achieved by using molecules that bind specifically by hydrogen bonding to the nucleobases. Another way to obtain the same effect is the recognition and binding of duplex structures *via* natural or synthetic minor groove binders.<sup>4</sup> Minor groove binders were originally a potent class of naturally occurring antibiotics that bind to duplex DNA specifically in the minor groove. Minor groove binders are long, flat molecules that can adopt a "crescent shape" that fits snugly into the minor groove to form close atomic contacts in the deep, narrow space formed between the two phosphate-sugar backbones in the double helix. They bind in the minor groove by either hydrogen bonds or hydrophobic interactions. With these powerful tools, genetically based diseases, as well as viral infections could be treated. Since, statistically, the base sequence of a 17-mer oligonucleotide occurs just once in the sequence of the human genome, extremely selective intervention ought to be possible with

oligonucleotides of this length. *Zamecnik and Stephenson* were the first to propose the use of synthetic antisense oligonucleotides for this purpose in 1978.<sup>5,6</sup>

Nowadays, unmodified as well as modified oligonucleotides can be prepared easily and very efficiently with the help of DNA-synthesizers by the phosphite triester method. This method was originally introduced by *Letsinger*<sup>7</sup>. The method is explained in detail in the experimental part of this thesis.

To be successful in practical applications antisense oligonucleotides must comply with several requirements.<sup>8</sup> (1) The complex formed between the oligonucleotide and its complementary sequence must be sufficiently stable under physiological conditions. (2) The interaction between the oligonucleotide and the target sequence must be specific. (3) Half-live time of the oligonucleotide has to be sufficiently long under *in vivo* conditions to show the desired effect. (4) Cell membrane permeability is essentially for the oligonucleotide hybrids to reach their site of action.

To increase binding affinity, different approaches exist. *Hélène et al.*<sup>9</sup> covalently linked intercalating agents to oligonucleotides to increase the affinity (Scheme 1). Intercalating agents, like acridine, are flat aromatic compounds which can stabilize oligonucleotide hybrids through hydrophobic and pi-stacking interactions with the base pairs.

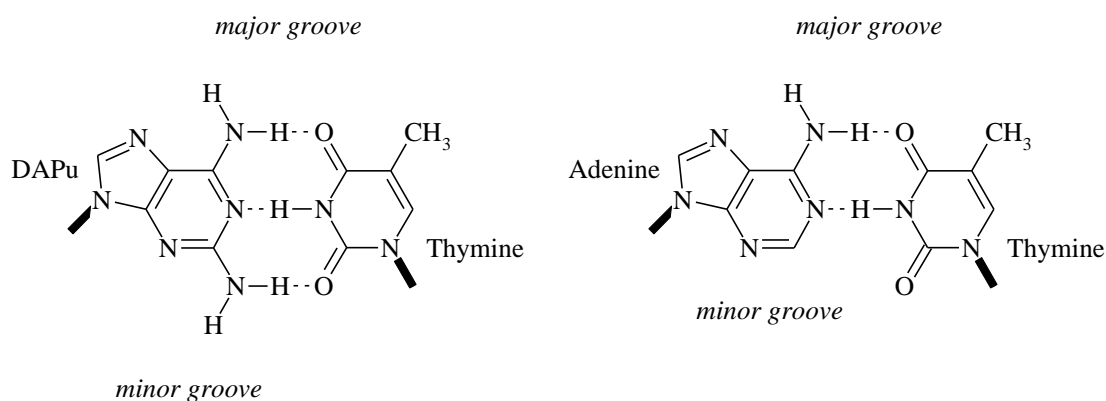


Scheme 1 Acridine bound to the 3'-end of an oligonucleotide.

Another possibility to increase  $T_M$  comprises the introduction of modified bases that form more stable *Watson-Crick* base pairs than the natural bases. 2,6-Diaminopurine (DAPu) for



example forms three hydrogen bonds with thymine, whereas the natural partner adenine is able to form only two hydrogen bonds (Scheme 2).<sup>10</sup>



**Scheme 2** Hydrogen bonds of the base pairs DAPu/T and A/T.

It is also possible to raise the  $T_M$  by altering the sugar moiety. A 9mer 2'-O-methyloligoribonucleotide hybrid duplex, for example, is around 10°C more stable than the corresponding unmodified DNA duplex.<sup>11</sup>

Adequate stability to nucleases and sufficient passage through membranes can be achieved by modification of the oligonucleotides.

The enzymes responsible for the degradation of nucleic acids (DNA, RNA), the nucleases (DNases, RNases), differ in their specificities. Unmodified antisense oligonucleotides can be degraded in organisms by single strand specific exonucleases within minutes. Since enzymatic hydrolysis of the phosphodiester backbone is a major problem, modification of the phosphodiester is an obvious approach. In an apparently slight change is to replace an oxygen by a sulphur atom. Phosphothionate polynucleotides have been described by *de Clerq and Eckstein* already in 1970.<sup>12</sup> Phosphorothioate antisense oligonucleotides are stable to snake venom phosphodiesterase and spleen phosphodiesterase, which are endonucleases. Another type of phosphate modification, the nonionic methylphosphonate oligonucleotides, were used for the first time by *Miller and Ts'O* in 1981.<sup>13</sup>

For the activity of any therapeutic agent a satisfactory bioavailability is essential. Activity of the antisense oligonucleotides is crucially affected by how well they reach, unmetabolized, their site of action. The mRNA, produced in the nucleus by transcription of the DNA, is translated into the corresponding protein on the ribosomes in the cytoplasm. To stop translation, the antisense oligonucleotides must pass through the plasma membrane into the interior of the cell. The plasma membrane is a natural barrier to many large or negatively charged molecules. Cellular uptake of oligonucleotides takes place better than expected for molecules with properties of its kind. The existence of an active transport of oligonucleotides by endocytosis is responsible for this. According to all the evidence, this mechanism is receptor mediated.<sup>14</sup> 3'-Derivatisation of oligonucleotides, as linking with acridine (mentioned above), appears to have a beneficial effect on both the ability to penetrate and the stability to nucleases.<sup>15</sup> An additional way to improve the penetration of antisense oligonucleotides, is the incorporation in liposomes<sup>16</sup> or the covalent attachment to nonspecific or specific carriers.<sup>17,18</sup>

Most of the oligonucleotides have been designed to inhibit translation and so are antisense agents, and only a few studies report efforts into the direction of transcriptional inhibition. The advantage of inhibition of the transcription is that the target gene occurs only once per cell while the corresponding mRNA may be present in many copies. However more important seems to be the disadvantage, which is accessibility of the target DNA sequence.

While antisense and antigene research boomed until the end of the last century, which is understandably since it could be the key to treat hereditary diseases, viral and bacterial infections and even cancer. However, the euphoria calmed down lately. Practical problems such as dose, efficacy and delivery turned out to be major obstacles, and that antisense research became much less popular than originally expected.

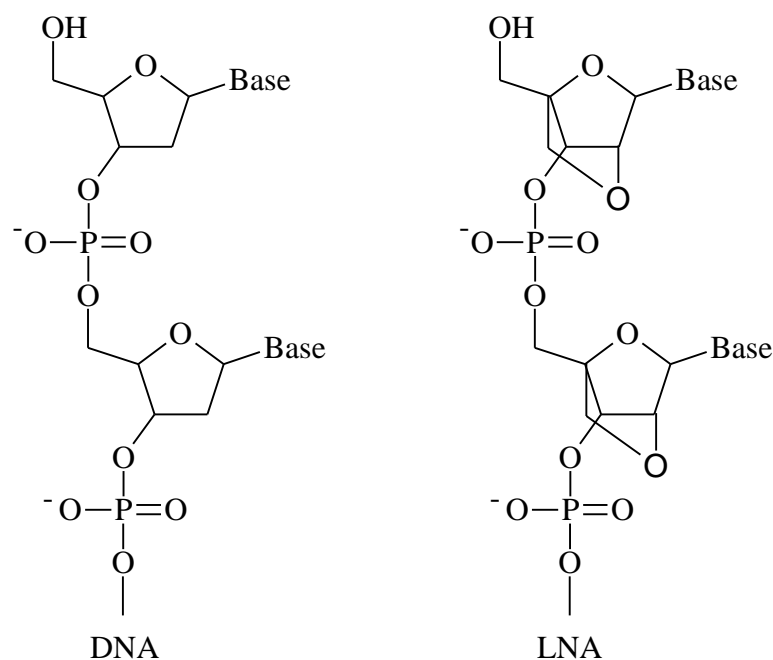
### 1.2.2 RNA Interference

RNA interference (RNAi) is one of the most exciting discoveries of the past decade in functional genomics. RNAi is rapidly becoming an important method to analyze gene functions in eukaryotes and holds the promise for the development of therapeutic gene silencing.<sup>19,20</sup>

Although the mechanisms for RNAi remain largely unknown, the steps required to generate the specific dsRNA oligonucleotides are clear. It has been shown that dsRNA duplex strands that are 21-26 nucleotides in length work most effectively in producing RNA interference. Selection of the right homologous region within the gene is also important. Factors such as the distance from start codon, the G/C content and the location of adenosine dimers are important when considering the use of dsRNA for RNAi.<sup>21</sup> There are several methods for preparing small interfering RNA (siRNA), such as chemical synthesis, in vitro transcription, siRNA expression vectors, and PCR expression cassettes.

### 1.2.3 Locked Nucleic Acid

Locked Nucleic Acid (LNA) was first described by *Wengel* and co-workers in 1998<sup>22</sup> as a novel class of conformationally restricted oligonucleotide analogues. LNA is composed of bicyclic nucleotides in which the 2'-oxygens and the 4'-carbon atoms are bridged with a methylene unit (Scheme 3). This bridge restricts the flexibility of the ribofuranose ring and locks the structure into a rigid bicyclic formation, conferring enhanced hybridization performance and exceptional biostability.

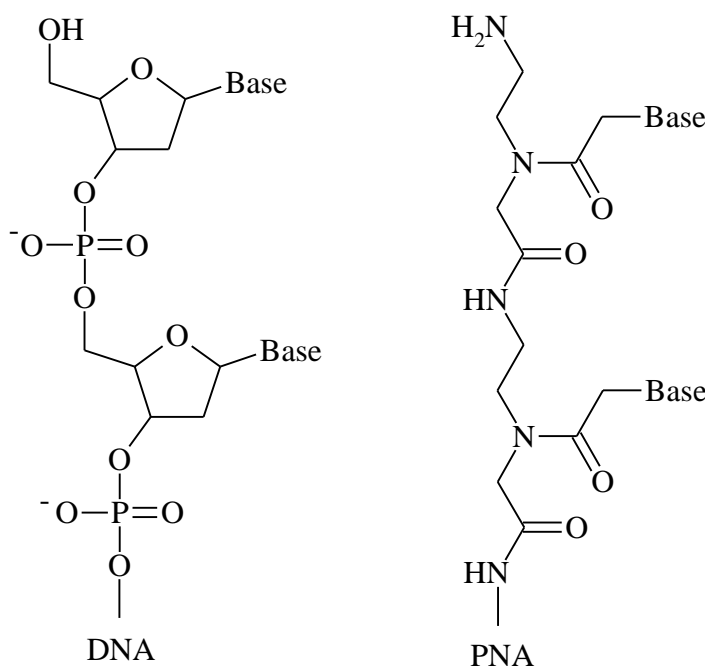


Scheme 3 Structural comparison between DNA and LNA.

### 1.2.4 Peptide Nucleic Acids

Peptide Nucleic Acids (PNA) was discovered by the *Nielsen* group.<sup>23-25</sup> In comparison with natural nucleic acids, where the nucleobases are attached to a sugar-phosphate chain, these compounds consist of nucleobases assembled on the string of a pseudopeptide backbone (Scheme 4). The most frequently used peptide nucleic acids are composed of a poly[*N*-(2-aminoethyl)glycine] backbone and the nucleobases are attached through an acetyl linkage.

Peptide nucleic acids, despite the achiral and uncharged backbone, retain an unsurpassed selectivity of base-pairing of native nucleic acids. There are many exciting biological properties of PNA (chemical and enzymatic stability, stable hybrid formation with both DNA and RNA, and (PNA)<sub>2</sub>-DNA triple helix formation).



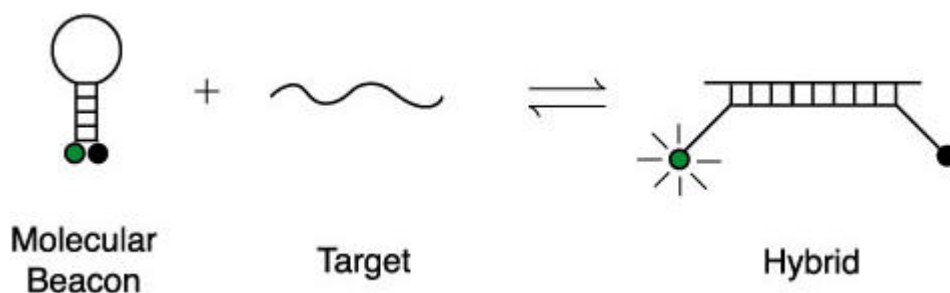
Scheme 4 Structural comparison between DNA and PNA.

### 1.2.5 Molecular Beacons

Molecular beacons are single-stranded oligonucleotide hybridization probes that form a *stem-and-loop* structure.<sup>26-32</sup> The loop contains a probe sequence that is complementary to a target sequence, and the stem is formed by the annealing of complementary sequences located on either side of the probe sequence. A fluorophore is covalently linked to the end of one arm and a quencher to the end of the second arm.

In the absence of targets, the probe does not fluoresce, because the stem places the fluorophore so close to the nonfluorescent quencher that they transiently share electrons, eliminating the ability of the fluorophore to fluoresce. When the probe encounters a target molecule, it forms a probe-target hybrid that is longer and more stable than the stem hybrid.

The rigidity and length of the probe-target hybrid precludes the simultaneous existence of the stem hybrid. Consequently, the molecular beacon undergoes a conformational reorganization that forces the stem hybrid to dissociate and the fluorophore and the quencher to move away from each other (Scheme 5).



Scheme 5 Principle of molecular beacons.

Molecular beacons can be used as amplicon detector probes in diagnostic assays. Because nonhybridized molecular beacons are non-fluorescent, it is not necessary to isolate the probe-target hybrids to determine the number of amplicons synthesized during an assay. Molecular beacons are added to the assay mixture before carrying out gene amplification and fluorescence is measured in real time. Furthermore, the use of molecular beacons provides an additional level of specificity. Because it is very unlikely that false amplicons or primer-dimers possess target sequences for the molecular beacons, the generation of fluorescence is exclusively due to the synthesis of the intended amplicons.

Molecular beacons with differently coloured fluorophores can be synthesized. This enables assays that simultaneously detect different targets in the same reaction. For example, multiplex assays contain a number of different primer sets, each set enabling the amplification of a unique gene sequence, e.g. from different pathogenic agents. A corresponding number of molecular beacons can be present, each containing a probe sequence specific for one of the amplicons, and each labelled with a fluorophore of a different colour. The colour of the resulting fluorescence identifies the pathogenic agent in the sample and the number of amplification cycles required to generate detectable fluorescence provides a quantitative measure of the number of target sequences present. Moreover, due to the inherent design of

gene amplification assays, the use of molecular beacons enables the detection of a rare pathogen in the presence of a much more abundant pathogen.

### **1.2.6 Probing and Mapping of RNA**

The many different functions of RNAs require specific interactions of these molecules with proteins, metals, other nucleic acids and substrates. The specificity of these interactions and their biological activities are determined by the three-dimensional structures of RNAs. The tertiary structure of RNA is formed by hydrogen bonding between functional groups of nucleosides in different regions of the molecule, by the coordination of polyvalent cations, and by stacking interactions in the double stranded regions of RNA. Knowledge of the tertiary structure of RNAs and the possibility to predict RNA folding from nucleotide sequences are of key importance for the design of functionally active polynucleotides, and for the selection of optimal oligonucleotide probes for the detection of specific RNAs and antisense oligonucleotides. The most widely used approach for investigations of RNA structure and functions is chemical and enzymatic probing in combination with theoretical methods. Physical methods like X-ray crystallographic<sup>33,34</sup> and NMR analysis<sup>35,36</sup> are powerful tools but have serious practical limitations. For both methods, large amounts of highly purified RNA are needed, and X-ray studies require high quality RNA crystals, which are difficult to grow.

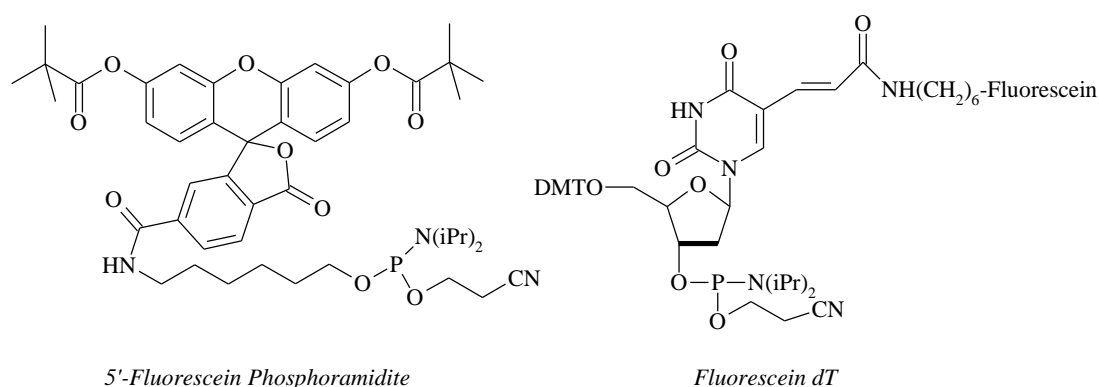
Chemical probing allows to detect structural motives like single stranded and double stranded regions, bulges and mismatches. Since most natural RNAs are globular molecules its important to distinguish nucleotides on the surface from those that are interior to solve the structure and to find potential drug targets.

### **1.2.7 Labelling**

Radioactive and fluorescence labelling of oligonucleotides are well established methods for faster and easier detection of oligonucleotides. The introduction of the labels may occur

---

during automated oligonucleotide synthesis or *via* the polymerase chain reaction. Alternatively, it may be done postsynthetically at either end of oligonucleotides. Labelled probes can be detected at very low concentrations in PAGE, on micro-array chips or in solution. For fluorescent labelling relatively big molecules (Scheme 6), which may influence the structure and binding properties of the oligonucleotides, are needed. In contrast, radioactive labelling allows the use of normal nucleotides, containing radioactive isotopes. Due to environmental and safety issues in the work with radioactive materials, optical detection particularly in diagnostics, is used whenever possible.



Scheme 6 Commercially available fluorescent phosphoramidites.

## 1.3 DNA and RNA Architecture

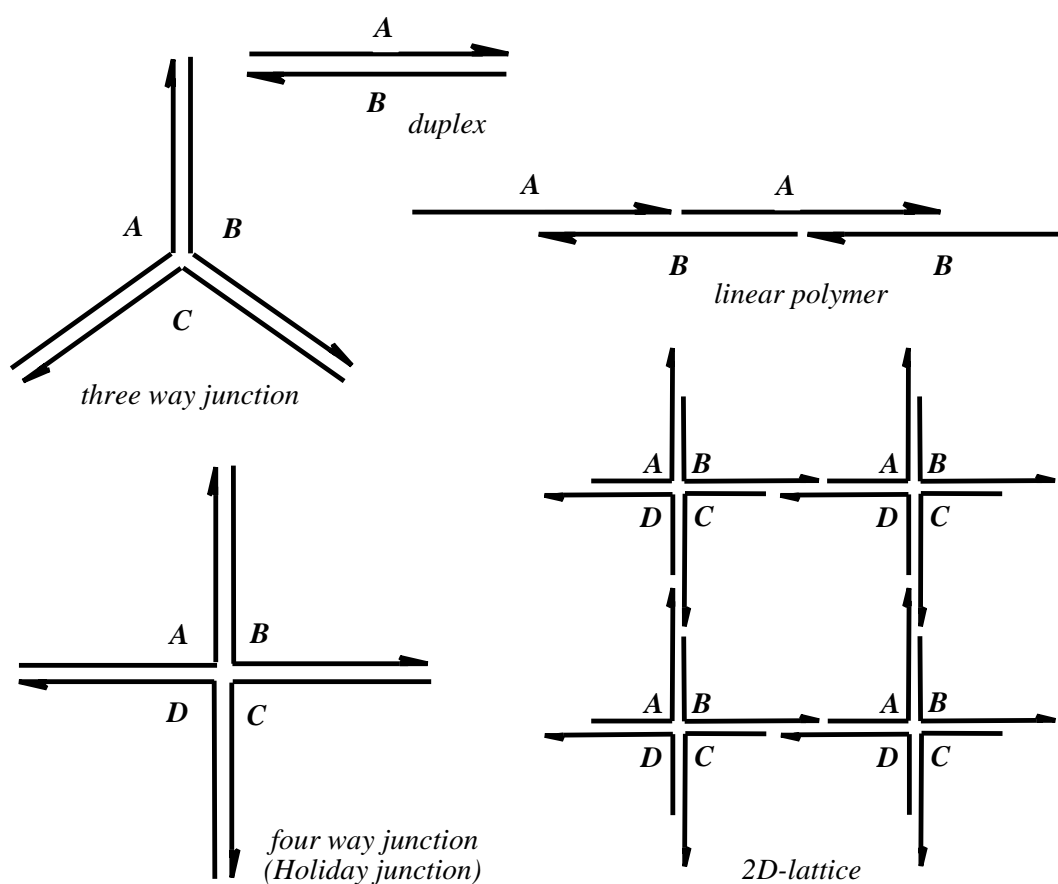
### 1.3.1 Branched DNA

DNA is an extraordinarily compact material used for information storage by every known form of life. The molecule's biochemical and biophysical properties have been well studied. Recently, there is increasing interest in this material's use for engineering purposes, such as the construction of nanomechanical devices and materials.

DNA nanotechnology is based upon the concept of using reciprocal exchange between DNA double helices or hairpins to produce branched DNA motifs or related structures. A variety of simple branched junction motifs, including the *Holliday Junction*, have been created, in which



there is a reciprocal exchange of strands between two helices. By allowing for reciprocal exchange between multiple helices, paranemic crossover (paranemic refers to a helix whose strands can be separated without unwinding), double crossover, and triple crossover motifs have been created that are significantly more rigid than other branched junctions (Scheme 7). The sequences of these unusual motifs are designed by an algorithm that attempts to minimize sequence symmetry.<sup>37</sup>

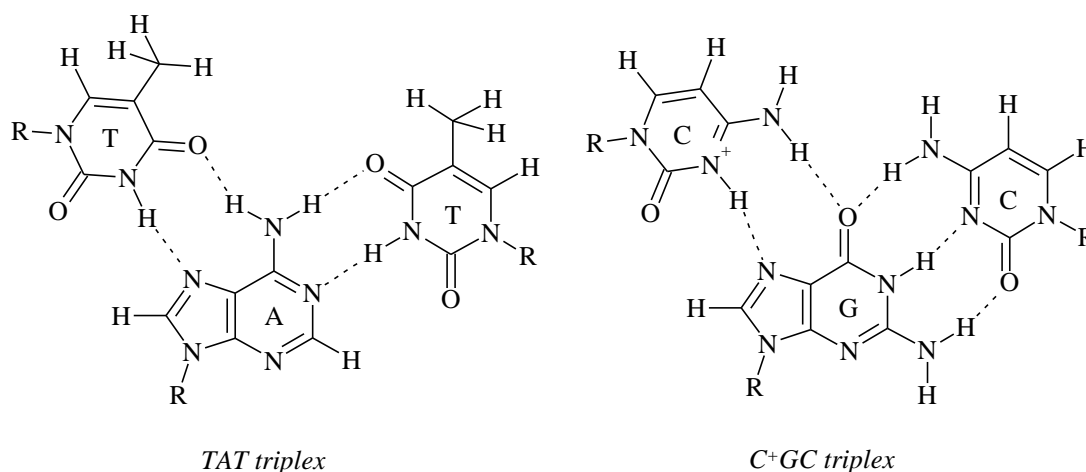


Scheme 7 Examples for one- and two-dimensional oligonucleotide architectures.

### 1.3.2 Triplex DNA

Since *Hoogsteen* and reverse *Hoogsteen* H-bonds require the presence of the purine bases A and G, triple helix formation with a third DNA and RNA strand is limited to homopurine sequences.<sup>38</sup> One active research area is, consequently, the preparation of base modifications which can also recognize pyrimidines. We can distinguish two different binding modes to homopurine sequences.

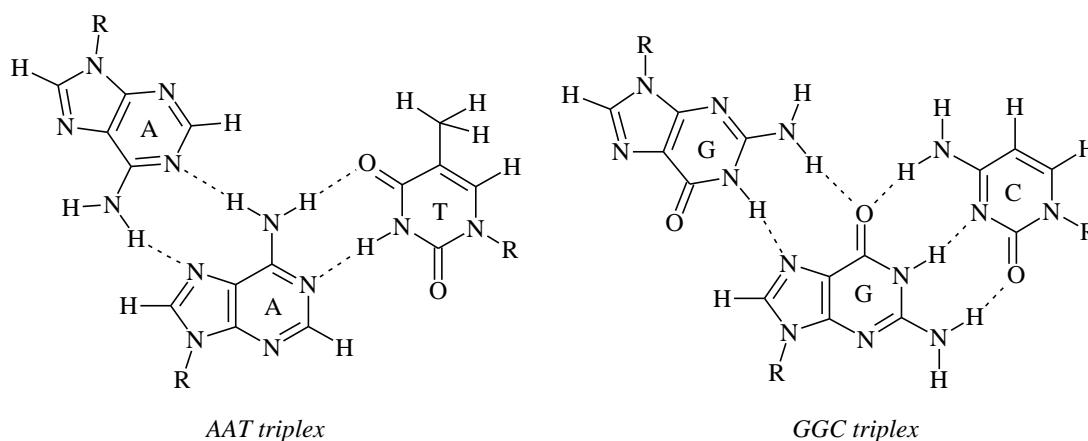
The Pyr: Pur: Pyr motif. In this motif, a thymine and cytosine containing DNA or RNA strand forms a triple strand with a homopurine sequence. T pairs with A and C pairs with G. Pairing occurs through formation of *Hoogsteen* base pairs. The *Hoogsteen* strand is parallel to the homopurine strands and antiparallel to the pyrimidine strand in the duplex (parallel binding). In order for the cytosine to form a stable *Hoogsteen* base pair with G it needs to be protonated at N3 (Scheme 8). The binding of the triplex is therefore strongly pH dependent. The binding is strong at low pH values and low at high pH values. The melting temperature of this type of triplex is therefore pH dependent.



Scheme 8 *Hoogsteen* base pairs.

The Pur: Pur: Pyr motif. Also in this motif, the third strand binds to the DNA in the major groove. Again, a homopurine strand in the duplex is required for triple helix formation. The

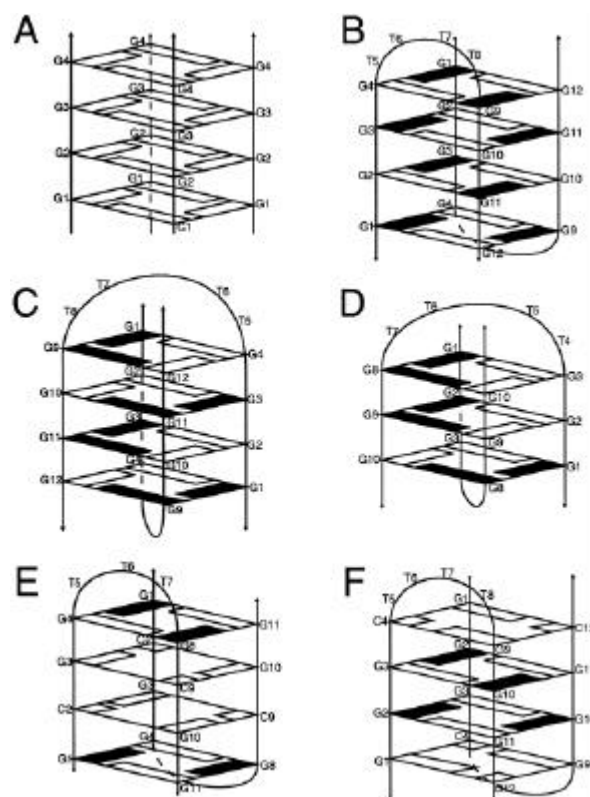
binding of the second homopurine strand in the triple strand is now antiparallel to the homopurine strand of the duplex (Scheme 9). Binding of the triplex is not pH dependent. The triplex H-bonds are of the reverse *Hoogsteen* type.



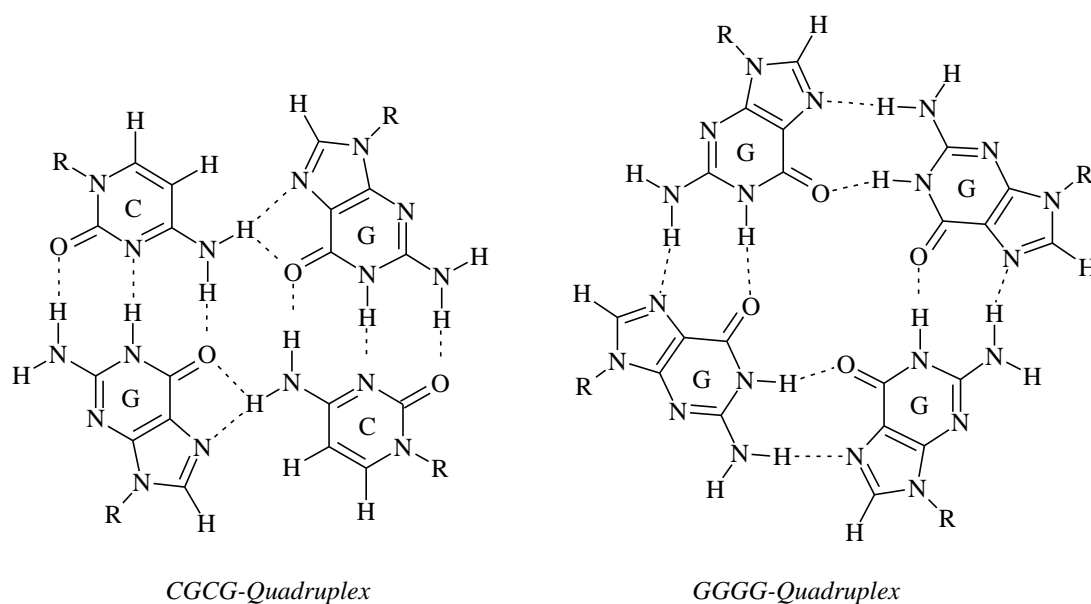
**Scheme 9** Reverse *Hoogsteen* base pairs.

### 1.3.3 Quadruplex DNA

DNA oligonucleotides that have repetitive tracts of guanine bases can form G-quadruplex structures that display an amazing number polymorphism (Scheme 10). Structures of several new G-quadruplexes have been solved recently that greatly expand the known structural motifs observed in nucleic acid quadruplexes. In addition base triads, base hexads, and quartets that contain cytosine stacking on the familiar G-quartets, have recently been identified. The current status of the diverse array of structural features in quadruplexes is described and used to provide insight into the polymorphism and folding pathways.<sup>39</sup>



Scheme 10 Schematic diagrams of a four-stranded linear quadruplex and some two-stranded dimeric hairpin quadruplexes representing x-ray crystal structures.<sup>39</sup> A solid line represents the sugar phosphate backbone. A solid circle indicates the 5'-end of the strand and an arrow indicates the 3'-end of the strand. Completely shaded rectangles indicate *syn* guanine residues, clear rectangles indicate *anti* guanine residues, and clear squares indicate *anti* cytosine residues (see Scheme 11).



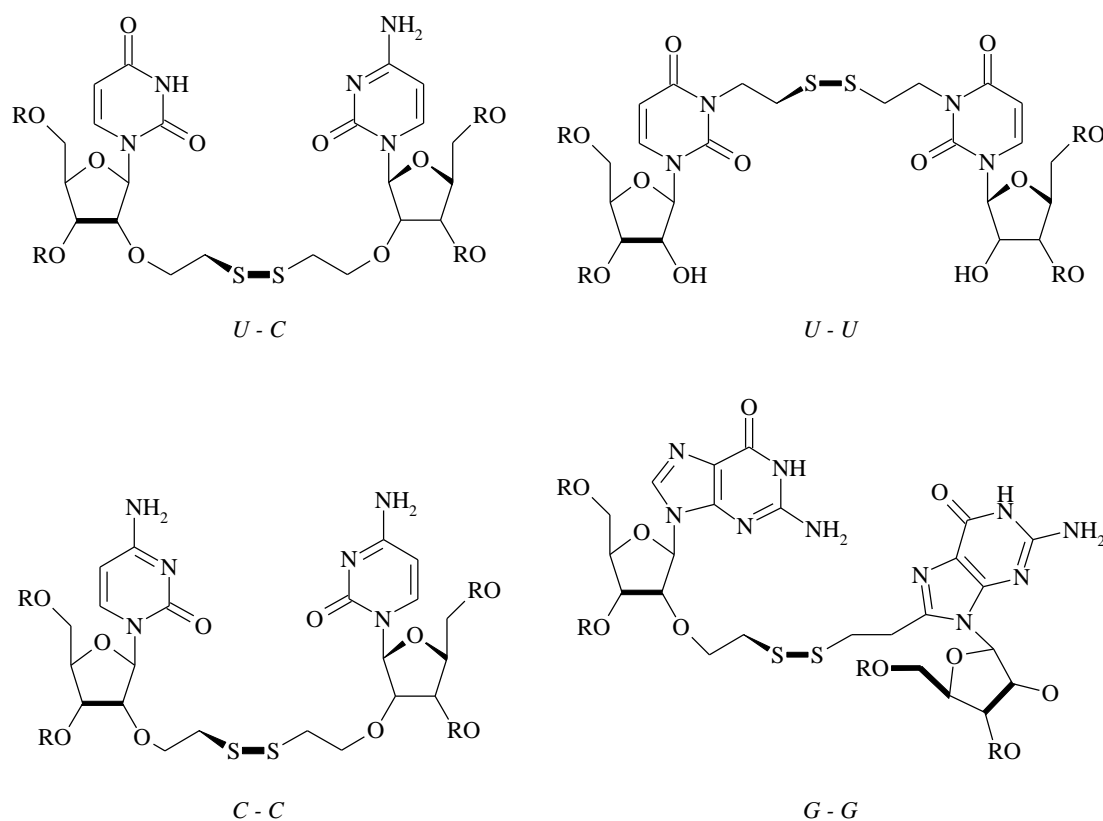
Scheme 11 Hydrogen bonds formed in quadruplexes.

### 1.3.4 Cross-Linked DNA

A most successful approach to stabilize oligonucleotides is to connect the strands that form the helical structure with a cross-link.<sup>40-45</sup> Methods to cross-link nucleic acids can generally be divided into two categories. In the first group, cross-links are formed using an exogenous reagent, like a (bis)electrophile. Because (bis)electrophiles can react with nearly all of the nucleophilic sites on the bases, these reagents often have little or no sequence specificity and form complex mixtures of cross-linked adducts.<sup>46-48</sup> Although some natural products like mitomycin C and synthetic compounds such as cisplatin and psoralen can form lesions at specific sites, these reagents require the presence of specific sequence patterns within a target to generate the cross-link.<sup>49</sup> In some cases, cross-link formation by alkylating agents can also have other effects, such as disrupting base stacking.

Cross-links can also be placed into oligonucleotides site specifically labelled with modified nucleosides that present reactive groups (Scheme 12). Positioning of the reactive groups in proximity on opposing strands of a helix allows the formation of a cross-link. This strategy requires optimisation of both, the loci to be bridged as well as the chemistry to form the cross-

link.<sup>50</sup> An preferred location for incorporation of an intrastrand cross-link is at the terminus of the helical structure. For example one end of a duplex can be covalently linked by bridging the 3'- and 5'-terminal hydroxyl groups to create a hairpin like structure.<sup>51</sup>



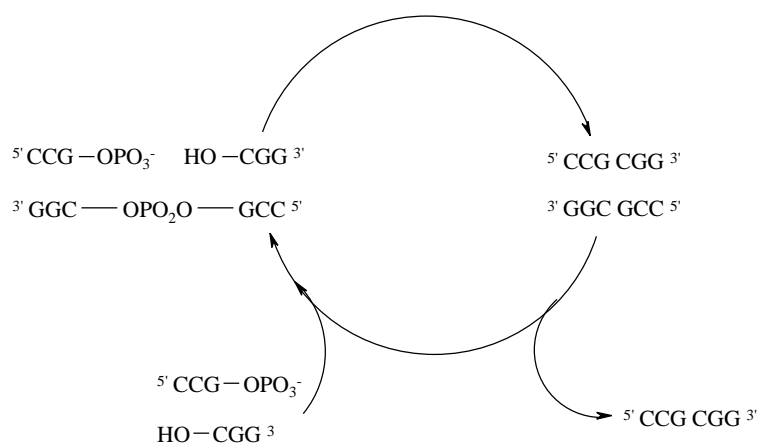
**Scheme 12** Chemical structure of disulfid RNA cross-links used by *Glick*<sup>51</sup> to cross-link modified yeast tRNA<sup>Phe</sup>.

## 1.4 Templated, Non-Enzymatic Reactions with Oligonucleotides

The first non-enzymatic DNA-templated reaction was reported by *Naylor* and co-workers in 1966, using polyadenosine as a template for the ligation of two thymidine hexanucleotides.<sup>52</sup> However, the low yield of 5% after 4 days rendered the chemistry of little practical use. The next significant advance in this field did not come until 1984, when *Orgel* and co-workers

successfully synthesized dGGCGG using a dCCGCC template and activated guanosine and cytidine monomers.<sup>53</sup>

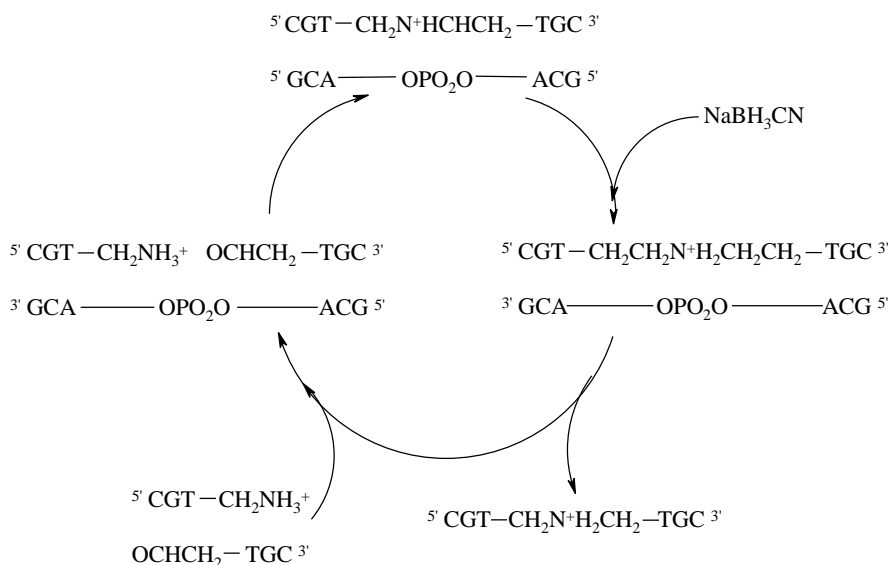
Unfortunately, this methodology was also hampered by poor reaction efficiency. A modest 17% yield was achieved and numerous byproducts from untemplated reactions were observed in the product mixture. In 1986, *von Kiedrowski* and co-workers proposed a potential solution to this problem with their report of the first autocatalyzed DNA-templated ligation reaction. A self-complementary hexanucleotide was used to template the ligation of two trinucleotides (Scheme 13). Since the resulting ligation product was identical to the original template, two template molecules become available upon dissociation of the duplex to participate in the subsequent catalytic cycle.<sup>54</sup> Despite the fact that the yield for this reaction was only 12% and catalytic turnover of the template was minimal due to the stability of the native DNA duplex, the design of a catalytically active template laid the conceptual foundation for much of the work that later followed in this field.



**Scheme 13** Autocatalyzed ligation of self complementary DNA template.

The discovery that backbone-modified nucleotides could be incorporated into DNA strands without significantly hindering the binding affinity between the modified strand and its complementary DNA strand lead *Lynn* and co-workers to develop a DNA-templated ligation strategy utilizing the imine condensation reaction.<sup>55</sup>

To apply the imine condensation reaction to DNA ligation, oligonucleotides bearing a 5'-amino or a 3'-aldehyde functionality, respectively, were synthesized. Upon combination of the reacting oligonucleotides with complementary template, association occurred, followed by the condensation reaction to give the imine ligated product (Scheme 14).



**Scheme 14** Cycle of DNA-templated ligation via reductive amination.

*Kool* and co-workers carried out some DNA-templated nucleophilic substitution reactions. Reaction of 5'-iodothymidine oligonucleotide with an oligonucleotide bearing a 3'-phosphorothioate anion in the presence of a DNA template resulted in the ligated oligonucleotide.<sup>56</sup>

Upon introduction of a single base-pair mismatch between, the reaction rate decreased 2000-fold relative to that of the correctly matched substrates. *Kool* subsequently went on to demonstrate the practical use of this high template fidelity for the detection of single point mutations in DNA.<sup>57</sup>

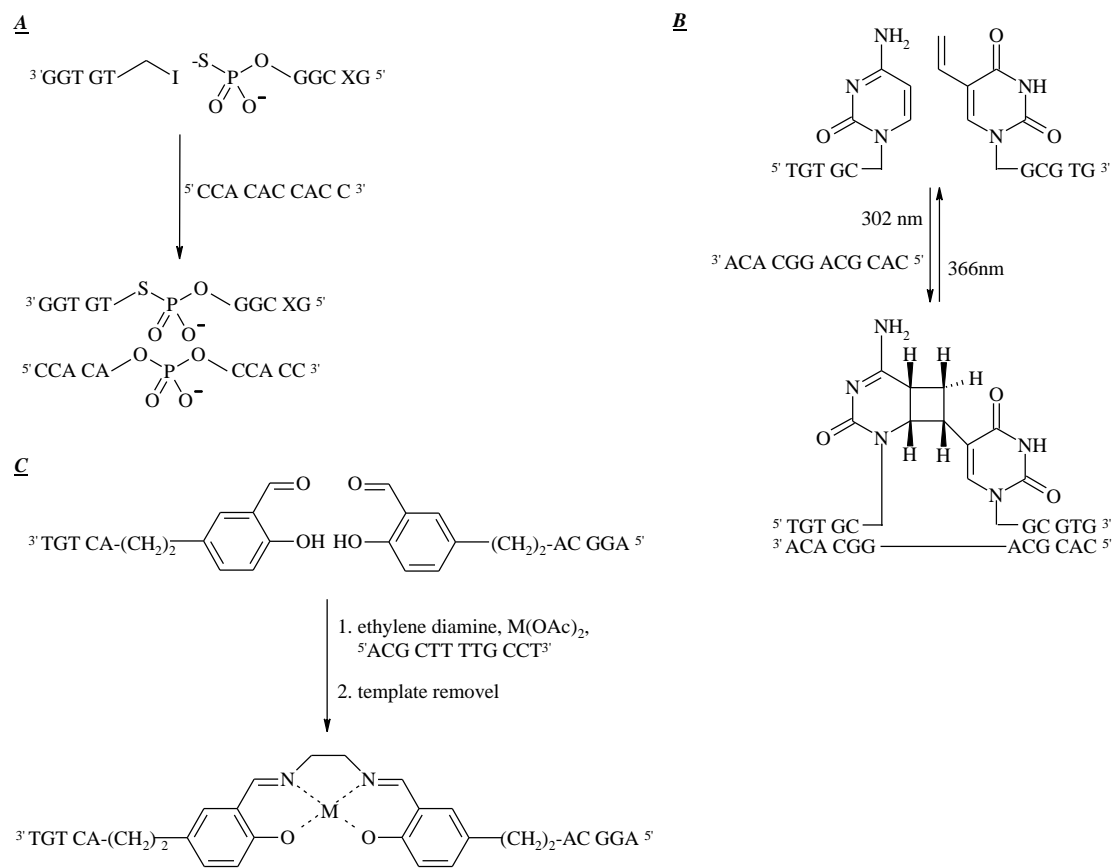
*Saito* and co-workers used photoligation in the DNA-templated synthesis of oligonucleotides. Upon irradiation of 3'-cytosine and 5'-vinyldeoxyuridine with 366 nm light in the presence of



a DNA template, the ligated complex was formed. Irradiation of the product with 302 nm light effected the reverse reaction, regenerating the starting materials.<sup>58</sup>

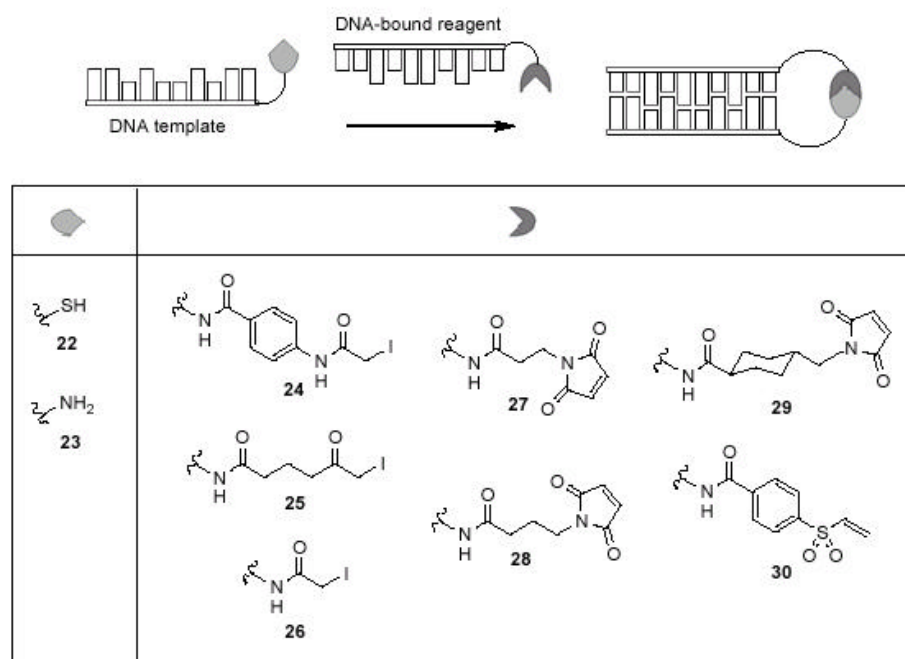
The use of this methodology to perform multiple concomitant ligation reactions was also demonstrated by irradiation of five hexanucleotides in the presence of a complementary DNA template to produce the desired 30-mer oligonucleotide product. With this work, Saito and co-workers have demonstrated that photoligation of modified nucleotides is a viable method for DNA-templated ligation reactions, and that this method possesses the added benefit over previously presented backbone ligation methods in that the reaction is reversible.

*Sheppard* designed a ligation reaction in which the product was a DNA-metallosalen complex capable of acting as a catalyst in subsequent reactions.<sup>59</sup> To synthesize the metallosalen complex, 5'-salicylaldehyde and 3'-salicylaldehyde were reacted with the complementary template, ethylenediamine, and either  $\text{Mn}(\text{OAc})_2$  or  $\text{Ni}(\text{OAc})_2$ . Upon removal of the template, the desired Mn(II) or Ni(II) DNA-metallosalen complex was obtained (Scheme 15). The metal ion was found to play a key role in templating complex formation. Thus, in the presence of  $\text{Mn}(\text{OAc})_2$ , 65% yield was obtained, but only a 4% yield of unmetallated DNA-salen was obtained when  $\text{Mn}(\text{OAc})_2$  was omitted from the reaction mixture. Using this chemistry, *Sheppard* introduced the DNA-templated synthesis of new organometallic reagents with potential applications in targeted nucleic acid cleavage, biosensors, and catalysis.<sup>60</sup>

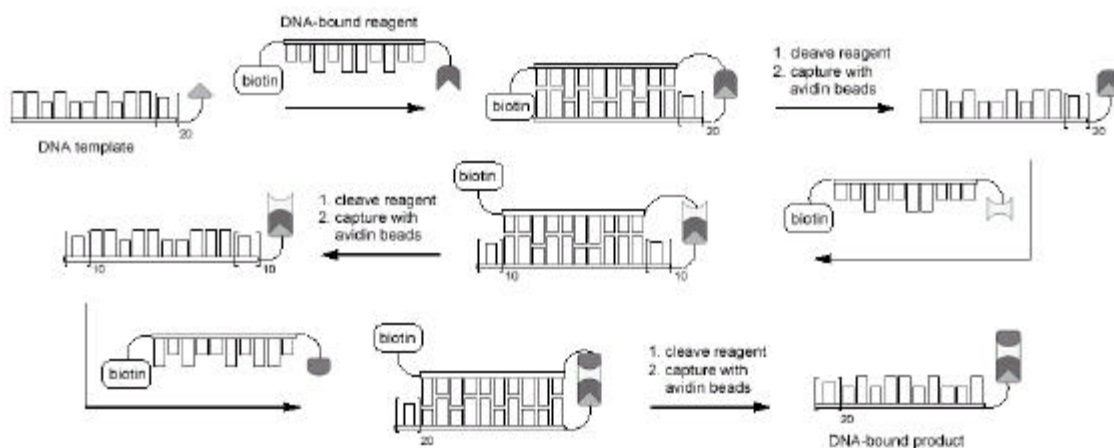


**Scheme 15** **A** nucleophilic substitution<sup>5</sup>, **B** photoligation<sup>6</sup>, **C** metallosalen complexation<sup>7</sup>.

*Liu* and co-workers extended the concept of DNA-templated synthesis to the specific combination of small molecules. In this approach, small molecule substrates and reagents are covalently attached to DNA templates. Upon annealing of the complementary templates, reagent and substrate are brought in close proximity, promoting the desired reaction (Scheme 16). Since the time of their initial report<sup>61</sup>, *Liu* and coworkers have developed this methodology to encompass a broad range of chemical transformations, and have demonstrated its potential for generating combinatorial libraries in solution and directing multistep small-molecule syntheses (Scheme 17).<sup>62</sup>



**Scheme 16** Conjugates employed in DNA-templated addition and nucleophilic substitution reactions.<sup>61</sup>



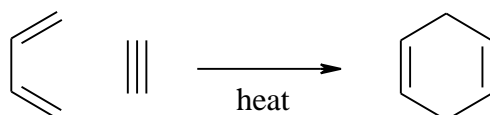
**Scheme 17** DNA-templated multistep small-molecule synthesis.<sup>62</sup>

## 1.5 The Diels-Alder Reaction

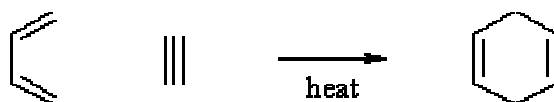
The most elegant and useful reaction is named after the discoverers, the two German chemists Otto *Diels* (1876-1954) and Kurt *Alder* (1902-1958). The work on this reaction brought them the *Nobel Prize* in 1950.

The *Diels-Alder* reaction is a concerted addition reaction of a conjugated diene to an alkene (the dienophile) to produce a cyclohexene. This reaction belongs to a larger class known as [2 + 4] cycloadditions, which are characterized by the formation of a ring by a process involving two  $\pi$ -electrons of one reactant and four  $\pi$ -electrons of the other. Such reactions tend to be electronically favoured because the transition state involves six circularly delocalized  $\pi$  - electrons, much like in benzene. It has, therefore, aromatic character and is particularly stabilised. (By comparison, [2 + 2] and [4 + 4] cycloadditions tend to be much slower.)

The simplest example is the reaction of 1,3-butadiene with ethene to form cyclohexene:

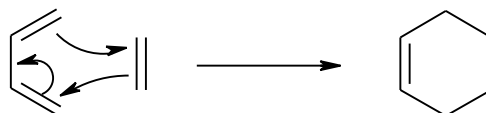


The analogous reaction of 1,3-butadiene with ethyne giving 1,4-cyclohexadiene is also known:



Since the reaction forms a cyclic product, via a cyclic transition state, it is also called a "*cycloaddition*".

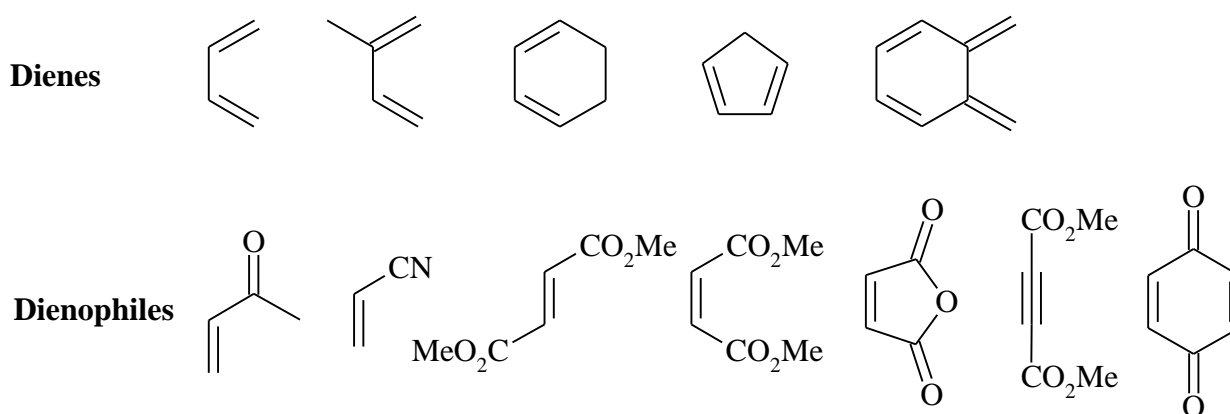
The reaction is a concerted process:



In concerted reactions, bond making and bond breaking occurs simultaneously. Due to that reaction mechanism, no intermediates are observed.

The high degree of regio- and stereoselectivity (due to the concerted mechanism), renders the *Diels-Alder* reaction a very powerful reaction, which is widely used in synthetic organic chemistry. The reaction is usually thermodynamically favoured due to the conversion of two  $\pi$ -bonds into two new, stronger  $\sigma$ -bonds. The two reactions shown above require harsh reaction conditions, but the normal *Diels-Alder* reaction is favoured by electron withdrawing groups on the electrophilic dienophile and by electron donating groups on the nucleophilic diene.

Some common examples of the reactants are shown below:

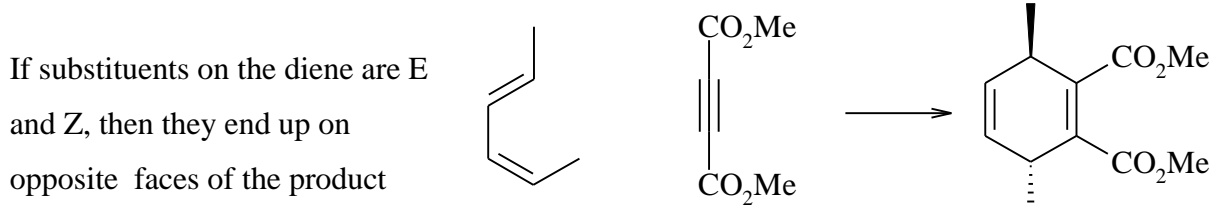
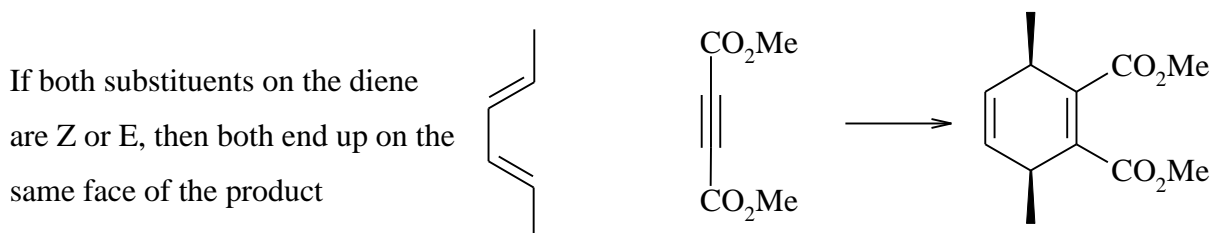
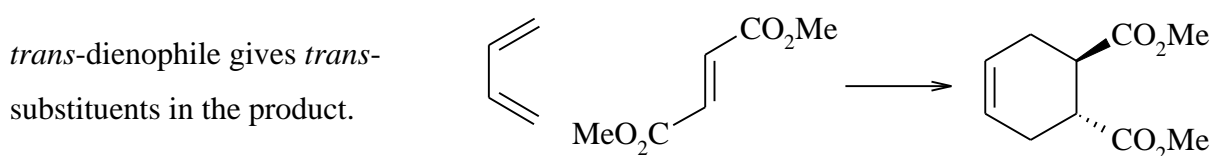
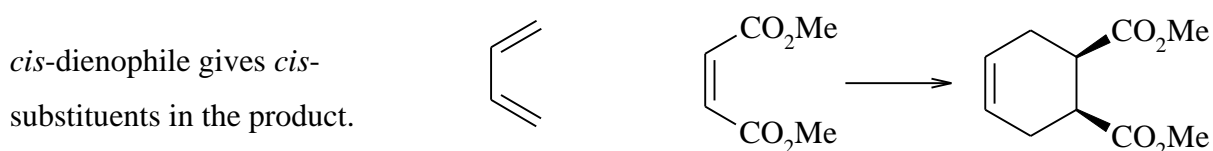


## 1 INTRODUCTION

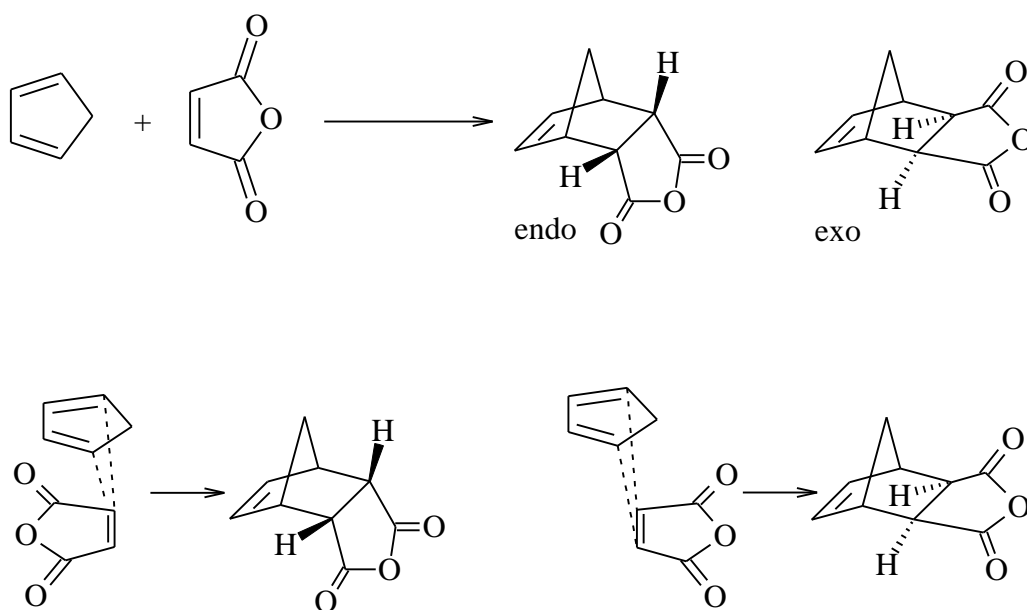
---

The *Diels-Alder* reaction is stereospecific with respect to both the diene and the dienophile. Addition is syn on both components.

This is illustrated by the examples below:



The reaction can also give stereoisomeric products depending on whether the dienophile lies under (*endo*) or away (*exo*) from the diene in the transition state. The *endo* product is usually the major product with maleimides as dienophiles since the  $\pi$ -electrons of the diene can interact with those of the carbon-oxygen double bonds when the molecules are aligned over each other.



Diene and dienophile aligned directly over each other gives the endo product (dienophile under or in = endo)

Diene and dienophile staggered with respect to each other gives the exo product (dienophile exposed or out = exo)

In the past decade “Organic Chemistry in Water” has become an active field of research.<sup>63-65</sup> A large number of reactions can be carried out in water without any specific disadvantages, but the discovery that an aqueous medium can actually promote reactions has further encouraged research in this area. Perhaps more than any other organic conversion, the *Diels-Alder* reaction has clearly manifested the advantage of an aqueous reaction medium. An aqueous medium can facilitate synthetic procedures, but can also be beneficial to organic reactions in terms of enhanced reaction rates, yields or stereochemistry.

Early reviews mention the significance of solvent polarity for *Diels-Alder* reactions.<sup>66</sup> *Desimoni* investigated a wide variety of *Diels-Alder* reactions (homo, hetero, intramolecular)<sup>67,68</sup> and concluded that in most cases the acceptor number (AN) of the solvent is the responsible property. The AN of a solvent describes the ability of a solvent to act as an electron pair acceptor and solvents are thought to reduce the LUMO of the reactants in *Diels-Alder* reactions through this mechanism (similar to Lewis acids). Evidently this pattern is

related to the hydrogen bond donating capacity of the solvent. Although this approach can certainly be criticized because it oversimplifies the influence of a solvent, the assumption that solvents can partly influence *Diels-Alder* reactions by affecting the molecule orbitals of the reactants makes sense and is true for most *Diels-Alder* reactions. However, not all reaction systems are as sensitive towards such interactions and in a few cases the donor number or cohesive density (solvent-solvent interactions) of the solvent are dominant.<sup>69</sup>

Pericyclic reactions, like *Diels-Alder* reactions, have attracted attention in the field of organic reactivity in water because these reactions were thought, as a result of their relatively apolar activated complex, not to be influenced by the solvent.

The first *Diels-Alder* reaction in water was actually carried out by the discoverers, *Diels* and *Alder*.<sup>70</sup> However, considering the hydrophylicity of the used reagents, maleic acid and furan, the use of water as solvent was rational. In the following decades few examples of *Diels-Alder* reactions in water were reported, but once more just reagents that readily dissolve in water were involved.<sup>71,72</sup>

Breslow's initial experiments revealed a 30 to 700-fold acceleration of several common *Diels-Alder* reactions.<sup>73</sup> In his paper, he briefly attributes this acceleration to hydrophobic effects: "Since in the *Diels-Alder* reaction of, e.g., cyclopentadiene with methyl vinyl ketone the transition state brings together two nonpolar groups, one might expect that in water this reaction could be accelerated by hydrophobic interactions".

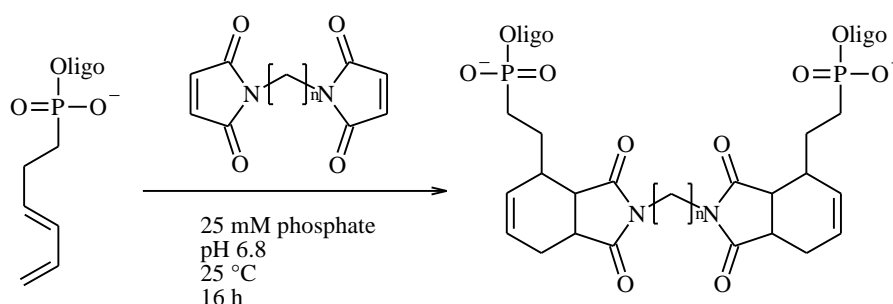
Further studies showed that water not only accelerates the *Diels-Alder* reaction, water also increases the stereoselectivity of the addition.<sup>74-76</sup> The endo/exo ratio is increased up to a factor of five if using water instead of organic solvents. This trend is partly attributed to the increased polarity of the medium, but the dramatic increase at high water contents is primarily the result of hydrophobic effects which favor the endo transition state (the most compact activated complex).

*NeXstar Pharmaceuticals* presented in 2001 the *Diels-Alder* bioconjugation of 5'-end diene-modified oligonucleotides (Scheme 18).<sup>77</sup> This has so far been the only reported work of *Diels-Alder* reactions with modified oligonucleotides in water. A 3,5-hexadiene-moiety was linked via the phosphodiester method to the 5'-end of a 28mer oligodeoxyribonucleotide. The



diene-modified oligonucleotides were bioconjugated in 25mM phosphate, pH = 6.8, at 25°C to 60°C with 2 to 12 equivalents of the maleimides. They observed complete transformation within 2 h.

For the linkage of two oligonucleotides they incubated the same oligonucleotide solution with 0.33 equivalents of 1,6-bismaleimido-hexane at 25°C and observed formation of the dimer of about 80% based on the bismaleimide.



Scheme 18 Linkage of 5'-end diene-modified oligonucleotides.<sup>77</sup>

## 1.6 Bioconjugation

Bioconjugation is defined as the linking of biomolecules to other biomolecules, polymers, small molecules, surfaces or metals. Bioconjugation is a critical enabling component of *in vitro* and *in vivo* diagnostics and *in vivo* therapies. The 'language' of bioconjugation has not changed in 15 years. Bioconjugation requires identifying a conjugation scheme that forms a stable linkage between the molecules, yet does not affect the inherent function of either coupling partner. Examples of biomolecules used in conjugates include enzymes, antibodies, peptides (synthetic and natural), oligonucleotides (synthetic and natural) and carbohydrates. Other types of molecules widely conjugated to biomolecules include fluorescent reagents, metal chelates and drugs. Yet another type of conjugation is the attachment (immobilization) of bio-molecules to solid surfaces such as plastics, glass, metal aggregates and beads, which has broad applications in genomics, proteomics and the diagnostics industry in general.

The ideal bioconjugation couple has to fulfil several criteria. First, the reactive moieties must react efficiently, yet must not cross-link with the biomolecule itself. Secondly, the linkers

need to be reactive enough to couple with high efficiency, yet stable enough so as to be stored in solution for long periods. Finally, the linkage should be stable over broad pH and temperature ranges, while still allowing cleavage to be effected if desired. It is also extremely important that no non-specific (i.e. non-covalent) binding/sticking of one biomolecule to the other biomolecule occurs which would lead to high background interference in any assay. It would be further advantageous if the functional reactive moieties could be modified for incorporation onto a biomolecule synthesized using standard solid phase methods.

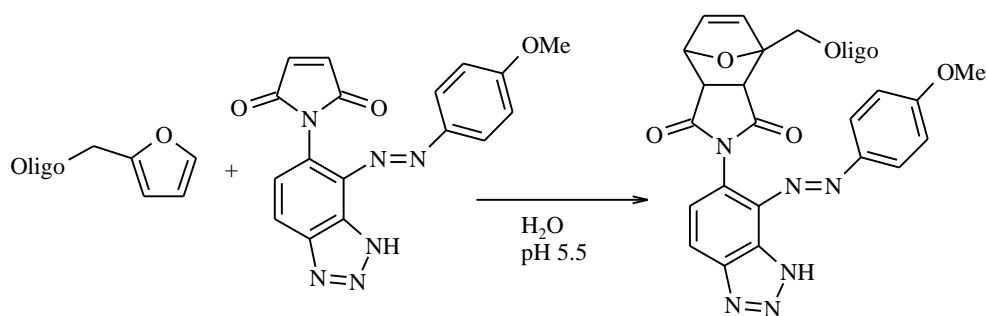
One of the critical components of many nucleic acid based diagnostic assays is an oligonucleotide with a reactive functionality that can be used to couple with labels, other biomacromolecules, or even microchips. Traditionally, either a primary thiol or an amine has been used for this purpose. Thiols are unstable and difficult to work with, and both chemistries require relatively unstable coupling partners.

In 2001 covalent modification and surface immobilization of nucleic acids via the *Diels-Alder* bioconjugation method was published by *Sebesta et al.*<sup>78</sup> They describe the two commonly employed methods for constructing bioconjugates of oligonucleotides, i.e. the introduction of the chemical modifier via automated synthesis and the post synthetic condensation. They report the progress toward a complementary method for preparing covalently modified oligonucleotides by a post-solid phase synthesis method relying on a cycloaddition reaction. Specifically, the highly selective reaction between a diene and a dienophile (a *Diels-Alder* cycloaddition) has been exploited for covalent biomolecule modification. Conceptually, the inertness and chemoselectivity of the *Diels-Alder* reactants offer advantages in bioconjugation applications. For example, competing hydrolysis of reactants under aqueous experimental conditions is less of a concern in a diene/dienophile condensation and the *Diels-Alder* process is actually accelerated in aqueous solvents. Furthermore, due to the high Chemo-selectivity of dienes possess for reactions with dienophiles, the *Diels-Alder* cycloaddition constitutes a previously untapped dimension of chemical orthogonality for the covalent modification of nucleic acids and other biopolymers.

They present direct comparison of the *Diels-Alder* bioconjugation method with other established techniques for covalent biomolecule modification, and describe the immobilization of cyclohexadiene-modified polymers on a maleimide modified surface.

The addition of an external label such as a fluorophore can be a disadvantage. Since most labels have appreciable biological properties in that they can associate with particular biomolecules in a non-covalent fashion, bioconjugation can lead to reduced and, in some cases, total probe inactivity. Additionally, any excess labeled probe has to either be removed from the assay or internally masked prior to analysis. This leads to extra separation procedures or the use of complicated and expensive probes.

Based on *Diels–Alder* cycloadditions and surface enhanced resonance Raman scattering (SERRS), *Graham et al* presented in 2002<sup>79</sup> a new approach for the detection of oligonucleotides. This method provides unique signals of the desired product using a simple probe without use of separation steps at ultra low concentrations. SERRS requires the presence of a colored moiety that will adsorb onto a metal surface. This produces enhanced Raman scattering at ultra low concentration levels and with a high degree of molecular specificity. In this new approach a small chemical tag is added to a probe molecule (Scheme 19). The tag is invisible to the detection technique of SERRS and is only made SERRS active by use of a developing agent that reacts specifically with the tag to produce the label. As the new species has a different molecular structure, the signal produced is unique to that species and shows differences to that of the developing reagent. Unlike fluorescence, this enables detection without separation.



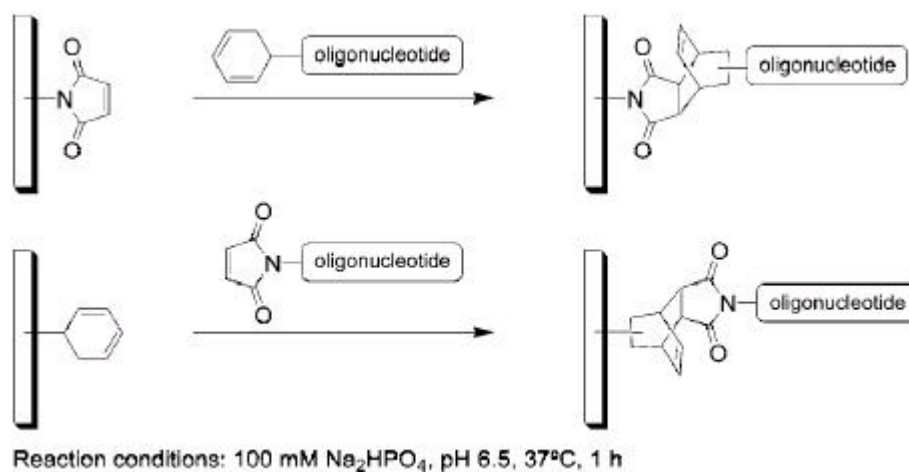
**Scheme 19** Bioconjugation via *Diels–Alder* reaction for surface enhanced resonance Raman scattering (SERRS).<sup>79</sup>

In 2003 *Leuck et al*<sup>80</sup> presented a method which is compatible with the presence of other chemical functionalities like amino groups and can be applied under particularly mild

## 1 INTRODUCTION

---

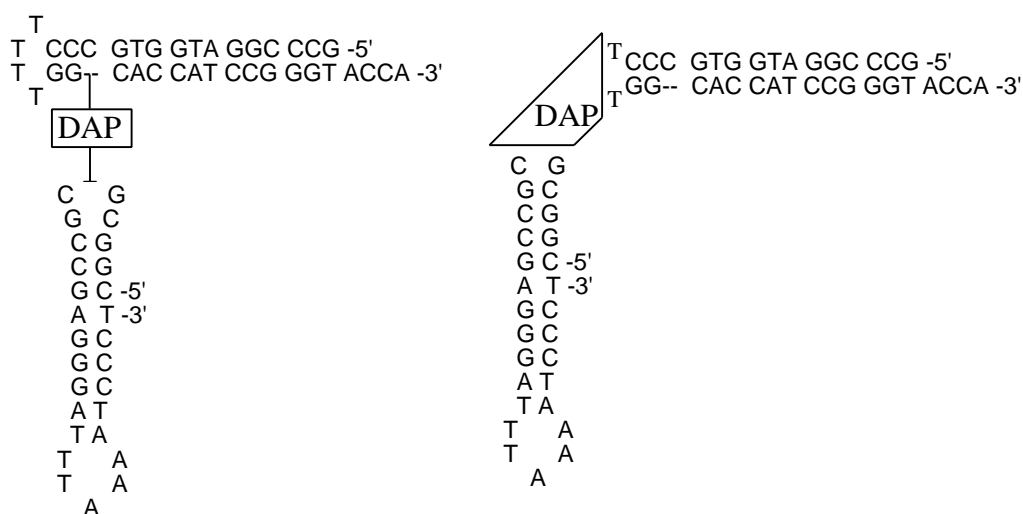
conditions, such as aqueous buffers without co-solvents, neutral pH and moderate temperature. They demonstrate the utility of aqueous *Diels-Alder* reactions for the bioconjugation of diene-modified oligonucleotide probes, and the covalent attachment of diene and maleimide functionalized oligonucleotides to a variety of glass surfaces (Scheme 20).



Scheme 20 Immobilization of modified oligonucleotides *via* the *Diels-Alder* reaction.<sup>80</sup>

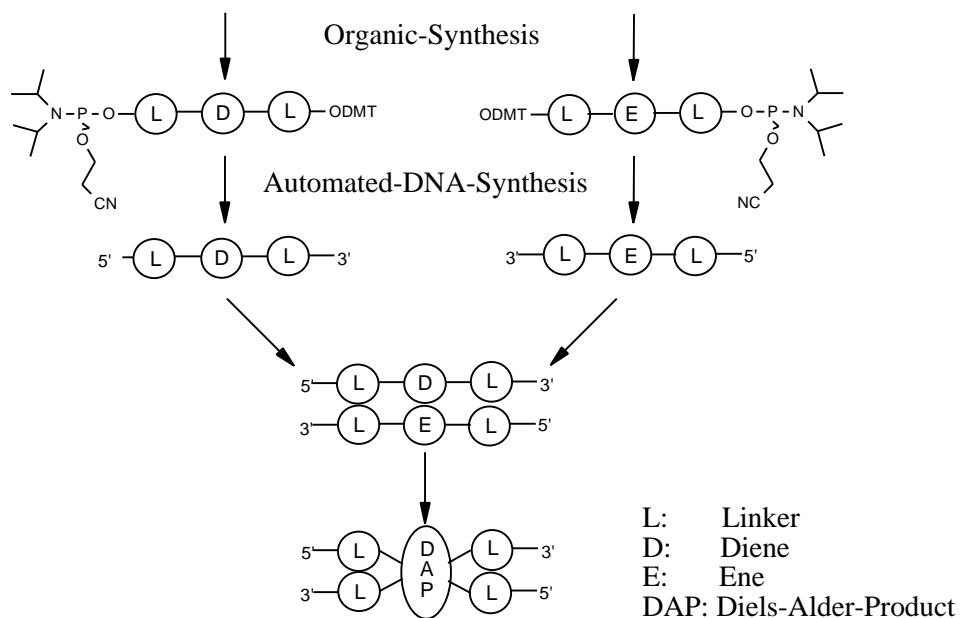
## 1.7 Aim of this Work

The overall goal of this research project is the development of a method for the assembly of larger DNA or RNA structures from smaller, well-defined secondary structural modules. One such target structure, a t-RNA mimic, is shown in Scheme 21. The target molecule could be composed of two subunits linked together, giving a tRNA mimic, that instead of the complex core structure<sup>81-86</sup>, between the acetylation and the anticodon branche, contains a simple chemical cross-link. One possibility consists in the linking of the two subunits *via* the *Diels-Alder* reaction. The reaction between diene and dienophile, reactive groups which are relatively stable against unwanted derivatisation, in aqueous solution via the *Diels-Alder* reaction is known to be favored because of the hydrophobic effect. Experiments with model oligodeoxyribonucleodides should help to determine the feasibility of this approach.



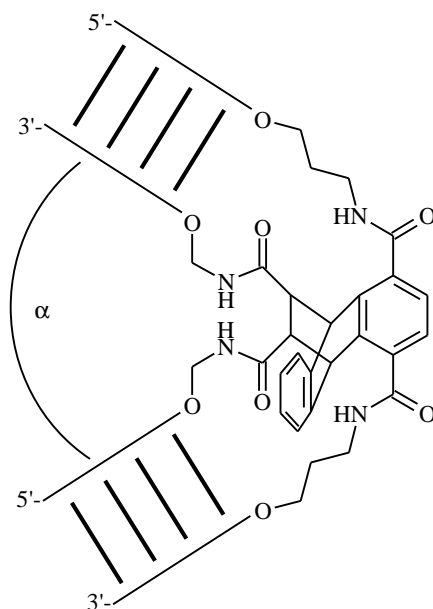
**Scheme 21** Illustration two different types of tRNA mimics. The acetylation site, the anti codon and parts of the stems correspond to tRNA<sup>leu</sup>, while the complex core structure is replaced by a simple *Diels-Alder* product.

Creation of our tRNA mimics can be divided into three major parts (Scheme 22). First one has to synthesize ene- and diene-phosphoramidite building blocks which then can be used for automated DNA synthesis on a DNA synthesizer. Finally one has to carry out the cross-linking of the ene- and the diene-modified oligonucleotides.



**Scheme 22** Strategy for the synthesis of ene- and diene-modified oligonucleotides and the cross-linking of the corresponding duplex.

Ene- and diene-modifications containing linkers of different length might, furthermore, allow the creation of cross-linked duplexes which are bent by a certain angle ( $\alpha$ ) (Scheme 23).



Scheme 23 Illustration of a kink in a modified duplex generated by a *Diels-Alder* adduct of a modified duplex with different linkers.





## 2 EXPERIMENTAL PART

### 2.1 Definitions

#### 2.1.1 Absorbance

The absorbance ( $A$ ) is the logarithm to base ten of the reciprocal of the spectral internal transmittance ( $T$ ).

$$A = -\log T$$

The reading displayed by most commercially available photometers is the absorbance, because it is proportional to the concentration according to the Lambert-Beer Law.

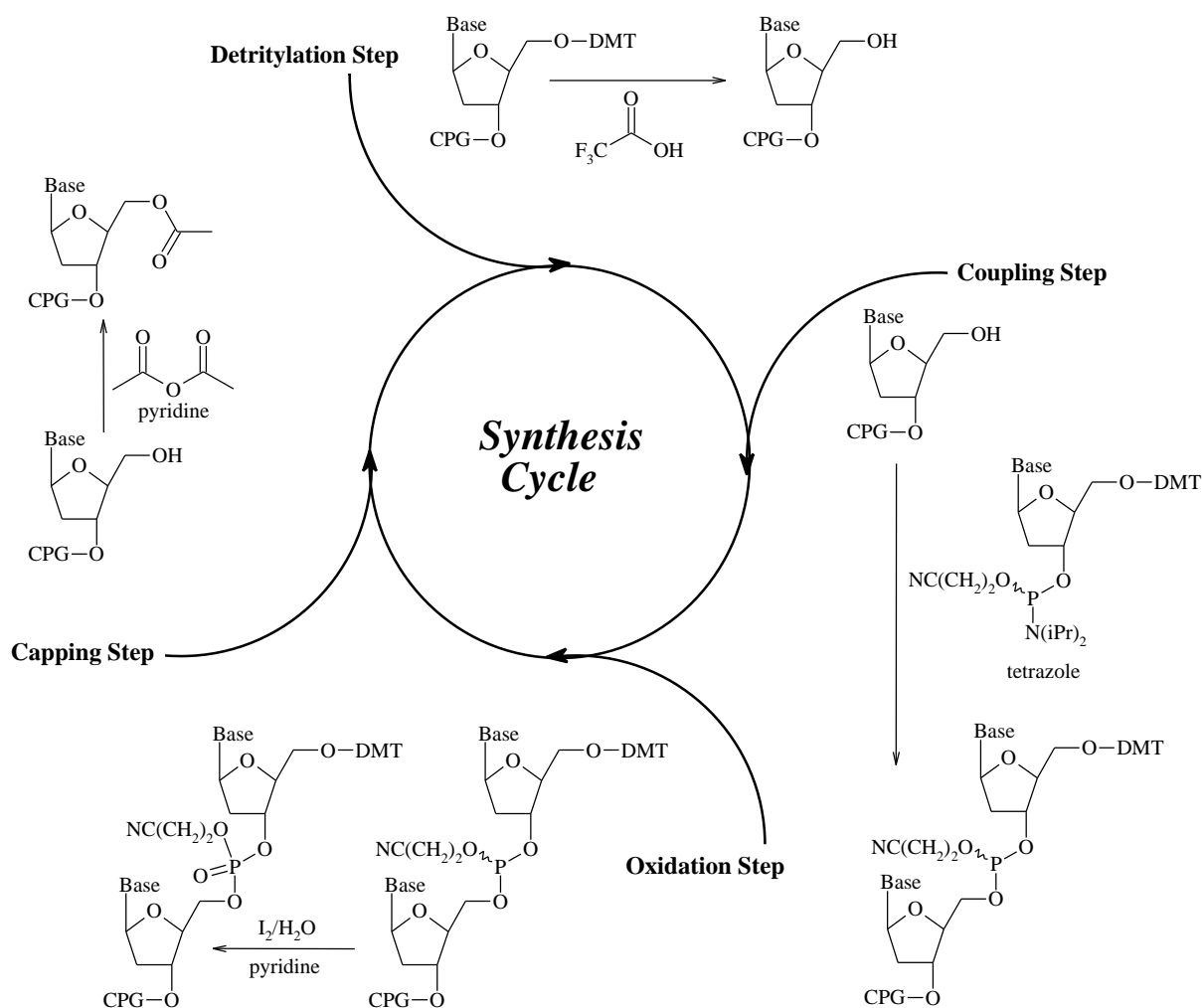
#### 2.1.2 Automated Oligonucleotide Synthesis

DNA synthesis is performed with the growing DNA chain attached to a solid support so that excess reagents can be removed by filtration. No purification steps are required between the cycles. The support material is usually a form of silica or a polymer, such as polystyrene. The starting material is the solid support derivatized with the nucleoside, which will finally be the 3' hydroxyl end of the oligonucleotide (Scheme24).<sup>87-105</sup>

The first step of the synthesis cycle is treatment of the derivatized solid support with acid to remove the DMT group. This will free the 5'-hydroxyl for the coupling reaction. An activated intermediate is created by simultaneously adding the phosphoramidite nucleoside monomer and tetrazole, a weak acid, to the reaction column. The tetrazole protonates the nitrogen of the phosphoramidite, making it susceptible to nucleophilic attack. This intermediate is so reactive that addition is complete within 30 seconds.

The capping step terminates any chains that did not undergo the addition. Since the unreacted chains have a free 5'-OH group, they can be terminated or capped by acetylation of the hydroxy group. Capping is done with acetic anhydride and 1-methylimidazole. The growing chains, that reacted successfully with the DMT protected phosphoramidite are not affected by

this step. Although capping is not ultimately required for DNA synthesis, it is highly recommended because it minimizes the length of the impurities and facilitates their separation from the final product.



**Scheme 24** Chain elongation cycle during automated DNA synthesis.

Finally, the internucleotide linkage is converted from the phosphite to the more stable phosphotriester. Iodine is used as the oxidizing agent and water as the oxygen donor. After oxidation, the DMT group is removed with a protic acid, trichloroacetic acid.

This cycle is repeated until chain elongation is complete.

The oligonucleotide is cleaved from the support by a one hour treatment with concentrated ammonium hydroxide which also removes the cyanoethyl phosphate protecting groups. The protecting groups on the exocyclic amines of the bases are removed by heating the crude DNA solution in ammonium hydroxid, at 55 °C.

### 2.1.3 Circular Dichroism

Circular Dichroism (CD)<sup>106,107</sup> is observed when optically active matter absorbs left and right hand circular polarized light slightly differently. It is measured with a CD spectropolarimeter. The CD is a function of wavelength. Different types of secondary structure present in peptides, proteins and nucleic acids Show distinct types of CD spectra. The analysis of CD spectra can therefore yield valuable information about secondary structure of biological macromolecules. A-, B- and Z-DNA can be differentiated by their typical CD spectra.

### 2.1.4 Extinction Coefficient

Constant used in the Beer-Lambert Law which relates the concentration of the substance being measured (in moles) to the absorbance of the substance in solution at a specific wavelength.<sup>108</sup>

$$\epsilon = A / (c * d)$$

### 2.1.5 Hyperchromicity

An increase in the optical density of a solution with nucleic acids in it such that it is able to absorb more ultraviolet radiation, which occurs when the double-stranded nucleic acid molecules denature into single-stranded molecules (Figure 1).

Hyperchromicity is the percentage change of the absorbance relative to the absorbance at the beginning of the experiment.

$$\text{Hyperchromicity} = (A - A_0) / A_0 * 100$$

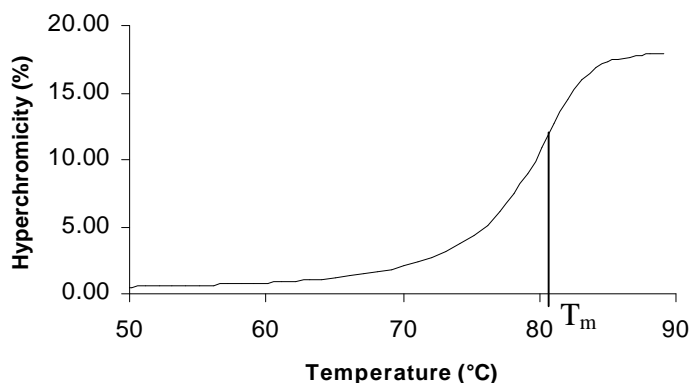


Figure 1 Hyperchromicity of an oligonucleotide duplex.

For DNA, hyperchromicity is typically calculated from the temperature dependent absorbance at 260 nm.

### 2.1.6 Lambert-Beer Law

Named after the two scientists Johann Heinrich Lambert (1728-1777) and August Beer (1825-1863), this law states the correlation between the absorbance  $A$ , the path length traversed, and the concentration of the absorbent substance:

$$A = c * d * \epsilon$$

where the concentration  $c$  is stated in mol/l and the path length  $d$  in cm. The proportionality constant, the relative extinction coefficient  $\epsilon$ , is a substance-specific function of the wavelength.

### 2.1.7 Loading Capacity

Amount of nucleoside (usually in mole), coupled on the surface, in ratio to the weight of the solid support (in grams).

### 2.1.8 Melting Temperature

The melting temperature ( $T_m$ ), characterizes the stability of the DNA hybrid formed between an oligonucleotide and its complementary strand (Figure 2). The melting temperature corresponds to the temperature at which 50% of a given oligonucleotide is bound to its complementary strand and so is dependent on the binding affinity between two oligonucleotides. The  $T_M$  corresponds to the temperature at which the change of hyperchromicity is the biggest, the maximum of the first derivative, which corresponds to zero in the second derivative.

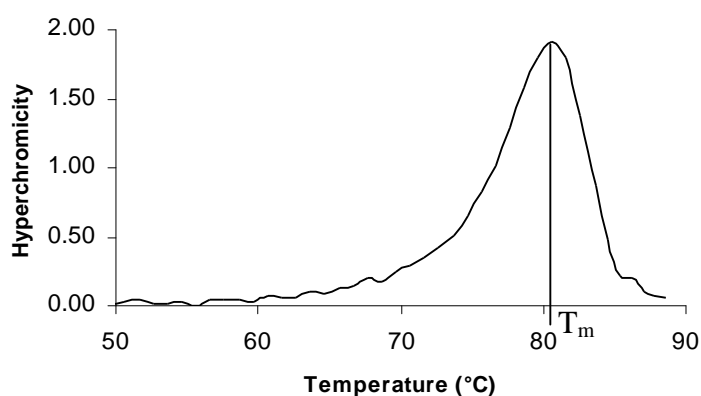


**Figure 2** First derivative of the melting curve of an oligonucleotide duplex

To estimate  $T_M$  for unmodified double stranded oligonucleotides with a length of 12-20 base pairs at 0.1 M NaCl, the rule of *Wallace*<sup>109,110</sup> can be used.

$$T_M = (\text{number of AT bp}) * 2^\circ\text{C} + (\text{number of GC bp}) * 4^\circ\text{C}$$

The sequence: a GC-rich sequence has a higher melting temperature, since GC base pairs form three hydrogen bonds while AT base pairs form just two.

The strand concentration: high oligonucleotide concentrations favour duplex formation, which results in a higher melting temperature.

The salt concentration: high ionic strength results in a higher  $T_M$ . The cations interact with the negative charged back bones of the oligonucleotides and, due to the reduced repulsion, stabilize DNA duplexes.

### 2.1.19 Optical Density

One optical density (OD) unit of DNA is the amount of DNA that gives an absorbance reading of 1.0 at 260nm for a sample dissolved in 1.0 ml total volume of H<sub>2</sub>O, which is read in a 1 cm quartz cell. For oligonucleotides, 1 OD corresponds to approximately 33µg of DNA.

### 2.1.10 Transmittance

The transmittance ( $T$ ) is the ratio of the transmitted spectral radiant flux ( $I$ ) to the incident spectral radiant flux ( $I_0$ ) at a specific wavelength.

$$T = I / I_0$$

## 2.2 Abbreviations

### 2.2.1 Solvents

AcOAc	acetic anhydride	EtOAc	ethylacetate
AcOH	acetic acid	EtOEt	diethylether
CCl <sub>4</sub>	carbon tetrachloride	EtOH	ethanol
CDCl <sub>3</sub>	deuteriochloroform	H <sub>2</sub> O	water
CH <sub>2</sub> Cl <sub>2</sub>	dichloromethane	HCl	acid hydrochloricum
CH <sub>3</sub> CN	acetonitrile	Hex	hexane
CHCl <sub>3</sub>	chloroform	MeOD	deuteromethanol
D <sub>2</sub> O	deuterated water	MeOH	methanol
DMF	dimethylformamide	tBME	tertiary buthylmethylether
DMSO	dimethylsulphoxide	THF	tetrahydrofuran

### 2.2.2 Conditions

°C	degrees celsius	min	minute(s)
d	day(s)	o.n.	over night
h	hour(s)	rt	room temperature

### 2.2.3 Chemicals and Groups

(d)A	(deoxy)adenosin	DMT	4,4'-dimethoxytrityl
(d)C	(deoxy)cytidin	DMTCl	4,4'-dimethoxytrityl chloride
(d)G	(deoxy)guanosin	Gua	guanin
(d)Rib	(deoxy)ribose	Im	imidazole
(d)T	(deoxy)thymidin	LDA	lithium diisopropylamide
Ac	acetyl	Na <sub>2</sub> CO <sub>3</sub>	di sodium carbonate
Ade	adenin	NaCl	sodium chloride
AIBN	azoisobutyronitril	NaH	sodium hydride

## 2 EXPERIMENTAL PART

---

Bn	benzyl	NaHCO <sub>3</sub>	sodium hydrogen carbonate
Boc	<i>tert</i> -butoxycarbonyl	PAM	phosphoramidite
Bz	benzoyl	Ph	phenyl
Cyt	cytosin	TEA	triethylamine
DCC	1.3-dicyclohexylcarbodiimide	TEAAc	triethylammonium acetate
DIBAL-H	diisobutylaluminum hydride	TFA	trifluoroacetic acid
DMS	dimethylsulphide	Thy	thymine

---

### 2.2.4 Various Abbreviations

<sup>13</sup> C-NMR	carbon NMR	ml	milliliters
<sup>1</sup> H-NMR	proton NMR	mol	mole(s)
abs	absolute	mp	melting point
Abs <sub>x</sub>	absorption at x nanometers	mRNA	messenger ribonucleic acid
bp	boiling point	MS	mass spectrometry
CD	circular dichroism	mult	multiplet
d	doublet	mw	molecular weight
DA	Diels-Alder	nm	nanometers
DNA	deoxyribonucleic acid	NMR	nuclear magnetic resonance
ds	double strand	OD	optical density
e	extinction coefficient	q	quartet
eq	equivalent(s)	quint	quintet
ESI	electron spray ionosation	R <sub>f</sub>	retention factor
g	gram	RNA	ribonucleic acid
HPLC	high performance liquid chromatography	RP	reverse phase
IE	ion exchange	s	singlet
IR	infrared	sext	sextet
l	liters	ss	single strand
LC	liquid chromatography	t	triplet
M	molar (moles / liter)	TLC	thin layer chromatography
MF	molecular formula	TOF	time of flight
MALDI	matrix assisted laser desorption ionisation	t <sub>R</sub>	retention time
mg	milligramms	tRNA	transfer ribonucleic acid
		ul	microliters
		UV	ultraviolet

---



## 2.3 Instrumentation and Methods

### 2.3.1 NMR Spectrometry

**<sup>1</sup>H-NMR** spectra were recorded on a Bruker AC 300 MHz or a Bruker DRX 500 MHz spectrometer and are reported in  $\delta$  from Me<sub>4</sub>Si ( $\delta = 0.00$  ppm) or from CDCl<sub>3</sub> ( $\delta = 7.26$  ppm). The <sup>1</sup>H-NMR chemical shifts and coupling constants were determined assuming first-order behavior. Multiplicities are reported using the following abbreviations: s (singlet), d (doublet), t (triplet), q (quartet), m (multiplet), br (broad) or a suitable combination. The list of coupling constants (J; reported to the nearest 0.5 Hz) corresponds to the order of the multiplicity assignment.

**<sup>13</sup>C-NMR** spectra were recorded on a Bruker AC 300 MHz or a Bruker DRX 500 MHz spectrometer in CDCl<sub>3</sub> (unless otherwise stated) with the chemical shifts relative to CHCl<sub>3</sub> (77 ppm).

**<sup>31</sup>P-NMR** spectra were recorded on a Bruker AC 300 MHz or a Bruker DRX 500 MHz spectrometer in CDCl<sub>3</sub> with the chemical shifts relative to phosphorous acid.

The NMR data were evaluated with the programs, 1D WIN-NMR and 2D WIN-NMR, version 6.0, of Bruker.

### 2.3.2 UV Spectrometry

UV spectra were recorded with UV/VIS Spectrometer Lambda 16 of Perkin Elmer. The blank, spectra of pure solvent or buffer with the same UV-cell, was subtracted from measured spectra to receive corrected spectra.

### 2.3.3 IR Spectrometry

IR spectra were recorded as pure substance (solid or oil) using a Jasco FT/IR-460 plus spectrometer, with a Golden Gate Mk II ATR Accessory with Diamond Top-plate and KRS-5 lenses, and processed with the Spectra Manager of Jasco. They are reported using the following abbreviations : s, strong; m, medium; w, weak.

### 2.3.4 ESI Mass Spectrometry

For mass determination of oligonucleotides.

VG platform mass spectrometer, Micromass Instruments, Manchester, U.K..

Minimal sample concentration: 50 pmol/ $\mu$ l.

Measured in acetonitril/water (1:1), 2 % tetrylamin.

### 2.3.5 Melting Points

They were recorded using Büchi 510 (open capillaries, uncorrected values).

### 2.3.6 Melting Curves of Oligonucleotides

Cary 3E UV/VIS Spectrophotometer (Varian) with Cary Temperature Controller, Sample Transport Accessory and Multi Cell Block.

- Adsorption of the oligonucleotides was measured at 260 nm.
- The temperature gradient was 0.5 °C per minute.
- Measurement was interrupted at the end of each temperature ramp for 2 min.
- The system was flushed with nitrogen, 6 l / min, at temperatures below 20 °C.
- The samples were measured in UV transparent cells, 4 x 10 mm and 0.8 ml, from Hellma.

### 2.3.7 Automated DNA-Synthesis

#### DNA Synthesizer:

ABI 392 and 394 Nucleic Acid Synthesizers from Applied Biosystems.

Standard programs for 40 nmol, 0.2 μmol and 1.0 μmol DNA synthesis from Applied Biosystems.

Longer coupling time for some modified phosphoramidites needed.

Reagents for automated DNA-Synthesis (phosphodiester method):

Phosphoramidite solutions:	0.5 M in acetonitrile
Activator solution:	terazole in acetonitrile
Capping A:	acetic anhydride/ pyridine/THF
Capping B:	1-methylimidazole in THF
Oxidizer solution:	0.02 M iodine in water/pyridine/THF
Deblock solution:	3 % trifluoroacetic acid
Wash solution:	acetonitrile
Trityl assay:	dichloromethane

Manual cleavage and deprotection in aqueous ammonia at 55 °C for 15 hours.

### 2.3.8 Analytical TLC

All reactions were monitored by thin layer chromatography (TLC), which was carried out on 0.25 mm Macherey-Nagel silica gel-25 UV<sub>254</sub> precoated plates. The following reagents were used as detectors (dipping followed by heating):

**Anisaldehyde reagent** : 1 mL of anisaldehyde and 2 mL of concentrated sulfuric acid dissolved in 100 mL of glacial acetic acid.

**Potassium permanganate reagent** : 3.0 g KMnO<sub>4</sub>, 20 g K<sub>2</sub>CO<sub>3</sub>, 5.0 ml 5% NaOH and 300 ml water.

**Cerium reagent:** 5.0 g phosphomolybdic acid hydrate and 16 ml concentrated phosphoric acid were dissolved in 200 ml water. Finally 2.0 g cer(IV)-sulfate was added.

**Bromokresol green reagent :** 40 mg of bromokresol green indicator (3,3',5,5'-tetrabromo-m-kresolsulfon-phthalein) was dissolved in 100 mL of ethanol and treated with 0.1 M aqueous NaOH until a blue color appeared. Basic compounds give a deep blue, acid or weak acid compounds a yellow color.

**Ninhydrine reagent :** 0.2 g of ninhydrine was dissolved in 100mL of ethanol.

**Vanillin reagent:** 8.6 g vanillin and 2.5 ml concentrated sulfuric acid were dissolved in 200 ml ethanol.

### 2.3.9 Preparative Column Chromatography

Preparative liquid chromatography (LC) was performed with silica 60 A, 40-63  $\mu\text{m}$ , from sds (France). Silica gel was suspended, in starting eluent, before filled into column and then covered with sand. After the dissolved crude material was added, solvent, isocratic or gradient, was pumped through the column. Collected fractions were controlled by TLC.

### 2.3.10 HPLC

BIO-TEK Kontron Instruments: pump system 525, diode array detector 545V.

**Soft ware: Galaxie Chromatography Data System (Varian).**  
Column oven.

**IE-HPLC:** EC 125-4 NU, Macherey Nagel.

A: 20mM  $\text{KH}_2\text{PO}_4$  in  $\text{H}_2\text{O}/\text{CH}_3\text{CN}$  (4:1), pH 7.0.

B: 20mM  $\text{KH}_2\text{PO}_4$ , 1.0 M NaCl in  $\text{H}_2\text{O}/\text{CH}_3\text{CN}$  (4:1), pH 7.0.

for selfcomplementary oligonucleotides 10 M urea or pH 10.0.

**RP-HPLC:** LiChroCART 250-4, Merck  
A: 0.1 M triethyl ammonium acetate in water.  
B: acetonitrile.  
40 °C.

### 2.3.11 Oligonucleotide Desalting

SEP PAK<sup>®</sup> C-18 10x9 mm mini columns from Waters.

Conditioning with 10 ml of acetonitril and 10 ml water, followed by 10 ml of 0.3 M triethyl ammoniumacetat buffer, pH = 6.0.

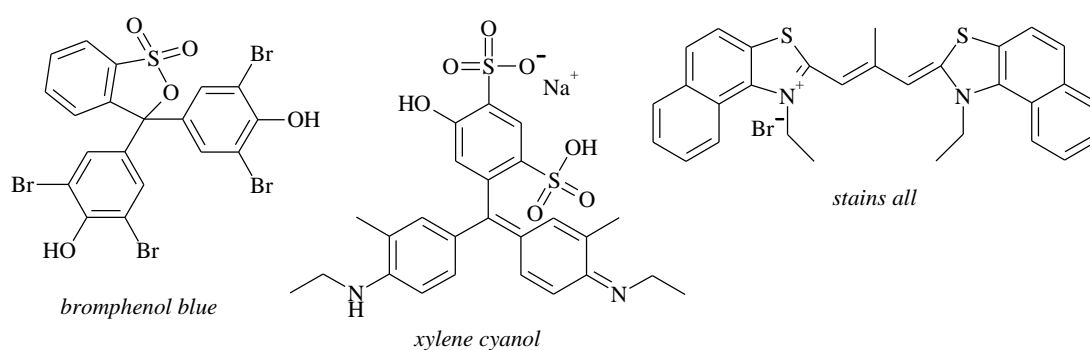
Loading of the crude oligonucleotide in 1 to 4 ml of 1.0 M triethyl ammoniumacetat buffer, pH = 6.0.

Washing with 10 ml of 0.3 M triethyl ammoniumacetat buffer, pH = 6.0, and 20 ml water.

Elution of the desalted oligonucleotide with 10 ml of methanol/water (3:2).

## 2.3.12 PAGE

Denaturing polyacrylamide gels were used analytically to control the quality of oligonucleotide solutions as well as to follow bio-conjugation and cross-linking experiments. As system we used a Mini-PROTEAN 3 electrophoresis module from Bio-Rad Laboratories. The gels were 0.75 mm thick 12% polyacrylamide, 1 x TBE (Tris-Borate-EDTA) and 10 M urea. The electrolyte was 1 x TBE. To reach stable conditions a prerun was performed before addition of the samples. The samples were mixed with 1 equivalent loading buffer (urea saturated formamide). To observe the migration bromphenol blue and xylene cyanol was added in one well (corresponds to about 12 resp. 55 bases). Oligonucleotides were visualized by staining the gels with *stains all* reagent (Scheme 25).



Scheme 25 Chemical structure of bromphenol, xylene cyanol and stains all.

Gels containing fluorescently labelled oligonucleotides were scanned, before staining, with a FLA-3000 scanner of Fujifilm. As scanning program we used BASReader 3.01 and for data processing Aida Image Analyzer v.3.10.

Stained gels were recorded in a Multi Image Light Cabinet of Alpha Innotech Corporation, and processed with Alphamanager v.5.5.

## 2.4 General Aspects

### 2.4.1 Chemicals

Chemicals used for organic synthesis were of highest quality obtainable from commercially suppliers (Fluka, Merk and Acros).

Solvents used in organic synthesis were of the quality needed from commercially suppliers.

Solvents for work up and FLC purification were of technical quality and additionally distilled and dried according to standard procedures.

Organic solvents used in HPLC were of super purity solvent (SPS) quality from Romil (Methanol 205, Acetonitril 230).

Ion exchange Water was used for synthesis work up.

Milli Q Water was used for HPLC and PAGE.

Solvents and reagents for the automated DNA-Synthesis were from Proligo (Hamburg) and Cruachem (Glasgow).

Deuterated solvents for NMR were of various suppliers.

### 2.4.2 General Methods

#### **General method A:**<sup>111-113</sup>

A solution of dimethyl-anthraquinone in 65% HNO<sub>3</sub> (10 ml / mmol) was stirred at 120 °C for 72 hr in a round bottom flask with a reflux condenser. To neutralize acidic gas, the reflux condenser was attached to a washing bottle containing a 1 M NaOH solution. After cooling down to 0 °C and filtration of the yellow reaction mixture, the remaining white powder was washed with ice water and dried at 120 °C under reduced pressure.

#### *Alternative method:*<sup>114</sup>

Heating of the reaction mixture to 220 °C, for 15 hr, in a autoclave (about 40 bar), followed of cooling down to 0 °C, filtration and washing with ice water. The remaining white powder then was dried at 120 °C under reduced pressure.

**Caution:** The aggressive conditions may destroy pressure and temperature control as well as the overpressure valve of the autoclave. While opening the autoclave, toxic gases ( $\text{NO}_x$ ) will escape.

**General method B:**<sup>115,116</sup>

A suspension of the anthraquinone derivative and activated zinc dust (300 mg / mmol, washed with 1 M HCl and  $\text{H}_2\text{O}$ ) in 12.5% aqueous ammonia (50 ml / mmol), was stirred at 80 °C in a round bottom flask with reflux condenser,. After 24 hr the suspension was filtrated and the residue was washed with hot 12.5% aqueous ammonia. The filtrate was concentrated under reduced pressure to half of the volume and then acidified with 2 M HCl to pH 1. The mixture was filtrated and the optained yellowish solid washed with little ice cold 2 M HCl followed by drying under reduced pressure.

**General method C:**<sup>117</sup>

A solution of dicarboxylic acid in absolute MeOH (10 ml / mmol) with a catalytic amount of concentrated  $\text{H}_2\text{SO}_4$ , was boiled at 80 °C in a round bottom flask with reflux condenser, for 5 hr. The dark solution was neutralized at room temperature with triethyl amine to pH 7. After evaporating MeOH the dimethyl ester was extracted with  $\text{CH}_2\text{Cl}_2$  and dried under reduced pressure.

**General method D:**<sup>118</sup>

To a solution of dimethyl ester in absolute  $\text{CH}_2\text{Cl}_2$  absolute MeOH (10 ml / mmol) was added. This mixture was then combined with 8 eq 3-aminopropanol and 30% NaOMe in MeOH ( 250  $\mu\text{l}$  / mmol). After heating for 2 hr at 70 °C, with a reflux condenser under argon atmosphere,  $\text{CH}_2\text{Cl}_2$  was evaporated under reduced pressure. The reaction mixture was then cooled down to 0 °C and filtrated. The remaining yellow solid was washed with little cold water and dried under reduced pressure.



**General method E:**

The diol was dissolved in absolute pyridine (20 ml / mmol) and 4,4'-dimethoxytrityl chloride in absolute pyridine (0.8 eq, 20 ml / mmol) was added dropwise over a period of about 2 hr. After stirring at room temperature for 3 hr the reaction was quenched by the addition of water. The crude product was isolated by liquid liquid extraction with CH<sub>2</sub>Cl<sub>2</sub> and dried in the rotation evaporator.

To avoid decomposition of the product on silica gel, the column was prepared with 5 ‰ triethyl amine containing solvent. Before addition of the crude product, the column was washed with pure solvent to get rid of surplus triethyl amine.

**General method F:**

To a suspension of (2 eq) tetrazol-diisopropyl-ammonium salt and (2 eq) 2-cyanoethyl-bis(N,N-diisopropyl)amino phosphite in absolute CH<sub>2</sub>Cl<sub>2</sub> (5 ml / mmol), one added the alcohol (1 eq) dissolved in absolute CH<sub>2</sub>Cl<sub>2</sub> (10 ml / mmol). After stirring at room temperature for 15 hr the reaction was quenched with NaHCO<sub>3</sub> aq and extracted with CH<sub>2</sub>Cl<sub>2</sub>. To avoid decomposition of the product on silica gel, the column was prepared with 5 ‰ triethyl amine containing solvent. Before addition of the crude product, the column was washed with pure solvent to get rid of surplus triethyl amine.

**General method G:**

Under argon, the diol (10 eq), in absolute THF (1 ml / mmol), was added dropwise to a suspension of sodium hydride (4 eq) in absolute THF (1 ml / mmol). After stirring for 15 hr at rt the dibromide, dissolved in absolute THF (1 ml / mmol) was added at rt and the reaction mixture was stirred for 1 hr at 80°C. The reaction mixture was then poured onto brine and extracted with EtOAc. After concentration under reduced pressure, excess diol was evaporated in a kugelrohr-oven.

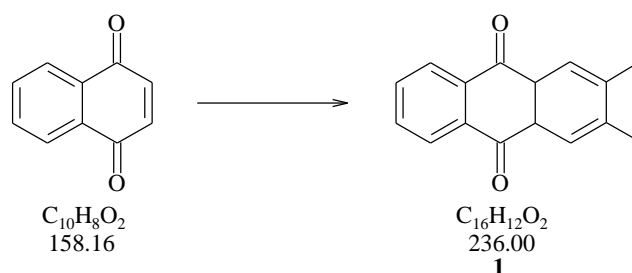
### **General method H:**

The amine (di-, triamine alternatively) in absolute  $\text{CH}_2\text{Cl}_2$  ( 1 ml / mmol) was added to maleic acid anhydride (1.1 eq / amino group) in absolute  $\text{CH}_2\text{Cl}_2$  ( 1 ml / mmol) and heated to 50 °C for 1 hr. After evaporation of the solvent, AcOAc (20 ml / mmol) and sodium acetate (1 g / mmol) was added. The suspension was to 80 °C for 3 hr, after being filtrated, the solvent was evaporated under reduced pressure.

## 2.5 Diene Phosphoramidites

### 2.5.1 Synthesis of 7<sup>119-125</sup>

#### 2,3-Dimethyl-anthraquinone (1)



In a 20 ml round bottom flask  $\alpha$ -1,4-naphthoquinone (1.58 g, 10 mmol) and 2,3-dimethyl-1,3-butadiene (822 mg, 10 mmol, 1 eq) were dissolved in 6 ml of toluene and stirred at 65 °C for 24 hr. Toluene was then evaporated and the residue dissolved in 100 ml of EtOH. O<sub>2</sub> was bubbled through the solution at 10 °C for 1.5 hr. After evaporating the EtOH, the residue was dissolved in H<sub>2</sub>O and extracted with EtOAc. The organic phase was washed with H<sub>2</sub>O and dried over Na<sub>2</sub>SO<sub>4</sub>. Evaporation of the solvent resulted in 2,3-dimethyl-anthraquinone (1) as red crystals.

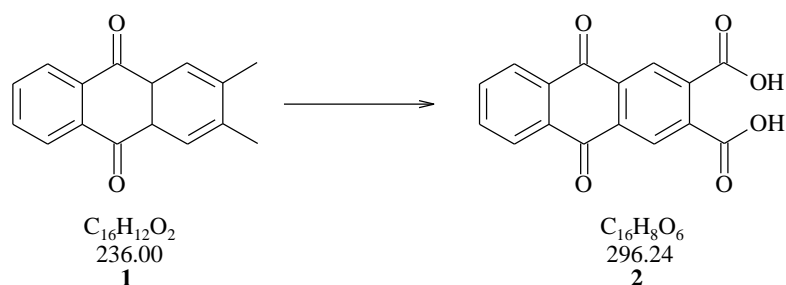
**Yield:** 2.0 g (8.6 mmol, 86%).

<sup>1</sup>H-NMR (CD<sub>3</sub>SOCD<sub>3</sub>, 300 MHz): 1.58 (s, 6 H), 3.47 (s, 2 H), 7.83-7.89 (m, 2 H), 7.91-7.94 (m, 2 H).

<sup>13</sup>C-NMR (CD<sub>3</sub>SOCD<sub>3</sub>, 75 MHz): 18.72, 30.24, 46.44, 123.19, 126.36, 133.65, 134.64, 197.95.

**R<sub>f</sub>** (Hex / EtOAc, 3 : 1): 0.52, discolours blue with cer reagent.

**9,10-Dioxo-9,10-dihydro-anthracene-2,3-dicarboxylic acid (2)**



According general method A.

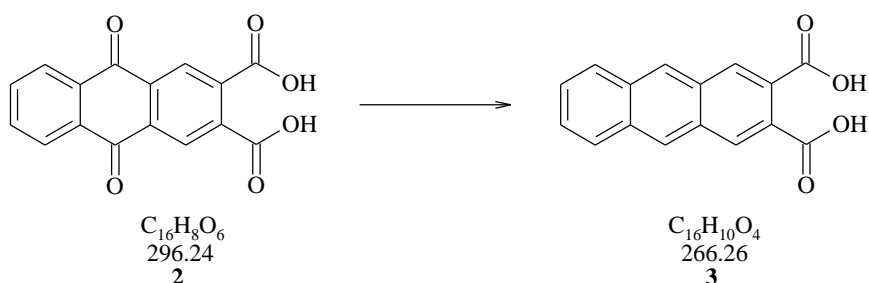
**Yield:** 57 %, as a yellow powder.

**$^1H$ -NMR** ( $CD_3SOCD_3$ , 300 MHz): 7.94-8.01 (m, 2 H), 8.22-8.28 (m, 2 H), 8.38 (s, 2 H).

**$^{13}C$ -NMR** ( $CD_3SOCD_3$ , 300 MHz): 126.81, 126.99, 133.14, 134.34, 134.88, 137.37, 167.44, 181.53.

**IR:** 3166, 1638, 1618  $cm^{-1}$ .

**mp:** (MeOH) 342 °C.

**Anthracene-2,3-dicarboxylic acid (3)**

Synthesized according to general method B.

**Yield:** 81 %, as a yellow powder.

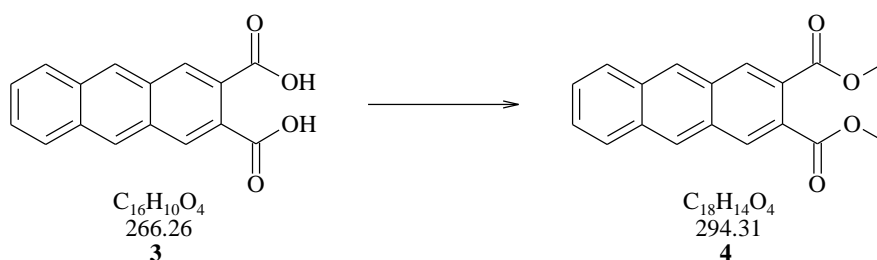
**$^1H$ -NMR** ( $CD_3SOCD_3$ , 300 MHz): 7.61-7.67 (m, 2 H), 8.14-8.18 (m, 2 H), 8.49 (s, 1 H), 8.78 (s, 2 H) .

**$^{13}C$ -NMR** ( $CD_3SOCD_3$ , 75 MHz): 126.90, 127.77, 128.36, 129.26, 130.09, 132.53, 168.72.

**IR:** 3135, 1701, 1674  $cm^{-1}$ .

**mp:** (MeOH) 345 °C.

### Anthracene-2,3-dicarboxylic acid dimethyl ester (4)



Synthesized according to general method C.

**Yield:** 60 %, as orange crystals.

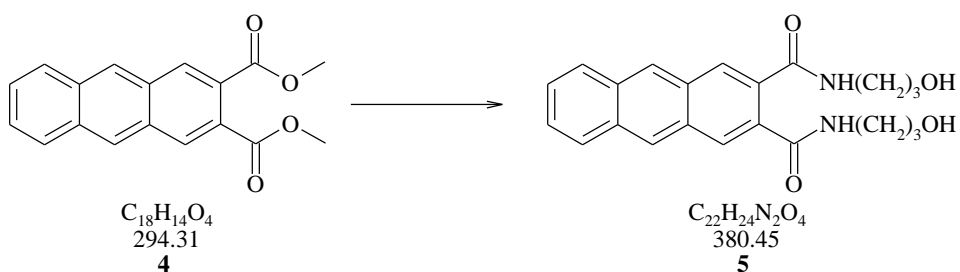
**<sup>1</sup>H-NMR** (CDCl<sub>3</sub>, 300 MHz): 3.99 (s, 6 H), 6.53-7.69 (m, 2 H), 8.00-8.10 (m, 2 H), 8.44 (s, 2 H), 8.51 (s, 2 H).

**<sup>13</sup>C-NMR** (CDCl<sub>3</sub>, 75 MHz): 52.67, 126.84, 127.56, 127.98, 128.40, 130.43, 131.28, 133.09, 168.17.

**IR:** 1717 cm<sup>-1</sup>.

**R<sub>f</sub>** (Hex / EtOAc, 7 : 3): 0.38, blue fluorescence.

**mp:** (EtOAc) 151 °C.

**Anthracene-2,3-dicarboxylic acid bis-[(3-hydroxy-propyl)-amide] (5)**

Synthesized according to general method C.

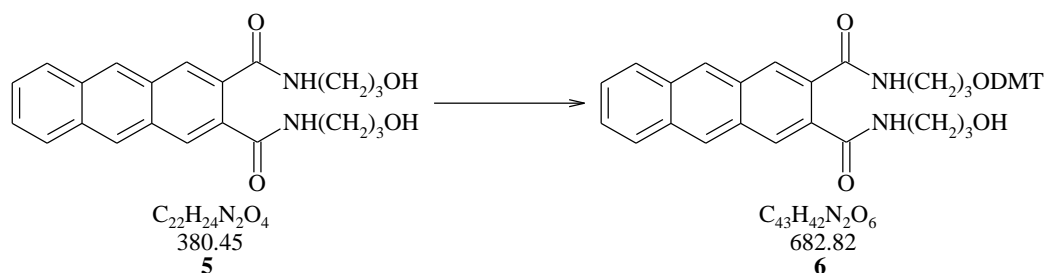
**Yield:** 41 %, as a transparent oil.

**$^1H$ -NMR** ( $CDCl_3$ , 300 MHz): 1.90 (p, 4 H,  $J = 6.6$  Hz), 3.52 (t, 4 H,  $J = 7.0$ ), 3.52 (t, 4H,  $J = 7.0$  Hz), 3.75 (t, 4 H,  $J = 6.2$  Hz), 7.55 (m, 2 H), 8.03 (m, 2 H), 8.10 (s, 2 H), 8.44 (s, 2 H).

**$^{13}C$ -NMR** ( $CDCl_3$ , 300 MHz): 33.21, 38.07, 60.60, 127.59, 128.35, 129.33, 129.55, 131.69, 133.76, 134.29, 171.95.

**$R_f$**  (tBME): 0.45, blue fluorescence.

**mp:** decomposition at 200 °C.

**Anthracene-2,3-dicarboxylic acid 2-({3-[bis-(4-methoxy-phenyl)-phenyl-methoxy]-propyl}-amide) 3-[(3-hydroxy-propyl)-amide] (6)**

Synthesized according to general method D.

**Yield:** 35 %, as a white solid.

**$^1\text{H-NMR}$**  ( $\text{CD}_3\text{SOCD}_3$ , 300 MHz): 1.86 (m, 4 H), 3.12 (t, 4 H,  $J=6.2$  Hz), 3.68 (s, 6 H), 6.89 (d, 4 H,  $J=8.8$  Hz), 7.18-7.42 (m, 9 H), 8.39 (m, 2 H).

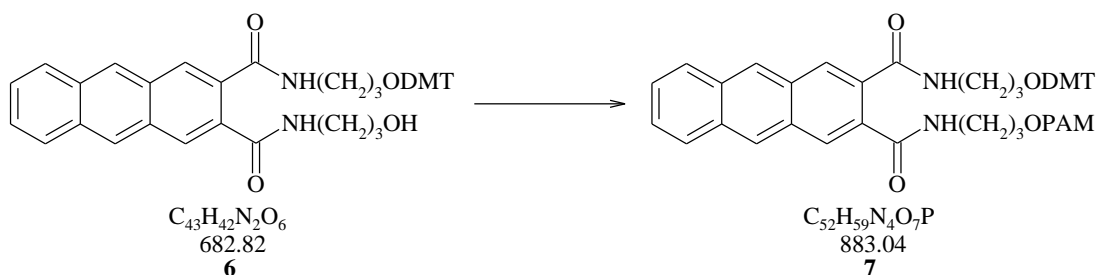
**$^{13}\text{C-NMR}$**  ( $\text{CD}_3\text{SOCD}_3$ , 75 MHz): 54.98, 85.35, 113.19, 126.60, 127.71, 127.84, 129.69, 129.91, 132.11, 133.77, 136.00, 145.26, 158.00, 168.11.

**$R_f$**  (EtOAc / MeOH, 3 : 1): 0.47, blue fluorescence and with cer reagent red discolourisation.

**mp:** decomposition.



**Diisopropyl-phosphoramidous acid 3-[(3-{3-[bis-(4-methoxy-phenyl)-phenyl-methoxy]-propylcarbamoyl}-anthracene-2-carbonyl)-amino]-propyl ester 2-cyano-ethyl ester (7)**



Synthesized according to general method E.

**Yield:** 31 %, as a white foam.

**<sup>1</sup>H-NMR** (CDCl<sub>3</sub>, 300 MHz): 1.07 (d, 12 H, *J* = 6.8 Hz), 1.11-1.30 (m, 2 H), 1.93-2.08 (m, 4 H), 2.37 (t, 2 H, *J* = 6.0 Hz), 3.31 (t, 2 H, *J* = 5.5 Hz), 3.41-3.65 (m, 4 H), 3.67 (s, 6 H), 3.70-3.91 (m, 4 H), 6.63 (d, 4 H, *J* = 12.0 Hz), 6.75-6.83 (m, 4 H), 7.12-7.20 (m, 7 H), 7.26-7.51 (m, 6 H), 7.93-8.02 (m, 2 H), 8.86 (d, 2 H, *J* = 11.3 Hz).

**<sup>13</sup>C-NMR** (CDCl<sub>3</sub>, 75 MHz): 20.21, 20.31, 24.50, 24.60, 38.21, 38.90, 42.97, 43.13, 55.21, 58.29, 62.39, 77.23, 86.48, 113.12, 123.04, 123.12, 124.99, 125.04, 126.34, 126.83, 127.85, 128.01, 128.54, 129.82, 132.06, 136.04, 144.40, 158.36, 169.03, 169.11.

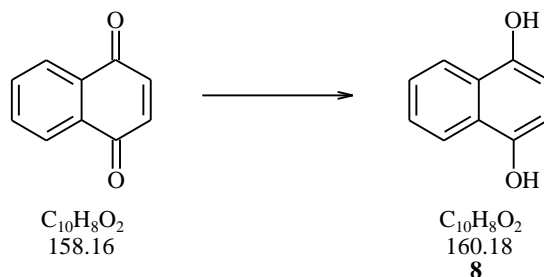
**<sup>31</sup>P-NMR** (CDCl<sub>3</sub>, 122 MHz): 148.20.

**R<sub>f</sub>** (EtOAc): 0.76, blue fluorescence and with cer reagent red discolourisation.

**mp:** decomposition.

## 2.5.2 Synthesis of 15<sup>126-130</sup>

### 1,4- Dihydroxynaphthalene (**8**)



A suspension of  $\alpha$ -1,4-naphthoquinone (5.0 g, 31.6 mmol) and activated zinc dust (2.0 g, 126 mmol, 4 eq, washed with 1 M HCl and H<sub>2</sub>O) in glacial acetic acid (75 ml) was treated with ultrasound. After 2 hr the color changed from dark brown to light yellow. The mixture was filtered and the residue was washed with EtOAc. The combined filtrates then were concentrated in vacuo to dryness **8** as a grey powder having a metallic luster.

**Yield:** 3.9 g (24.6 mmol, 78 %).

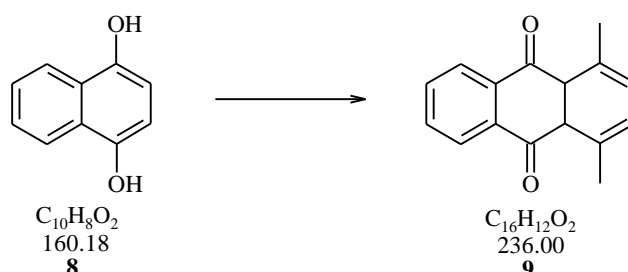
**<sup>1</sup>H-NMR** (CD<sub>3</sub>SOCD<sub>3</sub>, 300 MHz): 6.70 (s, 2 H), 7.43 (d, 2 H), 8.08 (d, 2 H), 9.33 (s, 2 H).

**<sup>13</sup>C-NMR** (CD<sub>3</sub>SOCD<sub>3</sub>, 75 MHz): 107.92, 121.88, 124.66, 125.33, 145.43.

**IR:** 747(s), 764 (s), 1061 (s), 1339 (s), 1598 (m), 1643 (m) cm<sup>-1</sup>.

**R<sub>f</sub>** (CH<sub>2</sub>Cl<sub>2</sub>): 0.11, UV active.

**mp:** (EtOAc) 192 °C.

**1,4-Dimethyl-anthraquinone (9)**

In a 50 ml round bottom flask with a reflux condenser 1,4-dihydroxynaphthalene (1.6 g, 10 mmol), acetonylacetone (1.14 g, 10 mmol, 1 eq), glacial acetic acid (7.5 ml) and concentrated hydrochloric acid (6.5 ml) were stirred at 120 °C for 24 hr. The dark, partly crystalline, solid was collected and washed with 50% acetic acid (10 ml) and then methanol (5 ml). Recrystallization from ethyl acetate and ethanol then gave **9** as yellow needles.

**Yield:** 1.53 g (6.5 mmol, 65 %).

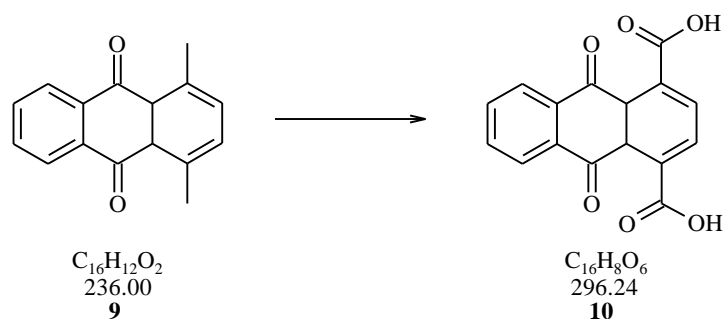
**<sup>1</sup>H-NMR** (CDCl<sub>3</sub>, 300 MHz): 2.78 (s, 6 H), 7.39 (s, 2 H), 7.55 (dd, 2 H, *J* = 5.8 and 3.5 Hz), 8.16 (dd, 2 H, *J* = 5.8 and 3.5 Hz).

**<sup>13</sup>C-NMR** (CDCl<sub>3</sub>, 300 MHz): 23.7, 126.4, 132.6, 133.3, 133.9, 137.2, 140.1, 185.7.

**R<sub>f</sub>** ( EtOAc / MeOH, 1 : 1): 0.85, UV active.

**mp:** (EtOH) 140-141 °C.

**9,10-Dioxo-9,10-dihydro-anthracene-1,4-dicarboxylic acid (10)**



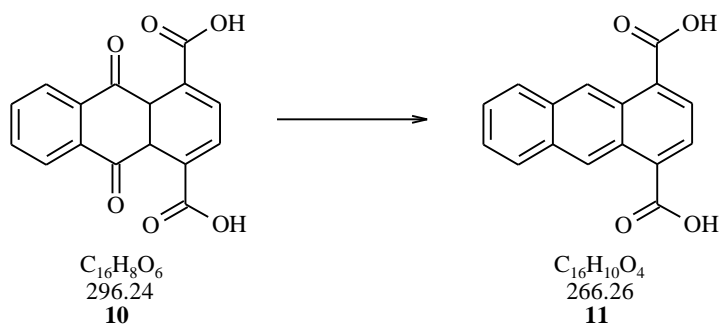
Synthesized according to general method A.

**Yield:** 40 %, as a white solid.

**$^1H$ -NMR** ( $CD_3SOCD_3$ , 300 MHz): 7.85 (s, 2 H), 7.93 (m, 2 H), 8.16 (m, 2 H), 12.63 (s, 2 H).

**$^{13}C$ -NMR** ( $CD_3SOCD_3$ , 75 MHz): 126.7, 129.9, 132.2, 132.6, 134.7, 136.5, 169.5, 181.4.

**mp:** (MeOH) >340 °C.

**Anthracene-1,4-dicarboxylic acid (11)**

Synthesized according to general method B.

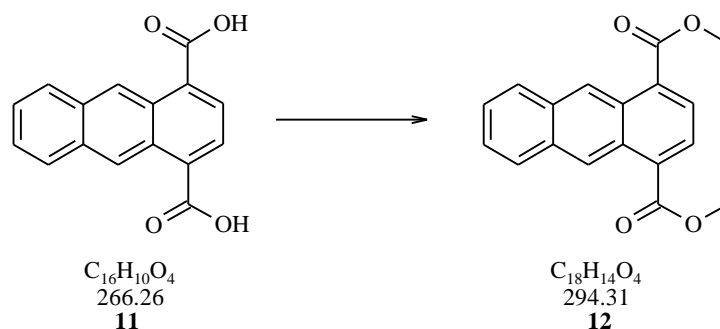
**Yield:** 49 %, as small yellow crystal plates.

**$^1H$ -NMR** ( $CDCl_3$ , 300 MHz): 7.6 (dd, 2 H,  $J = 6.5$  and  $3.1$  Hz), 8.14 (s, 2 H), 8.16 (m, 2 H), 9.46 (s, 2 H), 13.5 (br s, 2 H).

**$^{13}C$ -NMR** ( $CD_3SOCD_3$ , 300 MHz): 125.3, 126.9, 128.0, 128.3, 128.6, 131.6, 132.4, 168.5.

**mp:** (MeOH) 246 °C.

**Anthracene-1,4-dicarboxylic acid dimethyl ester (12)**



Synthesized according to general method C.

The product **12** was isolated from the crude mixture via LC (Hex / EtOAc, 7 : 3).

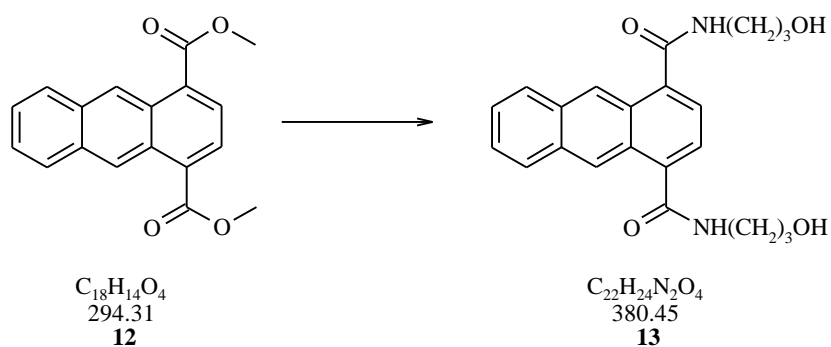
**Yield:** 65 %, as a yellow solid.

**<sup>1</sup>H-NMR** (CDCl<sub>3</sub>, 300 MHz): 3.99 (s, 6 H), 7.43-7.47 (m, 2 H), 8.00-8.01 (m, 4 H), 9.380 (s, 2 H).

**<sup>13</sup>C-NMR** (CDCl<sub>3</sub>, 75 MHz): 52.52, 76.60, 77.03, 77.45, 125.49, 126.62, 128.01, 128.58, 128.73, 131.58, 132.19, 167.58.

**R<sub>f</sub>** (Hex / EtOAc, 7 : 3): 0.52, yellow fluorescent.

**mp:** (EtOAc) 85-90 °C.

**Anthracene-1,4-dicarboxylic acid bis-[(3-hydroxy-propyl)-amide] (13)**

Synthesized according to general method D.

After drying under reduced pressure the product was purified by LC (EtOAc / MeOH, 3:1).

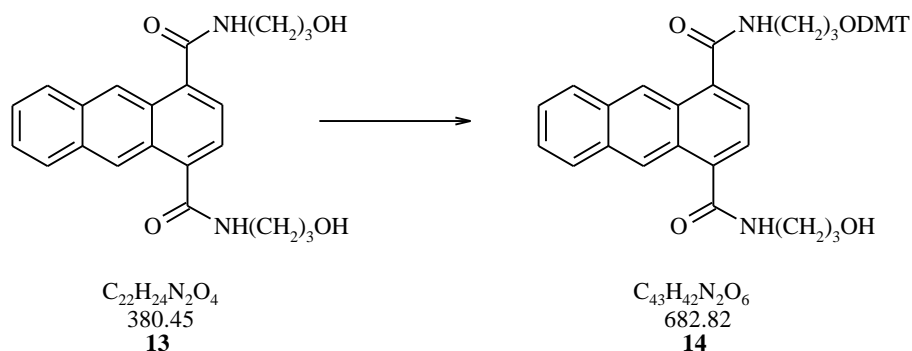
**Yield:** 87 %, as a yellowish solid.

**$^1H$ -NMR** ( $CD_3OD$ , 300 MHz): 1.98 (p, 4 H,  $J = 6.6$ ), 3.66 (t, 4 H,  $J = 7.0$ ), 3.79 (t, 4 H,  $J = 6.3$ ), 7.56-7.61 (m, 4 H), 8.05-8.08 (m, 2 H), 8.84 (s, 2 H).

**$^{13}C$ -NMR** ( $CD_3OD$ , 75 MHz): 34.13, 39.02, 61.52, 125.55, 126.67, 128.52, 130.14, 130.29, 134.29, 138.87, 172.93.

**$R_f$**  (EtOAc / MeOH, 1 : 1): 0.67, blue fluorescent.

**mp:** decomposition at 210 °C.

**Anthracene-1,4-dicarboxylic acid 1-({3-[bis-(4-methoxy-phenyl)-phenyl-methoxy]-propyl}-amide) 4-[(3-hydroxy-propyl)-amide] (14)**

Synthesized according to general method E.

Purification of the crude with LC (EtOAc / MeOH, 10:1).

**Yield:** 41 %, as a white solid.

**$^1H$ -NMR** (CDCl<sub>3</sub>, 300 MHz): 1.19-1.23 (m, 4 H), 1.87-1.98 (m, 4 H), 3.67 (s, 6 H), 3.70-3.87 (m, 4 H), 6.56-7.33 (m, 17 H), 7.48-7.59 (m, 2 H), 7.96-8.00 (m, 2 H), 8.86 (s, 2 H).

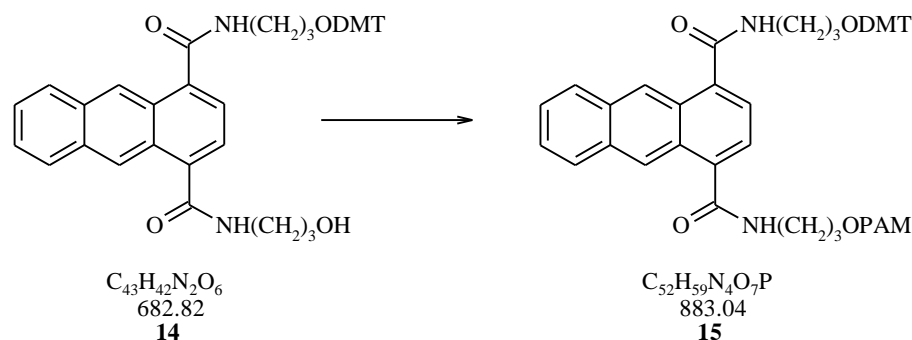
**$^{13}C$ -NMR** (CDCl<sub>3</sub>, 75 MHz): 54.98, 85.35, 113.19, 126.60, 127.71, 127.84, 129.69, 129.91, 132.11, 133.77, 136.00, 145.26, 158.00, 168.11.

**R<sub>f</sub>** (EtOAc / MeOH, 10:1): 0.64, yellow fluorescent and with cer reagent red discolourisation.

**mp:** decomposition.



**Diisopropyl-phosphoramidous acid 3-[(4-{3-[bis-(4-methoxy-phenyl)-phenyl-methoxy]-propylcarbamoyl}-anthracene-1-carbonyl)-amino]-propyl ester 2-cyano-ethyl ester (15)**



Synthesized according to general method F.

The crude was purified by LC (EtOAc).

**Yield:** 31 %, as a white foam.

**<sup>1</sup>H-NMR** (CDCl<sub>3</sub>, 300 MHz): 1.07 (d, 12 H, *J* = 6.8 Hz), 1.11-1.30 (m, 2 H), 1.93-2.08 (m, 4 H), 2.37 (t, 2 H, *J* = 6.0 Hz), 3.31 (t, 2 H, *J* = 5.5 Hz), 3.41-3.65 (m, 4 H), 3.67 (s, 6 H), 3.70-3.91 (m, 4 H), 6.63 (d, 4 H, *J* = 12.0 Hz), 6.75-6.84 (m, 2 H), 7.12-7.20 (m, 7 H), 7.24-7.34 (m, 3 H), 7.36-7.39 (m, 1 H), 7.45-7.51 (m, 2 H), 7.93-8.02 (m, 2 H), 8.86 (d, 2 H, *J* = 11.3 Hz).

**<sup>13</sup>C-NMR** (CDCl<sub>3</sub>, 375 MHz): 20.21, 20.30, 24.50, 24.60, 38.21, 38.90, 42.97, 43.13, 55.21, 58.29, 62.39, 86.48, 113.11, 123.04, 124.99, 126.34, 126.83, 127.89, 128.01, 128.54, 129.82, 132.06, 136.04, 136.83, 144.40, 158.36, 169.03, 169.11.

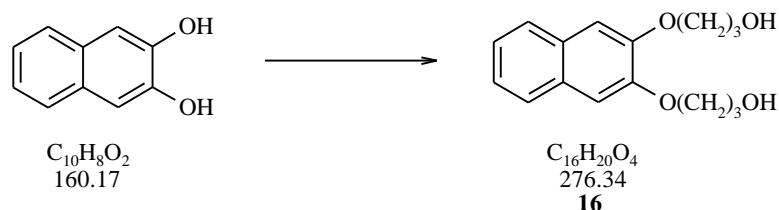
**<sup>31</sup>P-NMR** (CDCl<sub>3</sub>, 122 MHz): 148.20.

**HR-MS** (ESI<sup>+</sup>): C<sub>52</sub>H<sub>58</sub>N<sub>4</sub>NaO<sub>7</sub>P: calc.: 905.0186 g/mol, found: 905.0155 g/mol.

**R<sub>f</sub>** ( EtOAc ): 0.52, blue fluorescent and with cer reagent red discolourisation.

2.5.3 Synthesis of 18<sup>131-134</sup>

## 3-[3-(3-Hydroxy-propoxy)-naphthalen-2-yloxy]-propan-1-ol (16)



Under nitrogen atmosphere 2,3-dihydroxy-naphthalene (500 mg, 3.12 mmol) was added to a suspension of NaH (180 mg, 7.5 mmol, 2.4 eq) in absolute DMF (30 ml) and stirred for 1 hr at room temperature. After cooling down the reaction mixture to 0 °C, 3-bromo-1-propanol (0.85 ml, 9.37 mmol, 3 eq) in absolute DMF 10 ml was added dropwise. The reaction mixture was concentrated under reduced pressure and then purified by liquid chromatography with EtOAc as solvent. Concentration of the fractions gave pure 3-[3-(3-Hydroxy-propoxy)-naphthalen-2-yloxy]-propan-1-ol as white powder.

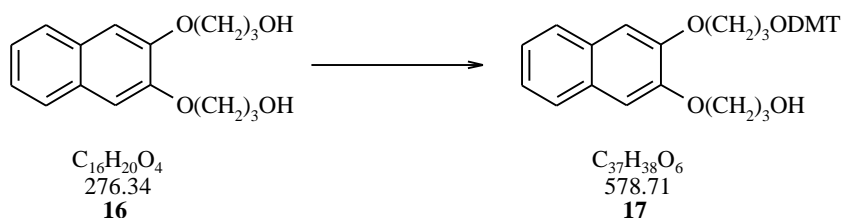
**Yield:** 390 mg (1.4 mmol, 47 %).

**<sup>1</sup>H-NMR** (CD<sub>3</sub>OD, 300 MHz): 2.07 (m, 4 H), 3.81 (t, 4 H,  $J = 6.3$  Hz), 4.21 (t, 4 H,  $J = 6.2$  Hz), 7.22 (s, 2 H), 7.26-7.29 (m, 2 H), 7.65-7.68 (m, 2 H).

**<sup>13</sup>C-NMR** (CD<sub>3</sub>OD, 75 MHz): 33.21, 60.07, 66.93, 108.94, 125.04, 127.33, 130.85, 150.34.

**R<sub>f</sub>** (EtOAc): 0.11, UV active.

**3-(3-{3-[Bis-(4-methoxy-phenyl)-phenyl-methoxy]-propoxy}-naphthalen-2-yloxy)-propan-1-ol (17)**



Synthesized according to general method D.

The crude was purified by LC (EtOAc / Hex, 1:1).

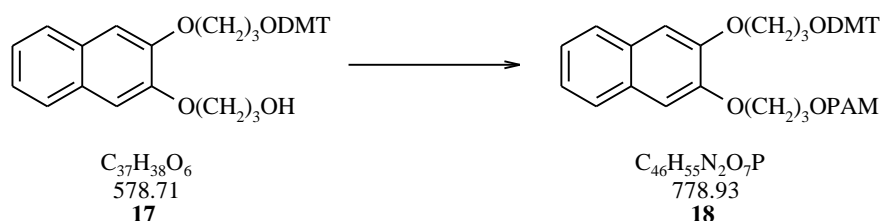
**Yield:** 33 %, as a white foam.

**$^1H$ -NMR** ( $CDCl_3$ , 300 MHz): 2.04-2.11 (m, 2 H), 2.15-2.23 (m, 2 H), 3.77 (s, 6 H), 3.77-3.83 (m, 2 H), 4.27 (t, 4 H,  $J = 5.9$  Hz), 6.76-6.81 (m, 4 H), 7.14-7.38 (m, 11 H), 7.43-7.46 (m, 2 H), 7.66-7.71 (m, 2 H).

**$^{13}C$ -NMR** ( $CDCl_3$ , 75 MHz): 29.71, 29.86, 31.55, 55.17, 59.61, 61.83, 65.55, 68.40, 85.87, 107.18, 107.43, 112.98, 124.10, 124.26, 126.28, 126.38, 126.58, 127.72, 128.15, 128.99, 129.45, 130.07, 136.43, 145.24, 148.64, 148.86, 158.29.

**$R_f$**  (EtOAc / Hex,1:1): 0.22, UV active and with cer reagent red discolourisation.

**mp:** decomposition.

**Diisopropyl-phosphoramidous acid 3-(3-{3-[bis-(4-methoxy-phenyl)-phenyl-methoxy]-propoxy}-naphthalen-2-yloxy)propyl ester 2-cyano-ethyl ester (18)**

Synthesized according to general method E.

The crude was purified by LC (EtOAc).

**Yield:** 95 %, as a white foam.

**$^1H$ -NMR** ( $CDCl_3$ , 300 MHz): 1.14-1.19 (m, 14 H), 2.08-2.19 (m, 4 H), 2.57 (t, 2 H,  $J = 6.2$  Hz), 3.31 (t, 2 H,  $J = 5.9$  Hz), 3.55-3.85 (m, 13 H), 4.09-4.25 (m, 4 H).

**$^{13}C$ -NMR** ( $CDCl_3$ , 300 MHz): 20.42, 20.51, 24.69, 24.74, 24.77, 24.84, 29.84, 30.10, 30.99, 31.09, 43.11, 43.28, 55.31, 58.34, 58.60, 60.21, 60.40, 60.63, 65.64, 66.15, 86.09, 108.04, 108.18, 113.15, 124.14, 124.18, 126.38, 126.77, 127.87, 128.32, 129.36, 129.44, 130.17, 136.61, 145.34, 149.36, 158.50.

**$^{31}P$ -NMR** ( $CDCl_3$ , 122 MHz): 148.40.

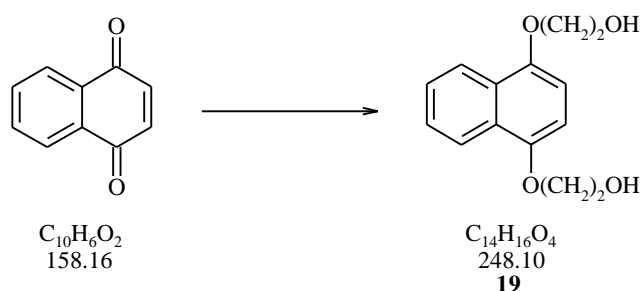
**HR-MS** (ESI<sup>+</sup>):  $C_{46}H_{55}N_2NaO_7P$ : calc.: 801.3644 g/mol, found: 801.3620 g/mol.

**$R_f$**  (EtOAc): 0.70, UV active and with cer reagent red discolourisation.

**mp:** decomposition.

### 2.5.4 Synthesis of **21**<sup>135-139</sup>

#### 2-[4-(2-Hydroxy-ethoxy)-naphthalen-1-yloxy]-ethanol (**19**)



In a separation funnel 1,4-naphthoquinone (2.75 g, 17 mmol) and sodium dithionite (2.75 g, 16 mmol) was added to H<sub>2</sub>O (30 ml) and diethylether (50 ml). After some shaking another sodium dithionite (3.75 g, 22 mmol) was added was added in two portions, shaking after each addition. The aqueous phase was removed, and the ethereal solution was washed with brine (20 ml) and dried over sodium sulfate. Removal of the solvent afforded a brownish solid which was combined with ethylene carbonate (3.3 g, 28 mmol, 2eq), tetraethylammonium bromide (1.0 g) and dimethylformamide (10 ml) and stirred at 150 °C for 8 hr. The mixture was then concentrated under reduced pressure and liquid liquid extraction with dichloromethane/ isopropanol (3/1) and water was done. Liquid column chromatography with ethylacetate then gave **19** as a dark solid.

**Yield:** 1.18 g (4.76 mmol, 28 %).

<sup>1</sup>H-NMR (CD<sub>3</sub>SOCD<sub>3</sub>, 300 MHz): 2.81 (s, 2 H), 4.30-3.81 (m, 8 H), 6.79 (s, 2 H), 7.56-7.30 (m, 2 H), 6.838-8.11 (m, 2 H).

<sup>13</sup>C-NMR (CDCl<sub>3</sub>, 75 MHz): 61.90, 70.15, 104.99, 121.84, 126.23, 126.60, 148.47.

## 2 EXPERIMENTAL PART

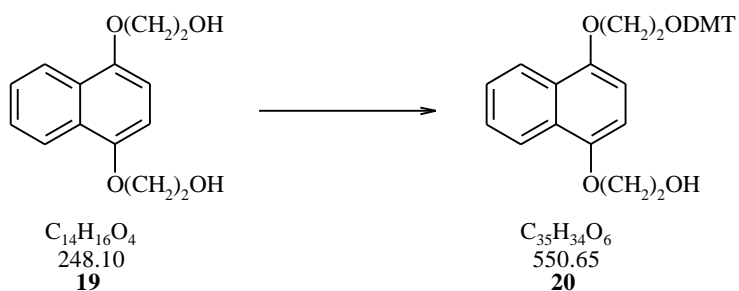
---

**IR:** 3413 (s), 2976 (m), 1629 (w), 1590 (s), 1443 (s), 1420 (m), 1383 (m), 1366 (m), 1351 (m), 1261 (s), 1229 (s), 1150 (m), 1093 (s), 1066 (s), 1030 (m), 901 (s), 893 (m), 885 (m), 794 (m), 763 (s), 742 (m)  $\text{cm}^{-1}$ .

**R<sub>f</sub>** (EtOAc): 0.48, UV active and blue discolourisation with cer reagent.

**mp:** (EtOH) 125-129 °C.

2-(4-{2-[Bis-(4-methoxy-phenyl)-phenyl-methoxy]-ethoxy}-naphthalen-1-yloxy)-ethanol  
(20)



Synthesized according to general method E.

The crude was purified by LC (EtOAc / Hex, 1:1).

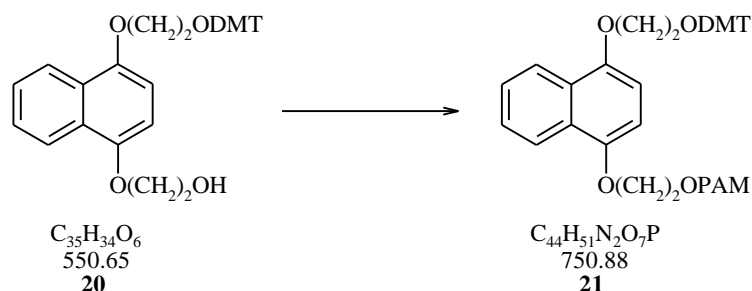
**Yield:** 43 %, as a beige oil.

**$^1H$ -NMR** (CDCl<sub>3</sub>, 300 MHz): 3.77 (s, 6 H), 4.07-4.14 (m, 4 H), 4.20-4.28 (m, 4H), 6.67-6.74 (m, 2 H), 6.79-6.84 (m, 4 H), 7.17-7.30 (m, 4 H), 7.39-7.43 (m, 4 H), 7.49-7.56 (m, 4 H), 8.17-8.37 (m, 1 H), 8.36-8.39 (m, 1 H).

**$^{13}C$ -NMR** (CDCl<sub>3</sub>, 75 MHz): 33.60, 39.67, 55.18, 60.38, 61.26, 61.90, 70.15, 85.87, 104.99, 113.03, 113.17, 121.84, 126.23, 126.60, 126.65, 136.47, 145.23, 148.47, 158.37.

**R<sub>f</sub>** ( EtOAc): 0.50, UV active and red discolourisation with cer reagent.

**mp:** decomposition.

**Diisopropyl-phosphoramidous acid 2-(4-{2-[bis-(4-methoxy-phenyl)-phenyl-methoxy]-ethoxy}-naphthalen-1-yloxy)-ethyl ester 2-cyano-ethyl ester (21)**

Synthesized according to general method F.

The crude was purified by LC (EtOAc / Hex, 1:1).

**Yield:** 94 %, as a beige foam.

**<sup>1</sup>H-NMR** (CDCl<sub>3</sub>, 300 MHz): 1.18-1.21 (m, 12 H), 1.55 (s, 2 H), 2.54-2.59 (m, 2 H), 3.51-3.54 (m, 2 H), 3.60-3.68 (m, 2 H), 3.77 (s, 6 H), 3.80-3.87 (m, 2 H), 4.26 (d, 4 H, *J* = 4.7 Hz), 6.69 (s, 2 H), 6.79-7.17 (m, 4 H), 7.19-7.30 (m, 3 H), 7.39-7.47 (m, 4 H), 7.49-7.55 (m, 4 H), 8.24-8.35 (m, 2 H).

**<sup>13</sup>C-NMR** (CDCl<sub>3</sub>, 75 MHz): 20.30, 20.39, 24.60, 43.08, 43.24, 55.21, 58.38, 58.62, 62.07, 62.30, 62.73, 68.19, 68.72, 68.82, 85.99, 104.50, 104.78, 113.08, 121.98, 122.03, 125.81, 125.83, 126.60, 126.72, 127.79, 128.26, 130.14, 136.25, 145.01, 148.67, 149.02, 158.43.

**<sup>31</sup>P-NMR** (CDCl<sub>3</sub>, 122 MHz): 148.40.

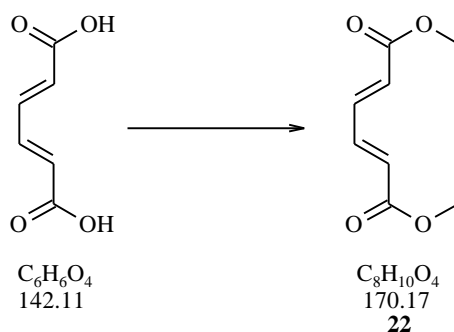
**HR-MS** (ESI<sup>+</sup>): C<sub>44</sub>H<sub>51</sub>N<sub>2</sub>NaO<sub>7</sub>P: calc.: 773.3331 g/mol, found: 773.3353 g/mol.

**R<sub>f</sub>** ( EtOAc / Hex, 1:1): 0.55, UV active and red discolourisation with cer reagent.



### 2.5.5 Synthesis of 25<sup>140-145</sup>

#### t,t-Hexa-2,4-dienedioic acid diethyl ester (22)



In absolute MeOH (100 ml) we dissolved trans,trans-muconic acid (1.94 g, 13.7 mmol) and added H<sub>2</sub>SO<sub>4</sub> (4 ml). After stirring at 70°C for 15 hr the reaction mixture was poured on saturated NaHCO<sub>3</sub> aq (150 ml) and extracted with EtOAc (200 ml). The aqueous phase was extracted two more times with EtOAc (100 ml). The combined organic phases then were washed with brine (200 ml), dried over Na<sub>2</sub>SO<sub>4</sub> and concentrated under reduced pressure. It resulted t,t-hexa-2,4-dienedioic acid diethyl ester as a white powder.

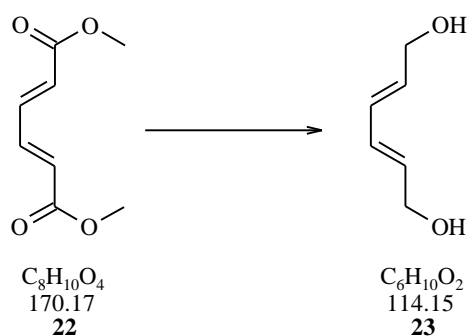
**Yield:** 2.44 g (12.3 mmol, 90%).

**<sup>1</sup>H-NMR** (CDCl<sub>3</sub>, 300 MHz): 1.28 (s, 6 H), 6.13-6.18 (m, 2 H), 7.23-7.31 (m, 2 H).

**<sup>13</sup>C-NMR** (CDCl<sub>3</sub>, 300 MHz): 14.19, 128.38, 140.77, 165.89.

**R<sub>f</sub>** (EtOAc): 0.76, UV active.

**mp:** (EtOAc) 75 °C.

**t,t-Hexa-2,4-diene-1,6-diol (23)**

At  $-78^{\circ}C$  1M DIBAL-H (123 ml, 123 mmol, 10eq, diisobutylaluminium hydride) was added slowly to t,t-hexa-2,4-dienedioic acid diethyl ester (2.44 g, 12.3 mmol) in absolute  $CH_2Cl_2$  (100 ml). The yellowish solution was heated up to room temperature in 2 hr and then stirred for 15 hr at room temperature. After 2 hr at  $40^{\circ}C$  the reaction mixture was cooled down to  $-78^{\circ}C$  and quenched with absolute EtOH (10 ml) followed by  $H_2O$  (20 ml). After heating up to room temperature the gel like mixture was extracted several time with MeOH by crushing in a mortar and centrifugation. The organic phases were concentrated under reduced pressure and the product purified by column chromatography with tBME. It resulted t,t-hexa-2,4-diene-1,6-diol as a white luster solid.

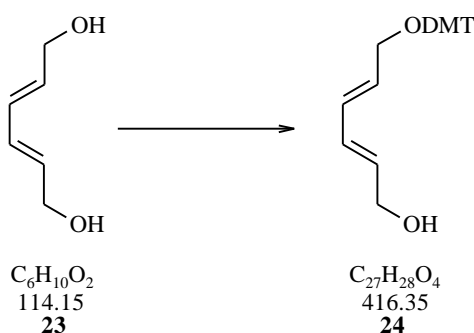
**Yield:** 980 mg (8.60 mmol, 70%).

**$^1H$ -NMR** ( $CDCl_3$ , 300 MHz): 1.35 (s br, 2 H), 4.19 (s br, 4 H), 5.79-5.88 (m, 2 H), 6.21-6.31 (m, 2 H).

**$^{13}C$ -NMR** ( $CDCl_3$ , 75 MHz): 63.40, 130.62, 132.59.

**$R_f$**  (EtOAc): 0.42, wake UV active and blue discolourisation with cer reagent.

**mp:** (EtOAc)  $106^{\circ}C$ .

**6-[Bis-(4-methoxy-phenyl)-phenyl-methoxy]-hexa-2,4-dien-1-ol (24)**

Synthesized according to general method E.

The crude was purified by LC (EtOAc / Hex, 2:3).

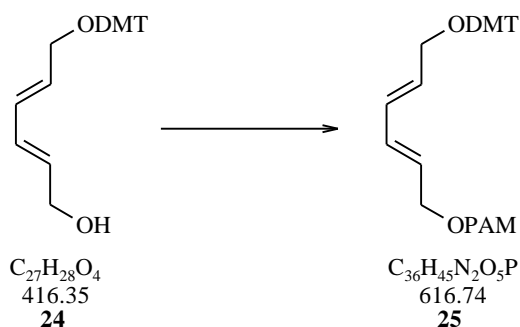
**Yield:** 52 %, as a transparent oil.

**$^1H$ -NMR** ( $CDCl_3$ , 300 MHz): 1.65 (s br, 1 H), 3.56-3.58 (m, 2 H), 3.70 (s, 6 H), 4.10-4.12 (m, 2 H), 5.67-5.81 (m, 2 H), 6.15-6.34 (m, 2 H), 6.75 (d, 4 H,  $J = 8.8$  Hz), 7.10-7.28 (m, 7 H), 7.36-7.39 (m, 2 H).

**$^{13}C$ -NMR** ( $CDCl_3$ , 75 MHz): 14.31, 21.15, 55.32, 60.52, 63.42, 64.29, 86.37, 113.22, 123.88, 126.83, 127.92, 128.21, 130.08, 131.01, 131.19, 131.79, 136.46, 145.19, 149.87, 158.55.

**$R_f$**  (EtOAc / Hex, 2:3): 0.13, UV active and red discolourisation with cer reagent.

**mp:** decomposition.

**Diisopropyl-phosphoramidous acid 6-[bis-(4-methoxy-phenyl)-phenyl-methoxy]-hexa-2,4(trans,trans)-dienyl ester 2-cyano-ethyl ester (25)**

Synthesized according to general method F.

The crude was purified by LC (EtOAc / Hex, 1:1).

**Yield:** 68 %, as a transparent glass.

**$^1H$ -NMR** ( $CDCl_3$ , 300 MHz): 1.23-1.36 (m, 14 H), 2.61 (t, 2 H,  $J = 5.9$  Hz), 3.61-3.73 (m, 4 H), 3.77 (s, 6 H), 3.78-3.89 (m, 2H), 4.22-4.30 (m, 2 H), 5.80-5.86 (m, 2 H), 6.37 (p, 2 H,  $J = 16.2$  Hz), 6.86 (d, 4 H,  $J = 9.0$  Hz), 7.12-7.40 (m, 7 H), 7.50 (d, 2 H,  $J = 7.4$  Hz).

**$^{13}C$ -NMR** ( $CDCl_3$ , 75 MHz): 14.26, 20.33, 20.43, 21.07, 24.58, 24.67, 24.76, 29.74, 43.02, 43.18, 55.18, 58.36, 58.61, 60.37, 63.78, 64.02, 64.20, 86.23, 113.13, 117.77, 126.76, 127.86, 128.10, 129.85, 129.94, 129.98, 130.03, 130.79, 131.34, 136.32, 145.16, 158.47.

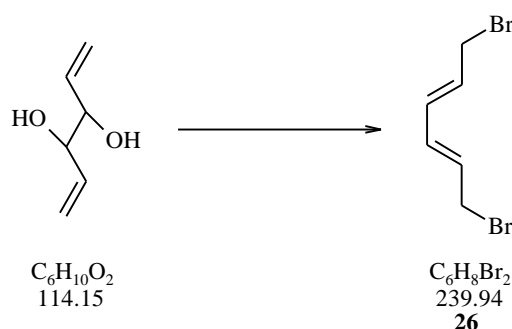
**$^{31}P$ -NMR** ( $CDCl_3$ , 122 MHz): 148.40.

**HR-MS** (ESI+):  $C_{36}H_{45}N_2NaO_5P$ : calc.: 639.2963 g/mol, found: 639.2946 g/mol.

**$R_f$**  (EtOAc / Hex, 1:1): 0.64, UV active and red discolourisation with cer reagent.

### 2.5.6 Synthesis of 29<sup>146-150</sup>

#### 1,6-Dibromo-hexa-2*t*,4*t*-diene (26)



A solution of hexa-1,6-diene-3,4-diol (1.50 g, 13.1 mmol) in absolute EtOEt (5 ml) was added dropwise, at 0°C, to phosphorus tribromide (2.24 g, 9.0 mmol, in excess) in absolute EtOEt (5 ml). After the addition was complete, the mixture was allowed to warm to room temperature. After 3 hr the reaction mixture was poured slowly into stirring ice-water and then was carefully neutralized with saturated aqueous sodium carbonate. The crude was extracted with ether and then purified by LC (EtOAc / MeOH, 19:1). The product is a strong lacrymator and should be handled in a fume hood.

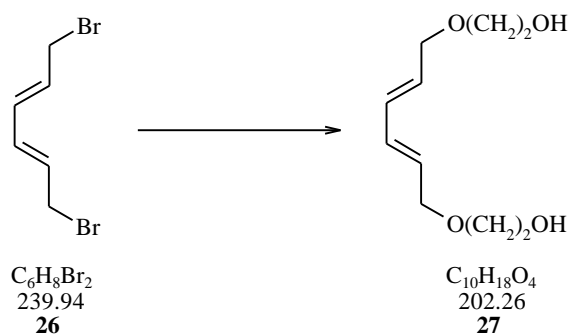
**Yield:** 2.63 g (11.4 mmol, 87 %).

**<sup>1</sup>H-NMR** (CDCl<sub>3</sub>, 300 MHz): 4.00 (d, 4 H, *J* = 7.7 Hz), 5.84-5.99 (m, 2 H), 6.21-6.31 (m, 2 H).

**<sup>13</sup>C-NMR** (CDCl<sub>3</sub>, 300 MHz): 32.50, 130.86, 133.25.

**R<sub>f</sub>** (tBME): 0.58, UV active.

**mp:** (EtOAc) 85-87 °C.

2-[6-(2-Hydroxy-ethoxy)-hexa-2*t*,4*t*-dienyloxy]-ethanol (27)

Synthesized according to general method G.

The crude was purified by LC (EtOAc / MeOH, 19:1).

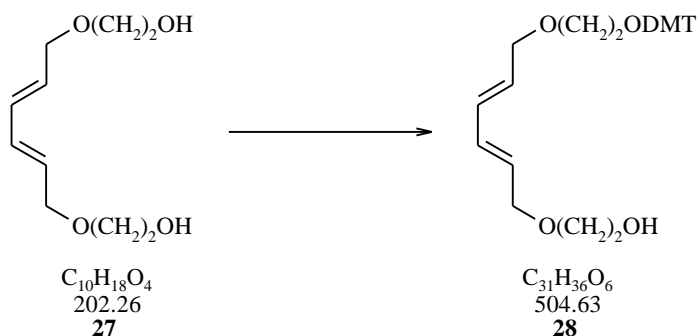
**Yield:** 24 %, as a yellowish oil.

**<sup>1</sup>H-NMR** (CDCl<sub>3</sub>, 300 MHz): 2.02 (s br, 2 H), 3.52-3.57 (m, 4 H), 3.73 (t, 4 H, *J* = 4.4 Hz), 4.05 (d, 4 H, *J* = 5.6 Hz), 5.71-5.80 (m, 2 H), 6.22-6.27 (m, 2 H).

**<sup>13</sup>C-NMR** (CDCl<sub>3</sub>, 75 MHz): 61.92, 71.26, 77.24, 129.90, 132.03.

**R<sub>f</sub>** (EtOAc): 0.12, UV active, with permanganate reagent yellow and with cer reagent blue discolourisation.

2-(6-{2-[Bis-(4-methoxy-phenyl)-phenyl-methoxy]-ethoxy}-hexa-2*t*,4*t*-dienyloxy)-ethanol  
(28)



Synthesized according to general method E.

The crude was purified by LC (EtOAc).

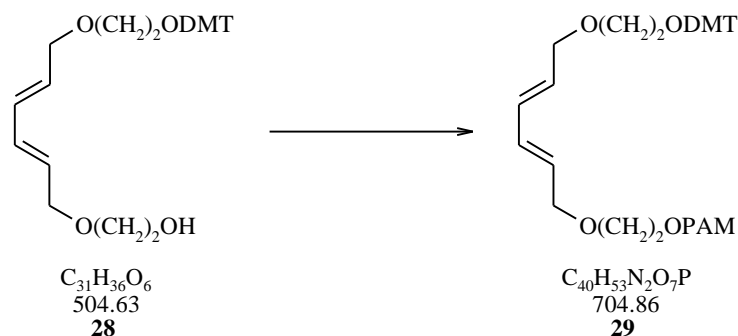
**Yield:** 30 %, as a transparent glass.

**$^1H$ -NMR** ( $CDCl_3$ , 300 MHz): 2.02 (s br, 2 H), 3.52-3.57 (m, 4 H), 3.73 (t, 4 H,  $J = 4.4$  Hz), 4.05 (d, 4 H,  $J = 5.6$  Hz), 5.71-5.80 (m, 2 H), 6.22-6.27 (m, 2 H), 6.77-6.82 (m, 4 H), 7.17-7.35 (m, 7 H), 7.45 (d, 2 H,  $J = 7.2$  Hz).

**$^{13}C$ -NMR** ( $CDCl_3$ , 75 MHz): 14.34, 21.17, 32.26, 60.36, 60.52, 62.07, 67.74, 69.45, 71.05, 71.43, 85.89, 113.12, 126.71, 127.82, 128.33, 129.62, 130.16, 130.62, 131.52, 132.25, 136.74, 145.46, 158.47.

**$R_f$**  (EtOAc): 0.48, UV active and red discolourisation with cer reagent.

**mp:** decomposition.

**Diisopropyl-phosphoramidous acid 2-(6-{2-[bis-(4-methoxy-phenyl)-phenyl-methoxy]-ethoxy}-hexa-2*t*,4*t*-dienyloxy)-ethyl ester 2-cyano-ethyl ester (29)**

Synthesized according to general method F.

The crude was purified by LC (EtOAc).

**Yield:** 98 %, as a transparent oil.

**$^1H$ -NMR** ( $CDCl_3$ , 300 MHz): 1.15-1.18 (m, 12 H), 1.54 (s, 2 H), 2.61 (t, 2 H,  $J = 6.4$  Hz), 3.20 (t, 2 H,  $J = 5.1$  Hz), 3.55-3.63 (m, 6 H), 3.77 (s, 6 H), 3.73-3.87 (m, 2 H), 4.06 (t, 4 H,  $J = 6.0$  Hz), 5.71-5.78 (m, 2 H), 6.24-6.28 (m, 2 H), 6.77-6.82 (m, 4 H), 7.17-7.35 (m, 7 H), 7.45 (d, 2 H,  $J = 7.2$  Hz).

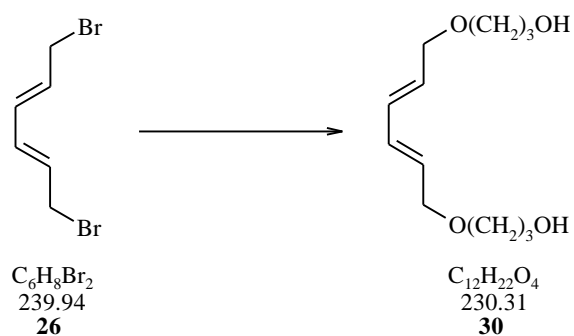
**$^{13}C$ -NMR** ( $CDCl_3$ , 75 MHz): 20.27, 24.52, 24.59, 24.62, 24.68, 42.98, 43.14, 55.21, 58.38, 58.63, 62.53, 62.78, 63.24, 69.68, 70.00, 70.09, 71.24, 71.32, 77.44, 113.03, 126.64, 127.74, 128.21, 129.72, 130.07, 130.30, 131.44, 132.03, 136.33, 145.07, 158.37.

**$^{31}P$ -NMR** ( $CDCl_3$ , 122 MHz): 148.78.

**HR-MS** (ESI<sup>+</sup>):  $C_{44}H_{60}N_2NaO_7P$ : calc.: 727.3488 g/mol, found: 727.3497 g/mol.

**$R_f$**  (EtOAc): 0.49, UV active and red discolourisation with cer reagent.



2.5.7 Synthesis of 32<sup>146-150</sup>3-[6-(3-Hydroxy-propoxy)-hexa-2*t*,4*t*-dienyloxy]-propan-1-ol (30)

Synthesized according to general method G.

The crude was purified by LC (EtOAc / MeOH, 19:1).

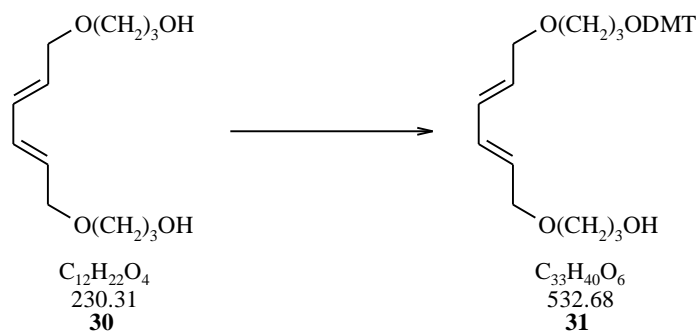
**Yield:** 24 %, as wet, transparent crystals.

**<sup>1</sup>H-NMR** (CDCl<sub>3</sub>, 300 MHz): 1.57-1.65 (m, 4 H), 2.39 (s br, 2 H), 3.43 (t, 4 H, *J* = 5.9 Hz), 3.61 (t, 4 H, 3.0 Hz), 3.98 (d, 4 H, *J* = 5.6 Hz), 5.68-5.77 (m, 2 H), 6.16-6.23 (m, 2 H).

**<sup>13</sup>C-NMR** (CDCl<sub>3</sub>, 75 MHz): 30.14, 62.78, 70.25, 71.01, 129.86, 131.97.

**R<sub>f</sub>** (EtOAc): 0.12, UV active, with permanganate reagent yellow and with cer reagent blue discolourisation.

**3-(6-{3-[Bis-(4-methoxy-phenyl)-phenyl-methoxy]-propoxy}-hexa-2*t*,4*t*-dienyloxy)-propan-1-ol (31)**



Synthesized according to general method E.

The crude was purified by LC (EtOAc / Hex, 2:3).

**Yield:** 59 %, as a transparent oil.

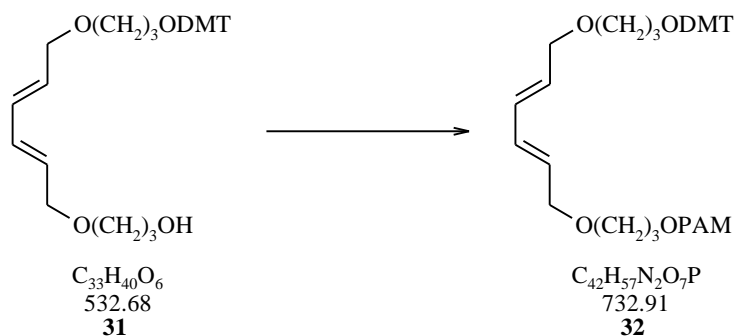
**<sup>1</sup>H-NMR** (CDCl<sub>3</sub>, 300 MHz): 1.80-1.87 (m, 4 H), 3.13 (t, 2 H, *J* = 5.9 Hz), 3.53-3.58 (m, 4 H), 3.76 (s, 6 H), 3.95-4.01 (m, 4 H), 4.07-4.14 (m, 2 H), 5.68-5.75 (m, 2 H), 6.18-6.23 (m, 2 H), 6.77-6.82 (m, 4 H), 7.18-7.31 (m, 7 H), 7.41 (d, 2 H, *J* = 7.0 Hz).

**<sup>13</sup>C-NMR** (CDCl<sub>3</sub>, 75 MHz): 14.34, 21.17, 30.60, 32.26, 55.33, 60.36, 60.52, 62.07, 67.74, 69.45, 71.05, 71.43, 85.89, 113.12, 126.71, 127.82, 128.33, 129.62, 130.16, 130.62, 131.52, 132.25, 136.74, 145.46, 158.47.

**R<sub>f</sub>** (EtOAc): 0.48, UV active and red discolourisation with cer reagent.

**mp:** decomposition.

**Diisopropyl-phosphoramidous acid 3-(6-{3-[bis-(4-methoxy-phenyl)-phenyl-methoxy]-propoxy}-hexa-2*t*,4*t*-dienyloxy)-propyl ester 2-cyano-ethyl ester (32)**



Synthesized according to general method F.

The crude was purified by LC (EtOAc).

**Yield:** 99 %, as a transparent glass.

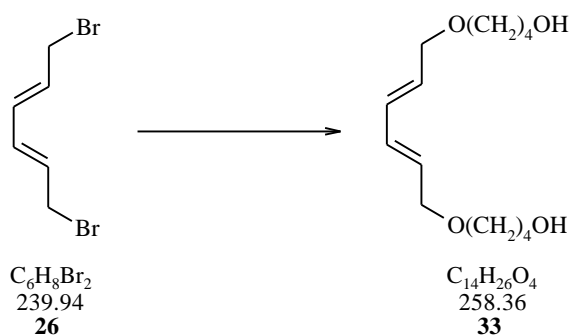
**<sup>1</sup>H-NMR** (CDCl<sub>3</sub>, 300 MHz): 1.09-1.19 (m, 16 H), 1.81-1.89 (m, 4 H), 2.58-2.63 (m, 2 H), 3.13 (t, 2 H, *J* = 6.2 Hz), 3.48-3.61 (m, 6 H), 3.71-3.85 (m, 2 H), 3.76 (s, 6 H), 3.97 (t, 2 H, *J* = 5.5 Hz), 5.67-5.76 (m, 2 H), 6.16-6.26 (m, 2 H), 6.77-6.83 (m, 4 H), 7.14-7.32 (m, 7 H), 7.41 (d, 2 H, *J* = 7.1 Hz).

**<sup>13</sup>C-NMR** (CDCl<sub>3</sub>, 300 MHz): 14.06, 20.31, 20.40, 22.99, 24.52, 24.61, 24.70, 30.44, 31.47, 31.57, 42.91, 43.08, 55.19, 58.19, 58.45, 60.22, 60.43, 60.66, 66.88, 67.60, 70.98, 71.05, 85.73, 112.97, 126.58, 127.69, 128.17, 130.01, 130.15, 131.60, 131.75, 136.57, 145.32, 158.31.

**<sup>31</sup>P-NMR** (CDCl<sub>3</sub>, 122 MHz): 147.72.

**HR-MS** (ESI<sup>+</sup>): C<sub>42</sub>H<sub>58</sub>N<sub>2</sub>O<sub>7</sub>P: calc.: 733.3981 g/mol, found: 733.3971 g/mol.

**R<sub>f</sub>** (EtOAc): 0.80, UV active and red discolourisation with cer reagent.

2.5.8 Synthesis of 35<sup>146-150</sup>4-[6-(4-Hydroxy-butoxy)-hexa-2*t*,4*t*-dienyloxy]-butan-1-ol (33)

Synthesized according to general method G.

The crude was purified by LC (EtOAc / MeOH, 9:1).

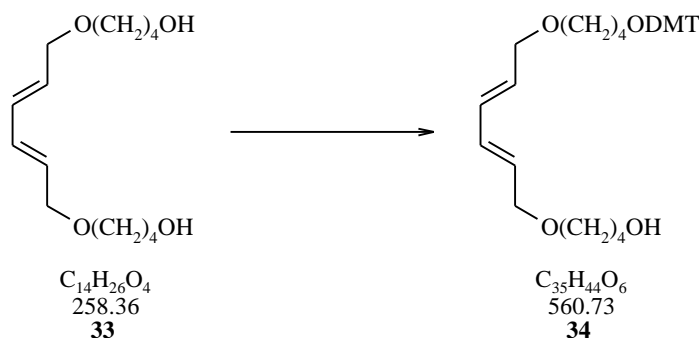
**Yield:** 17 %, as a yellowish oil.

**<sup>1</sup>H-NMR** (CDCl<sub>3</sub>, 300 MHz): 1.57-1.65 (m, 8 H), 2.39 (s br, 2 H), 3.43 (t, 4 H, *J* = 5.9 Hz), 3.61 (t, 4 H, 3.0 Hz), 3.98 (d, 4 H, *J* = 5.6 Hz), 5.68-5.77 (m, 2 H), 6.16-6.23 (m, 2 H).

**<sup>13</sup>C-NMR** (CDCl<sub>3</sub>, 75 MHz): 26.75, 30.14, 62.78, 70.25, 71.01, 129.86, 131.97.

**R<sub>f</sub>** (EtOAc / MeOH, 9:1): 0.40, UV active, with permanganate reagent yellow and with cer reagent blue discolourisation.

**4-(6-{4-[Bis-(4-methoxy-phenyl)-phenyl-methoxy]-butoxy}-hexa-2*t*,4*t*-dienyloxy)-butan-1-ol (34)**



Synthesized according to general method E.

The crude was purified by LC (EtOAc).

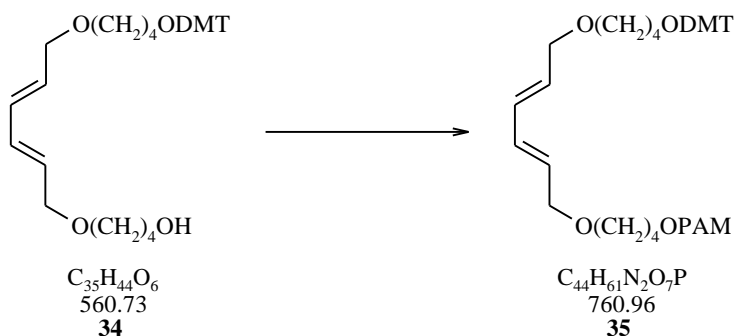
**Yield:** 37 %, as a beige solid.

**<sup>1</sup>H-NMR** (CDCl<sub>3</sub>, 300 MHz): 1.64 (s, 8 H), 3.04 (t, 2 H, *J* = 5.8 Hz), 3.37 (t, 2 H, *J* = 6.0 Hz), 3.45 (t, 2 H, *J* = 5.7 Hz), 3.60-3.77 (m, 2 H), 3.77 (s, 6 H), 3.98 (dd, 4 H, *J* = 5.9 and 15.5 Hz), 5.68-5.77 (m, 2 H), 6.15-6.26 (m, 2 H), 6.78-6.82 (m, 4 H), 7.15-7.32 (m, 7 H), 7.41 (d, 2 H, *J* = 7.1 Hz).

**<sup>13</sup>C-NMR** (CDCl<sub>3</sub>, 75 MHz): 26.71, 26.80, 30.25, 55.19, 62.78, 63.05, 70.22, 70.29, 70.89, 71.08, 112.95, 126.55, 127.68, 128.20, 129.54, 130.01, 130.45, 131.54, 132.15, 136.67, 145.36, 158.28.

**R<sub>f</sub>** (EtOAc): 0.44, UV active and red discolourisation with cer reagent.

**mp:** decomposition.

**Diisopropyl-phosphoramidous acid 4-(6-{4-[bis-(4-methoxy-phenyl)-phenyl-methoxy]-butoxy}-hexa-2*t*,4*t*-dienyloxy)-butyl ester 2-cyano-ethyl ester (35)**

Synthesized according to general method F.

The crude was purified by LC (EtOAc / Hex, 1:1).

**Yield:** 97 %, as a transparent oil.

**$^1H$ -NMR** ( $CDCl_3$ , 300 MHz): 1.14-1.17 (m, 14 H), 1.65 (t, 8 H,  $J = 3.0$  Hz), 2.61 (t, 2 H,  $J = 6.4$  Hz), 3.04 (t, 2 H,  $J = 5.8$  Hz), 3.35-3.44 (m, 4 H), 3.51-3.74 (m, 4 H), 3.77 (s, 6 H), 3.96 (t, 4 H,  $J = 6.8$  Hz), 5.68-5.77 (m, 2 H), 6.15-6.26 (m, 2H), 6.77-6.82 (m, 4 H), 7.15-7.32 (m, 7 H), 7.41 (d, 2 H,  $J = 12.2$  Hz).

**$^{13}C$ -NMR** ( $CDCl_3$ , 75 MHz): 20.32, 20.41, 24.52, 24.60, 24.70, 26.31, 26.72, 28.02, 42.90, 43.07, 55.19, 58.17, 58.42, 63.05, 69.95, 70.26, 70.94, 77.21, 112.95, 126.55, 127.67, 128.19, 130.01, 130.09, 130.15, 131.69, 136.66, 158.29.

**$^{31}P$ -NMR** ( $CDCl_3$ , 122 MHz): 147.45.

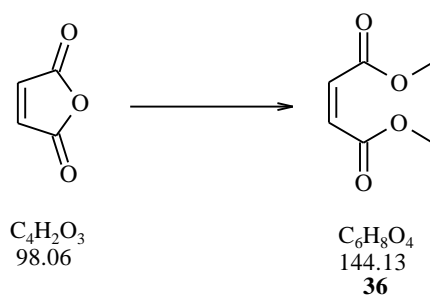
**HR-MS** (ESI+):  $C_{44}H_{62}N_2O_7P$ : calc.: 761.4294 g/mol, found: 761.4283 g/mol.

**$R_f$**  (EtOAc / Hex, 1:1): 0.67, UV active and red discolourisation with cer reagent.

## 2.6 Ene Phosphoramidites

### 2.6.1 Synthesis of 39<sup>151-153</sup>

#### Dimethyl maleate (cis-But-2-enedioic acid dimethyl ester) (36)



Synthesized according to general method C.

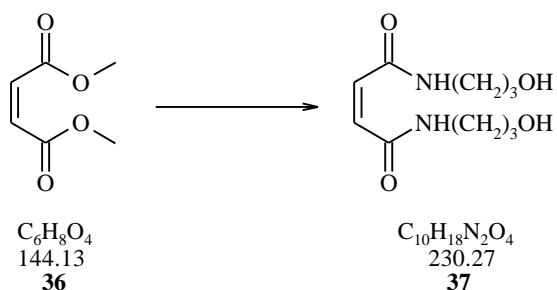
The crude was purified by LC (EtOAc).

**Yield:** 95 %, as a transparent oil.

**<sup>1</sup>H-NMR** (CDCl<sub>3</sub>, 300 MHz): 5.72 (s, 6 H), 8.19 (s, 2 H).

**<sup>13</sup>C-NMR** (CDCl<sub>3</sub>, 300 MHz): 52.01, 129.63, 165.51.

**R<sub>f</sub>** (EtOAc): 0.78, UV active.

**cis-But-2-enedioic acid bis-[(3-hydroxy-propyl)-amide] (37)**

Synthesized according to general method D.

The crude was purified by LC (EtOAc / MeOH, 1:1).

**Yield:** 65 %, as white foam which turns slightly red when stored at rt.

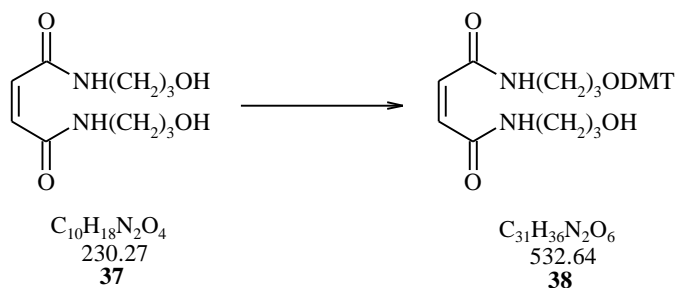
**$^1\text{H-NMR}$**  (MeOD, 300 MHz): 2.69 (t, 4 H,  $J = 4.0$  Hz), 3.20-3.28 (m, 4 H), 3.29-3.35 (m, 4 H), 6.83 (s, 2 H).

**$^{13}\text{C-NMR}$**  ( $\text{CD}_3\text{SOCD}_3$ , 75 MHz): 14.32, 30.06, 32.26, 32.38, 35.80, 36.54, 38.69, 57.75, 57.81, 58.36, 58.58, 78.71, 163.83, 169.15, 170.93.

**$R_f$**  (EtOAc / MeOH, 1:1): 0.37, UV active and yellow discolourisation with permanganate reagent.



**cis-But-2-enedioic acid {3-[bis-(4-methoxy-phenyl)-phenyl-methoxy]-propyl}-amide (3-hydroxy-propyl)-amide (38)**



Synthesized according to general method E.

The crude was purified by LC (EtOAc / Hex, 1:1).

**Yield:** 12 %, as a beige foam.

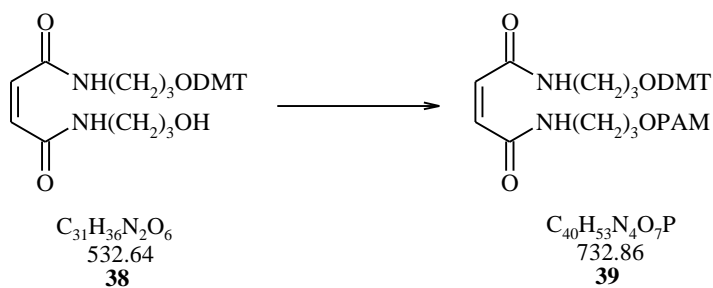
**<sup>1</sup>H-NMR** (CDCl<sub>3</sub>, 300 MHz): 2.69 (t, 4 H, *J* = 4.0 Hz), 3.20-3.28 (m, 4 H), 3.29-3.35 (m, 4 H), 6.83 (s, 2 H), 6.78-6.82 (m, 4 H), 7.15-7.32 (m, 7 H), 7.41 (d, 2 H, *J* = 7.1 Hz).

**<sup>13</sup>C-NMR** (CD<sub>3</sub>SOCD<sub>3</sub>, 75 MHz): 29.30, 29.57, 32.30, 32.49, 36.15, 36.32, 37.38, 38.21, 39.65, 39.70, 55.38, 58.59, 58.92, 59.26, 59.60, 61.56, 62.09, 77.58, 78.93, 113.32, 113.41, 126.89, 127.96, 128.02, 130.05, 130.16, 136.28, 145.10, 158.59, 169.27, 172.81.

**R<sub>f</sub>** (EtOAc/ Hex, 1:2): 0.47, UV active and red discolourisation with cer reagent.

**mp:** decomposition.

**Diisopropyl-phosphoramidous acid 3-(3-{3-[bis-(4-methoxy-phenyl)-phenyl-methoxy]-propylcarbamoyl}-(cis)acryloylamino-propyl ester 2-cyano-ethyl ester (39)**



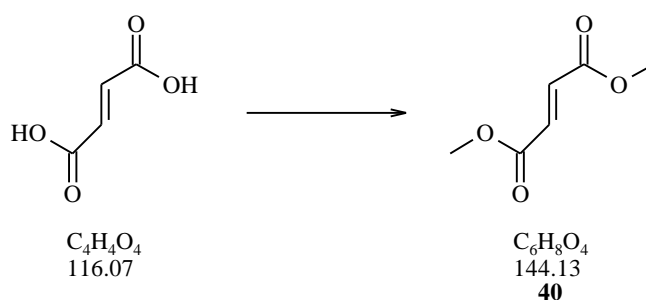
Synthesized according to general method F.

The crude was purified by LC (EtOAc / Hex, 1:1).

**Yield:** Product undergoes intramolecular maleimide formation.

2.6.2 Synthesis of 43<sup>150-154</sup>

## Dimethyl fumarate (t-But-2-enedioic acid dimethyl ester) (40)



Synthesized according to general method C.

The crude was purified by LC (EtOAc).

**Yield:** 100 %, as transparent crystals.

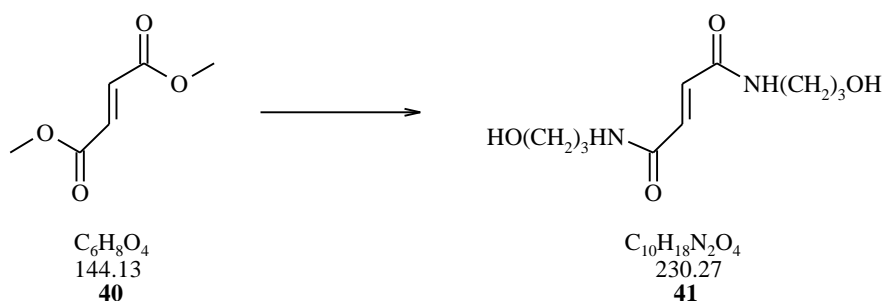
**<sup>1</sup>H-NMR** (CDCl<sub>3</sub>, 300 MHz): 3.79 (s, 6 H), 6.84 (s, 2 H).

**<sup>13</sup>C-NMR** (CD<sub>3</sub>SOCD<sub>3</sub>, 75 MHz): 52.29, 133.38, 165.35.

**R<sub>f</sub>** (EtOAc): 0.77, UV active.

**mp:** (EtOAc) 105 °C.

**t-But-2-enedioic acid bis-[(3-hydroxy-propyl)-amide] (41)**



Synthesized according to general method E.

The crude was purified by LC (EtOAc / MeOH, 2:1).

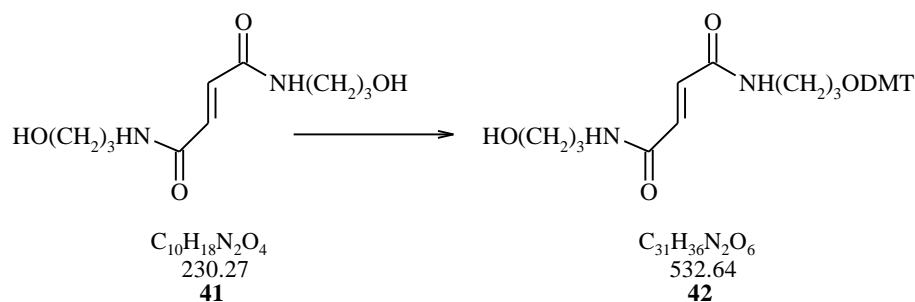
**Yield:** 74 %, as a transparent oil.

**<sup>1</sup>H-NMR** (CD<sub>3</sub>SOCD<sub>3</sub>, 300 MHz): 2.82 (t, 4 H, *J* = 7.0 Hz), 3.04-3.16 (m, 4 H), 3.44-3.49 (m, 4 H), 4.74-4.78 (m, 2 H).

**<sup>13</sup>C-NMR** (CD<sub>3</sub>SOCD<sub>3</sub>, 75 MHz): 14.32, 30.06, 32.26, 32.38, 35.80, 36.54, 38.69, 57.75, 57.81, 58.36, 58.58, 78.71, 163.83, 169.15, 170.93.

**R<sub>f</sub>** (EtOAc / MeOH, 2:1): 0.29, UV active and yellow discolourisation with permanganate reagent.

**t-But-2-enedioic acid {3-[bis-(4-methoxy-phenyl)-phenyl-methoxy]-propyl}-amide (3-hydroxy-propyl)-amide (42)**



Synthesized according to general method F.

The crude was purified by LC (EtOAc).

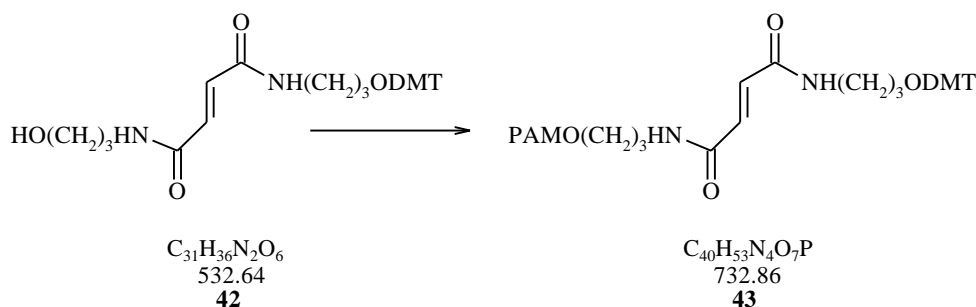
**Yield:** 45 %, as a yellowish foam.

**<sup>1</sup>H-NMR** (CDCl<sub>3</sub>, 300 MHz): 1.59-1.76 (m, 4 H), 3.07-3.14 (m, 2 H), 3.26-3.46 (m, 4 H), 3.52-3.58 (m, 2 H), 3.72 (s, 6 H), 6.76 (d, 4 H, *J* = 8.8 Hz), 7.14-7.25 (m, 7 H), 7.36 (d, 2 H, *J* = 7.0 Hz).

**<sup>13</sup>C-NMR** (CD<sub>3</sub>SOCD<sub>3</sub>, 75 MHz): 29.30, 29.57, 32.30, 32.49, 36.15, 36.32, 37.38, 38.21, 39.65, 39.70, 55.38, 58.59, 58.92, 59.26, 59.60, 61.56, 62.09, 77.58, 78.93, 113.32, 113.41, 126.89, 127.96, 128.02, 130.05, 130.16, 136.28, 145.10, 158.59, 169.27, 172.81.

**R<sub>f</sub>** (EtOAc): 0.53, UV active and red discolourisation with cer reagent.

**mp:** decomposition.

**Diisopropyl-phosphoramidous acid 3-(3-{3-[bis-(4-methoxy-phenyl)-phenyl-methoxy]-propylcarbamoyl}-(trans)acryloylamino-propyl ester 2-cyano-ethyl ester (43)**

Synthesized according to general method F.

The crude was purified by LC (EtOAc / Hex, 1:1).

**Yield:** 43 %, as a yellow foam.

**<sup>1</sup>H-NMR** (CDCl<sub>3</sub>, 300 MHz): 1.09-1.19 (m, 16 H), 1.81-1.89 (m, 4 H), 2.58-2.63 (m, 2 H), 3.13 (t, 2 H, *J* = 6.2 Hz), 3.48-3.61 (m, 6 H), 3.71-3.85 (m, 2 H), 3.76 (s, 6 H), 3.97 (t, 2 H, *J* = 5.5 Hz), 6.16-6.26 (m, 2 H), 6.77-6.83 (m, 4 H), 7.14-7.32 (m, 7 H), 7.41 (d, 2 H, *J* = 7.1 Hz).

**<sup>13</sup>C-NMR** (CDCl<sub>3</sub>, 75 MHz): 14.06, 20.31, 20.40, 22.99, 24.52, 24.61, 24.70, 30.44, 31.47, 31.57, 42.91, 43.08, 55.19, 58.19, 58.45, 60.22, 60.43, 66.88, 67.60, 70.98, 71.05, 85.73, 126.58, 127.69, 130.01, 130.15, 131.60, 131.75, 136.57, 145.32, 158.31.

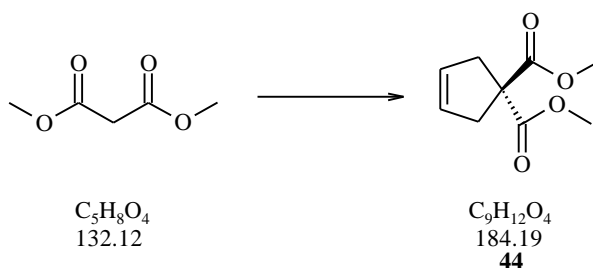
**<sup>31</sup>P-NMR** (CDCl<sub>3</sub>, 122 MHz): 148.65.

**R<sub>f</sub>** (EtOAc): 0.29, UV active and red discolourisation with cer reagent.

**mp:** decomposition.

### 2.6.3 Synthesis of **47**<sup>155</sup>

#### Cyclopent-3-ene-1,1-dicarboxylic acid dimethyl ester (**44**)



To a stirring solution of dimethylmalonate 10.56 g (9.18 ml, 80 mmol) in absolute DMF 150 ml, LiH 1.59 g (0.2 mol, 2.5 eq) was added slowly at 0°C under nitrogen atmosphere. After 2 hr at rt, one added cis-1,4-dichloro-2-buten 11.99 g (10.1 ml, 96 mmol, 1.2 eq) in absolute DMF. After 2 d stirring at rt, the beige suspension was diluted with Hex/tBME (200 ml, 4:1) and then poured on of ice-water 1 l. The organic layer was dried over sodium sulphate and evaporated under reduced pressure. Drying in the kugelrohr gave **44** as white crystals.

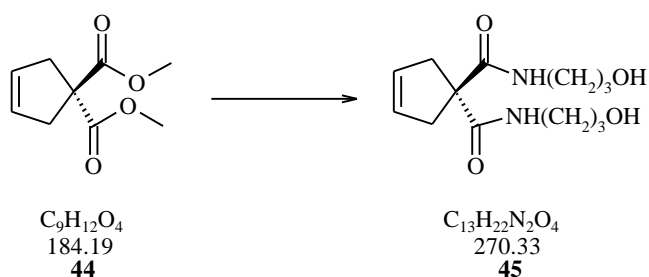
**Yield:** 10.7 g (58.4 mmol, 73 %).

<sup>1</sup>H-NMR (CDCl<sub>3</sub>, 300 MHz): 4.22 (s, 4 H), 3.73 (s, 6 H), 5.60 (s, 2 H).

<sup>13</sup>C-NMR (CDCl<sub>3</sub>, 300 MHz): 40.92, 52.82, 58.73, 127.78, 172.64.

**R<sub>f</sub>** (Hex/EtOAc, 11:1): 0.29, yellow discolourisation with permanganate reagent.

**mp:** (EtOAc) 61 °C.

**Cyclopent-3-ene-1,1-dicarboxylic acid bis-[(3-hydroxy-propyl)-amide] (45)**

Synthesized according to general method D.

The crude was purified by LC (EtOAc / MeOH, 1:1).

**Yield:** 98 %, as white solid.

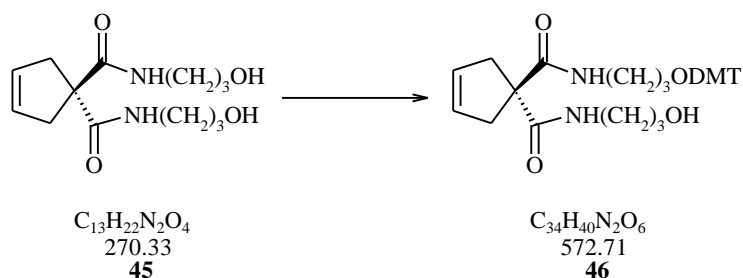
**<sup>1</sup>H-NMR** (CD<sub>3</sub>SOCD<sub>3</sub>, 300 MHz): 1.47-1.56 (m, 4 H), 3.02-3.13 (m, 4 H), 3.30-3.41 (m, 4 H), 4.45 (s br, 2 H), 5.56 (s, 2 H), 7.52 (t, 2 H, *J* = 5.9 Hz).

**<sup>13</sup>C-NMR** (CD<sub>3</sub>SOCD<sub>3</sub>, 75 MHz): 22.69, 32.14, 32.52, 35.83, 36.75, 58.53, 60.53, 128.41, 169.41, 172.14.

**R<sub>f</sub>** (EtOAc / MeOH, 1:1): 0.60, yellow discolourisation with permanganate reagent.



**Cyclopent-3-ene-1,1-dicarboxylic acid {3-[bis-(4-methoxy-phenyl)-phenyl-methoxy]-propyl}-amide (3-hydroxy-propyl)-amide (46)**



Synthesized according to general method E.

The crude was purified by LC (EtOAc).

**Yield:** 50 %, as a beige solid.

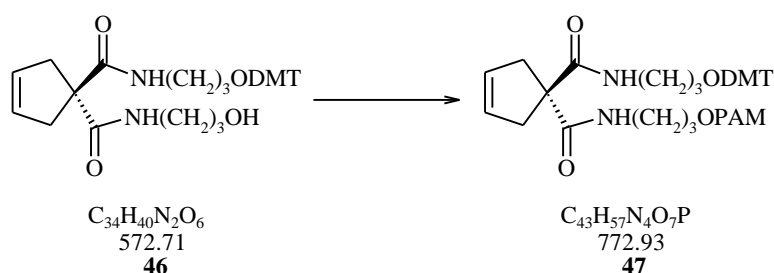
**$^1\text{H-NMR}$**  ( $\text{CDCl}_3$ , 300 MHz): 2.78-2.98 (m, 4 H), 3.22 (dt, 4 H,  $J = 26.5$  and  $5.9$  Hz), 3.31-3.41 (m, 6 H), 3.56 (t, 2 H,  $J = 5.1$  Hz), 3.80 (s, 6 H), 5.57 (s, 2 H), 6.81-6.87 (m, 4 H), 7.15-7.35 (m, 7 H), 7.41-7.42 (m, 2 H).

**$^{13}\text{C-NMR}$**  ( $\text{CDCl}_3$ , 75 MHz): 14.20, 21.06, 23.25, 28.99, 29.31, 32.15, 36.48, 38.08, 38.21, 41.79, 55.22, 59.20, 59.30, 60.41, 61.26, 62.14, 86.20, 113.10, 126.77, 127.84, 128.03, 129.94, 130.01, 136.04, 136.10, 144.89, 158.44, 169.89, 173.59, 174.29.

**$R_f$**  (EtOAc): 0.24, UV active and red discolourisation with cer reagent.

**mp:** decomposition.

**Diisopropyl-phosphoramidous acid 3- [ (1- {3- [bis- (4-methoxy-phenyl)-phenyl-methoxy]-propylcarbamoyl}-cyclopent-3-enecarbonyl)-amino]-propyl ester 2-cyanoethyl ester (47)**



Synthesized according to general method F.

The crude was purified by LC (EtOAc).

**Yield:** 59 %, as transparent viscous oil.

**$^1H$ -NMR** ( $CDCl_3$ , 300 MHz): 1.13-1.17 (m, 12 H), 1.19-1.30 (m, 2 H), 1.70-1.79 (m, 4 H), 2.63 t, 2H,  $J = 6.6$  Hz), 2.77-2.94 (m, 4 H), 3.09 (t, 2 H,  $J = 5.9$  Hz), 3.27-3.37 (m, 4 H), 3.50-3.67 (m, 4 H), 3.77 (s, 6 H), 5.55 (s, 2 H), 6.80 (d, 4 H,  $J = 8.8$  Hz), 7.16-7.29 (m, 7 H), 7.39 (d, 2 H,  $J = 7.0$  Hz).

**$^{13}C$ -NMR** ( $CDCl_3$ , 75 MHz): 20.46, 20.55, 24.73, 24.82, 29.59, 30.67, 30.77, 37.46, 38.09, 41.63, 41.81, 43.11, 43.27, 55.34, 58.39, 58.65, 59.65, 61.33, 61.38, 61.62, 113.23, 126.86, 127.94, 128.26, 128.67, 128.71, 130.14, 136.32, 145.09, 158.58, 173.23.

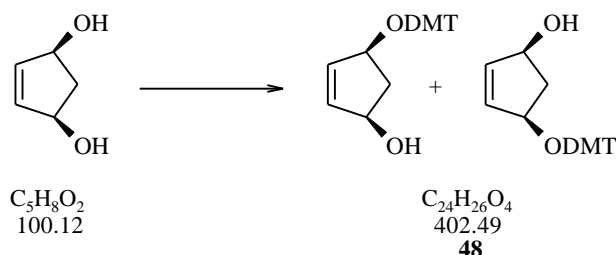
**$^{31}P$ -NMR** ( $CDCl_3$ , 122 MHz): 147.88.

**$R_f$**  (EtOAc): 0.63, UV active and red discolourisation with cer reagent.

**mp:** decomposition.

### 2.6.4 Synthesis of 49

#### 4-[Bis-(4-methoxy-phenyl)-phenyl-methoxy]-cyclopent-2-enol (48)



Synthesized according to general method E.

The crude was purified by LC (EtOAc / Hex, 1:1).

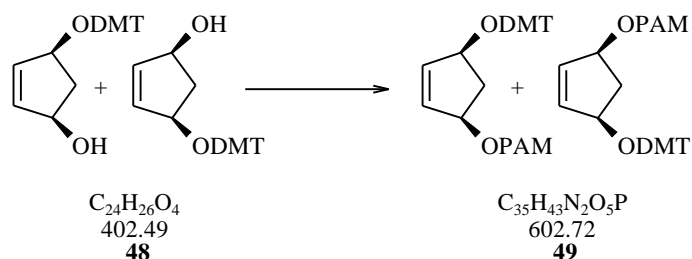
**Yield:** 71 %, as a white foam.

**$^1H$ -NMR** ( $CDCl_3$ , 300 MHz): 3.77 (s, 6 H), 4.07-4.14 (m, 2 H), 5.18 (d, 1 H,  $J = 5.5$  Hz), 5.77 (d, 1 H,  $J = 5.5$  Hz), 6.82 (d, 4 H,  $J = 8.5$  Hz), 7.17-7.30 (m, 3 H), 7.38 (d, 4 H,  $J = 8.8$  Hz), 7.49 (d, 2 H,  $J = 7.4$  Hz).

**$^{13}C$ -NMR** ( $CDCl_3$ , 75 MHz): 14.52, 43.26, 55.53, 74.93, 77.80, 87.06, 113.48, 124.08, 127.04, 128.18, 128.51, 130.45, 136.00, 136.27, 137.35, 146.04, 150.04, 158.80.

**$R_f$**  (EtOAc / Hex, 1:1): 0.35, UV active and red discolourisation with cer reagent.

**mp:** decomposition.

**Diisopropyl-phosphoramidous acid 4-[bis-(4-methoxy-phenyl)-phenyl-methoxy]-cyclopent-2-enyl ester 2-cyano-ethyl ester (49)**

Synthesized according to general method F.

The crude was purified by LC (EtOAc).

**Yield:** 96 %, as a yellowish resin like solid.

**<sup>1</sup>H-NMR** (CDCl<sub>3</sub>, 300 MHz): 1.12-1.19 (m, 12 H), 1.20-1.30 (m, 2 H), 1.56-1.74 (m, 2 H), 3.45-3.66 (m, 4 H), 3.80 (m, 6 H), 4.40-4.44 (m, 1 H), 4.48-4.45 (m, 1 H), 5.05-5.22 (m, 1 H), 5.74 (dd, 1 H, *J* = 5.5 and 25.7 Hz), 6.81-6.85 (m, 4 H), 7.20-7.42 (m, 7 H), 7.51 (d, 2 H, *J* = 8.5 Hz).

**<sup>13</sup>C-NMR** (CDCl<sub>3</sub>, 75 MHz): 20.21, 20.29, 20.44, 20.53, 23.06, 23.11, 23.14, 24.52, 24.59, 24.84, 41.87, 41.93, 42.13, 43.16, 43.33, 45.43, 45.52, 55.34, 55.37, 58.25, 58.31, 58.37, 58.54, 58.62, 75.42, 75.66, 75.74, 113.27, 126.82, 127.94, 128.42, 130.31, 134.49, 134.56, 134.65, 134.71, 135.76, 135.83, 137.26, 145.94, 158.63.

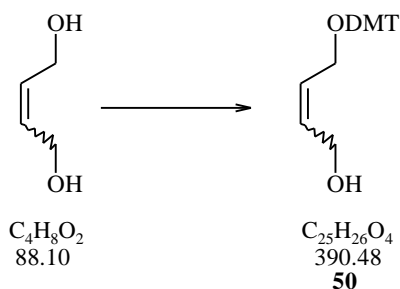
**<sup>31</sup>P-NMR** (CDCl<sub>3</sub>, 122 MHz): 148.20.

**R<sub>f</sub>** (EtOAc): 0.79, UV active and red discolourisation with cer reagent.

**mp:** decomposition.

### 2.6.5 Synthesis of 51

#### 4-[Bis-(4-methoxy-phenyl)-phenyl-methoxy]-but-2-en-1-ol (50)



Synthesized according to general method E.

The crude was purified by LC (EtOAc / Hex, 1:1).

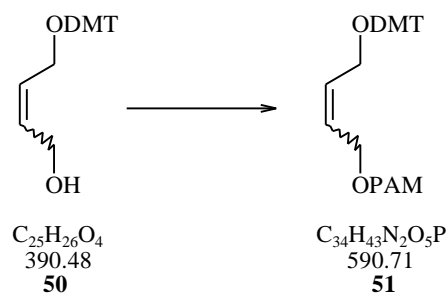
**Yield:** 68 %, as a transparent oil.

**$^1\text{H-NMR}$**  ( $\text{CDCl}_3$ , 300 MHz): 3.66-3.68 (m, 2 H), 3.77 (s, 6 H), 4.02 (m, 2 H), 5.67-5.80 (m, 2 H), 6.82 (d, 4 H,  $J = 8.8$  Hz), 7.17-7.34 (m, 7 H), 7.43 (d, 2 H,  $J = 7.4$  Hz).

**$^{13}\text{C-NMR}$**  ( $\text{CDCl}_3$ , 75 MHz): 55.33, 58.93, 60.14, 86.65, 113.25, 123.88, 126.89, 127.97, 128.19, 129.10, 130.08, 131.17, 136.16, 136.26, 145.01, 149.87, 158.56.

**$R_f$**  (EtOAc / Hex, 1:1): 0.41, UV active and red discolourisation with cer reagent.

**mp:** decomposition.

**Diisopropyl-phosphoramidous acid 4-[bis-(4-methoxy-phenyl)-phenyl-methoxy]-but-2-enyl ester 2-cyano-ethyl ester (51)**

Synthesized according to general method F.

The crude was purified by LC (EtOAc).

**Yield:** 96 %, as a transparent oil.

**$^1H$ -NMR** ( $CDCl_3$ , 300 MHz): 1.05-1.23 (m, 14 H), 2.55 (t, 2 H,  $J = 6.2$  Hz), 2.73 (t, 6.2 Hz), 3.77 (s, 6 H), 3.95-4.24 (m, 4 H), 5.61-5.78 (m, 2 H), 6.80 (d, 4 H,  $J = 8.8$  Hz), 7.15-7.33 (m, 7 H), 7.41 (d, 2 H,  $J = 7.0$  Hz).

**$^{13}C$ -NMR** ( $CDCl_3$ , 75 MHz): 20.21, 20.29, 20.38, 20.46, 23.03, 23.06, 23.14, 24.61, 24.69, 24.81, 43.09, 43.26, 45.43, 45.51, 55.35, 58.25, 58.32, 58.50, 58.75, 59.60, 59.84, 60.38, 76.74, 113.25, 126.84, 127.94, 128.28, 129.14, 129.18, 129.24, 130.14, 136.39, 145.11, 158.58.

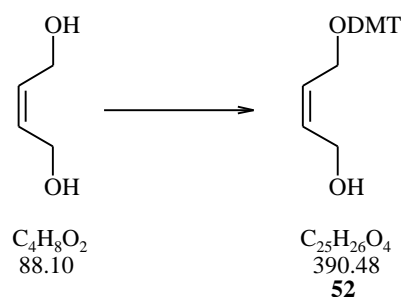
**$^{31}P$ -NMR** ( $CDCl_3$ , 122 MHz): 148.40.

**$R_f$**  (EtOAc): 0.65, UV active and red discolourisation with cer reagent.

**mp:** decomposition.

### 2.6.6 Synthesis of 53

#### 4-[Bis-(4-methoxy-phenyl)-phenyl-methoxy]-but-2(cis)-en-1-ol (52)



Synthesized according to general method E.

The crude was purified by LC (EtOAc / Hex, 2:3).

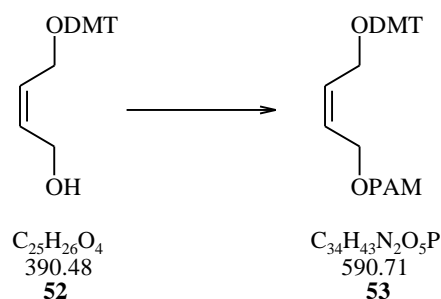
**Yield:** 72 %, as a transparent oil.

**$^1H$ -NMR** ( $CD_3SOCD_3$ , 300 MHz): 3.54 (d, 2 H,  $J = 3.7$  Hz), 3.73 (s, 6 H), 3.80 (t, 2 H,  $J = 4.4$  Hz), 5.58 (t, 2 H,  $J = 4.0$  Hz), 6.89 (d, 4 H,  $J = 8.8$  Hz), 7.19-7.40 (m, 9 H).

**$^{13}C$ -NMR** ( $CD_3SOCD_3$ , 75 MHz): 55.10, 57.10, 59.68, 85.73, 113.27, 126.49, 126.74, 127.69, 127.94, 129.66, 132.73, 135.82, 145.02, 158.11.

**$R_f$**  (EtOAc / Hex, 2:3): 0.49, UV active and red discolourisation with cer reagent.

**mp:** decomposition.

**Diisopropyl-phosphoramidous acid 4-[bis-(4-methoxy-phenyl)-phenyl-methoxy]-but-2(cis)-enyl ester 2-cyano-ethyl ester (53)**

Synthesized according to general method F.

The crude was purified by LC (EtOAc).

**Yield:** 97 %, as a transparent oil.

**$^1H$ -NMR** ( $CDCl_3$ , 300 MHz): 1.06-1.30 (m, 14 H), 2.55 (t, 2 H,  $J = 6.6$ ), 3.4-3.59 (m, 4 H), 3.64 (d, 2 H,  $J = 5.9$  Hz), 3.75 (s, 6 H), 3.77-3.82 (m, 4 H), 5.61-5.79 (m, 2 H), 6.80 (d, 4 H,  $J = 8.8$  Hz), 7.16-7.31 (m, 7 H), 7.41 (d, 2 H,  $J = 7.4$  Hz).

**$^{13}C$ -NMR** ( $CDCl_3$ , 75 MHz): 20.24, 20.33, 24.47, 24.57, 24.68, 42.97, 43.13, 55.21, 58.36, 58.62, 59.46, 59.71, 60.25, 86.33, 113.11, 117.56, 126.72, 127.82, 128.15, 129.01, 129.06, 129.11, 130.00, 136.27, 144.98, 158.45.

**$^{31}P$ -NMR** ( $CDCl_3$ , 122 MHz): 148.40.

**HR-MS** (ESI<sup>+</sup>):  $C_{34}H_{43}N_2O_5NaP$ : calc.: 613.2807 g/mol, found: 613.2810 g/mol.

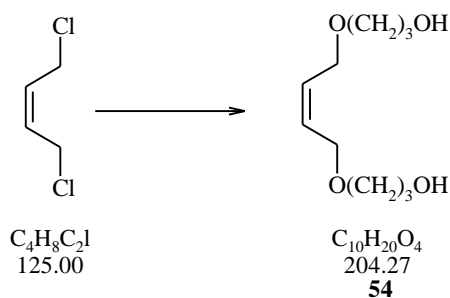
**$R_f$**  (EtOAc): 0.88, UV active and red discolourisation with cer reagent.

**mp:** decomposition.



### 2.6.7 Synthesis of 56<sup>156-160</sup>

#### 3-[4-(3-Hydroxy-propoxy)-but-2(cis)-enyloxy]-propan-1-ol (54)



Synthesized according to general method G.

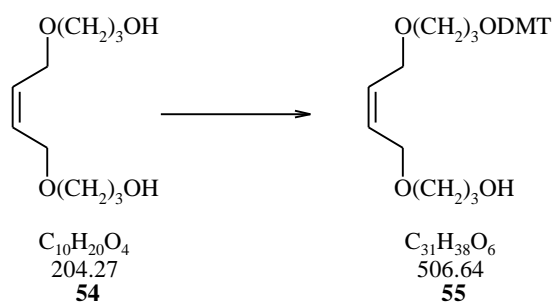
The crude was purified by LC (EtOAc / MeOH, 9:1).

**Yield:** 63 %, as a transparent oil.

<sup>1</sup>H-NMR (CDCl<sub>3</sub>, 300 MHz): 1.77-1.85 (m, 4 H), 2.49 (s br, 2 H), 3.59 (t, 4 H, *J* = 5.9 Hz), 3.74 (t, 4 H, *J* = 5.5 Hz), 4.03 (d, 4 H, *J* = 4.8 Hz), 5.70 (t, 2 H, *J* = 2.9 Hz).

<sup>13</sup>C-NMR (CDCl<sub>3</sub>, 75 MHz): 32.13, 61.41, 66.65, 69.19, 129.39.

**R<sub>f</sub>** (EtOAc / MeOH, 9:1): 0.47, yellow discolourisation with permanganate reagent.

**3-(4-{3-[Bis-(4-methoxy-phenyl)-phenyl-methoxy]-propoxy}-but-2(cis)-enyloxy)-propan-1-ol (55)**

Synthesized according to general method E.

The crude was purified by LC (EtOAc).

**Yield:** 48 %, as a transparent glass.

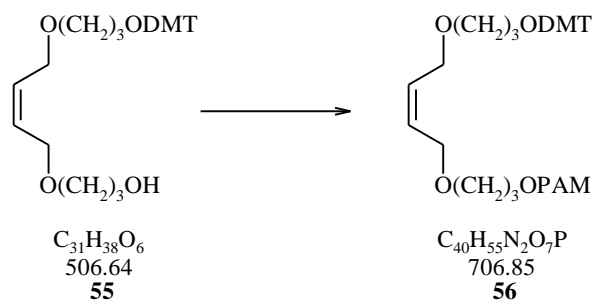
**<sup>1</sup>H-NMR** (CDCl<sub>3</sub>, 300 MHz): 1.76-1.90 (m, 4 H), 2.26 (t, 2 H, *J* = 5.2 Hz), 3.13 (t, 2 H, *J* = 6.2 Hz), 3.53-3.59 (m, 4 H), 3.77 (s, 6 H), 4.01 (t, 4 H, *J* = 5.2 Hz), 5.65-5.68 (m, 2 H), 6.78-6.83 (m, 4 H), 7.16-7.26 (m, 7 H), 7.41 (d, 2 H, *J* = 7.0 Hz).

**<sup>13</sup>C-NMR** (CDCl<sub>3</sub>, 75 MHz): 30.43, 32.08, 55.21, 60.23, 61.90, 66.57, 67.82, 69.44, 76.61, 85.74, 112.97, 126.61, 127.71, 128.15, 128.88, 129.75, 130.01, 136.54, 145.27, 158.31.

**R<sub>f</sub>** (EtOAc): 0.48, UV active and red discolourisation with cer reagent.

**mp:** decomposition.

**Diisopropyl-phosphoramidous acid 3-(4-{3-[bis-(4-methoxy-phenyl)-phenyl-methoxy]-propoxy}-but-2(cis)-enyloxy)propyl ester 2-cyano-ethyl ester (56)**



Synthesized according to general method F.

The crude was purified by LC (EtOAc).

**Yield:** 84 %, as a white solid.

**<sup>1</sup>H-NMR** (CDCl<sub>3</sub>, 300 MHz): 0.16-1.15 m, 14 H), 1.87 (t, 4 H,  $J = 6.3$  Hz), 2.61 (t, 2 H,  $J = 6.2$  Hz), 3.48-3.61 (m, 6 H), 3.77 (s, 6 H), 4.02 (d, 4 H,  $J = 4.4$  Hz), 5.67 (s br, 2 H), 6.80-6.86 (m, 4 H), 7.25-7.33 (m, 7 H, 7.43 (d, 2 H, 7.0 Hz).

**<sup>13</sup>C-NMR** (CDCl<sub>3</sub>, 75 MHz): 20.44, 20.53, 24.66, 24.75, 24.83, 29.84, 30.59, 31.61, 31.71, 55.33, 58.33, 58.58, 60.40, 66.79, 67.16, 67.90, 76.74, 85.89, 113.11, 126.73, 127.83, 128.32, 129.30, 129.58, 130.15, 136.71, 145.44, 158.47.

**<sup>31</sup>P-NMR** (CDCl<sub>3</sub>, 122 MHz): 148.78.

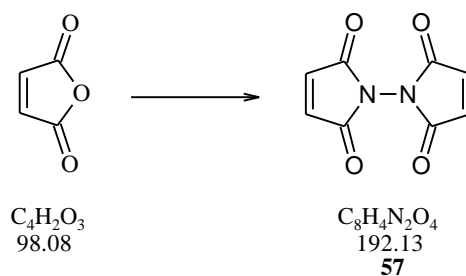
**R<sub>f</sub>** (EtOAc): 0.76, UV active and red discolourisation with cer reagent.

**mp:** decomposition.

## 2.7 Dimaleimides

### 2.7.1 Synthesis of 57<sup>161-167</sup>

#### [1,1']Bipyrrolyl-2,5,2',5'-tetraone (57)



Synthesized according to general method H.

The crude was purified by LC (EtOAc / Hex, 1:1).

**Yield:** 60 %, as a yellow solid.

**<sup>1</sup>H-NMR** (CDCl<sub>3</sub>, 300 MHz): 6.93 (s, 4 H).

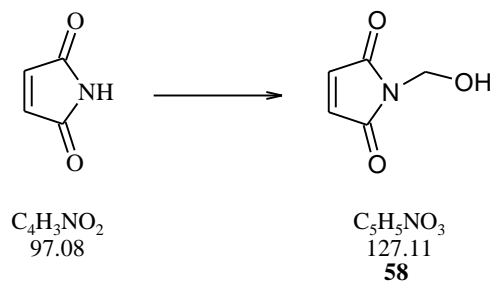
**<sup>13</sup>C-NMR** (CDCl<sub>3</sub>, 75 MHz): 133.82, 164.99.

**R<sub>f</sub>** (EtOAc): 0.54 UV active and yellow discolourisation with permanganate reagent.

**mp:** EtOAc)178 °C.

2.7.2 Synthesis of 59<sup>168-170</sup>

## 1-Hydroxymethyl-pyrrole-2,5-dione (58)



In NaOH (2.0 ml, 4.0 mM) we dissolved maleimide (200 mg, 2.0 mmol) and paraformaldehyde (100 mg, 3.3 mmol, 1.7 eq). After stirring for 3 h at 80 °C the reaction mixture was poured into water and extracted with EtOAc. The concentrated crude product was then purified by LC (EtOAc / Hex, 1:2).

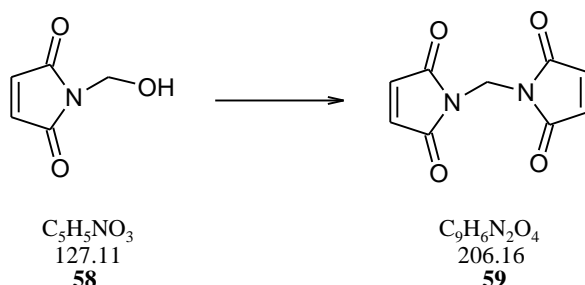
**Yield:** 196 mg (1.54 mmol, 77 %), as a white solid.

**<sup>1</sup>H-NMR** (CDCl<sub>3</sub>, 300 MHz): 3.07 (s br, 1 H), 5.07 (d, 2 H, *J* = 7.2 Hz), 6.75 (s, 2 H).

**<sup>13</sup>C-NMR** (CDCl<sub>3</sub>, 300 MHz): 61.14, 134.64, 170.09.

**R<sub>f</sub>** (EtOAc/Hex, 1:2): 0.2, UV active and yellow discolouration with permanganate reagent.

**mp:** EtOAc) 106 °C.

**N,N'-Methylenedimaleimide (59)**

In 10 ml absolute  $CH_2Cl_2$  we dissolved 140 mg (1.1 mmol) 1-hydroxymethyl-pyrrole-2,5-dione 140 mg (1.1 mmol) and 160 mg (1.65 mmol, 1.5 eq) maleimide 160 mg (1.65 mmol, 1.5 eq). We added  $BF_3 \cdot EtOEt$  250  $\mu l$  (1.0 mmol, 1 eq), diluted in absolute  $CH_2Cl_2$  2 ml and stirred for 4 h at 40 °C with a reflux condenser. The reaction mixture was then poured into water and extracted with EtOAc. The solvent was evaporated under reduced pressure and the crude was purified by LC (EtOAc).

**Yield:** 147 mg (0.72 mmol, 65 %), as a white solid.

**$^1H$ -NMR** ( $CDCl_3$ , 300 MHz): 3.73(s, 4 H), 6.73 (s, 2 H).

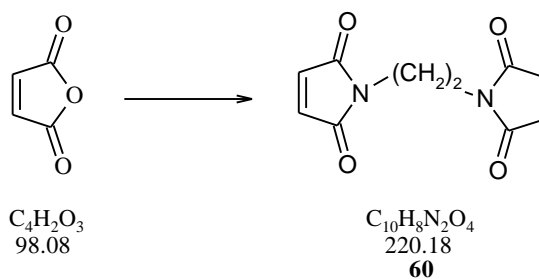
**$^{13}C$ -NMR** ( $CDCl_3$ , 75 MHz): 42.75, 134.17, 170.48.

**$R_f$**  (EtOAc): 0.65, UV active and yellow discolourisation with permanganate reagent.

**mp:** (EtOAc) 171 °C.

### 2.7.3 Synthesis of **60**<sup>171-172</sup>

#### N,N'-Ethylenedimaleimide (**60**)



Synthesized according to general method H.

The crude was purified by LC (EtOAc / Hex, 1:1).

**Yield:** 15 %, as a white solid.

**<sup>1</sup>H-NMR** (CDCl<sub>3</sub>, 300 MHz): 3.73(s, 4 H), 6.68 (s, 4 H).

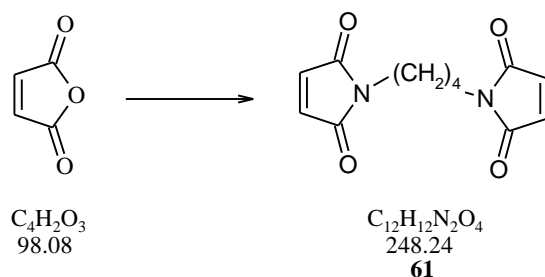
**<sup>13</sup>C-NMR** (CDCl<sub>3</sub>, 75 MHz): 36.50, 134.17, 170.48.

**R<sub>f</sub>** (EtOAc):0.60, UV active and yellow discolourisation with permanganate reagent.

**mp:** (EtOAc) 196 °C.

### 2.7.4 Synthesis of **61**<sup>173</sup>

#### N,N'-Tetramethylenedimaleimide (**61**)



Synthesized according to general method H.

The crude was purified by LC (EtOAc / Hex, 1:1).

**Yield:** 51 %, as a white solid.

**<sup>1</sup>H-NMR** (CDCl<sub>3</sub>, 300 MHz): 1.53-1.58 (m, 4 H), 3.47-3.54 (m, 4 H), 6.66 (s, 4 H).

**<sup>13</sup>C-NMR** (CDCl<sub>3</sub>, 300 MHz): 25.76, 37.17, 134.10, 170.74.

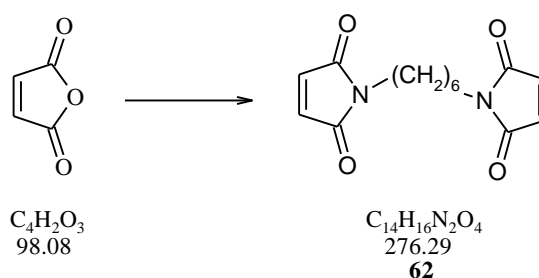
**R<sub>f</sub>** (EtOAc): 0.58, UV active and yellow discolourisation with permanganate reagent.

**mp:** (EtOAc) 206 °C.



### 2.7.5 Synthesis of **62**<sup>173</sup>

#### N,N'-Hexamethylenedimaleimide (**61**)



Synthesized according to general method H.

The crude was purified by LC (EtOAc / Hex, 1:1).

**Yield:** 60 %, as a white solid.

**<sup>1</sup>H-NMR** (CDCl<sub>3</sub>, 300 MHz): 1.20-1.29 (m, 4 H), 1.50-1.59 (m, 4 H), 3.47 (t, 4 H,  $J = 7.3$  Hz), 6.065 (s, 4 H).

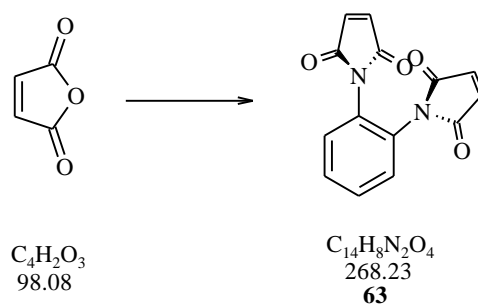
**<sup>13</sup>C-NMR** (CDCl<sub>3</sub>, 300 MHz): 26.15, 28.32, 37.67, 134.03, 170.84.

**R<sub>f</sub>** (EtOAc): 0.3, UV active and yellow discolourisation with permanganate reagent.

**mp:** (EtOAc) 144 °C.

### 2.7.6 Synthesis of **63**<sup>175-176</sup>

#### **N,N'-o-Phenylenedimaleimide (63)**



Synthesized according to general method H.

The crude was purified by LC (EtOAc).

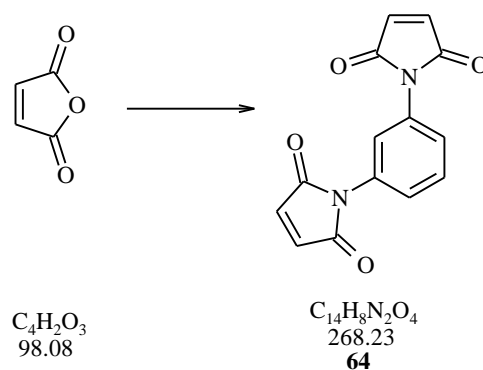
**Yield:** 23 %, as a white solid.

**<sup>1</sup>H-NMR** (CD<sub>3</sub>SOCD<sub>3</sub>, 300 MHz): 7.14 (s, 4 H), 7.46 (m, 2 H), 7.59 (m, 2 H).

**<sup>13</sup>C-NMR** (CD<sub>3</sub>SOCD<sub>3</sub>, 75 MHz): 128.41, 128.99, 129.60, 134.73, 168.69.

**R<sub>f</sub>** (EtOAc): 0.56, UV active and yellow discolourisation with permanganate reagent.

**mp:** (CH<sub>3</sub>CN) 243 °C.

**2.7.7 Synthesis of 64**<sup>177-178</sup>**N,N'-m-Phenylenedimaleimide (64)**

Synthesized according to general method H.

The crude was purified by LC (EtOAc).

**Yield:** 32 %, as a yellow solid.

**<sup>1</sup>H-NMR** (CD<sub>3</sub>SOCD<sub>3</sub>, 300 MHz): 7.20 (s, 4 H), 7.38 (m, 1 H), 7.40 (m, 2 H), 7.62 (m, 2 H).

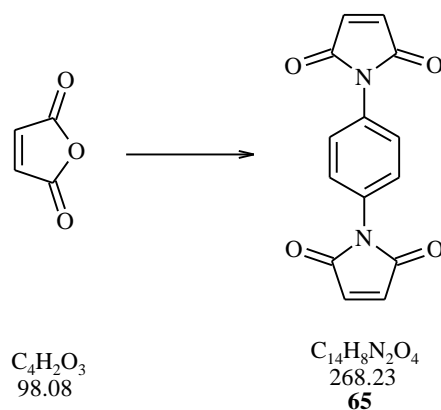
**<sup>13</sup>C-NMR** (CD<sub>3</sub>SOCD<sub>3</sub>, 75 MHz): 124.70, 125.92, 129.14, 131.98, 134.64, 169.57.

**R<sub>f</sub>** (EtOAc): 0.64, UV active and yellow discolourisation with permanganate reagent.

**mp:** ( Et OAc) 204 °C.

### 2.7.8 Synthesis of 65

#### N,N'-p-Phenylenedimaleimide (65)



Synthesized according to general method H.

The crude was purified by LC (EtOAc).

**Yield:** 37 %, as a yellow solid.

**$^1H$ -NMR** ( $CD_3SOCD_3$ , 300 MHz): 7.14 (s, 4 H), 7.46 (m, 2 H), 7.59 (m, 2 H).

**$^{13}C$ -NMR** ( $CD_3SOCD_3$ , 75 MHz): 127.36, 129.34, 134.67, 169.59.

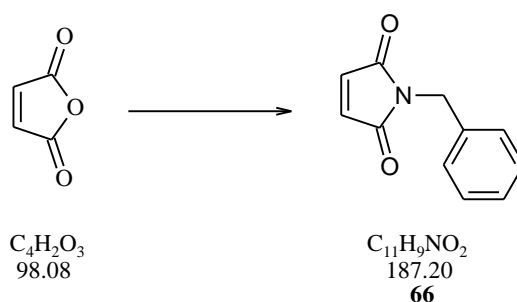
**R<sub>f</sub>** (EtOAc): 0.62, UV active and yellow discolourisation with permanganate reagent.

**mp:** (EtOAc) 346 °C.

## 2.8 Maleimides

### 2.8.1 Synthesis of **66**<sup>177-182</sup>

#### N-Benzylmaleimide (**66**)



Synthesized according to general method H.

The crude was purified by LC ( $CH_2Cl_2$ ).

**Yield:** 62 %, as transparent crystals.

<sup>1</sup>H-NMR ( $CDCl_3$ , 300 MHz): 4.66 (s, 2 H), 6.68 (s, 2 H), 7.23-7.34 (m, 5 H).

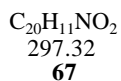
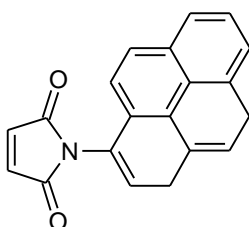
<sup>13</sup>C-NMR ( $CDCl_3$ , 300 MHz): 41.56, 76.74, 128.00, 128.53, 128.83, 134.34, 136.31, 170.55.

**R<sub>f</sub>** ( $CH_2Cl_2$ ): 0.54, yellow discolourisation with permanganate reagent.

**mp:** (EtOAc) 95 °C.

### 2.8.2 Synthesis of 67

#### N-(1-Pyrenyl)maleimide (67)



From Fluka.

**$^1H$ -NMR** ( $CD_3SOCD_3$ , 75 MHz): 7.05 (s, 2 H), 7.70-7.90 (m, 2 H), 8.00-8.32 (m, 7 H).

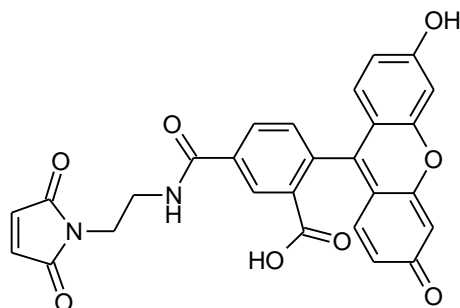
**$^{13}C$ -NMR** ( $CD_3SOCD_3$ , 75 MHz): 122.2, 123.5, 124.3, 125.2, 125.5, 126.0, 126.2, 126.9, 127.2, 127.3, 128.3, 128.4, 128.7, 130.3, 130.6, 131.3, 135.2, 170.9.

**$R_f$**  (EtOAc): 0.64, UV active and yellow discolourisation with permanganate reagent.

**mp:** (MeOH) 239 °C.

### 2.8.3 Synthesis of 68

*N*-[2-(2,5-Dioxo-2,5-dihydro-pyrrol-1-yl)-ethyl]-6-(6-hydroxy-3-oxo-3*H*-xanthen-9-yl)-isophthalamic acid (**68**)



$C_{27}H_{18}N_2O_8$   
498.40  
**68**

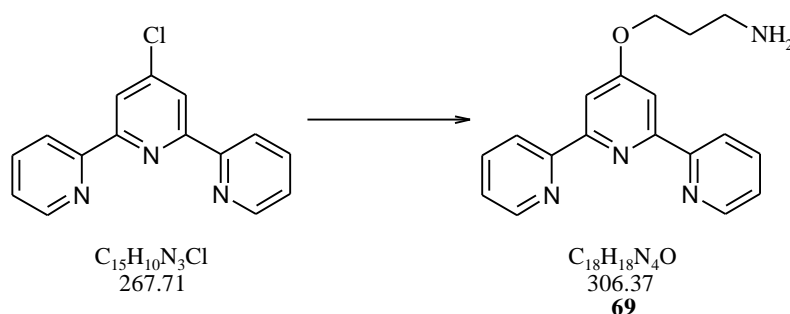
From Vector Laboratories (USA).

$\lambda_{em}$  520 nm

$\lambda_{ex}$  492 nm

## 2.8.4 Synthesis of 70

## 3-([2,2';6',2'']Terpyridin-4'-yloxy)-propylamine (69)



In 10 ml absolute DMSO we dissolved 63 mg (1.13 mmol, 1.2 eq) KOH, and 75  $\mu$ l (1.0 mmol, 1.1 eq) 3-amino-1-propanol. After stirring for 1 h at rt, we added 250 mg (0.93 mmol, 1 eq) 4-chloroterpyridine. The reaction mixture was heated for 1 h to 50 °C and then the solvent was evaporated under reduced pressure. The crude was extracted with  $CH_2Cl_2$  from water, dried over  $Na_2SO_4$  and solvent was evaporated. The product was used without further purification for the next step.

**Yield:** 171 mg (0.56 mmol, 60 %), as a beige solid.

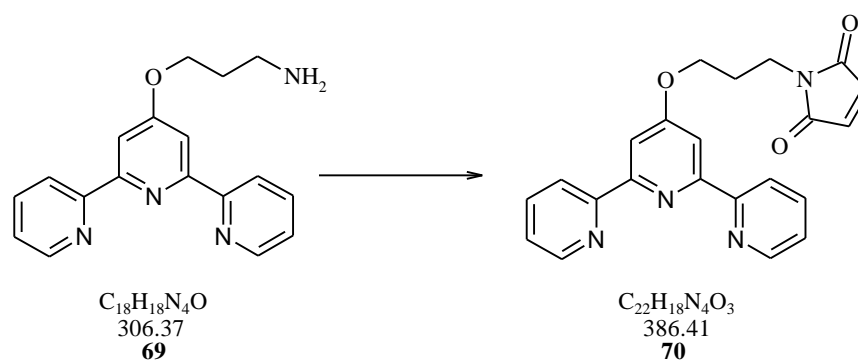
**$^1H$ -NMR** ( $CDCl_3$ , 300 MHz): 1.96-2.01 (m, 2 H), 2.91-2.96 (m, 2 H), 4.28-4.32 (t, 2 H,  $J = 6.2$  Hz), 7.24-7.32 (m, 2 H), 7.78-7.84 (m, 2 H), 7.98 (s, 2 H), 8.56-8.66 (m, 4 H).

**$^{13}C$ -NMR** ( $CDCl_3$ , 300 MHz): 32.86, 39.14, 66.19, 107.36, 121.15, 121.34, 121.39, 123.81, 124.28, 136.79, 149.03, 155.03, 156.12, 156.75, 157.09, 167.19.

**$R_f$**  (EtOAc/MeOH, 9:1): 0.5, UV active and yellow discolourisation with permanganate reagent.



## 1-[3-([2,2';6',2'']Terpyridin-4'-yloxy)-propyl]-maleimide (70)



Synthesized according to general method H.

The crude was purified by LC (EtOAc / MeOH, 8:2).

**Yield:** 45 %, as a brown solid.

**$^1H$ -NMR** (CDCl<sub>3</sub>, 300 MHz): 1.96-2.01 (m, 2 H), 2.91-2.96 (m, 2 H), 4.28-4.32 (t, 2 H,  $J = 6.2$  Hz), 6.37 (s, 2 H), 7.24-7.32 (m, 2 H), 7.78-7.84 (m, 2 H), 7.98 (s, 2 H), 8.56-8.66 (m, 4 H).

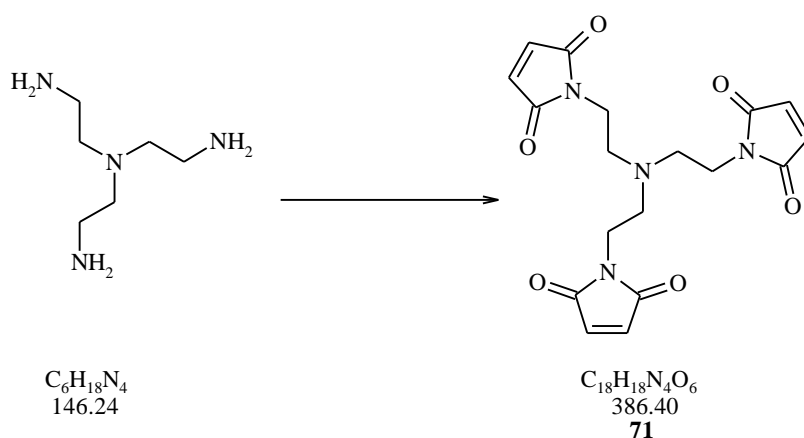
**$^{13}C$ -NMR** (CDCl<sub>3</sub>, 300 MHz): 32.86, 39.14, 66.19, 107.36, 121.15, 121.34, 121.39, 123.81, 124.28, 134.17, 136.79, 149.03, 155.03, 156.12, 156.75, 157.09, 167.19, 170.48.

**R<sub>f</sub>** (EtOAc/MeOH, 8:2): smeary spot from baseline to 0.75, UV active and yellow discolourisation with permanganate reagent.

## 2.9 Trimaleimide

### 2.9.1 Synthesis of 71<sup>173</sup>

#### Tris-(2-ethylenemaleimide)amine (71)



Synthesized according to general method H.

The crude was purified by LC (EtOAc / Hex, 1:1).

**Yield:** 53 %, as a light yellow solid.

**<sup>1</sup>H-NMR** (CDCl<sub>3</sub>, 300 MHz): 2.70 (t, 6 H, *J* = 6.2 Hz), 3.50 (t, 6 H, *J* = 6.6 Hz), 6.65 (s, 6 H).

**<sup>13</sup>C-NMR** (CDCl<sub>3</sub>, 300 MHz): 35.66, 51.67, 134.09, 170.63.

**R<sub>f</sub>** (EtOAc): 0.59, UV active and yellow discolourisation with permanganate reagent.

**mp:** 109 °C.

## 2.10 Oligodeoxyribonucleotide Synthesis

For reasons of simplicity we have decided to keep the compound numbers of the respective phosphoramidite building blocks also for the modifications after their incorporation into oligonucleotides.

For the synthesis of non modified oligodeoxyribonucleotides, common 0.2  $\mu\text{mol}$  synthesis has been carried out by using standard programs on ABI 392 and 394 Nucleic Acid Synthesizers from Applied Biosystems.

Modified oligodeoxyribonucleotides have been synthesized in 1.0  $\mu\text{mol}$  scale on the same apparatuses. Due to the lower coupling efficiency of some phosphoramidite building blocks, the coupling time was extended from 25 seconds to 5 minutes. During working time the time was extended by using the hold function of the apparatus, while for over night synthesis a modified program with generally extended coupling time was used.

The DNA synthesis was terminated with detritylation of the 5'-end (trityl of synthesis), and cleavage was accomplished manually.

After the automated DNA synthesis, the columns with the solid support bound oligodeoxyribonucleotides have been dried under reduced pressure to get rid of acetonitrile. The dried material was then transferred to a 1.5 ml screw micro tube. After adding 1.0 ml 25% aqueous ammonia the tubes have been shaken several times and were then incubated for 15 hours at 55°C in a heating block.

To get rid of the solid support, the supernatant of the centrifuged tubes was passed through a 0.45  $\mu\text{m}$  syringe filter. After careful lyophilization of the crude oligodeoxyribonucleotide solution, the white residue was dissolved in about 2 ml starting buffer and purified by reverse phase HPLC. The dried fractions were desalted via Sep-Pak<sup>®</sup> Cartridges from Waters. After repeated lyophilization was ready for MS, PAGE, bioconjugation and cross-linkage.

### 2.10.1 Oligodeoxyribonucleotides for Ene-Diene Cross-Linkage

In the following Tables (Table 1-2) synthesised oligonucleotides and their most important physical data are shown.

Table 1 Oligodeoxyribonucleotides containing electron poor ene- or anthracene-moieties.

seq. name	sequence (5' → 3')	length [bases]	extinct. $\epsilon$	mass – H <sup>+</sup> calc.	mass – H <sup>+</sup> meas.	$\Delta$ mass [g/mol]
				L/(mol*cm)	[g/mol]	[g/mol]
N1	CTG AAT CGA CCG GTA TCA G T	20	194100	6117	6117	0
N2	ACT GAT ACC GGT CGA TTC AG	20	195500	6117	6117	0
D1	CTG AAT CGA C <b>15</b> C GGT ATC AGT	21	194100	6558	6558	0
E1	ACT GAT ACC G <b>39</b> G TCG ATT CAG	21	195500	6408	3043	- 3365
E2	ACT GAT ACC G <b>43</b> G TCG ATT CAG	21	195500	6407	6441	+ 34

Table 2 GC-rich oligodeoxyribonucleotides containing ene- or anthracene-moieties.

seq. name	sequence (5' → 3')	length [bases]	extinct. $\epsilon$ L/(mol×cm)	mass – H <sup>+</sup> calc. [g/mol]	mass – H <sup>+</sup> meas. [g/mol]	$\Delta$ mass [g/mol]
N3	TGC CGA CGG CTC CGG ACG CGT GCG CAG GCC	30	267600	9210	9210	0
N4	TGC CGA CGG CTC	12	104500	3621	3621	0
N5	CGG ACG CGT GCG CAG GCC	18	163300	5526	5526	0
N6	GGC CTG CGC ACG CGT CCG GAG CCG TCG GCA	30	270400	9210	9211	+1
N7	GGC CTG CGC ACG CGT CCG	18	156500	5477	5477	0
N8	GAG CCG TCG GCA	12	115300	3670	3670	0
N9	TGC CGA CGG CTC T CGG ACG CGT GCG CAG GCC	30	267600	9514	9514	0
D2	TGC CGA CGG CTC <b>15</b> CGG ACG CGT GCG CAG GCC	31	267600	9653	9652	-1
D3	TGC CGA CGG CTC <b>18</b> CGG ACG CGT GCG CAG GCC	31	267600	9549	9549	0
D4	TGC CGA CGG CTC <b>32</b> CGG ACG CGT GCG CAG GCC	31	267600	9503	9503	0
D5	GGC CTG CGC ACG CGT CCG <b>15</b> GAG CCG TCG GCA	31	270400	9653	9653	0
D6	GGC CTG CGC ACG CGT CCG <b>18</b> GAG CCG TCG GCA	31	270400	9549	9549	0
D7	GGC CTG CGC ACG CGT CCG <b>32</b> GAG CCG TCG GCA	31	270400	9503	9502	-1
E3	GGC CTG CGC ACG CGT CCG <b>47</b> GAG CCG TCG GCA	31	270400	9541	9542	+1
E4	GGC CTG CGC ACG CGT CCG <b>56</b> GAG CCG TCG GCA	31	270400	9476	9477	+1
E5	GGC CTG CGC ACG CGT CCG <b>49</b> GAG CCG TCG GCA	31	270400	9372	9372	0
E6	GGC CTG CGC ACG CGT CCG <b>53</b> GAG CCG TCG GCA	31	270400	9360	9360	0
E7	GGC CTG CGC ACG CGT CCG <b>51</b> GAG CCG TCG GCA	31	270400	9360	9360	0

### 2.10.2 Hairpin and Hairpin-Mimic Oligodeoxyribonucleotides containing a Diene Moiety

In the following Tables (Table 3-5) synthesised oligonucleotides and their most important physical data are shown.

Table 3 Oligodeoxyribonucleotides for the fluorescein bioconjugation.

seq. name	sequence (5' → 3')	length [bases]	extinct. $\epsilon$	mass – H <sup>+</sup> calc. [g/mol]	mass – H <sup>+</sup> meas. [g/mol]	$\Delta$ mass [g/mol]
D8	TCG TGC AGC GTC GTT TTC GAC 15 CTG CAC GA	29	264100	9302	9301	-1
D9	ACG TGC CAG TGT TTT CAC T 32 G CAG GT	26	228900	7961	7962	+1
N10	CGG TAC TGA CTT TTG TCA GTA CCG	24	223300	7334	7334	0
N11	CGG TAC CTG ACT TTT GTC AGT ACC G	25	230500	7623	7623	0
D10	CGG TAC CTG ACT TTT GTC A 32 GTA CCG	25	230500	7916	7913	-3
N12	TCA CTG CAG AGT TTT CTC TGC AGT GA	26	242400	7951	7950	-1
D11	ACT GTA GTG C 15 G CAC TAC AGT	21	193500	9559	6558	-1
D12	CGA ACC TAC A 32 T GTA GGT TCG	21	194100	6454	6454	0
D13	TCA CTG CAG AGT 32 CTC TGC AGT GA	24	208200	7027	7025	-2

Table 4 Oligodeoxyribonucleotides for bioconjugation and dimaleimide linkage.

seq. name	sequence (5' → 3')	length [bases]	extinct. $\epsilon$ L/(mol $\times$ cm)	mass – H <sup>+</sup> calc. [g/mol]	mass – H <sup>+</sup> meas. [g/mol]	$\Delta$ mass [g/mol]
N13	TCT GAA TG	8	77700	2424	2424	0
N14	TAC G	4	39800	1173	1172	-1
N15	ATT GCT TTT GCA AT	14	129000	4243	4243	0
N16	ATT GCA AAA GCA AT	14	146000	4279	4279	0
D14	ATT GC <b>25</b> GCA AT	11	97200	3203	3204	+1
D15	ATT GC <b>32</b> GCA AT	11	97200	3319	3319	0
D16	ATT GC <b>29</b> GCA AT	11	97200	3291	3292	+1
D17	ATT GC <b>35</b> GCA AT	11	97200	3347	3348	+1
D18	<b>25</b> CT GAA TG	8	68900	2296	2296	0
D19	<b>32</b> CT GAA TG	8	68900	2412	2412	0
D20	<b>25</b> AC G	4	31800	1046	1046	0
D21	<b>32</b> AC G	4	31800	1162	1162	0
D22	CGG CG <b>32</b> C GCC GAG GGA TTT AAA ATC CCT	28	254000	8578	8577	-1
D23	GCC CGG ATG GTG CCC TTT TGG <b>32</b> CAC CAT CCG GGT ACC A	38	335600	11611	11611	0

Table 5 Oligodeoxyribonucleotides for templated dimaleimide cross-linkage.

seq. name	sequence (5' → 3')	length [bases]	extinct. $\epsilon$ L/(mol×cm)	mass – H <sup>+</sup> calc. [g/mol]	mass – H <sup>+</sup> meas. [g/mol]	$\Delta$ mass [g/mol]
N17	CTG AAT CGA CCG GTA TCA GT	20	194100	6116	6118	+2
N18	TAC CGG TCG ATT CAG	15	140000	4567	4568	+1
D24	CTG AAT <b>29</b> CGA CCG GTA TCA GT	21	194100	6381	6382	+1
D25	TAC CGG TCG <b>29</b> ATT CAG	16	140000	4832	4832	0
D26	CTG AAT <b>32</b> CGA CCG GTA TCA GT	21	194100	6409	6409	0
D27	TAC CGG TCG <b>32</b> ATT CAG	16	140000	4860	4860	0
D28	CTG AAT <b>35</b> CGA CCG GTA TCA GT	21	194100	6437	6437	0
D29	TAC CGG TCG <b>35</b> ATT CAG	16	140000	4888	4888	0



## 2.11 Cross-Linkage and Bioconjugation of Oligodeoxyribonucleotides

For reasons of simplicity we have decided to keep the compound numbers of the respective maleimides and dimaleimides also for the bioconjugate and the cross-linking bridge after the *Diels-Alder* reaction with the diene-modifications.

Pure oligodeoxyribonucleotide lyophilizates were dissolved in MQ water and the concentration was calculated via extinction coefficient, from the absorbance at 260 nm. Possible influence of ene- and diene building blocks on the extinction coefficient have been ignored for the calculation of the concentrations.

### 2.11.1 Ene-Diene Oligodeoxyribonucleotide Cross-Linkage

#### **Cross-Linking Experiments of Oligodeoxyribonucleotides containing a electron-poor Ene- Moiety with Oligodeoxyribonucleotides containing a Anthracene-Moiety**

For the incubation at different temperatures three times 1.0 ml oligonucleotide solution was prepared. Final concentration of both D1 and E2 were 5.0  $\mu\text{M}$ . Further 100  $\mu\text{l}$  0.1 M  $\text{NaH}_2\text{PO}_4$  (pH 7.0) and 400  $\mu\text{l}$  2.5 M NaCl was added to achieve final buffer concentrations of 10 mM  $\text{NaH}_2\text{PO}_4$  and 1.0 M NaCl.

The samples were heated up to 80 °C and slowly cooled down to get the duplex. The samples were then incubated for 7 days at 55 °C, 61°C and 100°C.

#### **Cross-Linking Experiments of GC-rich Oligodeoxyribonucleotides containing a Ene-Moiety with Oligodeoxyribonucleotides containing a Anthracene-Moiety**

Different solutions of 50  $\mu\text{l}$  volume, containing 5'000 pmol of diene modified oligodeoxyribonucleotide (D2, D3 and D4) and the same amount of ene modified oligodeoxyribonucleotide (E3 – E7), of complementary sequence, with 25 mM TEAAc (pH 5.5) and 0.1 M NaCl were prepared. The samples were heated up to 80 °C and slowly cooled

---

down to get the duplex. The samples were then incubated for 7 days at 50 °C, 70°C and 100°C.

### 2.11.2 Bioconjugation of Oligodeoxyribonucleotides with Maleimides and Linkage with Dimaleimides

#### Fluorescein Bioconjugation of Oligodeoxyribonucleotides

The diene modified oligodeoxyribonucleotides (D4-D7, D10 and D13) were incubated in 10mM phosphate buffer at pH 5.5, with 10 equivalents of fluoresceine maleimide at 20 to 30°C for 24 hours.

The modified oligodeoxyribonucleotides were incubated in purified dissolved form as well as directly after automated synthesis, still bound on solid support and with protected bases.

Dissolved fluoresceine labeled oligodeoxyribonucleotides were purified directly, and solid support bound ones after cleavage and deprotection in 25% aqueous ammonia at 55 °C, by RP HPLC. The dried fractions were desalted via Sep-Pak<sup>®</sup> Cartridges from Waters. The mass was determined from 10 µl aqueous solutions containing about 100 pmol/µl oligodeoxyribonucleotide (Table 6).

Table 6 Identification of the isolated oligonucleotides via ESI-MS.

oligonucleotides	mass – H <sup>+</sup>	mass – H <sup>+</sup>	Δ mass
	calc. [g/mol]	meas. [g/mol]	
D4-68	10001	10002	+1
D7-68	10001	10001	0
D10-68	8414	8414	0
D13-68	7525	7525	0

### Bioconjugation and Dimaleimide Linkage of Oligodeoxyribonucleotides

Solutions of D15 were incubated in aqueous medium (10mM NaOAc buffer, pH 6.5) for 7 days at 20 °C with 10 equivalents of the maleimide-derived dienophiles shown in.

After RP HPLC and desalting via Sep-Pak<sup>®</sup> Cartridges the masses were determined from aqueous solutions containing 50-500 pmol/μl oligodeoxyribonucleotide (Table 7).

Table 7 Identification of the isolated oligonucleotides via ESI-MS.

oligonucleotides	mass – H <sup>+</sup>	mass – H <sup>+</sup>	Δ mass
	calc. [g/mol]	meas. [g/mol]	
D15-58	3345	3346	+1
D15-66	3505	3507	+2
D15-67	3615	3615	0
D15-62	3594	3595	+1
D15-70	3705	3705	0
D15-68	3817	3817	0

Diene modified oligodeoxyribonucleotides were incubated in aqueous media (10 mM TEAAc buffer, pH 5.5) with 10 to 100 equivalents (solubility dependent) of different dimaleimides.

After RP HPLC and desalting via Sep-Pak<sup>®</sup> Cartridges the masses were determined (Table 8).

Table 8 Identification of the isolated oligonucleotides via ESI-MS.

oligonucleotides	mass - H <sup>+</sup>	mass - H <sup>+</sup>	$\Delta$ mass	oligonucleotides	mass - H <sup>+</sup>	mass - H <sup>+</sup>	$\Delta$ mass
	calc.	meas.			calc.	meas.	
	[g/mol]	[g/mol]	[g/mol]		[g/mol]	[g/mol]	[g/mol]
D4-63	9771	9772	+1	D10-60	8136	8136	0
		9789	+18	D13-60	7247	7247	0
D4-64	9771	9789	+18	D15-71	3705	3704	-1
D4-65	9771	9789	+18	D15-62	3595	3595	0
D4-65	9723	9722	-1	D18-62	2573	2573	0
		9742	+19	D22-62	8855	8855	0
D4-57	9695	9713	+19	D23-62	11887	11888	+1

The oligodeoxyribonucleotide dimaleimide bioconjugates were incubated in aqueous media (10 mM TEAAc buffer, pH 5.5) with 1 to 10 equivalents of diene modified oligodeoxyribonucleotides at 20 °C to 70 °C.

The reactions were controlled by denaturing PAGE and MS.

### Oligodeoxyribonucleotide Templated Dimaleimide Cross-Linkage

Couples of complementary diene modified oligodeoxyribonucleotides were incubated in aqueous media (0.1mM Tris-HCL buffer, pH 4.2 and 100mM NaCl) with 1 to 3 equivalents of different dimaleimides. The reaction mixtures were heated up to 70 °C and slowly cooled down to achieve the duplex formation.

The reaction was followed by, recording melting curves, denaturing PAGE and MS. After RP HPLC and desalting via Sep-Pak<sup>®</sup> Cartridges the masses were determined (Table 9).

Table 9 Identification of the isolated oligonucleotides via ESI-MS.

oligonucleotides	mass	mass	$\Delta$ mass
	calc.	meas.	
	[g/mol]	[g/mol]	[g/mol]
D24-60-D25	11434	11433	-1
D24-61-D25	11462	11459	-3
D24-62-D25	11490	11490	0
D24-60-D29	11490	11488	-2
D26-60-D27	11490	11487	-3
D26-61-D27	11518	11515	-3
D26-62-D27	11546	11542	-4
D26-71-D27	11656	11653	-3
D28-60-D29	11546	11542	-4
D28-61-D29	11574	11570	-4
D28-62-D29	11602	11599	-3

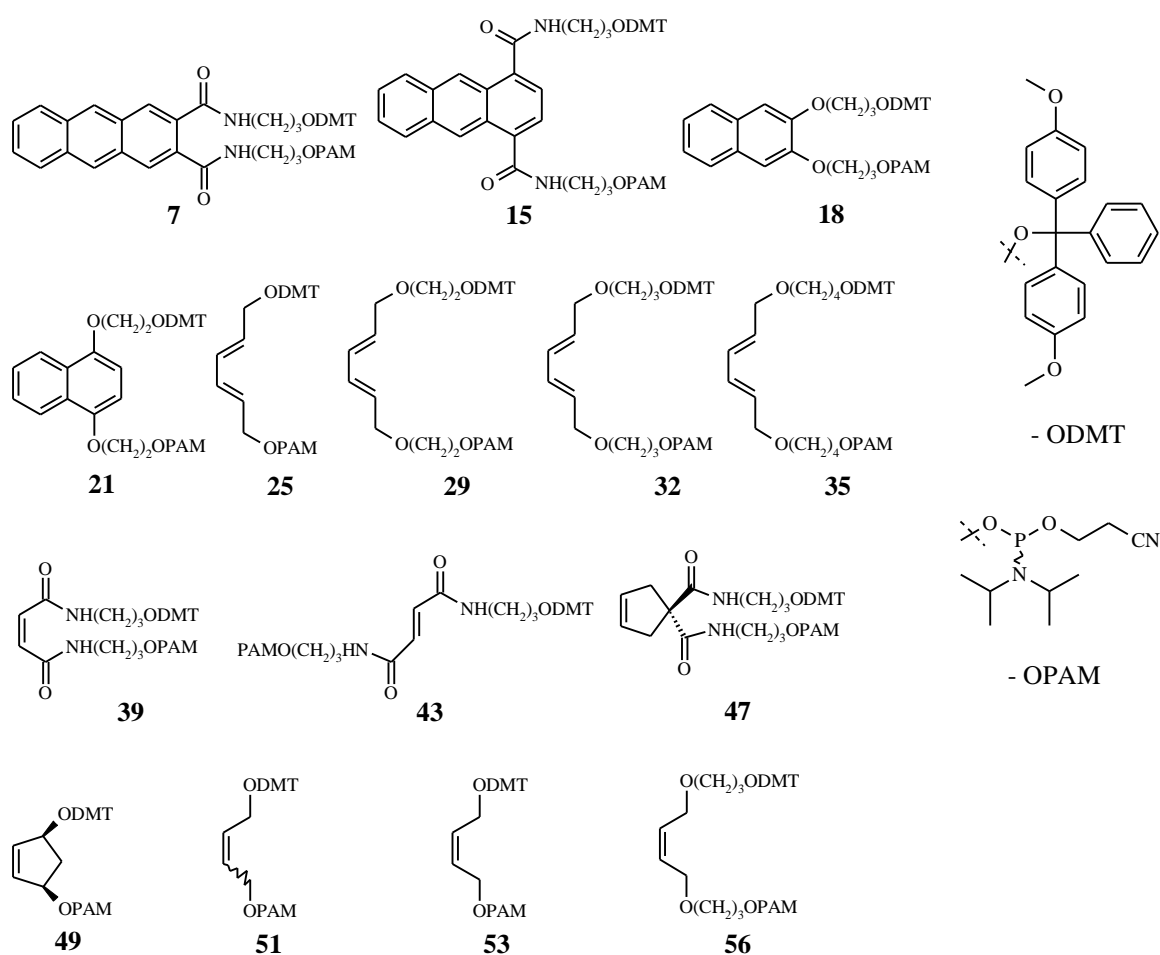


### 3 RESULTS AND DISCUSSION

#### 3.1 Synthesis of the Building Blocks and the Modified Oligonucleotides

##### 3.1.1 Synthesis of Phosphoramidites

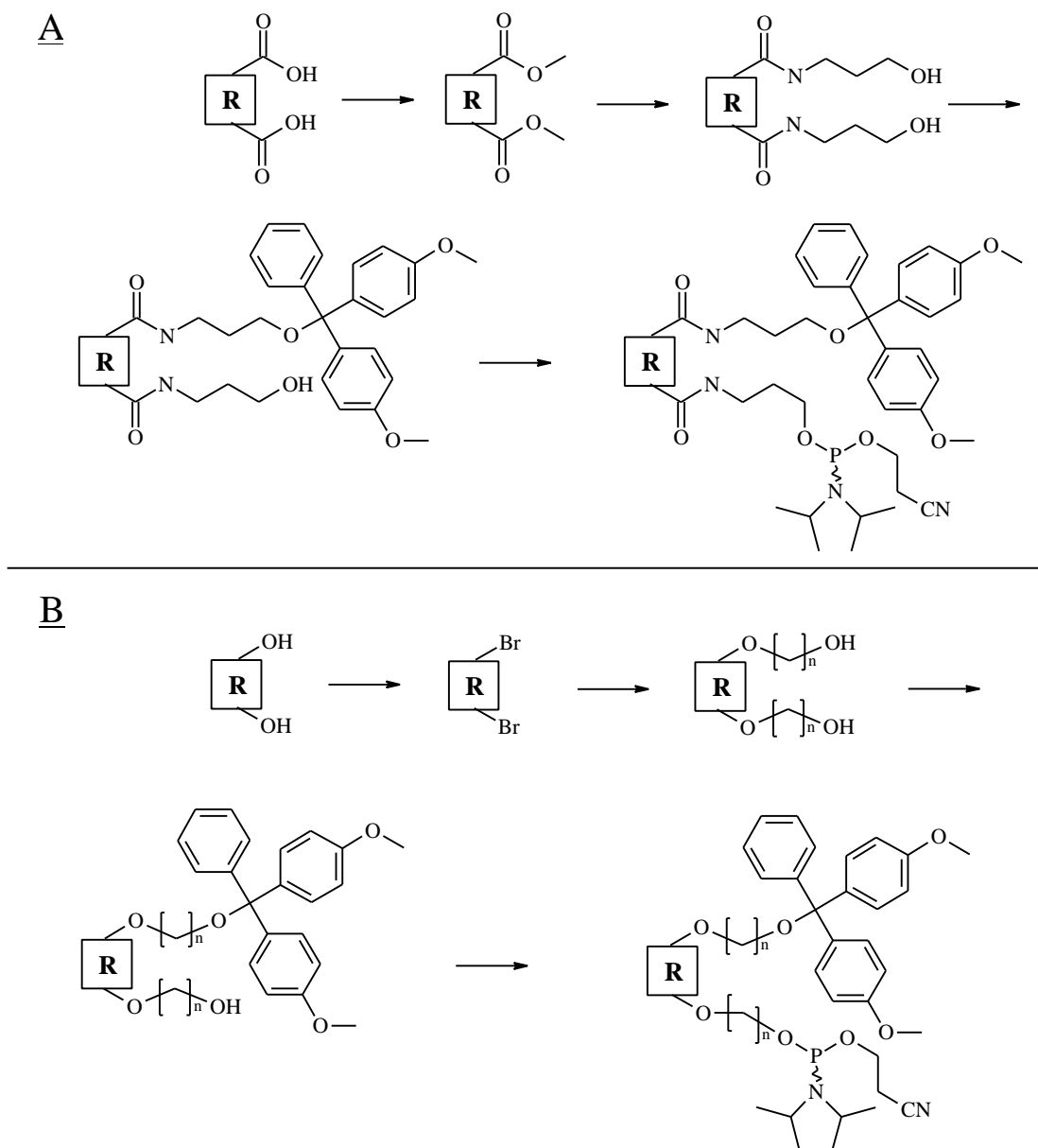
For the automated synthesis of modified oligodeoxyribonucleotides, a variety of diene- and ene-phosphoramidites was synthesized (Scheme 25).



Scheme 25 Phosphoramidites synthesized and used in this work.

### 3 RESULTS AND DISCUSSION

The general methods described in the experimental part led generally to pure phosphoramidites in reasonable overall yields. Enes and dienes were used as derivatives of the corresponding alcohols or acids. They were further derivatised with spacer groups. The latter were either alkyl-diols, which were linked via ether bonds, or aminoalkyl alcohols, which were linked through amide bonds (Scheme 26).



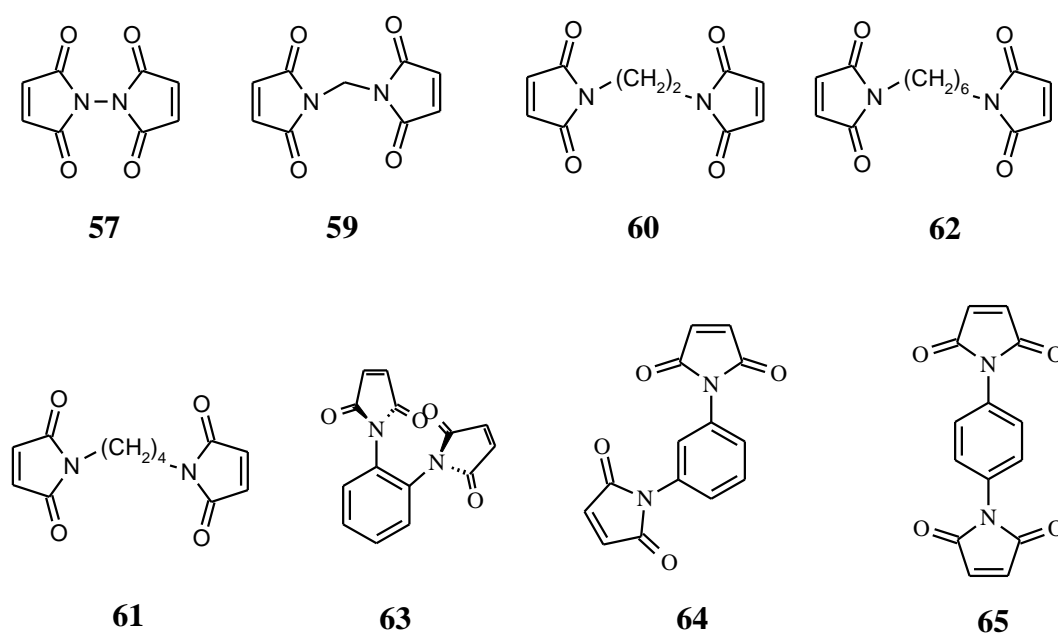
**Scheme 26** Schematic illustration of the synthesis path of phosphoramidites with amide-spacers (**A**) and ether-spacers (**B**).



The ether bond-linked dialcohols eventually turned out to have clear advantages. Thus, some of the amide derivatives gave rise to side-reactions (e.g. intramolecular imide formation) during their preparation. Intramolecular imide formation was also the major reason for the failure of oligodeoxyribonucleotide synthesis with diene building block **7** and ene building block **39**. Furthermore, all bis-amides were rather difficult to purify, due to their much higher polarity. Once obtained in pure form, however, the phosphoramidites proved to be stable upon storage in the fridge. On the other hand with all types of phosphoramidites decomposition was observed when stored in solution. Even when stabilized with silver, traces of HCl led to decomposition of the phosphoramidite, if deuterated chloroform was not passed through basic allox before it was used as solvent for NMR.

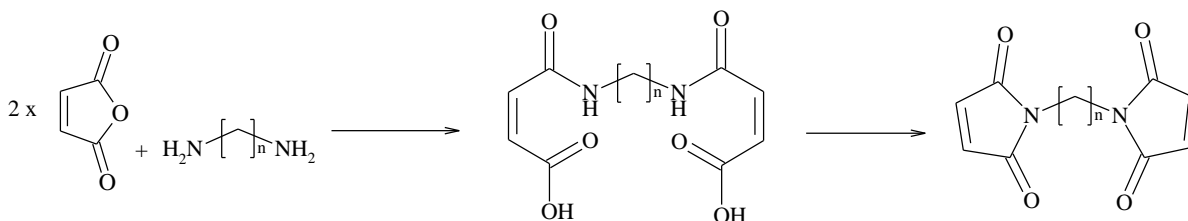
### 3.1.2 Synthesis of Dimaleimides

Dimaleimides with various linkers of different length and flexibility (Scheme 27) were synthesized. This set of dienophiles, provided a large set of different derivatives, which were tested in the cross-linkage experiments with diene-modified oligonucleotides.



Scheme 27 Dimaleimides synthesized and used in this work.

Most of the dimaleimides were synthesized from maleic acid anhydride and diamines *via* amid formation followed by condensation (Scheme 28). While amide formation happened immediately upon combining anhydride and diamine in dichloromethane, heating in acetic acid anhydride containing dry sodium acetate was needed for the condensation to the maleimides and dimaleimides.

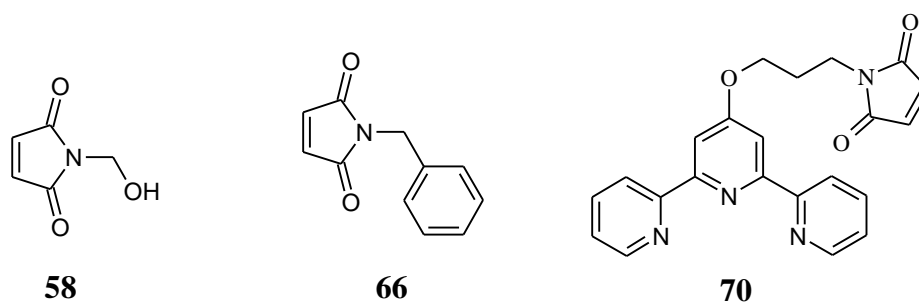


Scheme 28 Synthesis of the dimaleimides.

Too high temperatures or heating for too long, during the condensation step, led to the formation of insoluble black material and to a dramatic decrease in yield. The purified and dried dimaleimides showed good stability. Under basic aqueous conditions, however, hydrolysis of the maleimide rings was observed already at room temperature. For more detailed information on the yields of the individual dimaleimides see chapter 2.7.

### 3.1.3 Synthesis of Maleimides

Several maleimides (Scheme 29) were synthesized from maleic acid anhydride and amines in the same way as described for the dimaleimides in chapter 3.1.2.

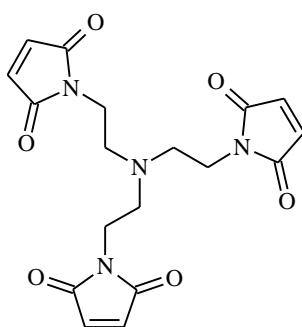


Scheme 29 Maleimides synthesized in this work.

Maleimides **58** and **66** were easy to synthesize and purify in good yields (77% and 62%). The synthesis of the terpyridine **70** was more difficult due to problems in the purification steps. It was obtained in an overall yield of 27%.

### 3.1.4 Trimaleimide Synthesis

Tris-(2-ethylenemaleimido)amine (**71**, Scheme 30) was synthesized in the same way as the maleimides and the dimaleimides. Tris(2-aminoethyl)amine was added to maleic acid anhydride in dichloromethane, followed by condensation in acetic acid anhydride in the presence of sodium acetate. Standard purification *via* column chromatography led to pure tris-(2-ethylenemaleimido)amine in a moderate yield (53%).



**71**

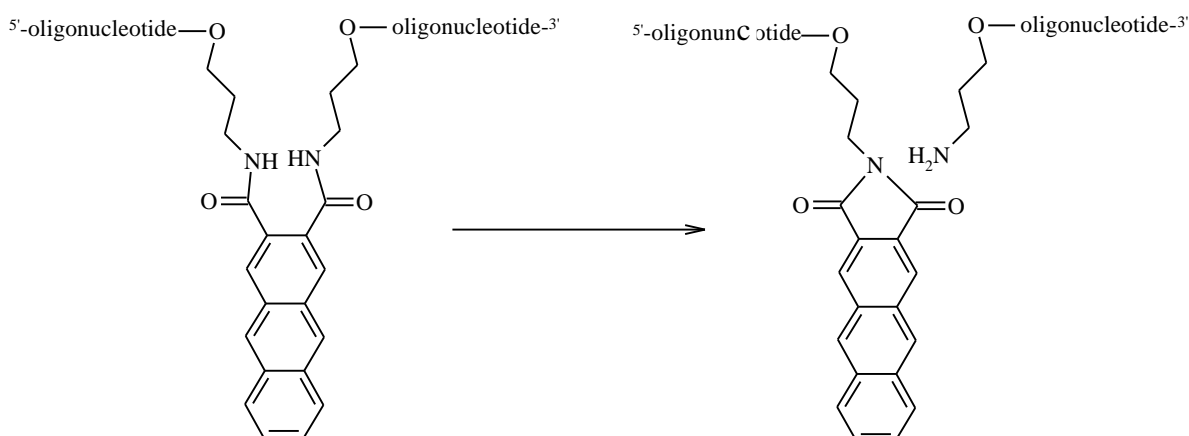
Scheme 30 Trimaleimide synthesized in this work.

## 3.2 Oligodeoxyribonucleotide Synthesis

The phosphoramidites described in chapter 3.1 contain both functional groups needed for the phosphoramidite method. Due to that they are compatible with most aspects of the automated DNA synthesis. They can be placed at the 3'-end, the 5'-end or anywhere in the middle of a sequence. The phosphoramidites were well soluble in absolute acetonitrile. Generally, 0.1 M solutions were used, except for 1,4-anthracene derivative **15**, which was used as 0.05 M solution to avoid crystallisation during the synthesis. Coupling times for the ene and diene building blocks were extended from the usual 25 seconds to up to five minutes in order to achieve maximum coupling yields. Internal trityl assay (*via* conductivity) or manual trityl assay (*via* absorbance) were used to calculate the coupling efficiencies. Coupling efficiencies

varied from 98% to 40%. While most of the modified oligonucleotides needed for our studies could be synthesized this way, incorporation of the building blocks **7** and **43** failed.

It was possible to assemble modified oligodeoxyribonucleotides with the 2,3-anthracenedicarboxylic acid derivative **7** on solid support, but intramolecular imide formation during the deprotection with aqueous ammonia at 55 °C allowed only isolation of fragmented oligonucleotides (Scheme 31).



Scheme 31 The presumed way of intramolecular imide formation observed with a 2,3-anthracenedicarboxylic acid derivative.

Oligodeoxyribonucleotides containing fumarate building block **43**<sup>1</sup> always showed a difference between calculated and measured mass of about +34 daltons. This difference in mass hints to the oxidation of the double bond of the fumaric acid derivative. Such oxidation leads to oligodeoxyribonucleotides which are, because of the missing functional group, useless for *Diels-Alder* reactions.

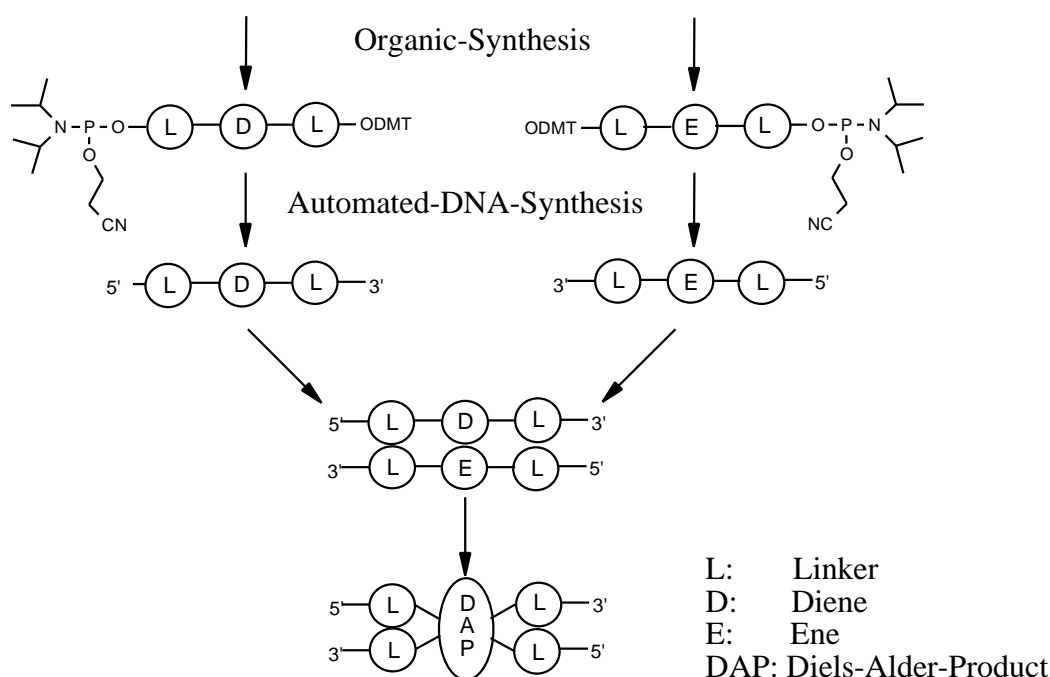
RP HPLC at 40 °C gave the modified oligodeoxyribonucleotides in pure form. For RP HPLC as well as in the desalting procedure with the Sep Pak<sup>®</sup> C<sub>18</sub>-columns of *Waters*, conditioning of the columns and sample preparation with 100 mM TEAAc was essential to avoid heavy losses of material.

<sup>1</sup> For reasons of simplicity we have decided to keep the compound numbers of the respective phosphoramidite building blocks also for the modifications after their incorporation into oligonucleotides.

### 3.3 Cross-Linkage of Ene- and Diene-Modified Oligodeoxyribonucleotides

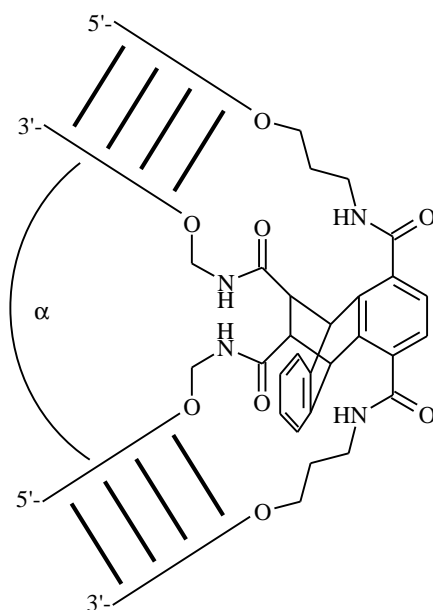
#### 3.3.1 First Experiments Towards the Direct Cross-Linking of Two Hybridised Strands

In this chapter we describe our efforts aimed at the direct cross-linking of two complementary oligodeoxyribonucleotides. In each of the two strands, one nucleotide has been replaced by a diene or a dienophile building block. *Diels-Alder* reaction between the two partners should result in a cross-linked duplex (Scheme 32). We first attempted a classical *Diels-Alder* reaction, i.e. an electron rich diene and an electron poor dienophile. Anthracene derivatives and fumaric as well as maleic acid were chosen as reactive groups.



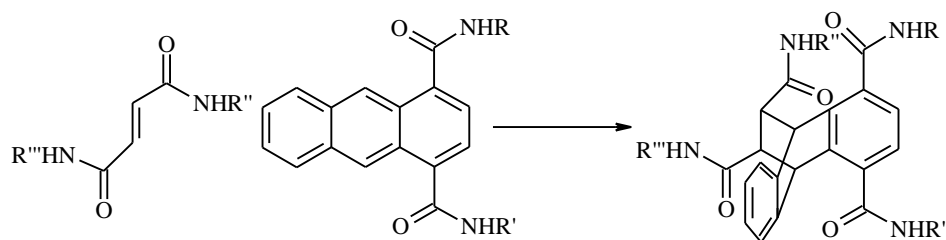
**Scheme 32** Direct cross-linking of two strands in DNA *via* the *Diels-Alder* reaction.

Subsequent studies should then show if it were possible to design DNAs with defined structural motifs, such as bends by using linkers of different lengths in the two strands (Scheme 33). This approach might be a first step towards the synthesis of mimics of functional nucleic acids.



**Scheme 33** Illustration of a kink in a duplex generated by a *Diels-Alder* adduct.

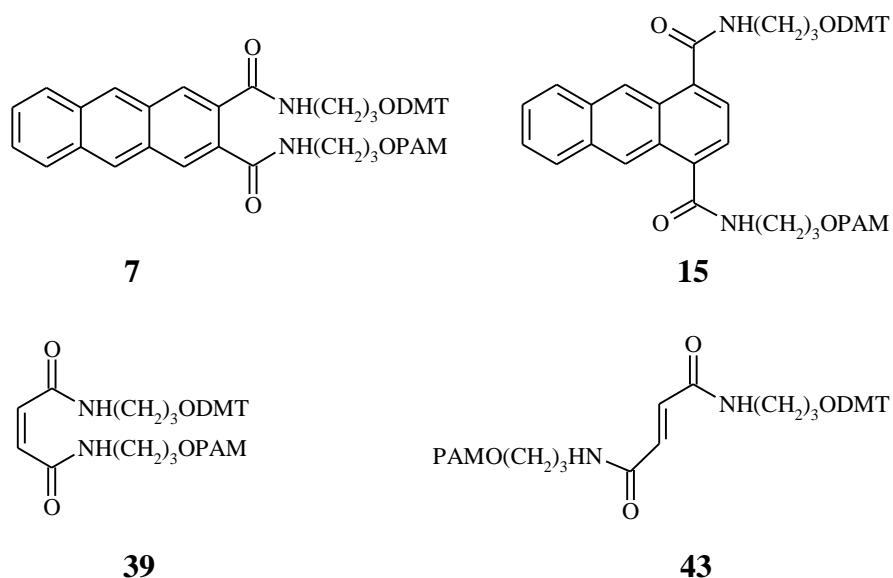
Anthracene derivatives were chosen to take advantage of the hydrophobic effect and to obtain a rigid *Diels-Alder* product (Scheme 34).



**Scheme 34** Attempted *Diels-Alder* reaction.

To bridge the distance between the phosphate backbones and to get a certain flexibility, derivatives bearing 3-amino-1-propanol linkers on both sides were used. Molecular modeling with the program Insight II predicted this length of linker to be optimal.

As mentioned earlier, connection of the linkers *via* an amide group turned out to have serious disadvantages. Compounds with two 3-amino-1-propanol linkers (**5**, **13**, **37** and **41**) are very polar and the yield of the reactions decreased because of loss during the work up. In addition to that the two amide groups of 2,3-anthracene derivatives and maleic acid derivatives can undergo intramolecular cyclisation by imide formation. Probably due to this latter fact, the synthesis of the maleic acid phosphoramidite (**39**) and the oligodeoxyribonucleotide synthesis with the 2,3-anthracene phosphoramidite (**7**) failed (Scheme 35). Compound **7** was successfully coupled during automated DNA synthesis, but the oligomer was cleaved under deprotection conditions. Efforts to replace the amide groups by ether groups failed.



**Scheme 35** Ene- and diene-phosphoramidite building blocks.

Incorporation of the 1,4-anthracene derivative (**15**) into oligodeoxyribonucleotides as well as deprotection and purification was successful. A coupling efficiency of 85 % was obtained with this building block. Due to the limited solubility of the phosphoramidite it was not possible to increase the coupling efficiency by the use of phosphoramidite solutions of higher concentration.



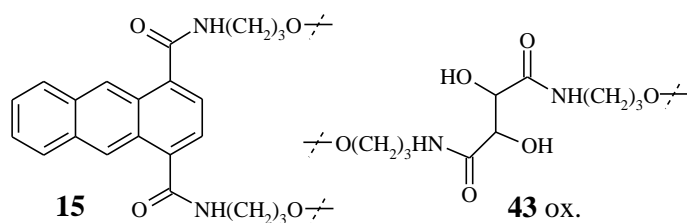
Only a low coupling efficiency of 25% could be achieved with the fumaric acid phosphoramidite **43**. The mass spectra of the deprotected and purified sequence, showed a difference of +34 compared to the calculated mass. Further investigations showed that addition of H<sub>2</sub>O to the double bond of fumaric acid derivatives can take place under basic aqueous conditions<sup>183-186</sup> as well as during the oxidation step in the automated DNA synthesis. This fact explains the observed difference in mass and why no *Diels-Alder* reaction could be observed.

**Table 10** Duplex sequences and incorporated building blocks; Comparison of melting temperatures.

oligonucleotides	0.01M NaCl		1.0M NaCl	
	T <sub>m</sub> [°C]	Δ T <sub>m</sub> [°C]	T <sub>m</sub> [°C]	Δ T <sub>m</sub> [°C]
N1/N2	59.5	+3.0	66.5	+3.0
D1/E2	56.5	0.0	63.5	0.0

N1 5'-CTG AAT CGA CCG GTA TCA GT-3'  
N2 3'-GAC TTA GCT GGC CAT AGT CA-5'

D1 5'-CTG AAT CGA C <sup>15</sup> C GGT ATC AGT-3'  
E2 3'-GAC TTA GCT G <sup>43 ox.</sup> G CCA TAG TCA-5'



The melting points of both, the modified and the unmodified duplex are 7 °C higher at high salt concentration compared to low concentration (Table 10). Interesting is the fact that the modified duplex, at both salt concentrations, is just destabilized by 3 °C. One could expect that modifications of this size, placed in the middle of the sequence should disturb  $\pi$ -stacking in a way that the hybrid would behave like two flexibly linked 10 base pair sequences, rather than a 20 base pair sequence.

$\pi$ -stacking is a very important factor for the stability of DNA duplexes. Based on the high melting temperatures,  $\pi$ -stacking seems to be intact in the modified duplex. The modifications are either taking part in the  $\pi$ -stacking or, what is more likely, are looped out of the helical

structure. A small destabilization, as observed, would be in agreement with such looped-out structure.

To circumvent oxidation of the ene-modified oligodeoxyribonucleotide (E2) during deprotection, we tried to react the purified diene modified sequence (D1) in aqueous buffer (10 mM NaH<sub>2</sub>PO<sub>4</sub>, 1.0M NaCl, pH 5.5) to the still solid supported and protected ene sequence (E2) followed by cleavage from the support, deprotection and purification. No cross linkage was observed according to denaturing PAGE. Since we could not find out whether the ene was already oxidized during the DNA synthesis, we can not establish the reason for the failure. An alternative explanation could simply be the absence of duplex formation between the solid supported strand with the protected nucleobases and the complementary strand in solution.

Melting experiments of the modified and the corresponding unmodified duplex show the expected sigmoid curves which visualize the highly cooperative denaturation of the duplex (Figure 3). In the case of the unmodified duplex, two transitions were observed. The reason for this was, however, not further investigated.

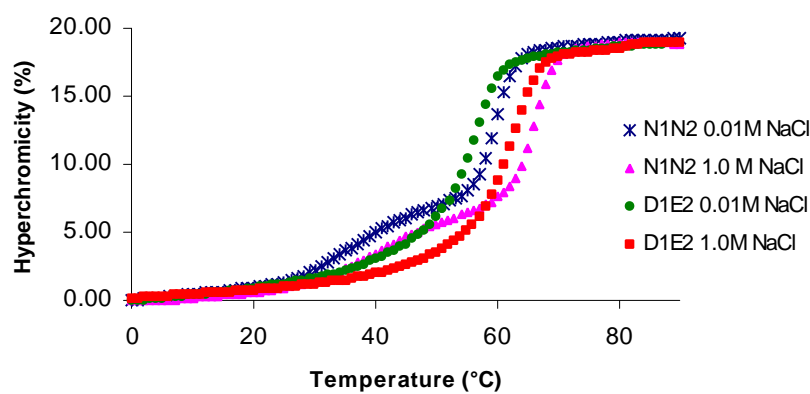
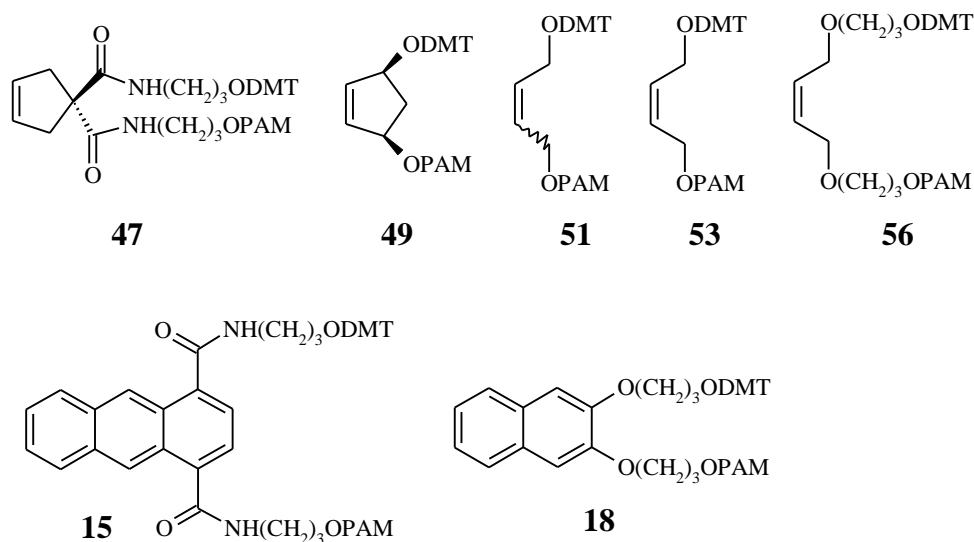


**Figure 3** Melting curves of the natural- and the “ene”-diene ( oxidised fumaric acid building block after addition of H<sub>2</sub>O); Conditions: 1.0 μM duplex in 10 mM NaH<sub>2</sub>PO<sub>4</sub> (pH 5.5) at different salt concentrations.

### 3.3.2 Cross-Linking Experiments of GC-rich Oligodeoxyribonucleotides Containing Electron-Rich Ene- and Diene-Modifications

After the first attempt with electron poor dienophile building blocks (chapter 3.2.1) did not lead to the expected results, new ene-phosphoramidites, without electron withdrawing groups at the ene-function, were synthesized (Scheme 36). To have the possibility of combining different complementary ene- and diene-oligonucleotides, an additional diene-phosphoramidite (**18**) was synthesized. To avoid the negative effects of amide groups in the molecules, ether type linkages (**56** and **18**) or no additional linkers were used (**49**, **51** and **53**), with the exception of **47**, which was still used as the di-amide.



**Scheme 36** Phosphoramidites used for the synthesis of modified, GC-rich oligodeoxyribonucleotides.

All the phosphoramidites shown in Scheme 36 could be incorporated into oligonucleotides. Coupling efficiencies in the automated DNA synthesis of phosphoramidites without linkers, however, was poor. In particular, the cyclopentene derivative **49** was rather bad ( $\leq 10\%$ ). Steric hindrance in combination with the rigidity of the building block is a possible explanation for this phenomenon.

Because the new ene-building blocks are not electron poor they are expected to be less reactive in the *Diels-Alder* reaction. In order to incubate the duplex at higher temperature without denaturation, a different oligodeoxyribonucleotide sequence was used than the one used in the former experiments. Since a higher temperature was likely to be required for the Diels-Alder reaction, due to the lower reactivity of the dienophile, the length of the oligonucleotides and the GC-content was increased. In addition we planned to use high salt concentrations to further support hybrid formation. This should allow formation of the duplex even at elevated temperatures and should, thus, increase the chances of a successful cross-linking reaction.

### 3 RESULTS AND DISCUSSION

To compare the melting temperatures of the modified duplexes, the respective unmodified duplex was synthesized. Additionally all combinations of the unmodified 30 base long oligodeoxyribonucleotides and the complementary 12 and 18 nucleotide sequences were prepared (Table 11). These shorter sequences correspond to the ones flanking the ene- and diene-building blocks in the analogous modified oligonucleotides (Table 11).

**Table 11** Melting temperatures of the unmodified duplex and different combinations of its parts at different salt concentration and oligonucleotide sequences of several unmodified sequences relevant for interpreting the  $T_m$ 's.

oligonucleotides	0.01M NaCl		1.2M NaCl	
	$T_m$ [°C]	$\Delta T_m$ [°C]	$T_m$ [°C]	$\Delta T_m$ [°C]
N3/N6	58.5	0.0	85.5	0.0
N3/N7/N8	42.5	-16.0	72.5	-13.0
N6/N4/N5	42.5	-16.0	72.5	-13.0
N4/N5/N7/N8	42.5	-16.0	72.5	-13.0
N3 N6	5'-TGC CGA CGG CTC CGG ACG CGT GCG CAG GCC-3' 3'-ACG GCT GCC GAG GCC TGC GCA CGC GTC CGG-5'			
N3 N7/N8	5'-TGC CGA CGG CTC-----CGG ACG CGT GCG CAG GCC-3' 3'-ACG GCT GCC GAG-5' 3'-GCC TGC GCA CGC GTC CGG-5'			
N4/N5 N6	5'-TGC CGA CGG CTC-5' 3'-CGG ACG CGT GCG CAG GCC-3' 3'-ACG GCT GCC GAG-----GCC TGC GCA CGC GTC CGG-5'			
N4/N5 N7/N8	5'-TGC CGA CGG CTC-5' 3'-CGG ACG CGT GCG CAG GCC-3' 3'-ACG GCT GCC GAG-5' 3'-GCC TGC GCA CGC GTC CGG-5'			

At low salt concentration the denaturation process of the sequence parts amongst themselves and with the complete complementary strand seems to be much less cooperative than the denaturation of the full-length duplex (Figure 4). This might be because there are two different systems, the 12 base pair and the 18 base pair duplexes. This should result in two

melting temperatures. The relatively flat curve could be the result of two melting temperatures which are so close together that the two transitions are not separate events anymore.

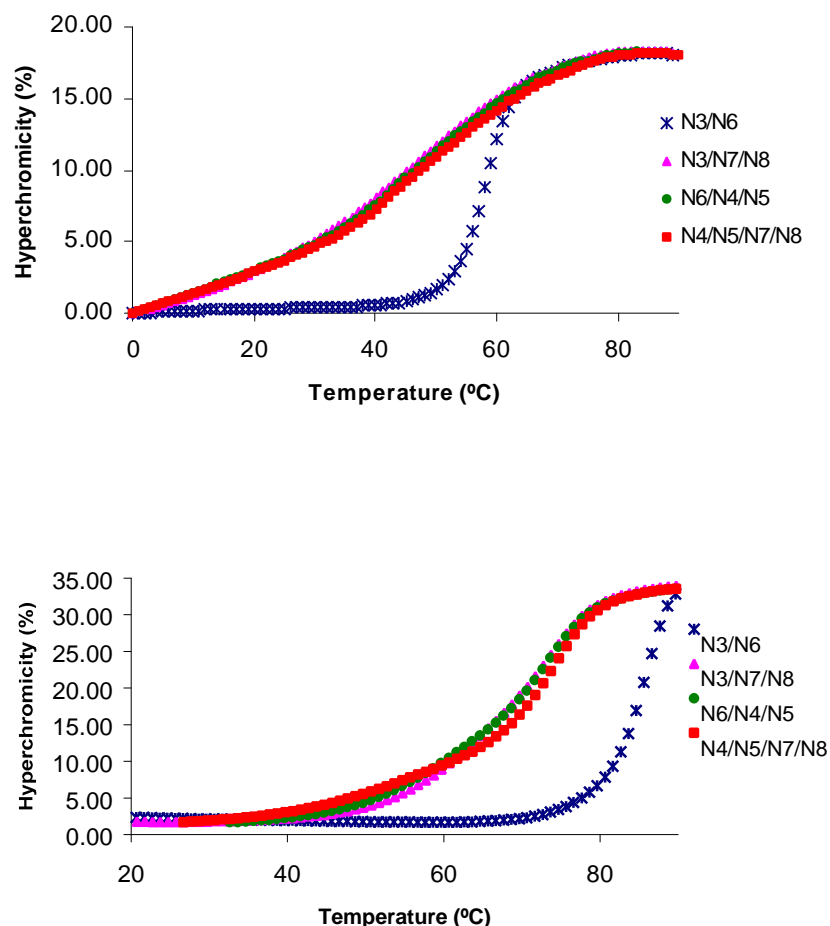


**Figure 4** Melting curves of the complementary oligonucleotides shown in Table 11. Conditions: 1.0  $\mu\text{M}$  oligonucleotide in 10 mM  $\text{NaH}_2\text{PO}_4$  (pH 5.5) at different salt concentrations (0.01 M NaCl - above and 1.2M NaCl - below).

Higher salt concentration shifts the curves to higher temperature. The shape of the melting curves is better defined than at low salt concentration. Below 60 °C one can guess a second transition, caused by the 12 base fragment. Since the change in absorbance, compared to the major transition, is so small, no exact second melting temperature can be calculated.

The change of the melting temperatures of approximately 30°C going from low to high salt concentration is reasonable for unmodified duplexes of this length (Table 11). Since the base composition in both strands is equal there is no difference in melting temperature between one complete strand with a complementary 12 bases long strand, compared with the complementary system. Finally in the system with all 4 fragments, just the denaturation of the 12 base pair duplex was observed. The ene- and diene-modifications were no longer incorporated in the middle of the sequence as it was done in the previous experiments. The dienes were placed after base 12 from the 5'-end, while the enes were placed after base 18 from the 5'-end of the complementary strand. In this way the ene-diene "pair" is flanked by a 12 base pair duplex on one and a 18 base pair duplex on the other side (Table 12).

The sequence containing the 1,4-anthracene derivative (D2) was paired with different ene-modified complementary sequences (Table 12). The melting temperatures in Table 12 were calculated from the melting curves shown in Figure 5.

The destabilizations observed for the different modifications were in the range of 7 °C to 9 °C. This was more than we expected after the experiments described in chapter 3.3.1. The difference between low and high salt concentration of the modified duplexes, of 27 °C, corresponds to the one of the unmodified duplex.

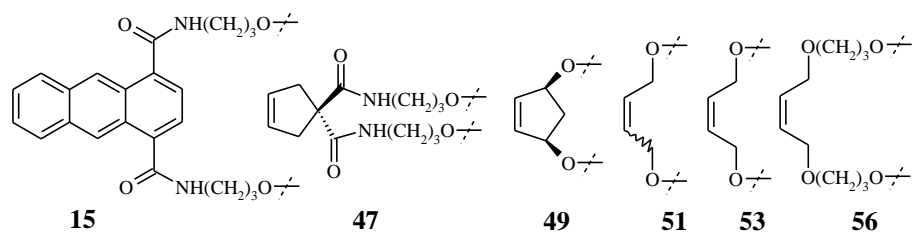


**Table 12** Melting temperatures of the unmodified duplex and the hybrids between the 1,4-anthracene modified strand (D2), paired with different ene-modified complementary strands (E3 **Y** = **47**, E4 **Y** = **56**, E6 **Y** = **53**, E7 **Y** = **51**) at different salt concentrations.

oligonucleotides	0.01M NaCl		1.2M NaCl	
	T <sub>m</sub> [°C]	Δ T <sub>m</sub> [°C]	T <sub>m</sub> [°C]	Δ T <sub>m</sub> [°C]
N3/N6	58.5	0.0	85.5	0.0
D2/E3	51.5	-7.0	78.5	-7.0
D2/E4	49.5	-9.0	78.5	-7.0
D2/E6	50.5	-8.0	78.5	-7.0
D2/E7	51.5	-7.0	78.5	-7.0

N3 5'-TGC CGA CGG CTC CGG ACG CGT GCG CAG GCC-3'  
 N6 3'-ACG GCT GCC GAG GCC TGC GCA CGC GTC CGG-5'

D2 5'-TGC CGA CGG CTC **15** CGG ACG CGT GCG CAG GCC-3'  
 EX 3'-ACG GCT GCC GAG **Y** GCC TGC GCA CGC GTC CGG-5'



The melting curves show just one transition, at low as well as at high salt concentration. A strong destabilization is observed going from the unmodified to the modified duplexes, while there is no significant difference between the different modified duplexes (Figure 5).

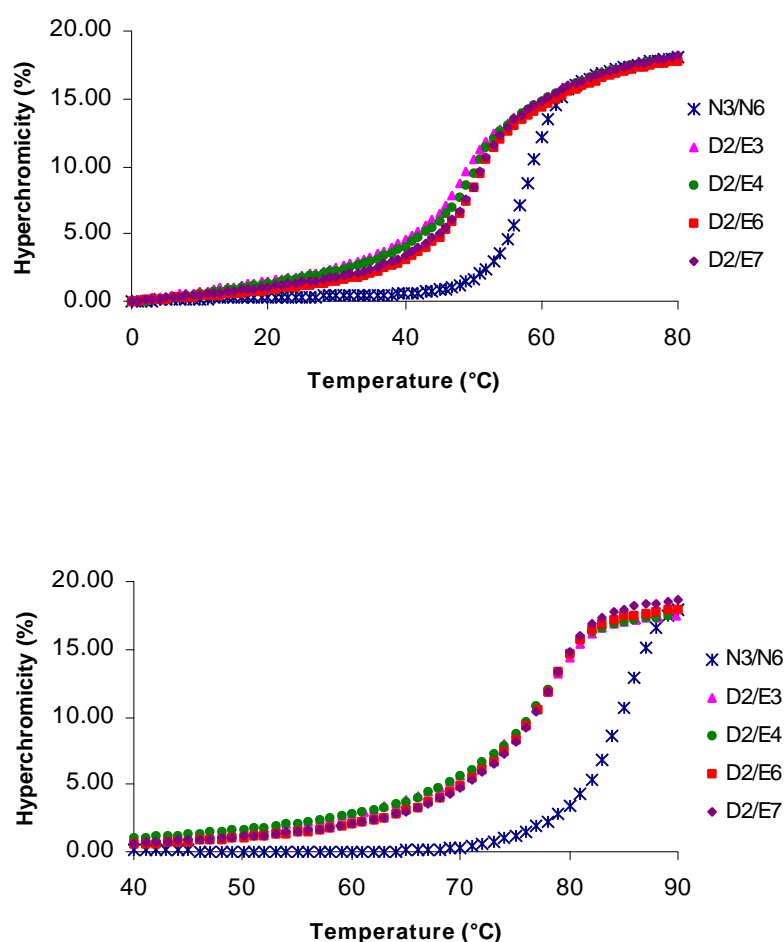


**Figure 5** Melting curves of the unmodified duplex and of the 1,4-anthracene modified strand paired with different ene-modified complementary strands. Conditions: 1.0  $\mu\text{M}$  duplex in 10 mM  $\text{NaH}_2\text{PO}_4$  (pH 5.5) at low (above) and high salt concentration (below).

Oligodeoxyribonucleotide D3 with the new diene-modification **18**, a 2,3-naphthalene derivative with 1,3-propandiol spacers, was paired with different ene-modified complementary strands.

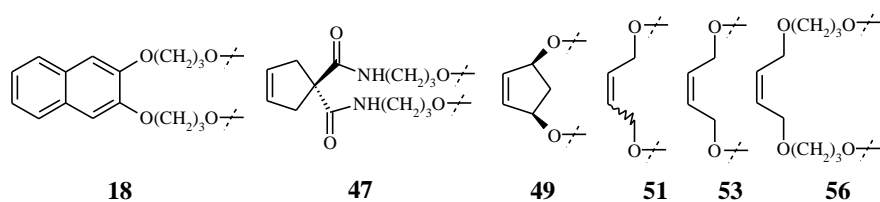
The duplexes between the 1,4-naphthalene derivative modified strand (D3) and the different ene-modified strands are destabilized by 5 °C, compared to the unmodified one. Higher salt concentration results again in a 27°C increase (Table 13).

**Table 13** Melting temperatures of the unmodified duplex and of the 1,4-anthracene-modified strand (D3) paired with different ene-modified complementary strands at different salt concentrations (E3 Y = **47**, E4 Y = **56**, E6 Y = **53**, E7 Y = **51**).

oligonucleotides	0.01M NaCl		1.2M NaCl	
	Tm [°C]	Δ Tm [°C]	Tm [°C]	Δ Tm [°C]
N3/N6	58.5	0.0	85.5	0.0
D3/E3	53.5	-5.0	80.5	-5.0
D3/E4	53.5	-5.0	80.5	-5.0
D3/E6	52.5	-6.0	80.5	-5.0
D3/E7	53.5	-5.0	80.5	-5.0

N3 5'-TGC CGA CGG CTC CGG ACG CGT GCG CAG GCC-3'  
N6 3'-ACG GCT GCC GAG GCC TGC GCA CGC GTC CGG-5'

D3 5'-TGC CGA CGG CTC **18** CGG ACG CGT GCG CAG GCC-3'  
EX 3'-ACG GCT GCC GAG **Y** GCC TGC GCA CGC GTC CGG-5'



All denaturation curves showed cooperative transitions at both salt concentrations (Figure 6).

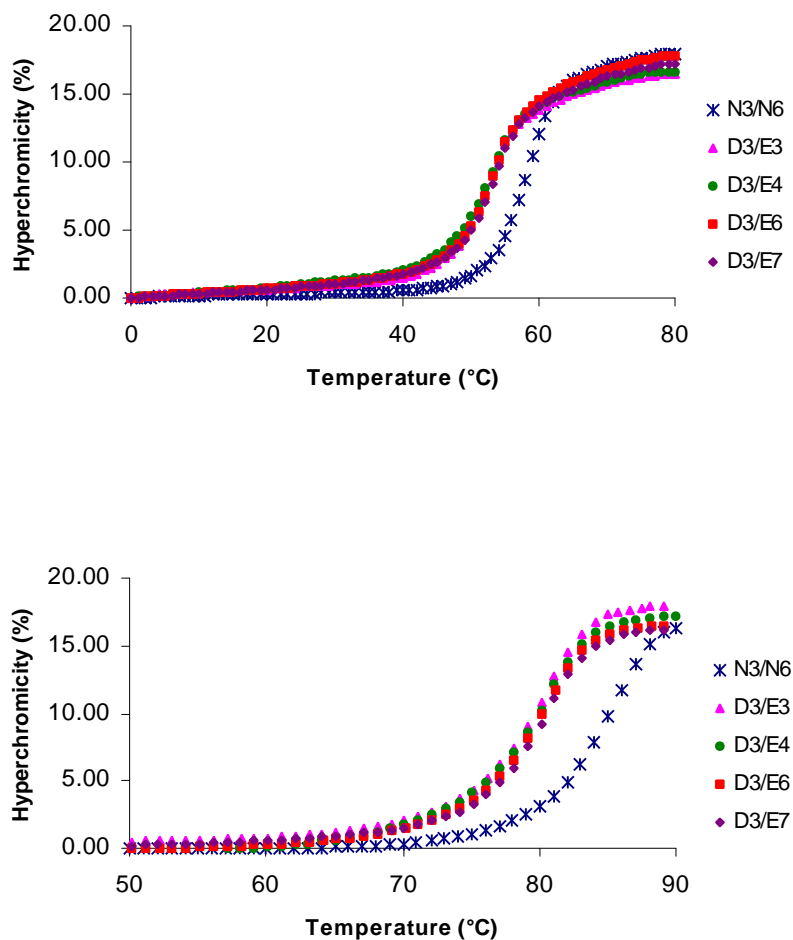


**Figure 6** Melting curves of the unmodified duplex and of the 2,3-naphthalene derivative (**18**) modified strand (D3) paired with different ene-modified complementary strands. Solutions of 1.0  $\mu\text{M}$  duplex in 10 mM  $\text{NaH}_2\text{PO}_4$  (pH 5.5) at low (above) and high salt concentration (below).

We tried to achieve cross-linkage of the different ene-diene duplexes by incubating them in aqueous buffer (25 mM TEAAc, 0.1 M NaCl, pH 5.5) at 50 °C. After two weeks of incubation, denaturing PAGE did not show any cross-linked product. Incubation at 70 °C, at which most of the strands should still be paired, also did not bring any cross linkage. Finally the samples were incubated at 100 °C in sealed micro tubes. These harsh reaction conditions

resulted in the slow degradation of the oligodeoxyribonucleotides; no cross linkage could be observed.

Apparently the ene-residues used here are too electron rich to undergo a *Diels-Alder* reaction at temperatures below 100°C. A further explanation could be the geometrical constraints given by the duplex geometry. The *Diels-Alder* reaction can only take place if the two partners are properly oriented. It is well possible, that, although model considerations predicted differently, this proper orientation is just not possible within the framework given by the duplex.

## 3.4 Cross-Linkage of Diene-Modified Oligodeoxyribonucleotides

### 3.4.1 Interstrand Cross-Linkage with Di-Functional Maleimides

As shown in chapter 3.1 and 3.2, our attempts directed towards the direct interstrand cross-linking of an ene/diene-modified duplex *via* the *Diels-Alder* reaction failed. The most likely reason were – in our opinion – the steric constraints imposed by the duplex geometry. This prevented the two reaction partners to adopt the proper arrangement for the reaction. The missing flexibility could be overcome by using a bifunctional (e.g. maleimide) reagent to cross-link two complementary diene-modified strands. Thus, we set out to explore this “indirect” possibility of interstrand cross-linking *via* the *Diels-Alder* reaction.

We used the three different diene-phosphoramidites of the building blocks shown in Table 14. They contain spacers of different lengths, which are connected *via* ether bonds to the diene-moiety. Spacers of different lengths were chosen in order to introduce different degrees of flexibility in the modified duplex, which was, again, expected to play an important role.

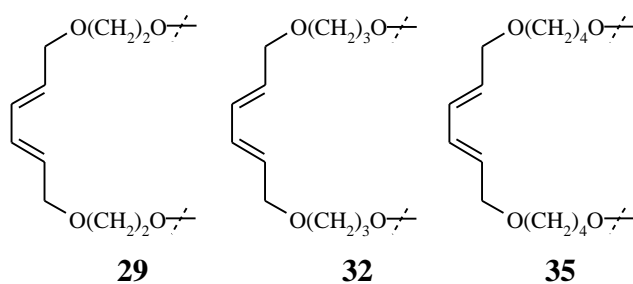
The different diene-building blocks, one at a time, were integrated into the strands opposite to each other, resulting in the oligonucleotide pairs shown in Table 14.

First, we investigated the pairing properties of the modified strands. The modified duplexes were compared with the unmodified duplex of the same sequence, just without the diene-building blocks. The  $T_m$ -values in Table 14 were calculated from the melting curves in Figure 7.

**Table 14** Melting temperatures of the natural and diene-modified duplexes, at 100 mM NaCl and the oligonucleotide sequences with the corresponding diene-phosphoramidites.

oligonucleotides	mp [°C]	$\Delta$ mp [°C]
N17/N18	49.5	0
D24/D25	30.5	-19.0
D26/D27	32.5	-17.0
D28/D29	33.0	-16.5
D24/D29	27.5	-22.0

N17	5'-CTG AAT CGA CCG GTA TCA GT-3'
N18	3'-GAC TTA GCT GGC CAT-5'
D24	5'-CTG AAT <b>29</b> CGA CCG GTA TCA GT-3'
D25	3'-GAC TTA <b>29</b> GCT GGC CAT-5'
D26	5'-CTG AAT <b>32</b> CGA CCG GTA TCA GT-3'
D27	3'-GAC TTA <b>32</b> GCT GGC CAT-5'
D28	5'-CTG AAT <b>35</b> CGA CCG GTA TCA GT-3'
D29	3'-GAC TTA <b>35</b> GCT GGC CAT-5'



Melting curves of the unmodified and the modified duplex as well as of a duplex with different diene-modifications in the two complementary strands show sigmoidal shapes with one transition (Figure 7).

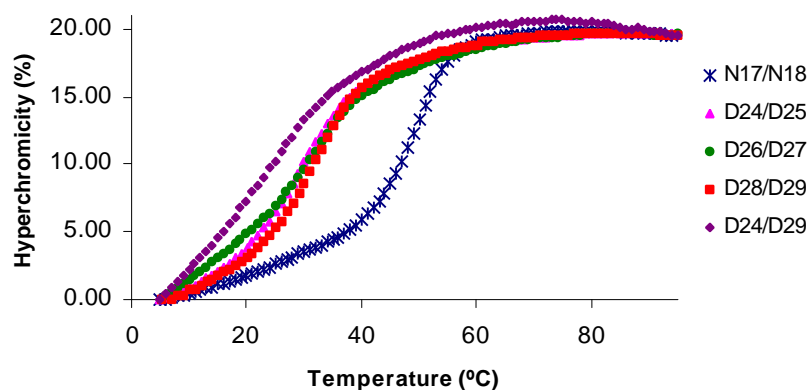
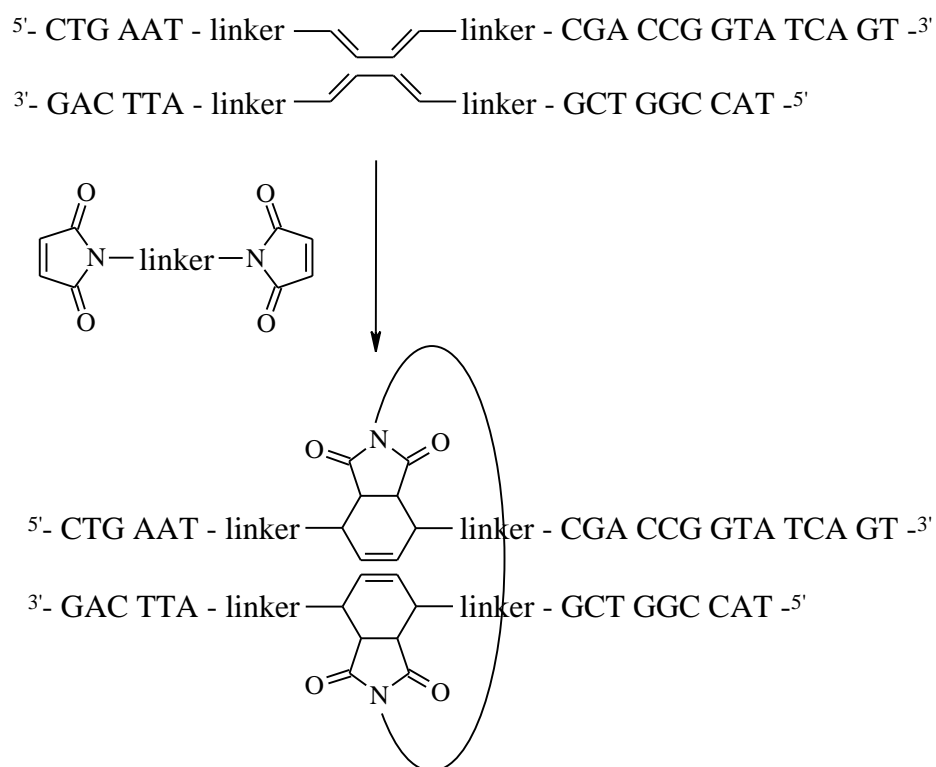


**Figure 7** Melting curves of the natural and diene-modified duplexes. Conditions: 1.0  $\mu$ M duplex in 10 mM TrisHCl (pH 4.2) and 100mM NaCl.

Within the experimental error of the melting experiments, all duplexes with the same modification in both strands showed the same degree of destabilization. We observed an average destabilization of 18 °C compared to the unmodified duplex. In the case of the duplex with unequal modifications in the complementary strands, an even larger destabilization of 22°C was found. Destabilizations of these dimensions show that the modifications do not support a continuous duplex. The observed melting temperatures are even lower than the one of the longer partial duplex. The  $T_m$  of the shorter stem, which is estimated between 15 °C and 20, °C was not observed.

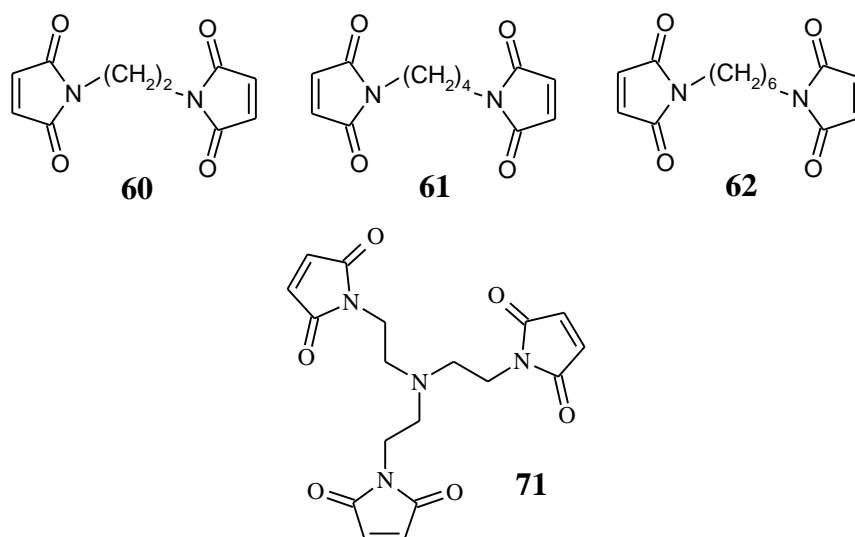


In a next step, the diene-modified duplexes were incubated in aqueous solution, at room temperature, under slightly acidic conditions (10 mM TrisHCl, pH 5.2), with the different dimaleimides. The expected cross-linking process is illustrated in Scheme 37.



Scheme 37 Schematic illustration of the cross-linkage of a diene-modified oligodeoxyribonucleotide duplex with a dimaleimide.

To determine the influence of the dimaleimide bridge, dimaleimides with alkyl chain linkers of different lengths were used in the cross-linking experiments. In addition, a trimaleimide was included in these studies (Scheme 38).



**Scheme 38** Dimaleimides and trimaleimide used to cross-link diene-modified oligodeoxyribonucleotides.

The cross-linking process was monitored by melting curve experiments. We first recorded the melting curve of a solution of duplex D24/D25, modified with the ethleneglycol spaced butadiene **29**, in 10 mM TrisHCl (pH 5.2) and 100 mM NaCl. Straight after adding one equivalent of dimaleimide **62** a second melting curve was recorded, which was still congruent with the first one. The solution was then incubated at 25 °C and additional melting experiments were taken after three days and one week. The different stage of the cross-linking reaction are shown in Figure 8. The melting curves reveal a rise in duplex stability. The curve taken after three days shows the presence of some non-cross-linked (lower transition) and some cross-linked material. After seven days, only cross-linked duplex is observed.

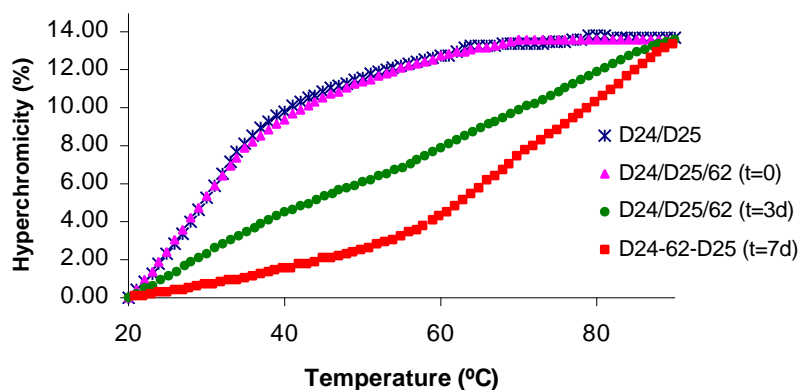


**Figure 8** Melting curves of different stages of a cross-linking experiment of the duplex D24/D25 with the dimaleimide **62**. Reaction times are indicated in days. Conditions: 1.0  $\mu$ M duplex in 10 mM TrisHCl (pH 4.2) and 100 mM NaCl.

After establishing an approximate reaction time required for this type of cross-linking, an extended study involving the diene-modified duplexes D24/D25, D26/D27 and D28/D29 with the maleimides **60-62** was performed. The different modified duplexes were incubated under the same conditions as mentioned above with two equivalents of the different dimaleimides, one at a time. After one week of incubation, the solutions were desalted and analysed by denaturing PAGE (Figure 9). The two bands of the modified 16 and 21 bases long complementary sequences D26 and D27 can be observed in lane 2 of the gel, serving as controls. The following lanes of the gel, show the different reaction products. An additional band, which corresponds to the respective cross-linked duplexes, can be seen in all reactions. In lane 3, an additional band with slightly higher mobility than the cross-linked duplex is observed. Mass spectrometry showed only the masses of the educts and the cross-linked product. We have, at present, no firm explanations for the existence of two different species with the same mass.

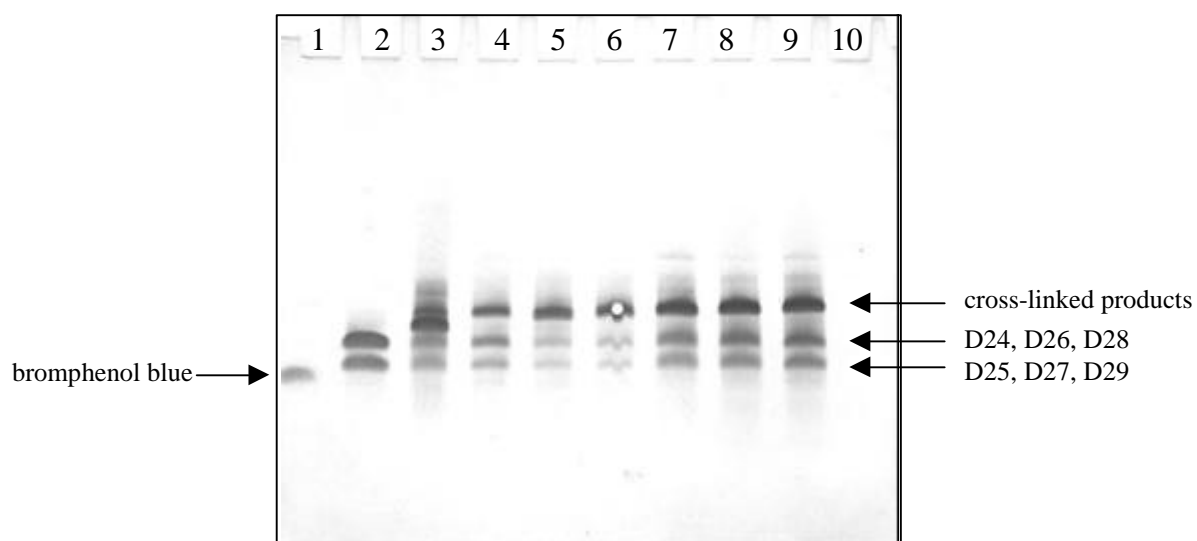
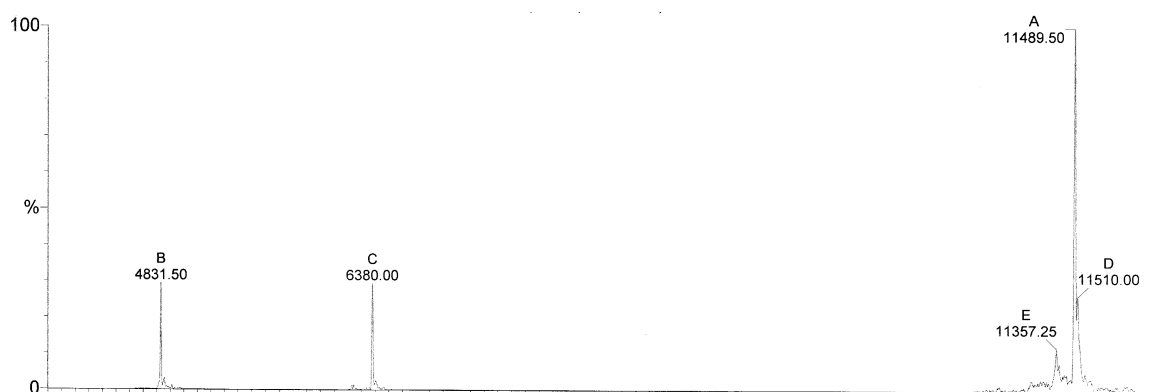


Figure 9 Denaturing PAGE of the modified and partially cross-linked oligodeoxyribonucleotides after incubation with 2 equivalents of dimaleimide.

Lanes: 1 dye, 2 D26/D27, 3 D24/D25/61, 4 D26/D27/60, 5 D26/D27/61, 6 D26/D27/62, 7 D28/D29/60, 8 D28/D29/61, 9 D28/D29/62, 10 empty.

The mass spectra of duplex D24/D25 after incubation with two equivalents of dimaleimide **62**, for one week at 25 °C (Figure 10), shows the mass of the two single strands D24 (B) and D25 (C), and the mass of the cross-linked duplex D24-62-D25 (A). The sample was desalted but not further purified. A very interesting aspect is the absence of peaks with the mass corresponding to single strands that reacted with the dimaleimide without subsequent cross-linkage. Since the reactions were carried out in the presence of an excess of dimaleimide, this product might – a priori – be expected. The absence of these products, however, indicates that the *Diels-Alder* reaction of the dimaleimide with the first strand is slow, while the cross-linkage to the complementary strand is fast. So the first reaction is the rate limiting step.



**Figure 10** ES-MS of the crude material obtained from the cross-linking reaction of the duplex D26/D27 with the dimaleimide **62**.

The reaction mixtures obtained from the cross-linking reactions were further purified with RP HPLC. The cross-linked products were obtained in high purity for further investigations. A dramatic increase of the melting temperature was observed after cross-linking of the modified duplex D24/D25 with each of the three dimaleimides (Table 15). Obviously, the stability increases with the length of the cross-linking chain. While the 1,2-ethylenedimaleimide linked duplex (D24-60-D25) is 19 °C more stable than the modified duplex (D24/D25), the longer dimaleimide linkers rise the melting temperature by 45 °C and 53 °C. The 1,6-hexamethylen cross-linked duplex shows a second transition at 68 °C (Table 15).

**Table 15** Melting temperatures of the ethyleneglycole linked bis-diene-modified duplex D24/D25<sup>1</sup> and the cross-linked duplexes after the reaction with the dimaleimides **60-62** at 100mM NaCl.

oligonucleotides	T <sub>m</sub> [°C]	Δ T <sub>m</sub> [°C]
D24/D25	30.5	0
D24-60-D25	59.5	+19.0
D24-61-D25	75.5	+45.0
D24-62-D25	67.5 / 83.5	+37.0 / +53.0

D24	5'-CTG AAT <b>29</b> CGA CCG GTA TCA GT-3'
D25	3'-GAC TTA <b>29</b> GCT GGC CAT-5'

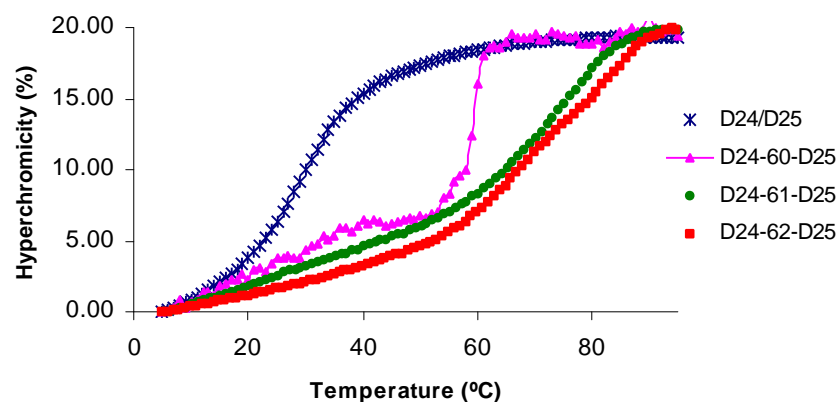
**29**

**60**                      **61**                      **62**

The cross-linked duplex can also be regarded as two connected hairpin mimics, which may denaturate at different temperatures. What we observe at 67.5 °C might therefore correspond to the denaturation of the six base pair stem of the shorter hairpin and the 84 °C transition would consequently correspond to the melting of the longer stem. We assume that in the cross-linked duplex D24-61-D25 the analogous two transitions are simply not resolved. Therefore, only one apparent transition with an average T<sub>m</sub> is observed (Figure 11).

<sup>1</sup> For reasons of simplicity we have decided to keep the compound numbers of the respective dimaleimides also for the cross-linking bridge after the *Diels-Alder* reaction with the diene-modifications.



**Figure 11** Melting curves of the ethyleneglycole linked bis-diene-modified duplex D24/D25 and the cross-linked duplexes after the reaction with the dimaleimides **60-62**. Conditions: 1.0  $\mu$ M duplex in 10 mM TrisHCl (pH 4.2) and 100mM NaCl.

The strands with the 1,3-propanediol spaced building blocks D26/D27 were, in addition to the three dimaleimides, also reacted with tris-(2-ethlenemaleimide)amine (**71**). The melting curves of the product duplexes are shown in Figure 12. All cross-linked duplexes show two more or less pronounced transitions, which become more obvious in the curves of the first derivate (Figure 13).

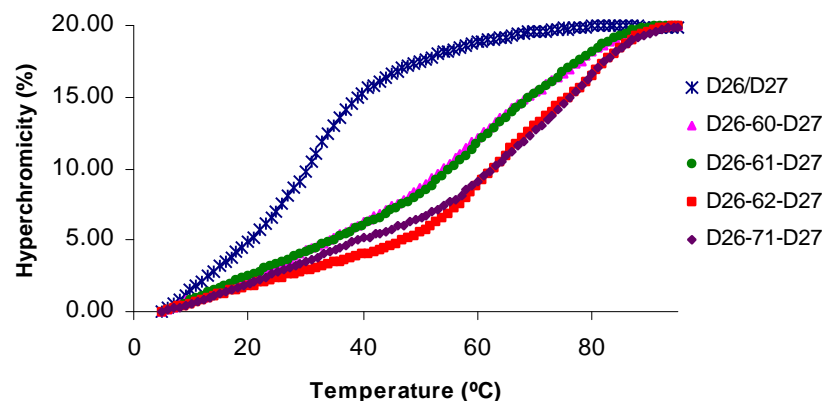


**Figure 12** Melting curves of the 1,3-propanediol bis-diene-modified duplex D26/D27 and the cross-linked duplexes after the reaction with the dimaleimides **60-62** as well as the trimaleimide **71**, at 100mM NaCl.

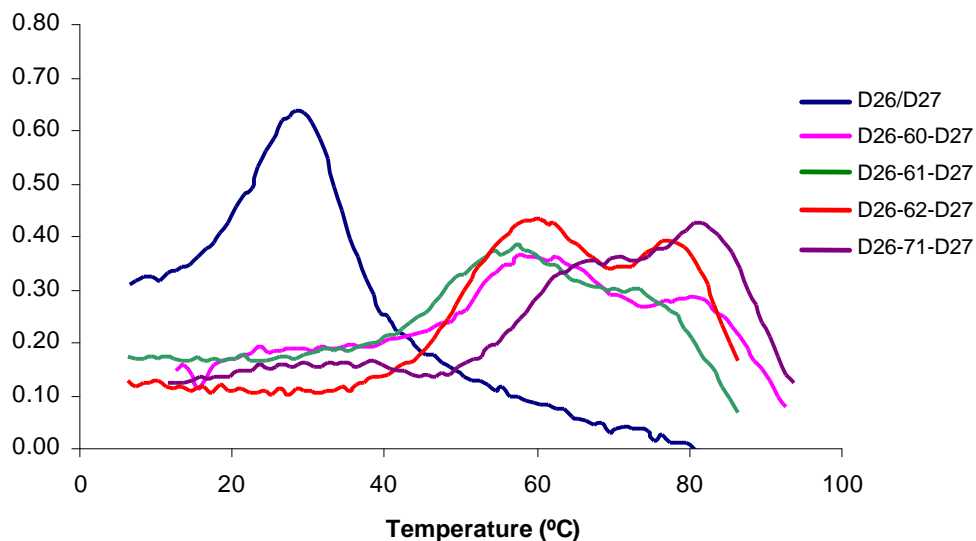


Figure 13 First derivate of the melting curves shown in Figure 12.

While a large difference in stability was observed in the previous melting experiment between the product with the short linker and the two others, all three cross-linked hybrids showed very similar melting curves (Figure 14) and transition temperatures in the present series (Table 16). Apparently, the present duplex (D26/D27) with somewhat extended spacers connecting the dienes into the phosphate backbones of the two strands possesses more flexibility and, thus, better tolerates the relatively short ethyleneglycol linker of the dimaleimide **60**.

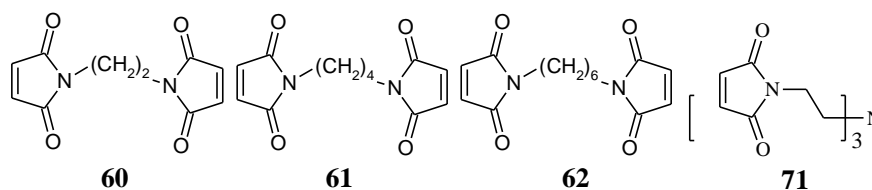
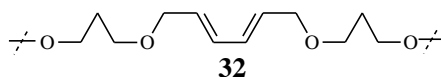


The analogous experiment with trimaleimide **71** gave rise to a cross-linked duplex just as with the dimaleimides. MS analysis showed that the third maleimide was unreacted. It provides, thus, an additional reactive function, which is available for further conjugation or modification.

**Table 16** Melting temperatures of the 1,3-propanediol linked, bis-diene-modified duplex D26/D27 and the cross-linked duplexes after the reaction with the dimaleimides **60-62** as well as the trimaleimide **71**, at 100mM NaCl.

oligonucleotides	T <sub>m</sub> [°C]	Δ T <sub>m</sub> [°C]
D26/D27	32.5	0
D26-60-D27	60.5 / 78.5	+28 / +46.0
D26-61-D27	60.5 / 78.5	+28 / +46.0
D26-62-D27	63.5 / 80.5	+31 / +48.0
D26-71-D27	64.5 / 80.5	+32 / +48.0

D26 5'-CTG AAT **32** CGA CCG GTA TCA GT-3'  
 D27 3'-GAC TTA **32** GCT GGC CAT-5'



Cross-linkage of the duplexes containing the 1,4-butanediol spaced modification **35** results, again in a considerable stabilization. Two transitions are observed with all three dimaleimides (Figure 14).

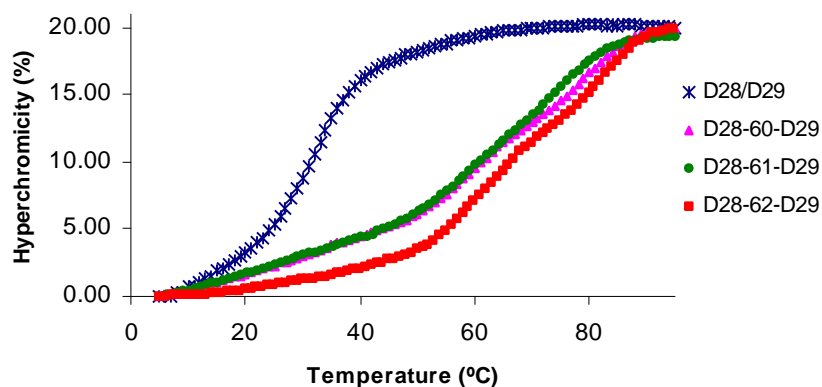


Figure 14 Melting curves of the 1,4-butanediol linked, bis-diene-modified duplex D24/D25 and the cross-linked duplexes after the reaction with the dimaleimides **60-62**. Conditions: 1.0  $\mu$ M duplex in 10 mM TrisHCl (pH 4.2) and 100mM NaCl.

One slight difference was observed, however: while in the previous two series a steady increase in stability was observed with increasing length of the cross-linker, the middle sized, 1,4-butane derived cross-linker was the least stable of all three products (Table 17), although the differences are relatively small.

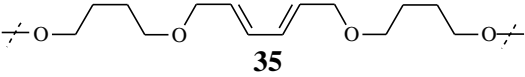
**Table 17** Melting temperatures of 1,4-butanediol, linked bis-diene-modified duplex D24/D25 and the cross-linked duplexes after the reaction with the dimaleimides **60-62** at 100mM NaCl.

oligonucleotides	T <sub>m</sub> [°C]	Δ T <sub>m</sub> [°C]
D28/D29	33.0	0
D28-60-D29	59.5/80.5	+26.5 / +47.5
D28-61-D29	59.5/76.5	+26.5 / +43.5
D28-62-D29	63.5/82.5	+30.5 / +49.5

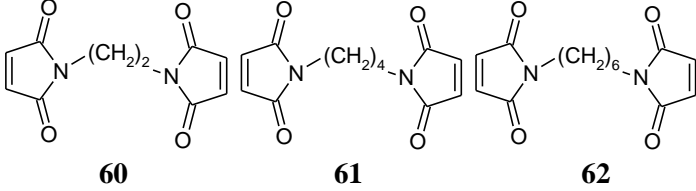
D28	5'-CTG AAT <b>35</b> CGA CCG GTA TCA GT-3'
D29	3'-GAC TTA <b>35</b> GCT GGC CAT-5'



**35**

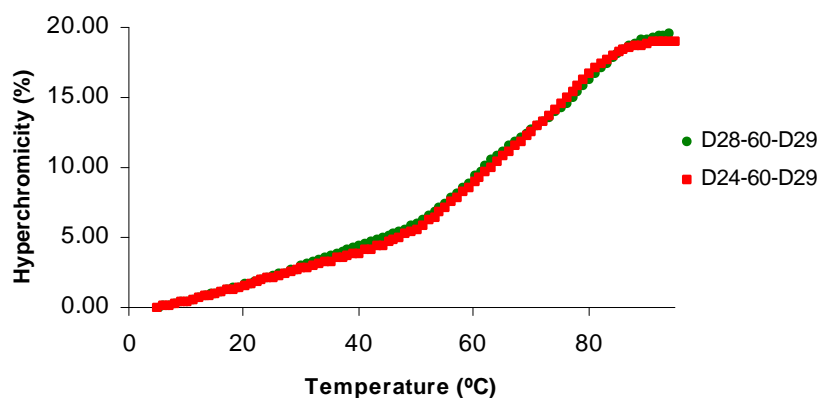
  



**60**                      **61**                      **62**

Finally, we also investigated – in one case – the cross-linking reaction of two complementary strands containing non-identical diene-modifications. For this purpose, the duplex D24/D29, prepared from building blocks **29** and **35**, respectively, was incubated with dimeleimide **60** under the same conditions as described before (Table 18).

Only marginal differences were obtained compared to the product obtained with the duplex containing identical dienes. Figure 15 shows the melting curve obtained in this reaction. It is nearly superimposable to the one obtained in the previous cross-linking experiment of the duplex D28/D29 with dimaleimide **60**.



**Figure 15** Melting curves of the cross-linked duplexes D28/D29, with the same diene-modifications in both strands, and D24/D29 with the short diene-modification **29** in the first and the long one **35** in the second strand, with ethylenedimaleimide (**60**). Conditions: 1.0  $\mu$ M duplex in 10 mM TrisHCl (pH 4.2) and 100mM NaCl..

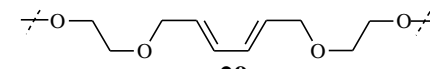
**Table 18** Comparison of melting temperatures of the cross-linked duplexes D28/D29 and D24/D29 linked *via* dimaleimide **60**.

oligonucleotides	T <sub>m</sub> [°C]	Δ T <sub>m</sub> [°C]
D28-60-D29	59.5/80.5	0
D24-60-D29	58.5/77.5	-1.0 / -3.0

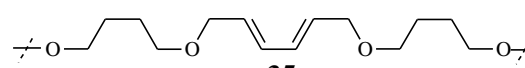
  

D24	5'-CTG AAT <b>29</b> CGA CCG GTA TCA GT-3'
D28	5'-CTG AAT <b>35</b> CGA CCG GTA TCA GT-3'
D29	3'-GAC TTA <b>35</b> GCT GGC CAT-5'

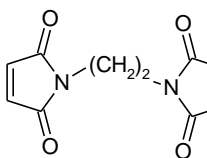
  



**29**



**35**



**60**

We subsequently compared the influence of the spacer length in the diene-modifications, on the stability of cross-linked duplexes. Therefore, the following tables contain the T<sub>m</sub>s of the different duplexes cross-linked with a given dimaleimide. We assume, that the transition at higher temperature correspond to the melting of the longer hairpin-moiety (as described before). The melting temperatures of the different duplexes, cross-linked with the ethylene-bridge (**60**) indicate an increasing stability towards longer alkyl spacers in the diene-modifications. While the first extension of the spacers in the phosphate backbones results in a stabilisation of 19 °C, the second extension had just an additional stabilising effect of 2 °C. This fact indicates the necessity of a minimal flexibility of the diene-modifications, which is not warranted in the case of the cross-linked duplex D24-60-D25 (Table 19).

Table 19 Melting temperatures of the ethylenedimaleimide (**60**) cross-linked duplexes, at 100mM NaCl.  $\Delta T_m$  refers to the transition at higher temperature.

oligonucleotides	T <sub>m</sub> [°C]	$\Delta T_m$ [°C]
D24-60-D25	59.5	0
D26-60-D27	60.5/78.5	+19.0
D28-60-D29	59.5/80.5	+21.0

The melting temperatures of all duplexes linked with dimaleimide **61** are in the same range (Table 20). The largest difference in stability among the duplexes is 3 °C, which is almost within the experimental tolerance. The longer dimaleimide **61** seems to compensate the missing flexibility of the short diene-modifications observed in cross-linking with dimaleimide **60**.

Table 20 Melting temperatures of the tetramethylenedimaleimide (**61**) cross-linked duplexes, at 100mM NaCl.  $\Delta T_m$  refers to the transition at higher temperature.

oligonucleotides	T <sub>m</sub> [°C]	$\Delta T_m$ [°C]
D24-61-D25	75.5	0
D26-61-D27	60.5/78.5	+3.0
D28-61-D29	59.5/76.5	+1.0

Also the comparison of the diene-modified duplexes cross-linked with dimaleimide **62** does not result in large differences. The slightly lower T<sub>m</sub> of the cross-linked duplex D28-62-D29, with the longest diene-modification, could indicate the beginning of a decrease of stability caused by excessive flexibility of the diene – dimaleimide combination (Table 21).

Table 21 Melting temperatures of the hexamethylenedimaleimide (**62**) cross-linked duplexes, at 100mM NaCl.  $\Delta T_m$  refers to the transition at higher temperature.

oligonucleotides	$T_m$ [°C]	$\Delta T_m$ [°C]
D24-62-D25	67.5/83.5	0
D26-62-D27	63.5/80.5	+3.0
D28-62-D29	63.5/82.5	+2.0

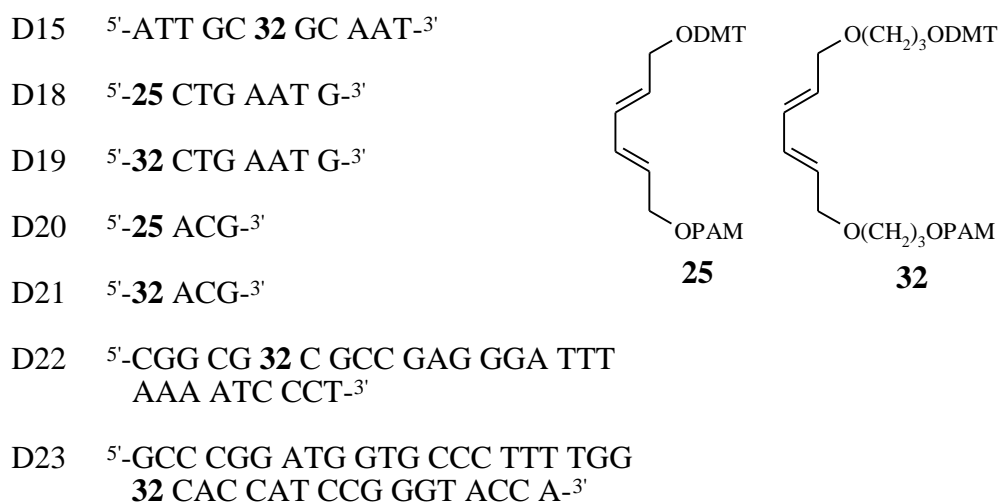
There seems to exist a minimal flexibility of the cross-link part, which is dependent on the length of the spacers in the diene-modification and of the length of the dimaleimide linker to result in a good duplex stabilization. Once, this flexibility is reached, longer spacers and linkers have a minor influence on duplex stability. Table 22 gives an overview of the  $T_m$ s observed with the different cross-linked duplexes.





### 3.4.2 Experiments Towards the Cross-Linking of Non-complementary DNAs with Dimaleimide Reagents

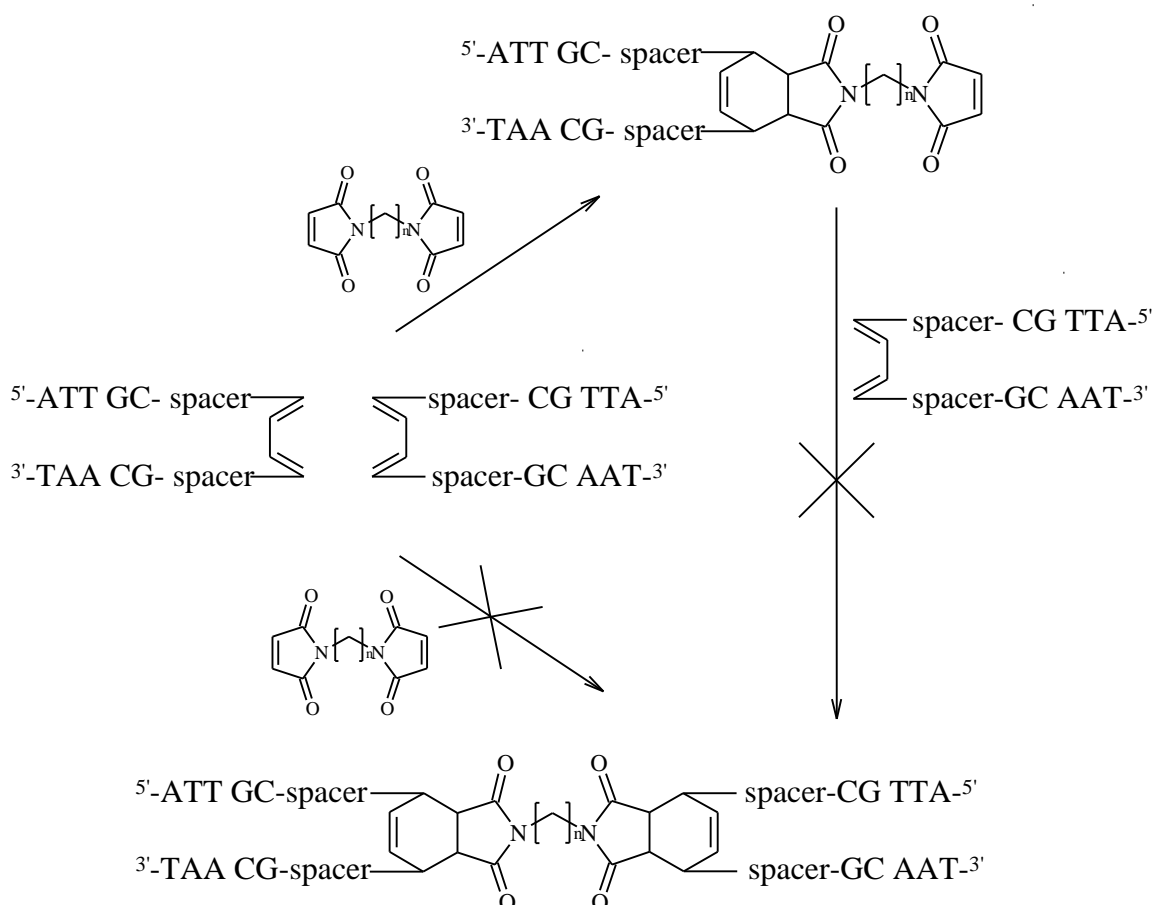
Here we describe our efforts to cross-link diene-modified oligodeoxyribonucleotides, which are not complementary. For this purpose, several oligodeoxyribonucleotides bearing a diene-modification in different places were synthesized using phosphoramidites **25** and **32**. The different modified oligodeoxyribonucleotides prepared this way are shown in Scheme 39.



Scheme 39 Sequences of different diene-modified oligonucleotides used in this study.

### 3 RESULTS AND DISCUSSION

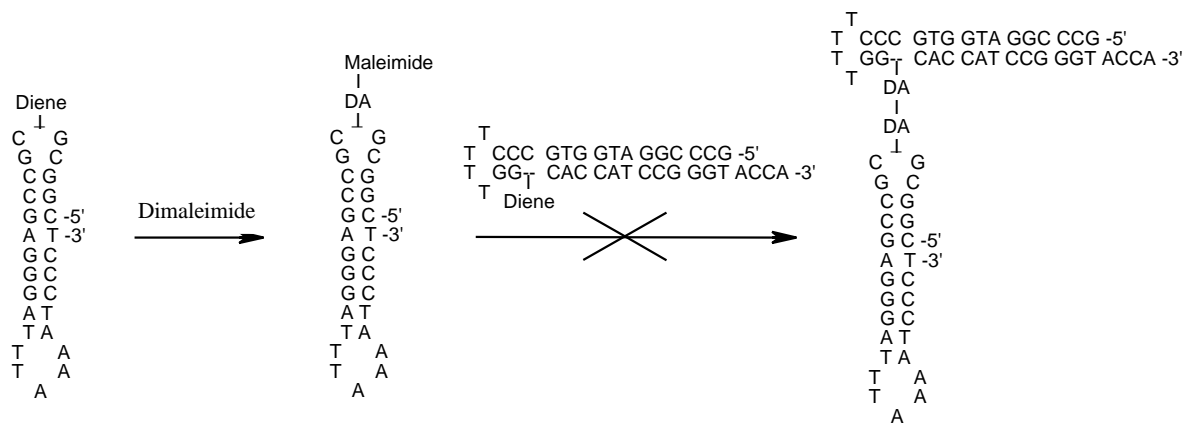
Incubation of the different diene-modified oligodeoxyribonucleotides (Scheme 40) with 0.5 equivalent of dimaleimide **62**, in aqueous media, resulted in a partial dimaleimide conjugation to single strands. In no case, however, linkage of two strands *via* the dimaleimide could be detected, neither by denaturing PAGE analysis nor by mass spectrometry.



**Scheme 40** Linkage of hairpin mimics *via* *Diels-Alder* reaction, with the hairpin mimic – dimaleimide adduct as the only product.

To gain more detailed insight into the problem, and to have the possibility of interconnecting two different diene-modified oligodeoxyribonucleotides, the experiment was divided into two steps. First, one type of oligodeoxyribonucleotide was incubated with an excess of the dimaleimide to obtain the respective conjugate. After isolation and characterisation of these

first adducts they were incubated with one equivalent of the second, diene-modified nucleic acid (Scheme 41).



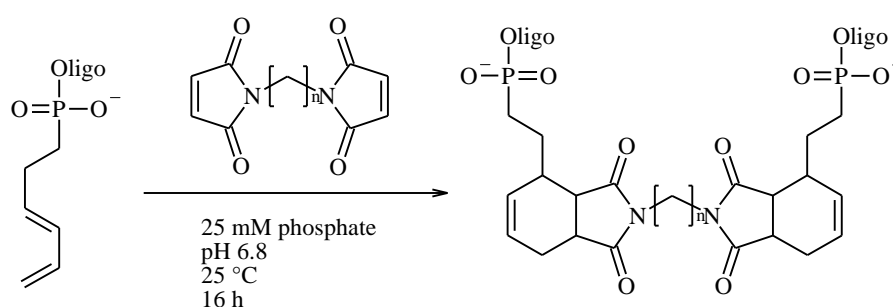
**Scheme 41** Stepwise linking of different diene-modified DNAs with difunctional maleimides.

The mono-adducts could be isolated in good yields. Their identity was verified by mass spectroscopy. However, neither denaturing PAGE nor MS showed any sign of successful linkage of two strands in subsequent reactions.

### 3 RESULTS AND DISCUSSION

---

In 2001 *Hill et al.*<sup>77</sup> mentioned the successful cross-linkage of a 5'-end diene-modified, truncated, oligodeoxyribonucleotide of the sequence 5'-CCA GTA CAA GGT GCT AAA CGT AAT GG<sup>-3'-3'</sup>-T<sup>-5'-5'</sup>-T<sup>-3'</sup>, using conditions similar to ours. They reported an 80 % yield, relative to the dimaleimide, of the cross-linked oligodeoxyribonucleotide after treatment with 0.33 equivalents of 1,6-hexamethyldimaleimide (**62**). No experimental or analytical details were given (Scheme 42).



Scheme 42 Conjugation reaction described by *Hill et al.*<sup>77</sup>

Surprisingly this remains the only hint to a successful linkage of non-complementary oligonucleotides. In other reports of non-enzymatic templated linkage of oligonucleotides bearing a big variety of modifications via different reaction types, no or very little linkage was observed in the absence of a template.<sup>59-62</sup>

### 3.5 Bioconjugation of Diene-Modified Oligodeoxyribonucleotides

As described in the previous chapters, we could successfully realise the cross-linkage of two complementary diene-modified DNA strands with dimaleimides. Analogous cross-linking experiments with non-complementary nucleic acids, however, failed. The failure could be attributed to the second step of the process. While the formation of mono-adducts *via* a *Diels-Alder* reaction took place quite readily, the second *Diels-Alder* reaction, the cross-linking, could not be observed. Apparently, template assistance is required for an efficient second step. We therefore decided to concentrate on the “first” reaction, i.e. the formation of mono *Diels-Alder* adducts. Some applications (and the scope) of this method for the bioconjugation of synthetic nucleic acids will be shown in this section.

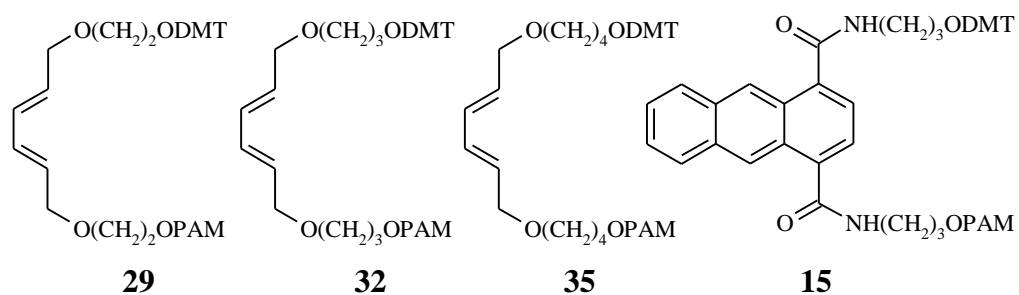
#### 3.5.1 Hairpin Mimics containing Diene-Building Blocks as Loop Replacements

The hairpin belongs to the most common secondary structural motifs found in nucleic acids.<sup>189</sup> In RNA, it is an essential element for the assembly of higher order structures. By enabling the proper folding, the hairpin contributes to the many functional properties of RNA. Extra stable hairpins containing four bases in the loop (tetraloops) have emerged as a distinct class of hairpins, which forms highly specific interactions with tetraloop receptor sites.<sup>189-191</sup> The hairpin motif is also found in DNA,<sup>192,193</sup> though to a much lesser extent due to the intrinsically double stranded nature of DNA. This central role of the hairpin as a structural and functional element has stimulated the design and synthesis of chemically modified hairpin analogs. Hairpin mimics can serve as tools for the investigation of structure and function of nucleic acids. In addition, they are increasingly gaining importance as building blocks for the construction of defined, nucleic acids based molecular structures.<sup>194</sup> Thus, the hairpin loop has been replaced with flexible oligo ethylene glycol linkers<sup>195-197</sup> as well as with more rigid aromatic derivatives<sup>198-202</sup> and metal complexes.<sup>203,204</sup> Furthermore, the construction of a stilbene-based hairpin mimic forming G-tetrad has been reported very recently.<sup>205,206</sup>

### 3 RESULTS AND DISCUSSION

---

Replacement of the loop region of a diene-building block would lead to a reactive hairpin mimic and, thus, add an additional level of functionality. To study the stability of diene-modified hairpin mimics, diene-phosphoramidites shown in Scheme 43 were incorporated into self complementary oligodeoxyribonucleotides.



Scheme 43 Phosphoramidites used for hairpin mimic synthesis.

The hairpin mimics were designed to have a five base pair stem. The different diene-building blocks served as a loop replacements. Their stabilities were compared with unmodified hairpins containing the same stem and a loop of four natural bases, A or T. The data are shown in Table 23.

**Table 23** Melting temperatures of the different diene-modified hairpin mimics and the respective T<sub>4</sub> and A<sub>4</sub> hairpins, at 100 mM NaCl.

oligonucleotides	T <sub>m</sub> [°C]	Δ T <sub>m</sub> [°C]
N15	57.8	0
N16	56.8	-1.0
D15	66.5	+8.7
D16	63.5	+5.7
D17	65.5	+7.7

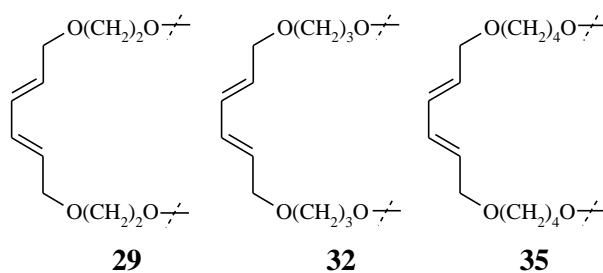
N15 5'-ATT GCT TTT GCA AT-3'

N16 5'-ATT GCA AAA GCA AT-3'

D15 5'-ATT GC **32** GC AAT-3'

D16 5'-ATT GC **29** GCA AT-3'

D17 5'-ATT GC **35** GC AAT-3'



The melting curves of the unmodified hairpins and the hairpin mimics all show sigmoidal shape, which indicates a cooperative melting process (Figure 16).

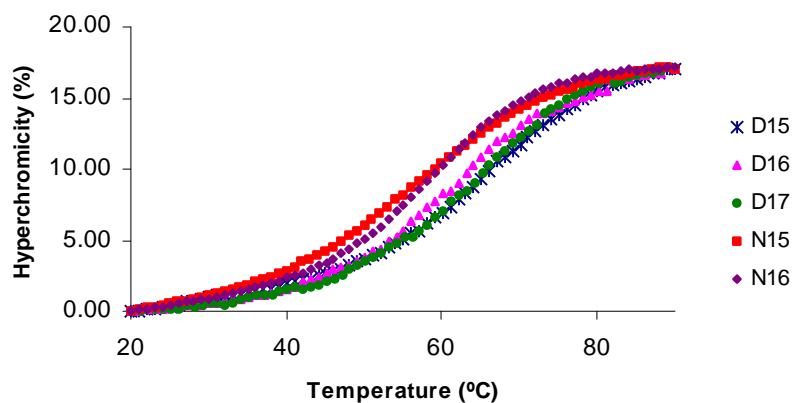


**Figure 16** Melting curves of different hairpin mimics and the respective T<sub>4</sub>- and A<sub>4</sub>-hairpins. Oligomer concentration 2.5  $\mu$ M, 10 mM Tris-HCl, 100 mM NaCl, pH 7.5.

Circular dichroism spectroscopy of diene-modified hairpin mimic D15 and of the corresponding unmodified hairpins was consistent with a B-form DNA (Figure 17). This structural information was later used for molecular modeling studies of the hairpin mimic structures.

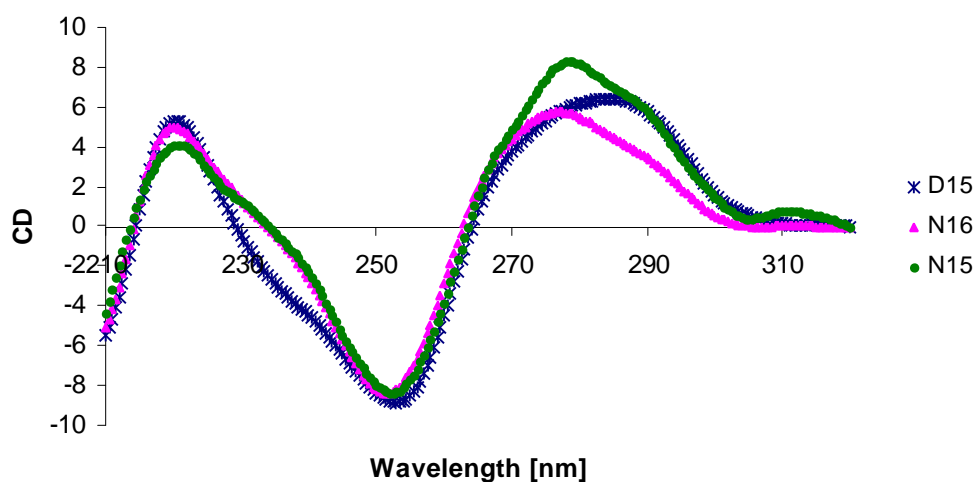


**Figure 17** CD spectra of the hairpins and the diene-modified hairpin mimic. Oligomer concentration 2.5  $\mu$ M, 10 mM Tris-HCl, 100 mM NaCl, pH 7.5.



The melting temperatures of the hairpins with the T<sub>4</sub>- and A<sub>4</sub>-loops, are about 57 °C while the hairpin mimics are between 5.7 °C and 8.7 °C more stable. Oligodeoxyribonucleotide D15 with building block **32** has the highest stability. One could expect to observe a correlation of the melting temperature versus spacer length, and a maximal melting temperature at a certain spacer length. In fact, however, the stabilities of the different hairpin mimics do not vary dramatically. Furthermore, considering the experimental error involved in the measurements, which is about ±1 °C, the three values are rather close. Thus the influence of the spacer length is, within these dimensions, not as big as it might have been expected.

Molecular modelling and structure optimisation with *Hyperchem*<sup>TM</sup> resulted in the models shown in Figure 18. The diene-function of the building blocks is positioned on the top of the hydrophobic core of the hairpins. The distance between the ring systems of the base pair next to the modification and the diene-function, corresponds approximately to the distances between the different base pairs. Since a butadiene is not likely to contribute substantially to  $\pi$ -stacking the close proximity of the linker and the bases of the stem is rather due to general hydrophobic interactions.

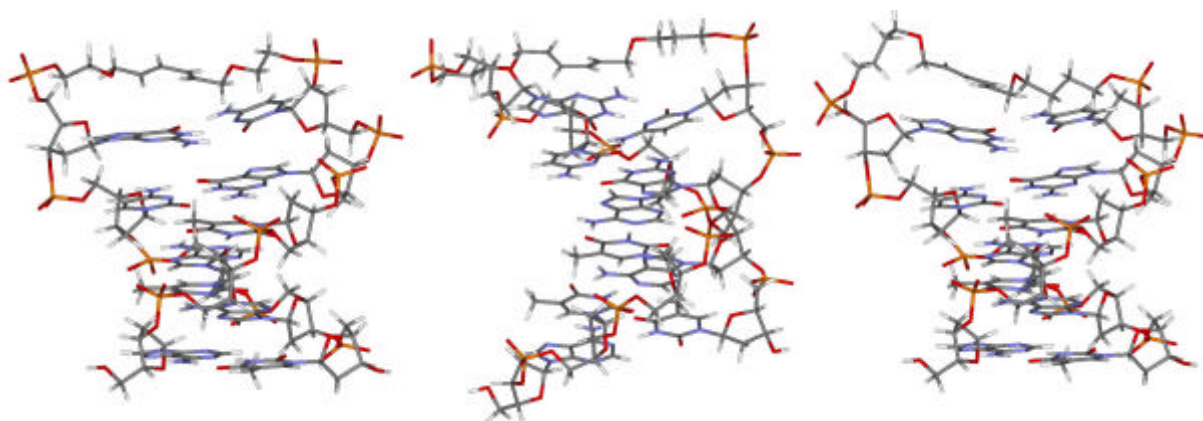


**Figure 18** Optimised structures of the hairpin mimics D16 (left), D15 (middle) and D17 (right), according to *amber* force field calculations (*Hyperchem*<sup>TM</sup>).

An increase in the melting temperature of 8.7 or 9.7°C was observed for D15 compared to the analogous hairpins containing a T<sub>4</sub> or A<sub>4</sub> loop, respectively. The melting curves (Figure 16) showed a single, cooperative transition. Furthermore, melting temperatures were independent of the oligomer concentration, which indicates a unimolecular process, i.e. formation and melting of the hairpin.

According to *amber* force field calculations (*HyperChem*<sup>TM</sup>), both possible diene conformations (i.e. *s-cis* and *s-trans*) form a stable hairpin-like secondary structure. The phosphate-phosphate distance between the two strands (17.7Å and 17.5Å for the *s-cis* and *s-trans* conformer, respectively) corresponds well with the 17.5Å observed in an ideal B-DNA. Since the *s-cis* isomer represents the relevant conformation for the subsequent *Diels-Alder* reaction, the hairpin mimic is presented in this orientation in Figure 19. The model shows the non-nucleotidic linker on top of the helix, bridging the two nucleic acid strands. The plane of the diene is oriented parallel to the adjacent base pair, providing the proper arrangement for reaction with dienophiles.

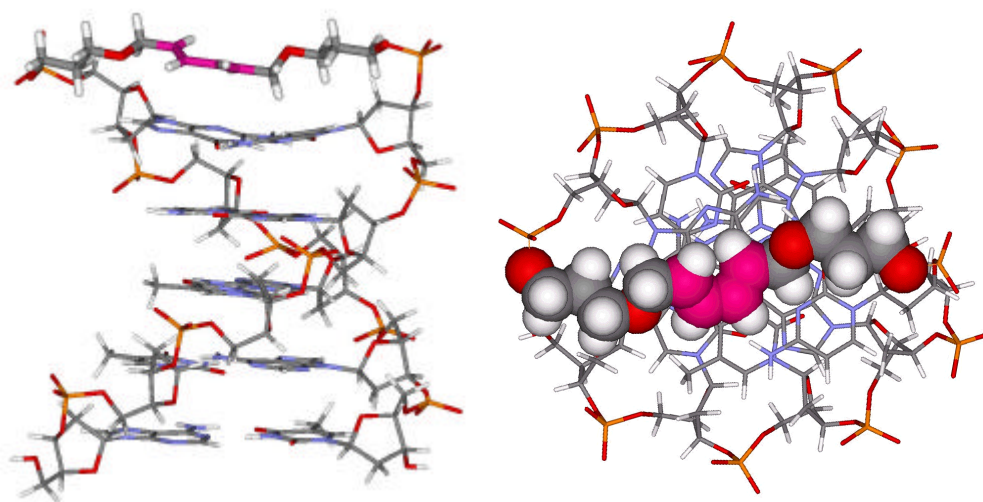


**Figure 19** Molecular model of 1,3-butadiene-derived DNA hairpin mimic D15 (*HyperChem*<sup>TM</sup> 7.0, *amber* force field); view perpendicular (left) and along the helical axis. The synthetic linker is displayed in a space filling representation (right) and the butadiene moiety is shown in the *s-cis* conformation.

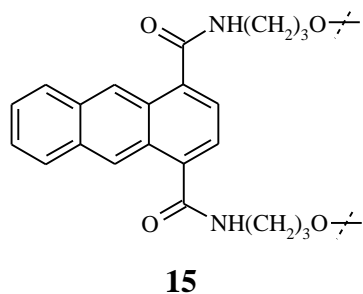
Finally the properties of the 1,4-anthracene derivative **15**, as loop replacement, was studied in a hairpin with a stem of 11 base pairs. Since the difference between a T<sub>4</sub>- and an A<sub>4</sub>-loop, according to previous studies is not too big, we compared this hairpin mimic just with the respective T<sub>4</sub>-hairpin (Table 24).

**Table 24** Melting temperatures of the 1,4-anthracene modified hairpin mimic and the corresponding T<sub>4</sub> hairpin, at 200 mM NaCl.

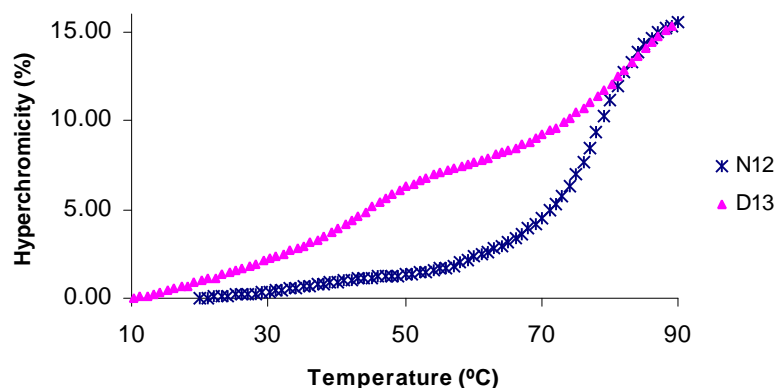
oligonucleotides	T <sub>m</sub> [°C]	Δ T <sub>m</sub> [°C]
N12	79.5	0
D13	45.5/86.0	+6.5

N12	5'-TCA CTG CAG AGT TTT CTC TGC AGT GA-3'
D13	5'-TCA CTG CAG AG <b>15</b> CTC TGC AGT GA-3'



While the T<sub>4</sub>-hairpin shows the expected sigmoid melting curve, the hairpin mimic shows two different transitions at 45.5 and 86 °C (Figure 20).



**Figure 20** Melting curves of the 1,4-anthracene hairpin mimic and the corresponding T<sub>4</sub>-hairpin. Solutions of 1.0 μM oligonucleotide in 10 mM NaH<sub>2</sub>PO<sub>4</sub> (pH 5.5) and 200 mM NaCl.

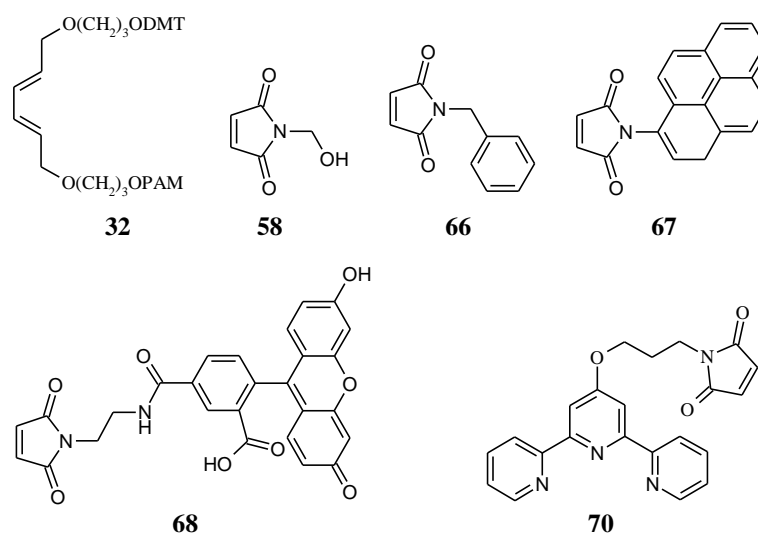
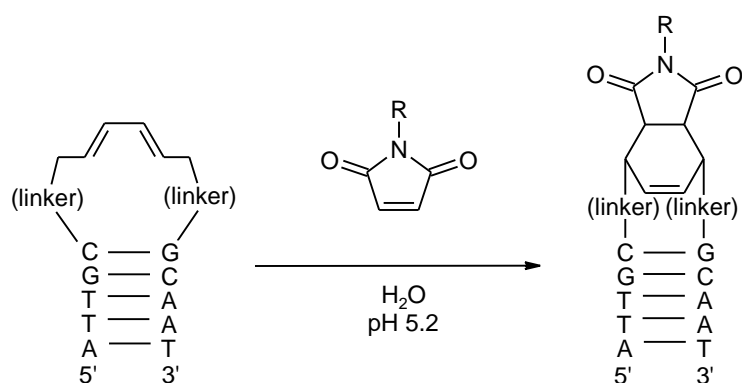
The higher melting temperature of the hairpin mimic shows a stabilisation of 6.5 °C compared with the T<sub>4</sub>-hairpin. This is in the same range as already observed with the butadiene building blocks. The lower melting temperature corresponds, according to calculations, to the denaturation of a duplex of about 10 base pairs.

Thus, this transition could arise from a partial duplex formed by one of the strands flanking the anthracene building block. On the other hand, it can not be excluded that the hairpin coexists with a duplex containing the anthracene building blocks in the middle. Such a behaviour was also observed with phenanthrene-modified, self-complementary oligonucleotides.<sup>202</sup>

Generally the tested diene-building blocks serve well as loop replacement in hairpins. The dimension of the stabilization is, compared with T<sub>4</sub>- and A<sub>4</sub>-looped hairpins, in the range of 5°C to 10°C. The importance of this new hairpin mimics becomes obvious in the following experiments where we show that, in addition to the higher stability, we concurrently inserted a novel functional group for bioconjugation under aqueous conditions.

### 3.5.2 Bioconjugation of Diene-Modified Hairpin Mimics

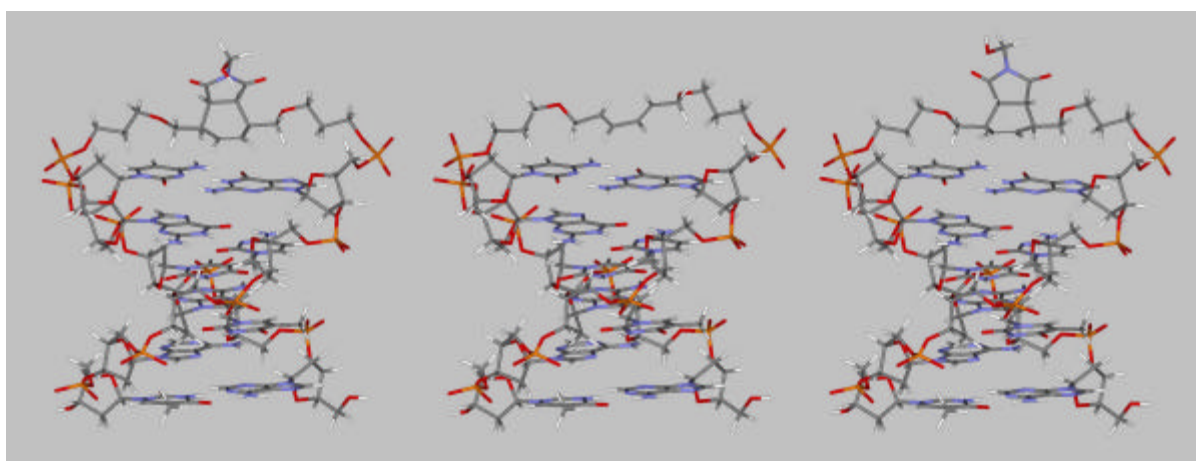
We next investigated the described hairpin mimics containing diene-building blocks as loop replacements regarding their reactivity towards functionalised maleimides. For this purpose the hairpin mimic D15, obtained with diene-building block **32**, was reacted with the series of different dienophiles shown in Scheme 44.



**Scheme 44** Illustration of the *Diels-Alder* reaction between the diene-modified hairpin mimic D15 and a maleimide (above). Diene-phosphoramidite building block (**32**) and the different maleimide derived molecules for the *Diels-Alder* bioconjugation (below).

D15 was chosen, because this hairpin mimic had previously turned out to be the most stable one in a series of three hairpins (chapter 3.5.1). We found that in aqueous media, under slightly acidic conditions, all maleimides undergo a [2+4] cycloaddition with the diene-modification of the hairpin mimic.

Thermal *Diels-Alder* reactions proceed through a concerted *syn* addition, therefore the imido group will maintain its *cis* geometry in the cycloadduct.<sup>187</sup> If the dienophile approaches the diene with its imido carbonyls'  $\pi$  system over the cyclohexadiene's  $\pi$  system, the *endo* product is formed. (*Endo* refers to the position of the dienophile's substituent relative to the saturated two-carbon bridge in the final product). If the dienophile orients itself with its substituent's  $\pi$ -systems pointing away from the cyclohexadiene's  $\pi$  system, then the *exo* stereoisomer is formed. The *endo* pathway is usually favored by far owing to a lowering of its transition state's energy as a result of this secondary  $\pi$  overlap (*Alder's rule*). Therefore, we can assume the preferred formation of the *endo* products in our experiments. Since the dienophile is symmetrical, this leaves us with two unique ways in which the two partners can approach each other. The two faces of the diene are rendered diastereofacial by the chiral nucleic acid. Therefore, we can obtain two diastereomeric products (Figure 21).

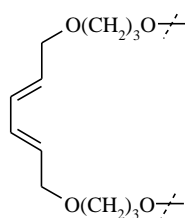
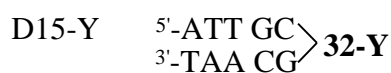
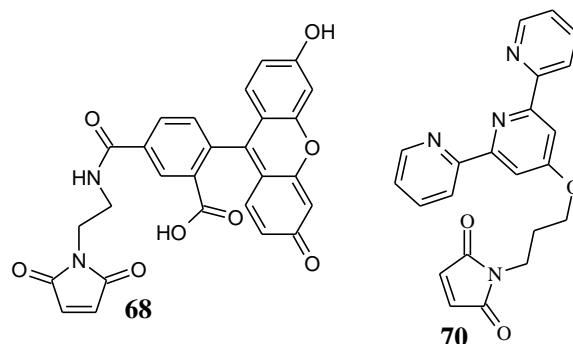
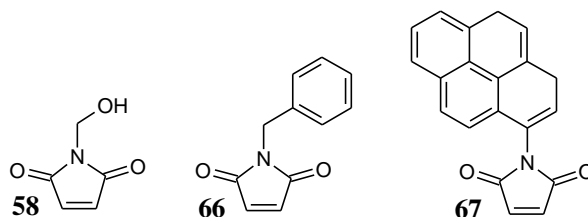


**Figure 21** Perpendicular view on molecular models of 1,3-butadiene-derived DNA hairpin mimic D15 (middle) and the *endo* bioconjugate D15-58, with orientation of the *Diels-Alder* product to the minor groove on the left and to the major groove on the right side (HyperChem<sup>TM</sup> 7.0, *amber* force field).

The obtained *Diels-Alder* adducts were subsequently purified by reverse phase HPLC, and analyzed by mass spectrometry. The pure oligomers were analysed by thermal denaturing experiments. The melting temperatures are given in Table 25. As can be seen from the data, all derivatives obtained by conjugation *via* the *Diels-Alder* reaction form stable hairpin structures. Although there is a variation in the stabilities of the different conjugates, in general they are comparable to the one of the parent hairpin mimic D15.

**Table 25** Melting temperatures of the hairpin mimic and the different bioconjugated diene-modified hairpin mimics at 100mM NaCl. The bioconjugated hairpin mimics are named after the respectively used maleimide (**Y** = **58**, **66**, **67**, **68** and **70**).

oligonucleotides	T <sub>m</sub> [°C]	Δ T <sub>m</sub> [°C]
D15	66.7	0
D15-58	64.2	-2.5
D15-62	66.3	-0.4
D15-66	66.5	-0.2
D15-67	57.5	-9.2
D15-68	67.1	+0.4
D15-70	59.7	-7.0

**32**



The shapes of the denaturing curves show a single, cooperative transition for all conjugates (Figure 22).

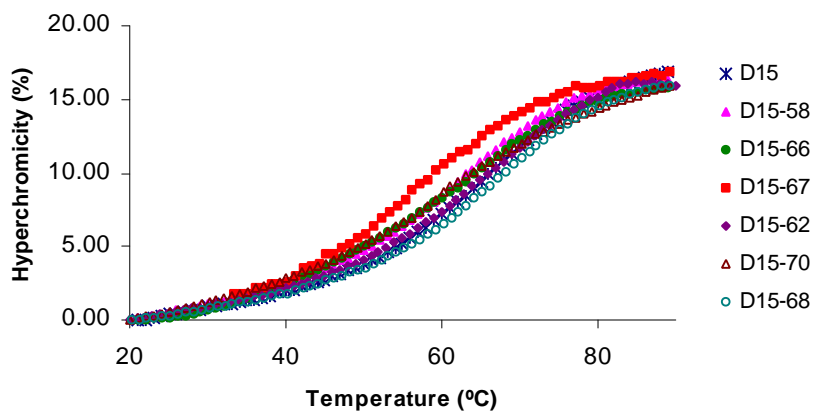


**Figure 22** Melting curves of the different bioconjugates synthesized via the *Diels-Alder* reaction. Oligomer concentration 2.5  $\mu\text{M}$ , 10 mM Tris-HCl, 100 mM NaCl, pH 7.5.

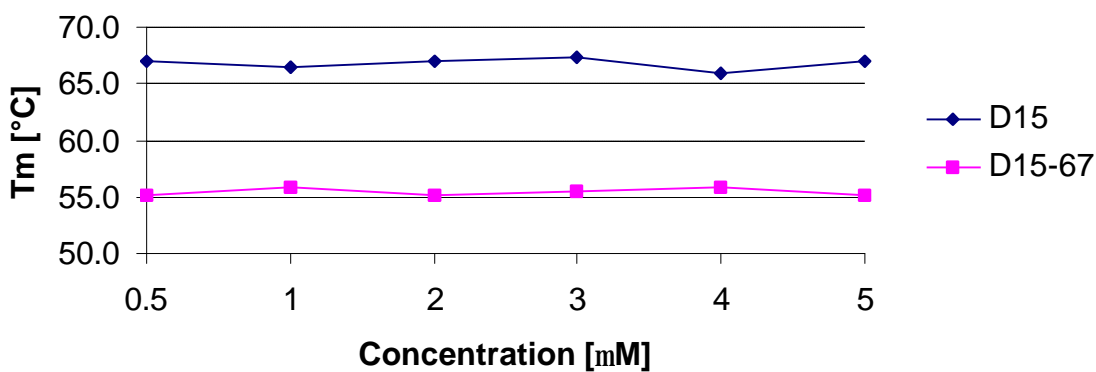


**Figure 23** Melting temperatures of hairpin mimic D15 and the pyrene bioconjugate D15-67, as a function of oligonucleotide concentration.

To verify that the observed transitions correspond to the melting of the hairpin structure, the dependence of the  $T_m$  on the oligomer concentration was established for the parent hairpin

D15 as well as for the pyrene conjugate D15-67. As it is expected for a unimolecular process, the  $T_m$  is independent from the oligonucleotide concentration over a range from 0.5 to 5.0  $\mu\text{M}$  (Figure 23).

Finally, circular dichroism spectra of the differently derivatised hairpin mimics were consistent with a B-form DNA (Figure 24).

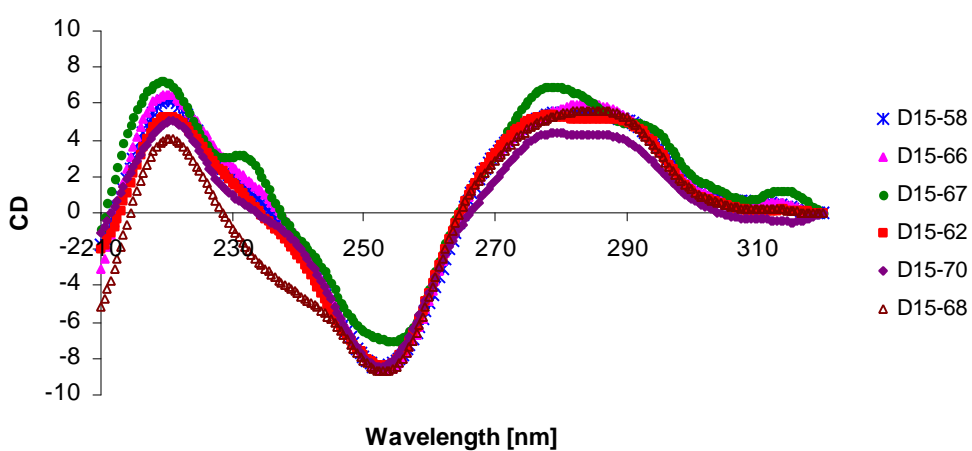


**Figure 24** CD spectra of the hairpin mimic and the different bioconjugates. Oligomer concentration 2.5  $\mu\text{M}$ , 10 mM Tris-HCl, 100 mM NaCl, pH 7.5.

With all the data collected, a model of the terpyridine conjugate was derived. Figure 25 shows a representation of this functionalised hairpin mimic.

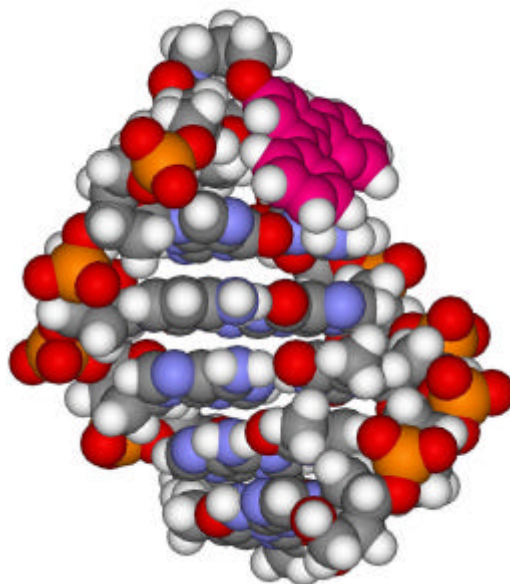
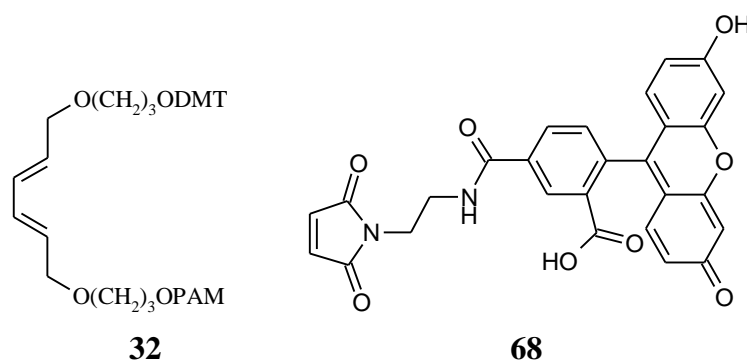


Figure 25 Molecular model of terpyridine bioconjugated 1,3-butadiene-derived DNA hairpin mimic D15-70 (HyperChem<sup>TM</sup> 7.0, *amber* force field). Perpendicular view displayed in a space filling representation. The terpyridine moiety (highlighted in red) is orientated to the major groove.

These results demonstrate, that the diene-modified hairpin mimic D15 is amenable to derivatisation though *Diels-Alder* reaction with suitable dienophiles. A variety of different groups can be attached to the hairpin loop, including aromatic residues, fluorescent dyes, metal coordinating ligands, as well as chemically reactive groups. The latter can serve as a site for attachment of further substituents.

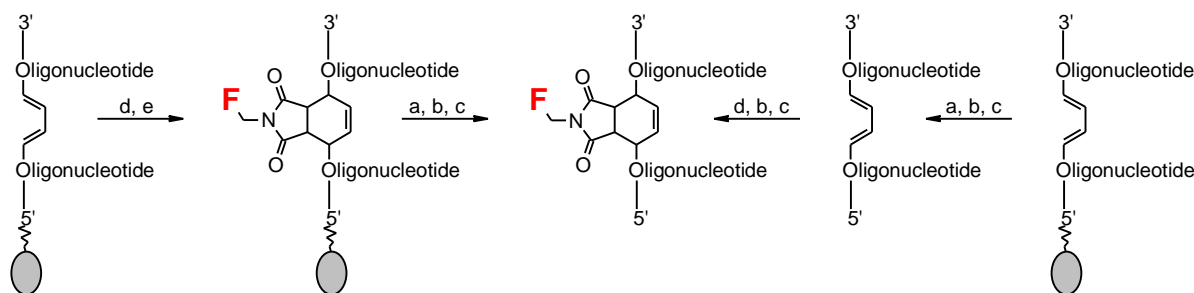
### 3.5.3 Fluorescein Bioconjugation of Oligodeoxyribonucleotides

As discussed in the previous chapter, diene-modified hairpins were found to react readily with different dienophiles. The obtained functionalised hairpin mimics formed stable secondary structures. We next extended these studies to nucleic acids containing *Diels-Alder* modifications in the stem.



**Scheme 45** Diene phosphoramidite building block (**32**) and fluorescein maleimide (**68**).

We concentrated on reactions with the fluorescein-derived maleimide **68** (Scheme 45). This brings the advantage of a straightforward detection of reacted vs. unreacted (or, in other words, labelled versus unlabelled) oligonucleotides. The fluorescein-modified single strands were prepared shown in Scheme 46. The labelling step involving reaction of the diene-modified oligonucleotide with the dienophile **68**, could be either done on solid support or in solution. Both of the two approaches have certain advantages and disadvantages. On solid support, the fluoresceine maleimide could be added as concentrated a solution. Excess of the fluoresceine maleimide was washed away from the immobilized oligodeoxyribonucleotides. The disadvantage, which can not be ignored, is that during the cleavage and deprotection procedure the imide function of the bioconjugate gets partially damaged by hydrolyses. This can be reduced, but not prevented, by deprotection at room temperature instead of 55 °C. The pure products were isolated after reverse phase HPLC.



**Scheme 46** Fluorescein labeling of diene-modified oligodeoxyribonucleotides on solid support and in solution: a) 25% aq ammonia, 55°C; b) HPLC; c) desalting; d) labeling with **68**; e) H<sub>2</sub>O, CH<sub>3</sub>CN washing.

The second, more conventional approach involved the bioconjugation of a purified modified oligodeoxyribonucleotide in aqueous solution. In this case, to get rid of the excess of fluorescein maleimide, the product had to be purified *via* HPLC. This additional purification step is time intense, but avoids hydrolysis of the imide function. Bioconjugation in solution is obviously to favor if time is not an issue.

We next investigated the influence of the modifications on duplex stability. The data given in Table 26 show that incorporation of building block **32** (N3/D7) leads to a decrease in T<sub>m</sub> of 13 °C compared to the unmodified 30mer duplex (N3/N6) at low salt concentration. If the diene-modification is placed opposite to an extra T (N9/D7) the decrease is reduced to 6 °C. The fluoresceine bioconjugated duplexes show a substantial further destabilisation of 19 °C and 15 °C respectively, depending on whether there was no extra base or if a T was positioned opposite to the *Diels-Alder* fluorescein modification..

The degree of destabilisation was substantially smaller at 0.2 M NaCl. Almost equal melting temperatures of the unmodified and the diene-modified (N3/D7) duplexes were obtained. The duplex N9/D7, where the diene building block forms a sort of a mismatch with a T of the complementary strand, however, is again destabilized by approximately 19 °C compared with the duplex N3/N6.

### 3 RESULTS AND DISCUSSION

Thus we can summarise that bioconjugation of the modified duplexes with fluorescein maleinimide results in a substantial destabilization of 15 - 20 °C (Table 26).

**Table 26** Melting temperatures of the unmodified duplexes, of the hybrides between unmodified and diene-modified strands and of the fluoresceine labelled hybrides at low and high salt concentrations.

oligonucleotides	0.01M NaCl		0.2M NaCl	
	T <sub>m</sub> [°C]	Δ T <sub>m</sub> [°C]	T <sub>m</sub> [°C]	Δ T <sub>m</sub> [°C]
N3/N6	71.0	0	86.0	0
N9/N6	70.5	-0.5	84.0	-2.0
N3/D7	58.0	-13.0	83.0	-3.0
N9/D7	65.0	-6.0	-----	-----
N3/D7-68	52.5	-18.5	67.5	-18.5
N9/D7-68	56.0	-15.0	-----	-----

N3 5'-TGC CGA CGG CTC CGG ACG CGT GCG CAG GCC-3'

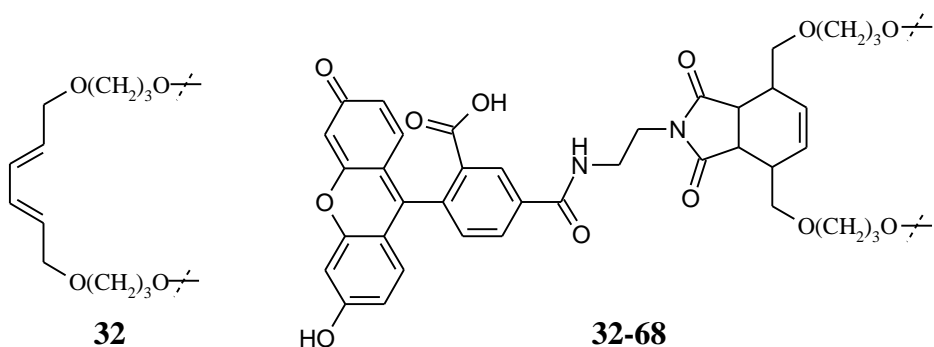
N6 5'-GGC CTG CGC ACG CGT CCG GAG CCG TCG GCA-3'

N9 5'-TGC CGA CGG CTC T CGG ACG CGT GCG CAG GCC-3'

D7 5'-GGC CTG CGC ACG CGT CCG **32** GAG CCG TCG GCA-3'

D7-68 5'-GGC CTG CGC ACG CGT CCG **32** GAG CCG TCG GCA-3'

**68**



The melting curves of the tested duplexes show build sigmoidal curves at 0.01 M as well as at 0.2 M NaCl concentration (Figure 26).

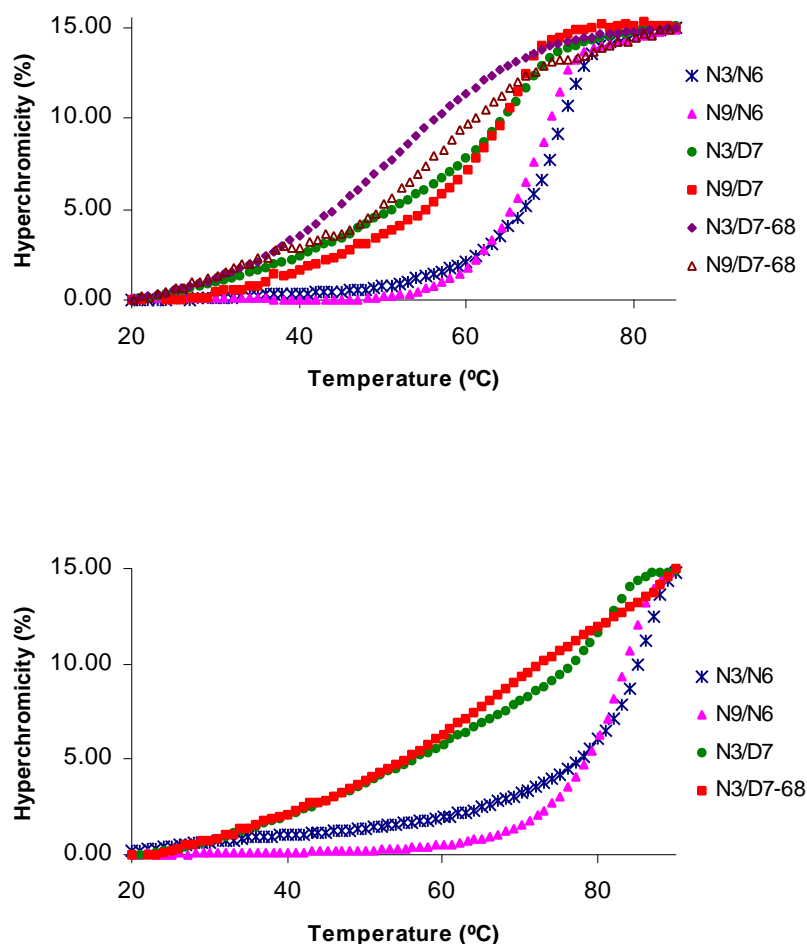


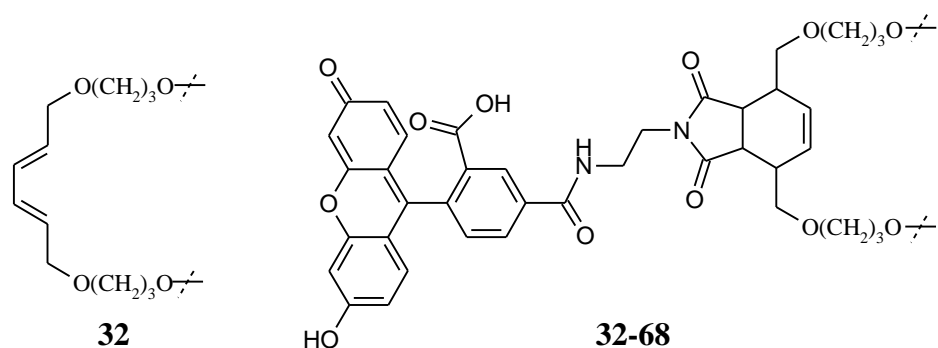
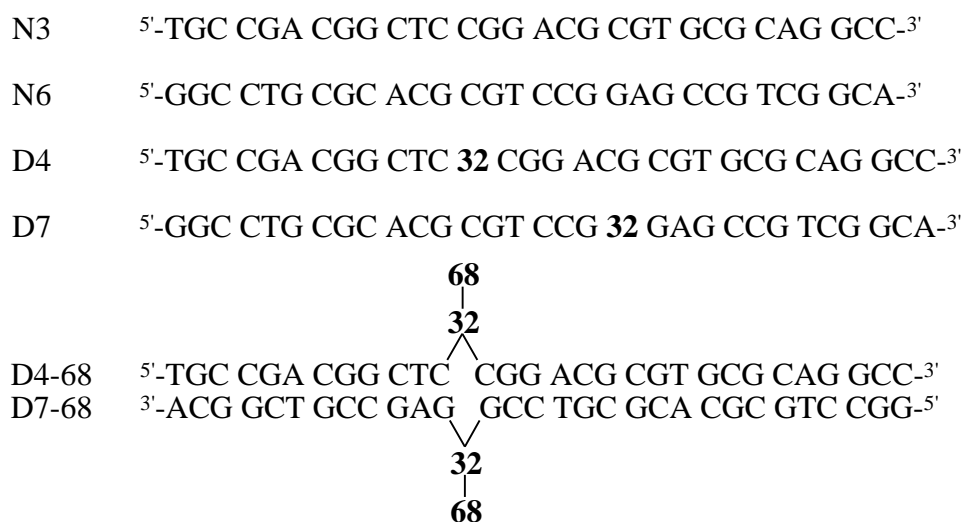
Figure 26 Melting curves of the duplexes between unmodified oligodeoxyribonucleotides and the corresponding unmodified, modified and fluorescein labelled complementary strands. Oligomer concentration 2.5  $\mu\text{M}$ , 10 mM Tris-HCl, pH 7.5 at low (above) and high salt concentration (below).

We furthermore examined the effect of a second fluorescein label which was placed right opposite to the first one (Table 27). A duplex containing two opposite dienes (D4/D7) is destabilised by 9  $^{\circ}\text{C}$  at both low and high salt conditions. Again, placement of one fluorescein *Diels-Alder* adduct (D4/D7-68) brings an additional 10 $^{\circ}\text{C}$  in destabilisation. The second fluorescein opposite to the first one, however, has no further influence (D4-68/D7-68).

### 3 RESULTS AND DISCUSSION

**Table 27** Melting temperatures of the unmodified duplexe, of the duplex of the respective diene-modified strands and of the duplex labelled with one and two fluoresceine maleimides at low and high salt concentrations.

oligonucleotides	0.01M NaCl		0.2M NaCl	
	Tm [°C]	Δ Tm [°C]	Tm [°C]	Δ Tm [°C]
N3/N6	71.0	0.0	86.0	0.0
D4/D7	62.0	-9.0	77.0	-9.0
D4/D7-68	51.5	-19.5	68.0	-18.0
D4-68/D7-68	51.0	-20.0	67.5	-18.5





Again, the melting curves show a cooperative melting process (Figure 27). These findings show that incorporation of dienes, either in one strand or in two strands in opposite positions leads to a considerable destabilisation of up to 10 °C. This is in disagreement to other observations in our group with non-nucleosidic building blocks containing a phenanthrene rather than a diene-moiety; those phenanthrene building blocks were very well tolerated in a DNA duplex.<sup>188</sup> *Diels-Alder* addition of a fluorescein maleimide brings a further strong decrease in duplex stability of approximately 10 °C. Apparently, the bulky substituent is not well tolerated. On the other hand, a second fluorescein opposite to the first one, has no effect at all.

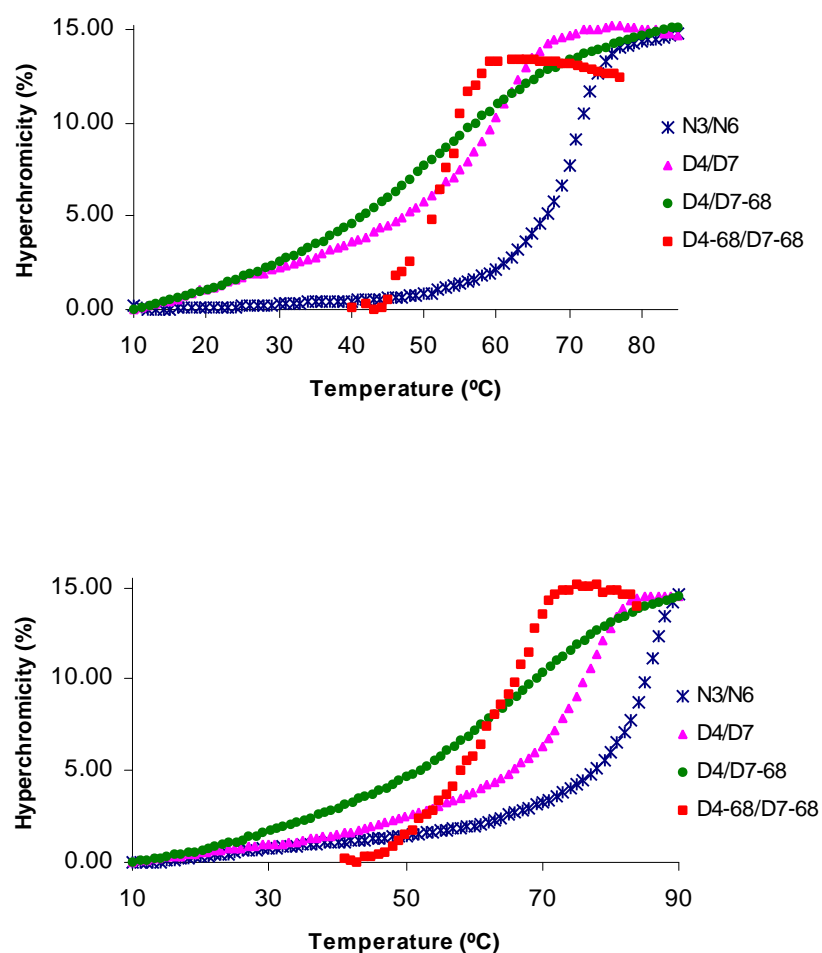


**Figure 27** Melting curves of natural, modified and fluorescein labelled duplexes. Oligomer concentration 2.5  $\mu$ M, 10 mM Tris-HCl, pH 7.5 at low (above) and high salt concentration (below).

Finally, different hairpins with a T<sub>4</sub>-loop were synthesized, to study the influence of a fluorescein modification in the stem part of the hairpin (Table 28). Hairpin N11 bears a C insertion, while D10 contains the diene insertion and D10-64 corresponds to D10 after bioconjugation.

At both salt concentrations, all insertions in the stem result in a dramatic decrease of the stability. The insertion of the natural base C lowers the melting temperature by 8.5 °C. The modified hairpin with the diene insertion shows a T<sub>m</sub> decrease of even a 14 °C compared to the respective unmodified hairpin (Table 28).

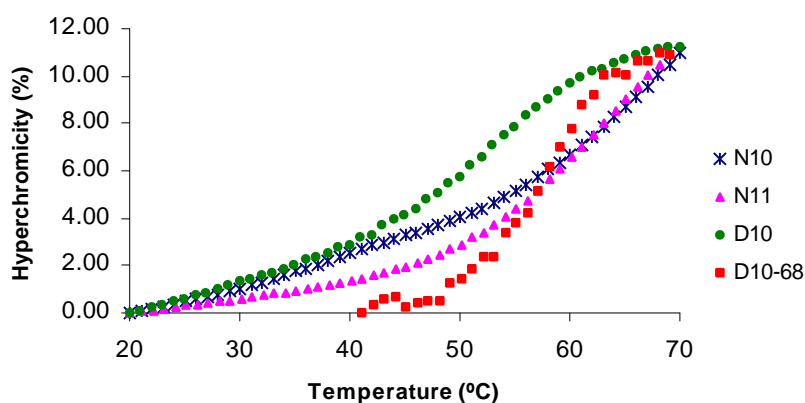
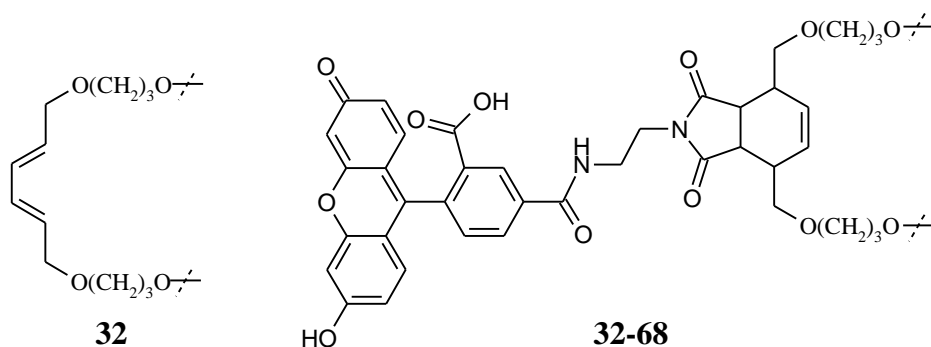
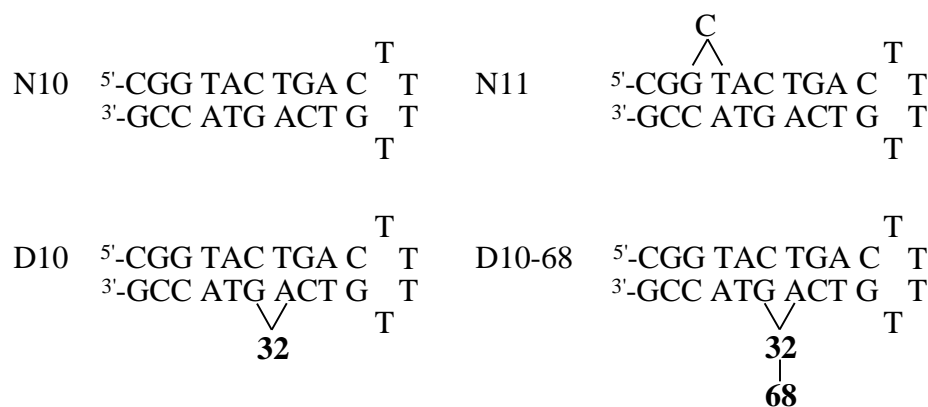


**Figure 28** Melting curves of unmodified, modified and fluorescein labelled hairpins Oligomer concentration 2.5 μM, 10 mM Tris-HCl, pH 7.5 at low (above) and high salt concentration (below).

**Table 28** Melting temperatures of unmodified, diene-modified and fluorescein labelled hairpins at different salt concentrations.

oligonucleotides	0.01M NaCl		0.2M NaCl	
	T <sub>m</sub> [°C]	Δ T <sub>m</sub> [°C]	T <sub>m</sub> [°C]	Δ T <sub>m</sub> [°C]
N10	59.0	0.0	69.0	0.0
N11	50.5	-8.5	63.5	-6.5
D10	43.5	-15.5	55.0	-14.0
D10-68	47.0	-12.0	57.5	-11.5



## 3.6 Conclusions

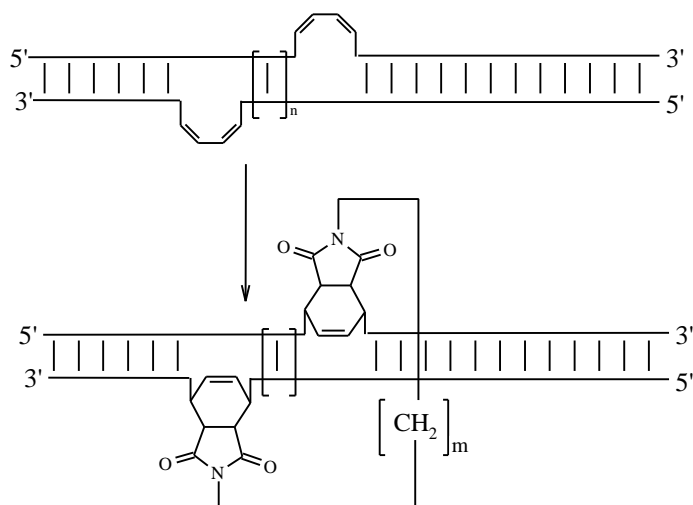
Phosphoramidites containing electron rich dienes are suitable building blocks for automated DNA synthesis. Self complementary oligodeoxyribonucleotides with a diene-building block serving as loop, form stabilized hairpin mimics. Diene-modified oligodeoxyribonucleotides react in aqueous media, as well as in organic solvents, with maleimide derivatives via the *Diels-Alder* reaction. Diene-modified complementary strands can be cross-linked with dimaleimides *via* the *Diels-Alder* reaction. Cross-linkage of non complementary diene-modified oligodeoxyribonucleotides, without a template, however, is not possible under the used conditions.

## 3.7 Outlook

Several additional experiments could be carried out with the methods developed in this work. Better understanding of the obtained results, by using additional modifications and cross-linking agents could top off the studies. In the following, we propose various potential applications of the cross-linking method based on this *Diels-Alder* reaction.

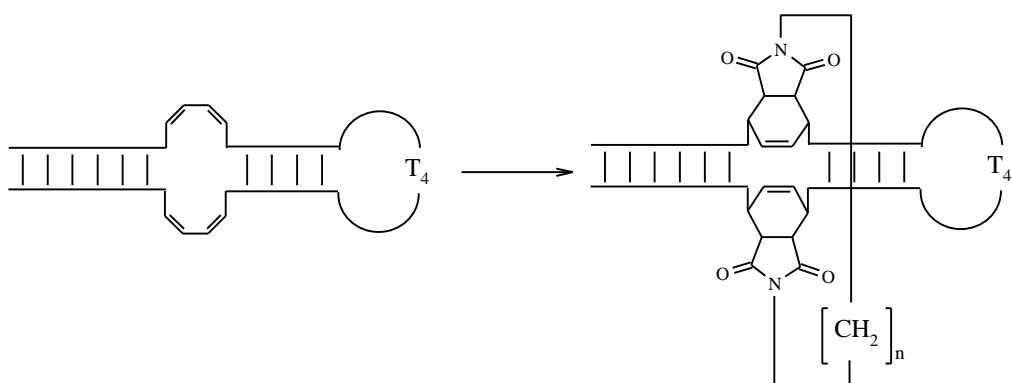
To investigate whether the stabilization of 48 °C, observed by cross-linkage of the duplex D26/D27 with dimaleimide **62**, is the highest reachable with hexadiene building blocks and dimaleimides, one had to repeat the experiments under consideration of dienes and dimaleimides with longer spacers and linkers respectively.

In several publications *Liu et al.*<sup>59-65</sup> observed that the reactivity in DNA-template assisted processes was rather insensitive to the distance between the reactive groups. Insertion of additional base pairs between the diene-building blocks on the complementary strands could show if this phenomenon is also valid for our system (Scheme 46).



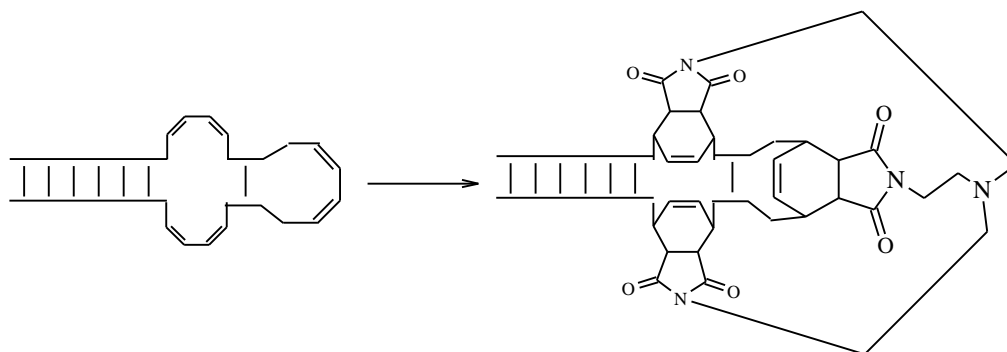
**Scheme 46** Dimaleimide cross-linkage of modified duplexes with diene-building blocks separated by  $n$  base pairs.

The stability of secondary structures of self complementary oligonucleotides, i.e. hairpins, could be increased *via* the cross-linkage of oligonucleotide with two diene-modifications (Scheme 47). Formation of these kind of “locked” structures should be similar to the one observed in the successful cross-linking of diene-modified duplexes.<sup>77,207</sup>



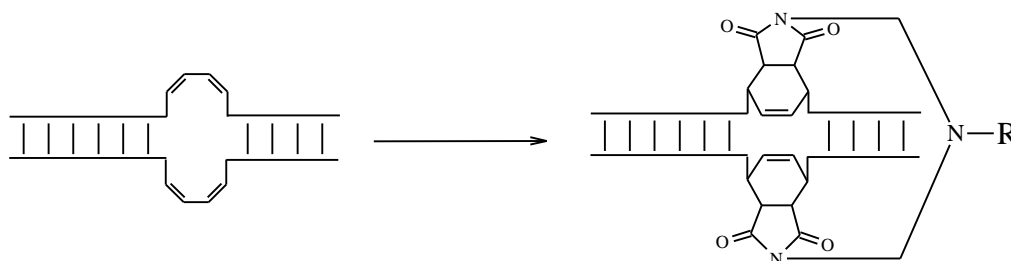
**Scheme 47** Dimaleimide cross-linkage of self complementary oligonucleotides bearing two diene-modifications.

Since our diene-phosphoramidites are synthetically equivalent to the phosphoramidites of the natural building blocks, there is no limitation of the number nor the place of incorporated diene-modifications in an oligonucleotide (Scheme 48). Even longer parts of an oligonucleotide could be replaced by the repeated insertion of one or several kind of diene-building blocks.



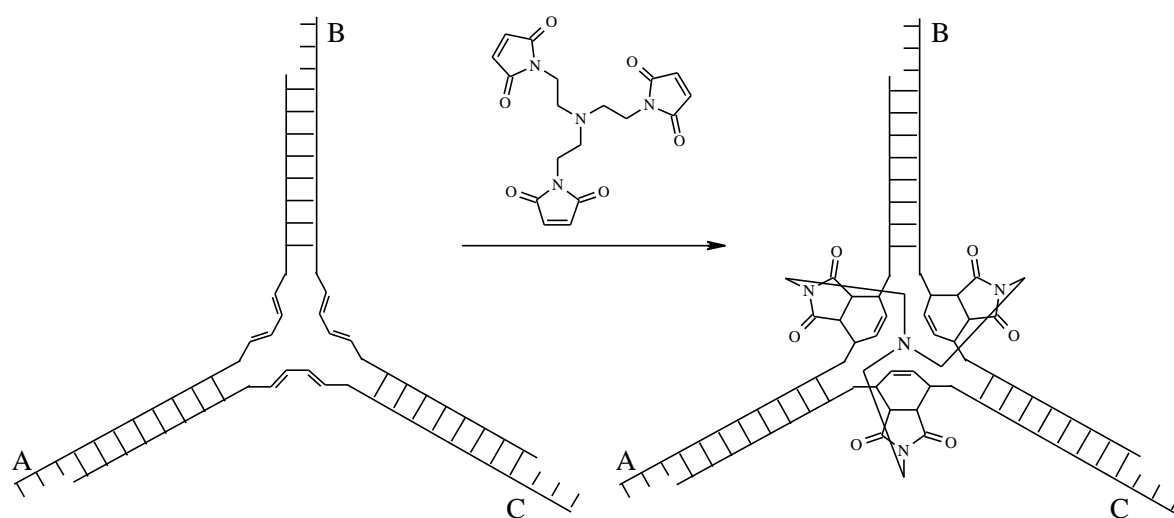
**Scheme 48** Cross-linkage of diene-modified self complementary oligonucleotides *via* a trimaleimide.

Dimaleimides with a further substitution would allow to realize cross-linkage and bioconjugation in one step (Scheme 49). One step in this direction, the cross-linkage with trimaleimide **71**, is already described in chapter 3.4.4 of this work. Similar to the maleimide bioconjugation<sup>[x]</sup>, functional groups, ligands towards metal complexation, fluorophores and many other moieties could be attached to the dimaleimides.

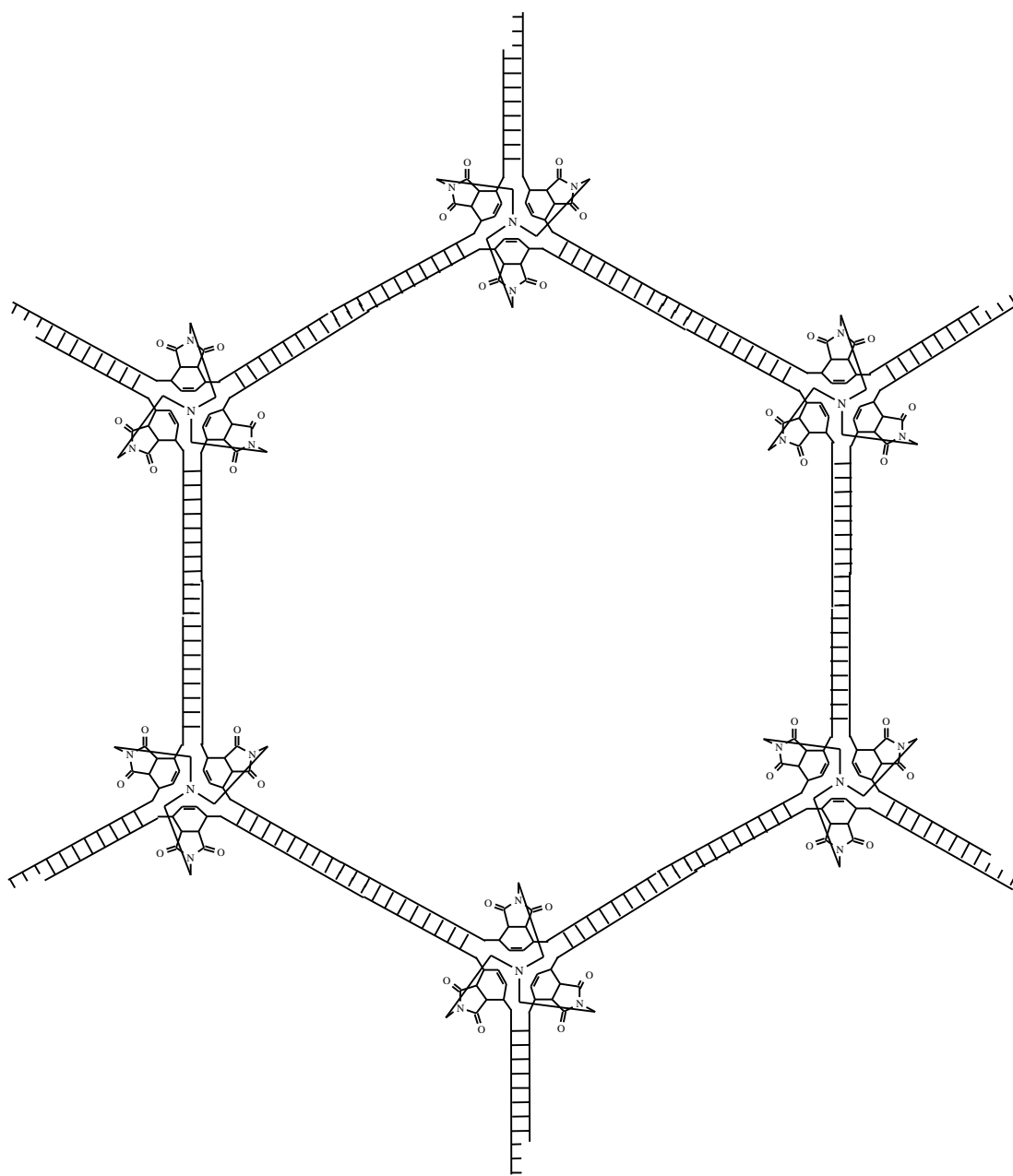


**Scheme 49** Cross-linking followed by bioconjugation with further substituted dimaleimides.

Cross-linking agents with more than two maleimides obviously allow cross-linking of more than two diene-modified oligonucleotides. Trimaleimide (**71**) could be used to cross-link diene-modified three way junctions (Scheme 50) under the same reaction conditions used for dimaleimide cross-linking. Scheme 51 shows a hypothetical two dimensional lattice built of cross-linked three way junctions.



**Scheme 50** Illustration of the cross-linking of a diene-modified tree way junction with trimaleimide (**71**).



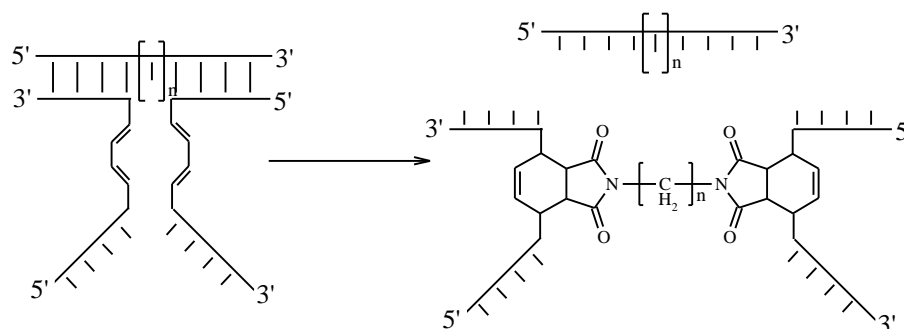
**Scheme 51** Illustration of a two dimensional oligonucleotide lattice built from trimaleimide cross-linked diene-modified three way junctions.

All our efforts towards cross-linking non-complementary diene-modified oligonucleotides failed. Since these experiments were carried out with the identical reactive groups and under the same reaction conditions used in the successful cross-linking of complementary diene-



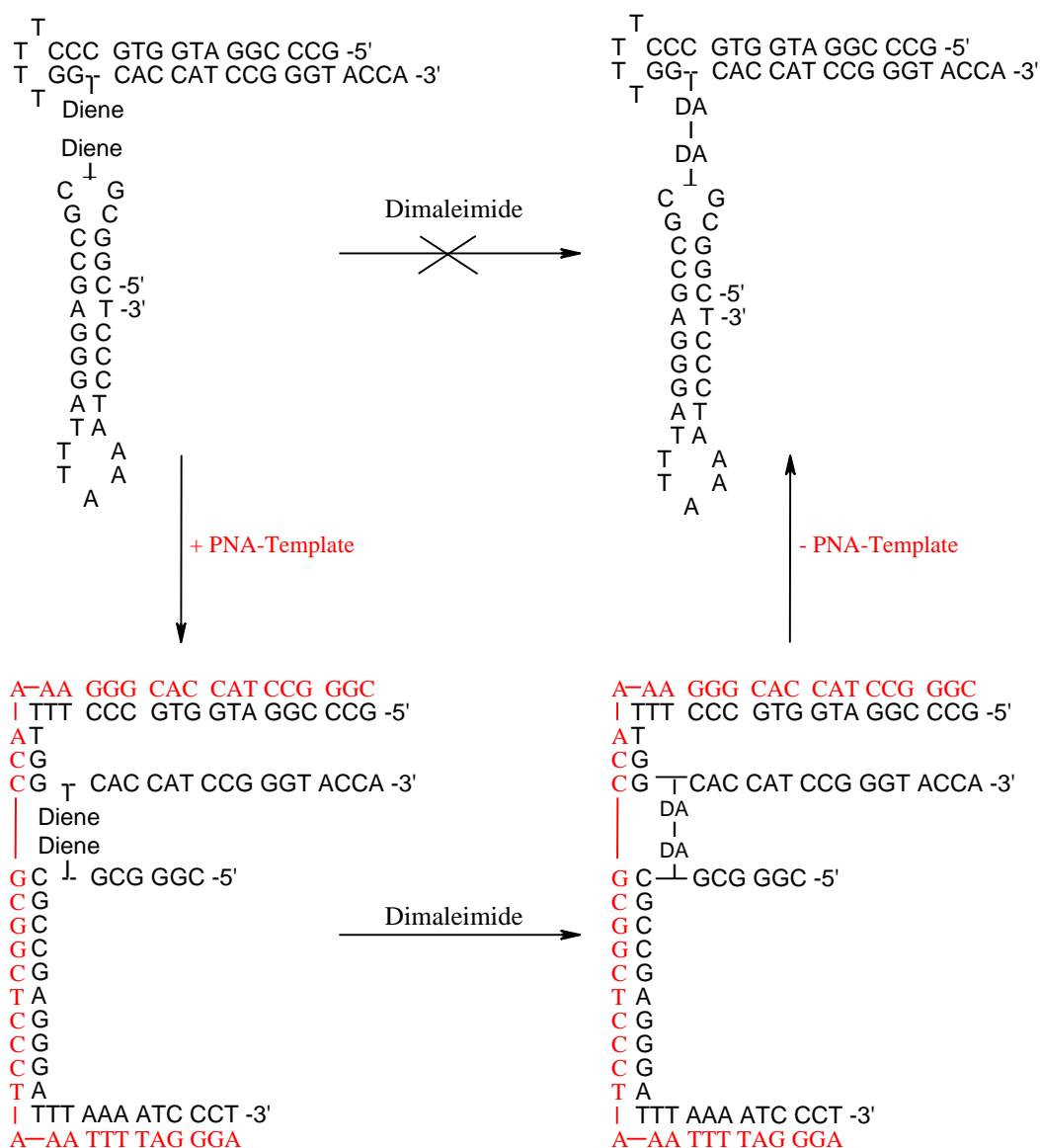
modified oligonucleotides, the missing sterical preorganisation seems to be responsible for this failure.

In the experiments reported in this work, the diene-modified oligodeoxyribonucleotides served, at the same time, as reactants and as templates. By the use of a third strand, which is complementary to parts of the sequences of two modified oligodeoxyribonucleotides, as template, it should be possible to cross-link non complementary strands (Scheme 52). Similar efficiency, as observed in the cross-linking of complementary diene-modified oligonucleotides, is expected in such experiments. The use of template strands bearing a different number of insertions could result in a better understanding of the necessity of preorganisation.



Scheme 52 Cross-linkage of non complementary strands with the help of a template strand.

Finally, while complementary oligonucleotides can serve as templates for non-complementary modified oligonucleotides without stable secondary structures, modified oligomers, like PNAs, which can form hybrids of increased stability might be used to template self complementary oligonucleotides (Scheme 53).



**Scheme 53** Alternative dimaleimide cross-linking of non-complementary diene-modified oligonucleotides, using a PNA-template for sterical preorganisation of the diene-modifications.

---

## 4 REFERENCES

- 1 Cogoni C. and Macino G., *Nature*, 399, **1999**, 166-169.
- 2 Cogoni C. and Macino G., *Science*, 286, **1999**, 2342-2344.
- 3 Gottesfeld, J. M., Neely, L., Trauger, J. W., Baird, E. E., Dervan, P. B., *Nature*, **1998**, 391, 468 – 471.
- 4 Kooter J.M., Matzke M.A. and Meyer P., *Trends Plant. Sci.*, 4, **1999**, 340-347.
- 5 Stephenson M. L., Zamecnik P. C., *Proc. Natl. Acad. Sci. U.S.A.*, **1978**, 75, 285.
- 6 Zamecnik P. C., Stephenson M. L., *Proc. Natl. Acad. Sci. U.S.A.*, **1978**, 75, 280.
- 7 Letsinger R. L., Lunsford W. B., *J. Am. Chem. Soc.*, **1976**, 98, 3655.
- 8 Uhlmann E., Peyman A., *Chemical Reviews*, **1990**, 90, 4, 544-584.
- 9 Hélène et al., *Proc. Natl. Acad. Sci.*, U.S.A., **1984**, 81, 3297.
- 10 Chollet A., Kawashima E., *Nucleic Acids Res.*, **1988**, 16, 305.
- 11 Inoue H., Hayase Y., Imura A., Iwai S., Miura K., Ohtsuka E., *Nucleic Acids Res.*, **1987**, 15, 6131.
- 12 De Clerq E., Eckstein F., Sternbach H., Morgan T. C., *Virology*, **1970**, 42, 421.
- 13 Miller P. S., McParland K. B., Jayaraman K., Ts’O P. O. P., *Biochemistry*, **1981**, 20, 1874.
- 14 Loke S. L., Stein C. A., Zhang X. H., Mori K., Nakanishi M., Subasinghe C., Cohen J. S., Neckers L. M., *Proc. Natl. Acad. Sci. U.S.A.*, **1989**, 86, 3474.
- 15 Vespieren P., Cornelissen A. W. C. A., Thoung N. T., Hélène C., Toulmé J. –J., *Gene*, **1987**, 61, 307.
- 16 Bayard B., Leserman L.D., Bisbal C., Lebleu B., *Eur. J. Biochem.*, **1985**, 151, 319.
- 17 Schell P. L., *Biochim. Biophys. Acta*, **1974**, 340, 324.
- 18 Schell P. L., *Biochim. Biophys. Acta*, **1971**, 240, 472.
- 19 Cheng J. C. et al., *Mol. Genet. Metab.*, **2003**, 80(1-2), 121-8.
- 20 Fire A. et al., *Nature*, **1998**, 391(6669), 806-11.
- 21 Hammond SM, Caudy AA, Hannon GJ. (2001) *Nature Rev Gen* **2**: 110-119.
- 22 Koshkin A.A., Singh S.K., Nielsen P., Rajwanshi V.K., Kumar R., Meldgaard M, Olsen C.E. and Wengel J., *Tetrahedron*, **1998**, 54, 3607-3630.
- 23 Egholm M., Buchardt O., Nielsen P.E. & Berg R.H., *J. Am. Chem. Soc.*, **1992**, 114, 1895-1897.

#### 4 REFERENCES

---

- 24 Egholm M., Nielsen P.E., Buchardt O. & Berg R.H., *J. Am. Chem. Soc.*, **1992**, 114, 9677-9678.
- 25 Egholm M., Buchardt O., Christensen L., Behrens C., Freier S., Driver D.A., Berg R.H., Kim S.K., Norden B. & Nielsen P.E., *Nature*, **1993**, 365, 566-568.
- 26 Bonnet G., Tyagi S., Libchaber A., Kramer F. R., *Proc Natl Acad Sci USA*, **1999**, 96, 6171-6176.
- 27 Marras S.A.E., Kramer F.R., and Tyagi S., *Genet Anal*, **1999**, 14, 151-156.
- 28 Marras S.A.E., Kramer F.R., and Tyagi S., *Nucleic Acids Res*, **2002**, 30, E122.
- 29 Mullah B., Livak K., *Nucleosides & Nucleotides*, **1999**, 18, 1311-1312.
- 30 Tyagi S., Bratu D.P., Kramer F.R., *Nat Biotechnol*, **1998**, 16, 49-53.
- 31 Tyagi S., Kramer F.R., *Nat Biotechnol*, **1996**, 14, 303-308.
- 32 Tyagi S., Marras S.A.E., Kramer F.R., *Nat Biotechnol*, **2000**, 18, 1191-1196.
- 33 Quigley G. J., Wang A. H. J., Seeman N. C., Suddath F. L., Rich A., Sussmann J. L., Kim S. H., *PNAS*, **1975**, 72, 4866.
- 34 Westhof E., Dumas P., Moras D., *JMB*, **1985**, 184, 119.
- 35 Moore P. B., *Curr. Opin. Struct. Biol.*, **1993**, 3, 340.
- 36 James J. K., Tinoco I. J., *NARes*, **1993**, 21, 3287.
- 37 Seeman N. C., *Angew. Chem. Int. Ed.*, **1998**, 37, 3220-3238.
- 38 Ekaterina I. Zagryadskaya, Felix R. Doyon, and Sergey V. Steinberg, *Nucleic Acids Res*. 2003 July 15, 31 (14): 3946–3953.
- 39 Kettani A., Bouaziz S., Gorin A., Zhao H., Jones R. A., Patel D. J., *J. Mol. Biol.*, **1998**, 282, 619-636.
- 40 Pinto A. L., Lippard S., *J. Biochem. Biophys. Acta.*, **1985**, 780, 167-180.
- 41 Borowy-Borowski H., Lipman R., Tomasz M., *Biochemistry*, **1990**, 29, 2999-3006.
- 42 Kirchner J. J., Hopkins P. B., *J. Am. Chem. Soc.*, **1991**, 4681-4682.
- 43 Sigurdsson S. T., Rink S. M., Hopkins P. B., *J. Am. Chem. Soc.*, **1993**, 115, 12633-12634.
- 44 Willis M. C., Hicke B. J., Uhlenbeck O. C., Cech T. R., Koch T. H., *Science*, **1993**, 262, 1255-1257.
- 45 Maillard J. T., Raucher S., Hopkins P. B., *J. Am. Chem. Soc.*, **1990**, 112, 2459-2460.
- 46 Kirchner J. J., Sigurdsson S. T., Hopkins P. B., *J. Am. Chem. Soc.*, **1992**, 114, 4021-4027.

- 
- 47 Maillard J. T., Weidner M. F., Kirchner J. J., Ribeiro S., Hopkins P. B., *Nucleic Acids Res.*, **1991**, 19, 1885-1891.
- 48 Tomasz M., Lipman R., Chowdary D., Pawlak J., Verdine G. L., Nakanishi K., *Science*, **1987**, 235, 1204-1208.
- 49 Sherman S. E., Gibson D., Wang A. H., Lippard S. J., *Science*, **1985**, 230, 412-417.
- 50 Webb T. R., Matteucci M. D., *J. Am. Chem. Soc.*, **1986**, 108, 2764-2765.
- 51 Glick G. D., *Biopoly.*, **1998**, 48, 83-96.
- 52 Naylor R., Gilham P. T., *Biochemistry*, **1966**, 5, 2722-2728 .
- 53 Inoue T., Joyce G. F. Grzeskowiak D., Orgel L. E., Brown J. M., Reese C. B., *J. Mol. Biol.*, **1984**, 178, 669-676.
- 54 von Kiedrowski G., *Angew. Chem. Int. Ed. Engl.*, **1986**, 25, 932-935.
- 55 Goodwin J. T., Lynn D. G., *J. Am. Chem. Soc.*, **1992**, 114, 9197-9198.
- 56 Xu Y., Karalkar N. B., Kool E. T., *Nature Biotechnology*, **2001**, 19, 148-152.
- 57 Fujimoto K., Matsuda S., Takahashi N., Saito I., *J. Am. Chem. Soc.*, **2000**, 122, 5646-5647.
- 58 Czapinski J. L., Sheppard T. L., *J. Am. Chem. Soc.*, **2001**, 123, 8618-8619.
- 59 Gartner Z. J, Liu D. R., *J. Am. Chem. Soc.*, **2001**, 123, 6961-6963.
- 60 Gartner Z. J., Kanan M. W., Liu D. R., *Angew. Chem., Int. Ed. Engl.*, **2002**, 41, 1796-1800.
- 61 Calderone C. T., Puckett J. W., Gartner Z. J., Liu D. R., *Angew. Chem., Int. Ed. Engl.*, **2002**, 41, 4104-4108.
- 62 Gartner Z. J., Kanan M. W., Liu D. R., *J. Am. Chem. Soc.*, **2002**, 124, 10304-10306.
- 63 Breslow R., *Acc. Chem. Res.*, **1991**, 6, 159.
- 64 Grieco P. A., *Aldrichim. Acta.*, **1991**, 24, 59.
- 65 Li C., *Chem. Rev.*, **1993**, 93, 2023.
- 66 Sauer J., Sustmann R., *Angew. Chem. Int. Ed. Engl.*, **1980**, 19, 779.
- 67 Desimoni G., Righetti P. P., *Tetrahedron*, **1991**, 47, 5857.
- 68 Desimoni G., Faita G., Pasini D., Righetti P. P., *Tetrahedron*, **1992**, 48, 1667.
- 69 Desimoni G., Faita G., Righetti P. P., Toma L., *Tetrahedron*, **1990**, 46, 7951.
- 70 Diels O., Alder K., *Ann. Chem.*, **1931**, 490, 243.
- 71 Carlson *et al.*, *J. Am. Chem. Soc.*, **1975**, 97, 5291.
- 72 Woodward R. B., Baer H., *J. Am. Chem. Soc.*, **1948**, 70, 1161.
-

#### 4 REFERENCES

---

- 73 Rideout D. C., Breslow R., *J. Am Chem. Soc.*, **1980**, 102, 7816.
- 74 Engberts J. B. F. N., *Pure Appl. Chem.*, **1995**, 67, 823.
- 75 Blokzijl W., Blandamer M. J., Engberts J. B. F. N., *J. Amer. Chem. Soc.*, **1991**, 113, 4241.
- 76 Breslow R., Maitra U., *Tetrahedron Lett.*, **1984**, 25, 1239.
- 77 Hill *et al.*, *J. Org. Chem.*, **2001**, 66, 16, 5352-5358.
- 78 Husar G. M., Anziano D. J., Leuk M., Sebesta D. P., *Nucleosides, Nucleotides and Nucleic Acids*, **2001**, 20, 559-566.
- 79 Fruk L., Grondin A., Smith E. W., Graham D., *Chem. Comm.*, **2002**, 2100-2101.
- 80 Latham-Timmons H. A., Wolter A., Roach J. S., Giare R., Leuk M., *Nucleosides, Nucleotides and Nucleic Acids*, **2003**, 22, 1495-1497.
- 81 Larkin D. C., Williams M. W., Martinis S. A., Fox G. E., *Nucleic Acids Res.*, **2002**, 30, 10, 2103-2113.
- 82 Dreher T. W., Goodwin J. B., *Nucleic Acids Res.*, **1998**, 26, 19, 4356-4364.
- 83 Helm M., Brulé H., Friede D., Giegé R., Pütz D., Florentz C., *RNA*, **2000**, 6, 1356-1379.
- 84 Hou Y. M., Zhang X., Holland J. A., Davis D. R., *Nucleic Acids Res.*, **2001**, 29, 4, 976-985.
- 85 Szmanski M., Barciszewski J., *Nucleic Acids Res.*, **2000**, 28, 1, 326-328.
- 86 Beuning P. J., Musier-Forsyth K., *Biopolymers*, **1999**, 52, 1, 1-28.
- 87 Pon R. T., Usman N., Ogilvie K.K., *Biotechniques*, **1988**, 6, 768-775.
- 88 McCollum C., Andrus A., *Tetrahedron Letters*, **1991**, 32, 4069-4072.
- 89 Kaufman J., Le M., Ross G., Hing P., Budiansky M., Yu E., Campbell E., Yoshimura V., Fitzpatrick V., Nadimi K., Andrus A., *Biotechniques*, **1993**, 14, 834-839.
- 90 Ana-Gen Technologies Inc., 1134 Aster Ave., Suite K, Sunnyvale, CA 94086. Tel: (408) 249-4362, Fax: (408) 249-4383.
- 91 Lint W., Vanaja E., Grant F. J., Lockhart P.G. and O'Hara P.J., *Biotechniques*, **1994**, 16, 408.
- 92 Sproat B. S. and Bannwarth W., *Tetrahedron Letters*, **1983**, 24, 5771-5774.
- 93 Adams S. P., Kavka K. S., Wykes E. J., Holder S. B., and Galluppi G. R., *J. Amer. Chem. Soc.*, **1983**, 105, 661-663.

- 
- 94 Caruthers M. H., *Academic Press*, **1987**, Orlando, FL.
- 95 Caruthers M. H., *Acc. Chem. Res.*, **1991**, 24, 278-284.
- 96 Caruthers M. H., *Science*, **1985**, 230, 281-285.
- 97 Urdea M. S., *Methods in Enzymology*, **1987**, 146, 22-41.
- 98 Ferretti L., Karnik S. S., Khorana H. G., Nassal M., and Oprian D. D., *Proc. Natl. Acad. Sci.*, **1986**, 83, 599-603.
- 99 Urdea M. S., Merryweather J. P., Mullenbach G. T., Coit D., Heberlein U., Valenzuela P., and Barr P. J., *Proc. Natl. Acad. Sci.*, **1983**, 80, 7461-7465.
- 100 Wright P., Lloyd D., Rapp W., and Andrus A., *Tetrahedron Letters*, **1993**, 34, 3373-3376.
- 101 Tanaka T. and Letsinger R. L., *Nucl. Acids. Res.*, **1982**, 10, 3249-3260.
- 102 Bartel D. P., and Szostak J. W., *Science*, **1993**, 261, 1411-1418.
- 103 Sinha N. D., *Methods in Molecular Biology*, **1993**, 20: Protocols for Oligonucleotides and Analogs, ed. S. Agrawal, Humana Press Inc., Totowa, NJ.
- 104 Ciccarelli R. B., Gunyuzlu P., Huang J., Scott C., and Oakes F. T., *Nucleic Acids Res.*, **1991**, 19, 6007-6013.
- 105 McCormick D. B. and Roth J. R., *Anal. Biochem.*, **1970**, 34, 226-236.
- 106 Walker J.M., ed., *Methods in Molecular Biology*, **1994**, Humana Press, 22, 219-244
- 107 G. Fasman, ed., *Circular Dichroism and the Conformational Analysis of Biomolecules*, *Plenum Press*, **1996**
- 108 Glasel, J.A., *BioTechniques.*, **1994**, 18, 1, 62-63.
- 109 Gait M. J., Ed. *Oligonucleotide Synthesis, A Practical Approach*, IRL-Press, Oxford, **1984**
- 110 Wallace R. B., Schaffer J., Murphy R. F., Bonner J., Itakura K., *Nucleic Acids Res.*, **1979**, 6, 3543
- 111 Garay R. O., Naarmann H., Müllen K., *Amer. Chem. Soc.*, **1994**, 27, 1922-27
- 112 Iyengar B. S., Dorr R. T., Alberts D. S., *J. Med. Chem.*, **1997**, 40, 23, 3734-38
- 113 Scholl, Boettger, *Chem. Ber.*, **1930**, 63, 2128-34
- 114 Voratnikov A. M., *J. Gen. Chem. USSR*, **1991**, EN, 61, 5.2, 1128-1130
- 115 Elbs K., *J. Prakt. Chem.*, **1890**, 41, 1-33
- 116 Martin, *J. Amer. Chem. Soc.*, **1936**, 58, 1441
-

#### 4 REFERENCES

---

- 117 Erb, Bernhard, Kucma, Jean-Philippe, Mourey, Sandrine, Struber, Fritz. *Chemistry-A European Journal*, **2003**, 9, 11, 2582-2588.
- 118 Gryko D. T., Jurrzak J., *Synlett*, **1999**, 8, 1310
- 119 Vorotnivov A. M., Kopranenkov V. N., *J. Gen. Chem. USSR*, **1991**, 61, 1128-1130.
- 120 Fairbourne, *J. Chem. Soc.*, **1921**, 119, 1576-1579.
- 121 Willgerot, Maffezzoli, *J. Prakt. Chem.*, **1910**, 2, 82, 208.
- 122 Seeliger W., Their W., *Justus Liebigs Ann. Chem.*, **1966**, 698, 158-166.
- 123 Dendrinis K., Jeong J., Huang W., Kalivretenos A., *Chem. Commun.*, **1998**, 4, 499-500.
- 124 Fatome M. et al., *Farmaco Ed. Sci.*, **1981**, 36, 8, 740-748.
- 125 Hamer, Rathbone, *J. Chem. Soc.*, **1943**, 247.
- 126 Ritchie E., Taylor W. C., *Aust. J. Chem.*, **1971**, 24, 2137-2150.
- 127 Iyengar B. S., Dorr R. T., Alberts D. S., Solyom A. M., Krutzsch M., Remers W. A., *J. Med. Chem.*, **1997**, 40, 23, 3734-3738.
- 129 Scholl, Boettger, *Chem. Ber.*, **1930**, 63, 2128-2134.
- 130 Zagotto G., Oliva A., Guano F., Menta E., Capranico G., Palumbo M., *Bioorg. Med. Chem. Lett.*, **1998**, 8, 2, 121-126.
- 131 Heilmayer W., Wallfisch B., Oliver Kappe C., Wentrup C., Gloe K., Kollenz G., *Supramolecular Chemistry*, **2003**, 15, 5, 375-383.
- 132 van Otterlo, Willem A. L., Ngidi, E. Lindani, de Koning, Charles B., *Tetrahedron Letters*, **2003**, 44, 34, 6483-6486.
- 133 Cheng Maosheng, Zhang Li, Yan Dong, Chen Egong, Shen Jianmin, *Zhongguo Yaowu Huaxue Zazhi*, **2002**, 12, 4, 187-193.
- 134 Kurebayashi H., Haino T., Usui S., Fukazawa Y., *Tetrahedron*, **2001**, 57, 41, 8667-8674.
- 135 Numata Shigeaki, Nagaoka Kazuya, *Jpn. Kokai Tokkyo Koho*, **1988**, 7.
- 136 Kuznetsova N. A., Stepanov B. I., *Izvestiya Vysshikh Uchebnykh Zavedenii, Khimiya i Khimicheskaya Tekhnologiya*, **1979**, 22, 9, 1139-41.
- 137 Cotton F. Albert, Donahue James P., Murillo Carlos A., *J. Amer. Chem. Soc.*, **2003**, 125, 18, 5436-5450.
- 138 Forss D. A., Hancox N. C., *Australian Journal of Chemistry*, **1956**, 9, 420-424.
- 139 Dolson M. G., Swenton J. S., *J. Amer. Chem. Soc.*, **1981**, 103, 9, 2361-2371.
-



- 
- 140 Schobert Rainer, Pfab Hermann, Mangold Anett, Hampel Frank, *Inorganica Chimica Acta*, **1999**, 291, 1-2, 91-100.
- 141 Walsh James G., Furlong Patrick J., Gilheany Declan G., *Journal of the Chemical Society, Chemical Communications*, **1994**, 1, 67-8.
- 142 Rubin Yves, Lin Sophia S., Knobler Carolyn B., Anthony John, Boldi Armen M., Diederich Francois, *J. Amer. Chem. Soc.*, **1991**, 113, 18, 6943-6949.
- 143 Naruta Yoshinori, Nagai Naoshi, Yokota Tadafumi, Maruyama Kazuhiro, *Chemistry Letters*, **1986**, 7, 1185-8.
- 144 Nakeda Kei, Shibata Yumiko, Sagawa Yukihiro, Urahata Makoto, Funaki Keishi, Hori Kozo, Sasahara Hiroya, Yoshii Eiichi, *Journal of Organic Chemistry*, **1985**, 50, 24 4673-4681.
- 145 Schneider Geza, Horvath Tibor, Sohar Pal, *Carbohydrate Research*, **1977**, 56, 1, 43-52.
- 146 Walsh James G., Furlong Patrick J., Gilheany Declan G., *Perkin Transactions 1: Organic and Bio-Organic Chemistry*, **1999**, 24, 3657-3665.
- 147 Yoshida et al., *Tetrahedron Lett*, **1979**, 1141-1142.
- 148 Karrer, Ringli, *Helv. Chim. Acta*, **1947**, 30, 866, 1771.
- 149 Farmer et al., *J. Chem. Soc.* **1927**, 2950
- 150 Spangler Charles W., McCoy Ray K., Dembek Alexa A., Sapochak Linda S., Gates Bradley D., *Perkin Transactions 1: Organic and Bio-Organic Chemistry*, **1989**, 1, 151-154.
- 152 Singh Jujhar, Nigam M. B., Sardana Vinod, Jain Padam C., Anand Nitya, *Organic Chemistry Including Medicinal Chemistry*, **1981**, 20B, 7, 596-597.
- 153 Baloniak Sylwester, Ludwiczak Rufina Stella, Melzer Ewa, *Polish Journal of Chemistry*, **1978**, 52, 6, 1249-1253.
- 154 Weygand et al., *Angew. Chem.*, **1953**, 65, 525-529.
- 155 Kang Ji-Hye, Chung Hye-Eun, Kim Su Yeon, Kim, Yerim Lee, Jeewoo Lewin, Nancy E., Pearce Larry V., Blumberg Peter M., Marquez Victor E., *Bioorganic & Medicinal Chemistry*, 2003, 11, 12, 2529-2539.
- 156 Chaudhari Sachin S., Akamanchi Krishnacharya G., Synlett, **1999**, 11, 1763-1765.
- 157 McGhee William D., Riley Dennis P., Christ Matthew E., Christ Kevin M., *Organometallics*, **1993**, 12, 4, 1429-1433.
-

#### 4 REFERENCES

---

- 158 Murdock K. C., Angier R. B., *Journal of Organic Chemistry*, **1962**, 27, 2395-2398.
- 159 Bobbitt J. M., Amundsen Lawrence H., Steiner Russell I., *Journal of Organic Chemistry*, **1960**, 25, 2230-2231.
- 160 Huisgen Rolf, Laschtuvka Erich, *Chemische Berichte*, **1960**, 93, 65-81.
- 161 Coogan M. P., Platts J. A., Haigh R. G., *Sulfur Letters*, **2002**, 25, 6, 251-257.
- 162 Kuznetsov Mikhail A., Kuznetsova Ljudmila M., Schantl Joachim G., Wurst Klaus, *European Journal of Organic Chemistry*, **2001**, 7, 1309-1314.
- 163 Kuznetsov M. A., Kuznetsova L. M., Schantl J, *Russian Journal of Organic Chemistry*, **2000**, 36, 6, 836-842.
- 164 Schulz Manfred, Kluge Ralph, Willscher Sabine, *Liebigs Annalen der Chemie*, **1987**, 8, 671-678.
- 165 Hoesch Lienhard, Koeppel Bruno, *Helvetica Chimica Acta*, **1981**, 64, 3, 864-889.
- 166 Leuenberger Christian, Hoesch Lienhard, Dreiding Andre S, *Helvetica Chimica Acta*, **1981**, 64, 4, 1219-1233.
- 167 Awad W. I., Kandile N. G., *Journal fuer Praktische Chemie*, **1979**, 321, 1, 8-12.
- 168 Tawney et al., *J. Org. Chem.*, **1961**, 26, 15-21.
- 169 Vail S. L., Pierce A. G., *J. Org. Chem.*, **1972**, 37, 391-397.
- 170 Sisido et al., *Tetrahedron Lett.*, **1968**, 5267-5269.
- 171 Makino Kenjiro, Masamoto Tsunezo, Yamada Kenichi, Kasahara Tatsuo, Asado Akio, *Jpn. Kokai Tokkyo Koho*, **1992**, 12.
- 172 Kovacic, Hein, *J. Amer. Chem. Soc.*, **1959**, 81, 1187-1189.
- 173 Cheronis J. C., Whalley E. T., Nguyen K. T., Eubanks S. R., Allen L. G., *J. Med. Chem.*, **1992**, 35, 9, 1563-1572.
- 174 Weissler Manfred, Kliem Hans-Christian, Sauerbrei Bernd, *PCT Int. Appl.*, **2002**, 74.
- 175 Lific et al., *Chem. Abstr.*, **1970**, 22, 118, 119-120.
- 176 Moore Wardt, *J. Amer. Chem. Soc.*, **1956**, 78, 2414.
- 177 Keana John F. W., Ogan Marc D., Lu Yixin, Beer Michael, Varkey J., *Journal of the American Chemical Society*, **1986**, 108, 25, 7957-7963.
- 178 Shiotani Masahisa, Sasaki Manji, *Jpn. Kokai Tokkyo Koho*, **1986**, 5.
- 179 Pal Bikash, Pradhan Prasun K., Jaisankar Parasuraman, Giri Venkatachalam S., *Synthesis*, **2003**, 10, 1549-1552.
-

- 
- 180 Einhorn Cathy, Durif Andre, Averbuch Marie-Therese, Einhorn Jacques, *Angewandte Chemie, International Edition*, **2001**, 40, 10, 1926-1929.
- 181 Borah Harsha N., Boruah Romesh C., Sandhu Jagir S., *Journal of Chemical Research, Synopses*, **1998**, 5, 272-273.
- 182 Chandrasekhar S., Takhi Mohamed, Uma G., *Tetrahedron Letters*, **1997**, 38, 46, 8089-8092.
- 183 Milas, Kurz, Anslo, *J. Amer. Chem. Soc.*, **1937**, 12, 59, 543.
- 184 Tanatar, *Chem. Ber.*, **1879**, 2293.
- 185 Kekule, Anscütz, *Chem. Ber.*, **1880**, 13, 215.
- 186 Egli Martin, Dobler Max, *Helv. Chim. Acta.*, **1989**, 72, 1136-1150.
- 187 Heilbronner E., Bock H., "Das HMO-Modell und seine Anwendung, Band 1, 2 und 3", *2. Auflage, Verlag Chemie*, **1978**.
- 188 Langenegger S. M., Häner R., *Helv. Chim. Acta*, **2002**, 85, 3414-3421.
- 189 Batey R. T., Rambo R. P., Doudna J. A., *Angew. Chem., Int. Ed Engl.* **1999**, 38, 2326-2343.
- 190 Hermann T., Patel D. J., *J. Mol. Biol.*, **1999**, 294, 829-849.
- 191 Moore P. B., *Annu. Rev. Biochem.*, **1999**, 68, 287-300.
- 192 Hilbers C. W., Haasnoot C. A. G., Debruin S. H., Joordens J. J. M., Vandermarel G. A., Vanboom J. H., *Biochimie*, **1985**, 67, 685-695.
- 193 Murchie A. I. H., Lilley D. M. J., *Methods Enzymol.*, **1992**, 211, 158-180.
- 194 Wengel J., *Organic & Biomolecular Chemistry*, **2004**, 2, 277-280.
- 195 Durand M., Chevrie K., Chassignol M., Thuong N. T., Maurizot J. C., *Nucleic Acids Res.*, **1990**, 18, 6353-6359.
- 196 Ma M. Y. X., Reid L. S., Climie S. C., Lin W. C., Kuperman R., Sumnersmith M., Barnett R. W., *Biochemistry*, **1993**, 32, 1751-1758.
- 197 Pils W., Micura R., *Nucleic Acids Res.*, **2000**, 28, 1859-1863.
- 198 Salunkhe M., Wu T. F., Letsinger R. L., *J. Am. Chem. Soc.*, **1992**, 114, 8768-8772.
- 199 Letsinger R. L., Wu T. F., *J. Am. Chem. Soc.*, **1995**, 117, 7323-7328.
- 200 Lewis F. D., Kalgutkar R. S., Wu Y. S., Liu X. Y., Liu J. Q., Hayes R. T., Miller S. E., Wasielewski M. R., *J. Am. Chem. Soc.*, **2000**, 122, 12346-12351.
- 201 Yamana K., Yoshikawa A., Nakano H., *Tetrahedron Lett.*, **1996**, 37, 637-640.
- 202 Stutz A., Langenegger S. M., Häner R., *Helv. Chim. Acta*, **2003**, 86, 3156-3163.
-

#### 4 REFERENCES

---

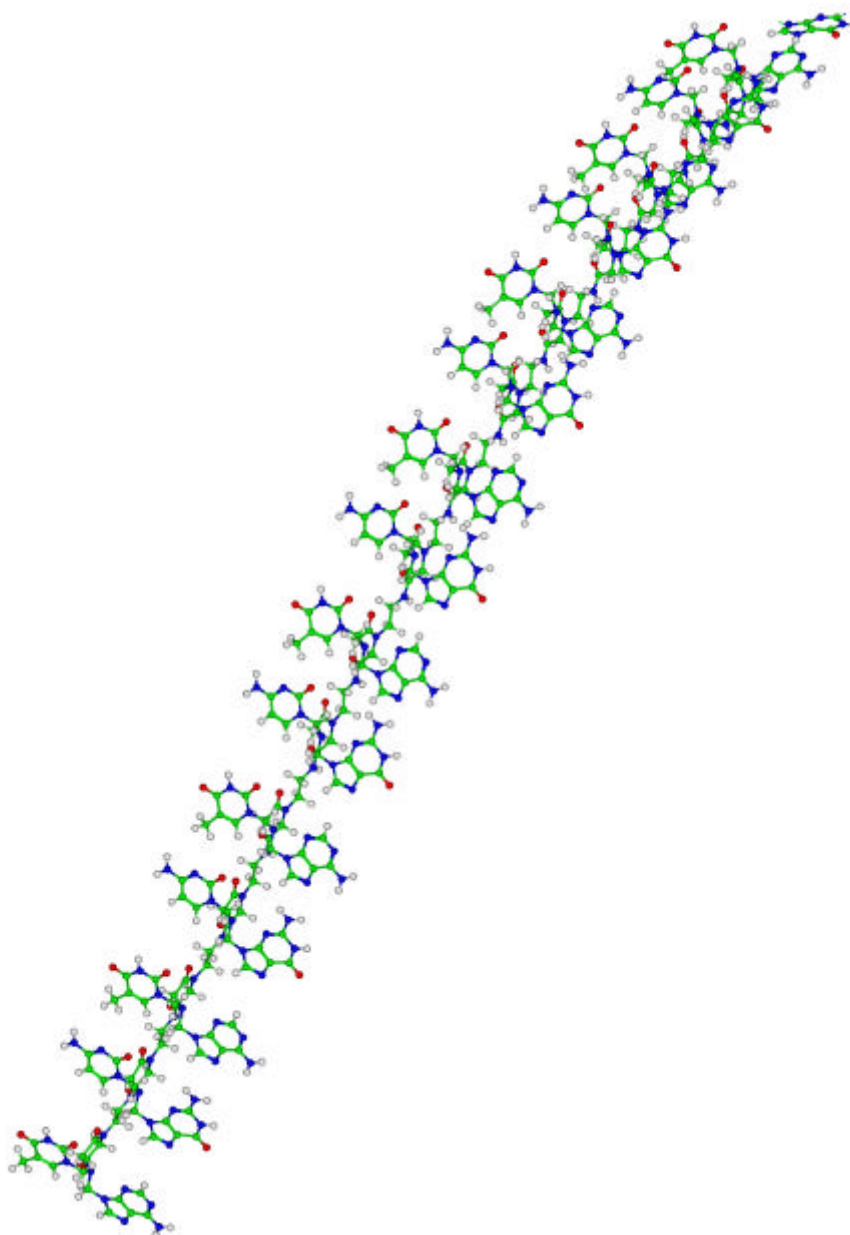
- 203 Lewis F. Helvoigt D., S. A., Letsinger R. L., *Chem. Commun.* **1999**, 327-328.
- 204 Czapinski J. L., Sheppard T. L., *ChemBioChem* **2004**, 5, 127-129.
- 205 Lewis F. D., Wu Y., Zhang L., *Chem. Commun.* **2004**, 636-637.
- 206 Bianke G., Häner R., *ChemBioChem*, **2004**; 5, 1063-1068.
- 207 Maglott E. J., Glick G. D., *Nucleic Acids Res.* **1998**, 26 (5): 1301–1308

## 5 APPENDIX

### 5.1 Proposal 2003

# Janus PNA

**Triple helix formation for once different.**



February 2003



## Abstract

In this proposal we describe a possible synthesis for what we call Janus PNA. A PNA backbone functionalised with a Base-Pair-Recognition-Motive in each building block should be able to recognise a DNA-Duplex. Higher melting points are expected through backbone interactions and  $\pi$ -stacking, while Watson-Crick interactions are responsible for the sequence recognition.

## Introduction

Janus is the Roman god known as the custodian of the universe. He is the god of beginnings and the guardian of gates and doors. He is lord over the first hour of every day, the first day of the month and January, the first month of the year. Two heads back to back represent Janus, each looking in opposite directions. His double-faced head appears on many Roman coins. Originally, one face was bearded and one was not, most likely representing the sun and the moon. In his right hand he holds a key. He was worshipped at the beginning of planting time, harvest, marriages, births and other important beginnings in a person's life.

In 1966 Cristol and Lewis<sup>1</sup> published an article about the synthesis and the properties of 5,5a,6,11,11a,12-Hexahydro-5,12:6,11-di-o-benzenonaphtacene. Due to its symmetric look they proposed the trivial name "januesene".

In 1994, Lehn et al.<sup>2</sup> presented the synthesis of three molecules containing the same sequences of H-bonding sites on both sides. For this reason they named them Janus molecules. They also proposed binding studies and self-assembly features towards supramolecular structures, formed from different combinations of the mentioned Janus molecules (Fig.1).

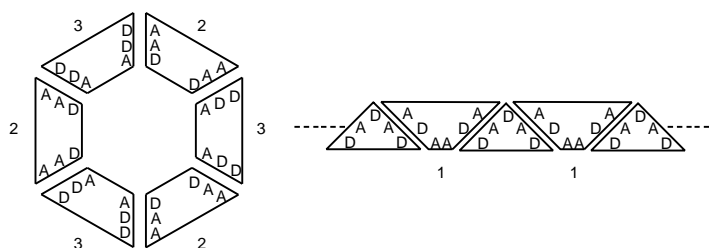


**Figure 1:** Cyclic and linear supramolecular structure of Janus molecule adducts. D and A represent hydrogen bond donating and accepting sites.

Two years later, Lehn et al.<sup>3</sup> published the binding properties of two Janus type heterocycles designed to recognize a cytosine-uracil mismatched base-pair. These heterocycles were inserted, in a wedgelike fashion, between the bases forming a triad motif with maximum number of Watson-Crick interactions (Fig.2). The binding properties of the CU-wedges were assessed by analysing the <sup>1</sup>H-NMR spectral changes occurring upon titration of a CDCl<sub>3</sub> solution with the lipophilic derivatives N-propyluracil and 1-(3,5-di-tert-butylbenzyl)cytosine.

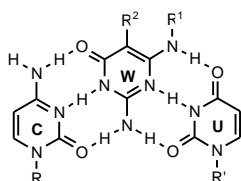


**Figure 2:** Watson-Crick interactions of the CU-wedges in a CU mismatched base-pair.

Here, we suggest the creation of polymers that contain branches of base-pair recognising Janus molecules. With suitable combination of Janus molecules and backbone we expect the polymer to wedge specific into a target DNA duplex to form a stable triplex like tertiary structure (Fig.3). In contrast to usual triplex formation, we would break up all Watson-Crick interactions of the DNA duplex and replace them by new ones between each single strand and our Janus polymer, in this way duplicating the number of hydrogen bonds.

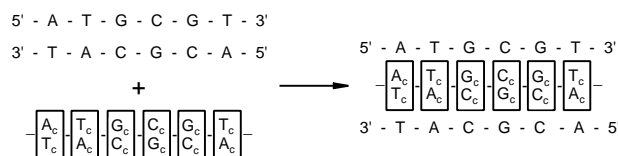


**Figure 3:** Wedge of the Janus polymer into DNA. c = complementary.



We decided to design the base-pair recognising part (the branches) by connecting the bases of the two base-pairs in a way that the H-bond acceptors and donors face away from the center of the new molecule (Fig.4). Since the bases have the possibility to stay in one plane some additional  $\pi$ -stacking interactions can be expected.

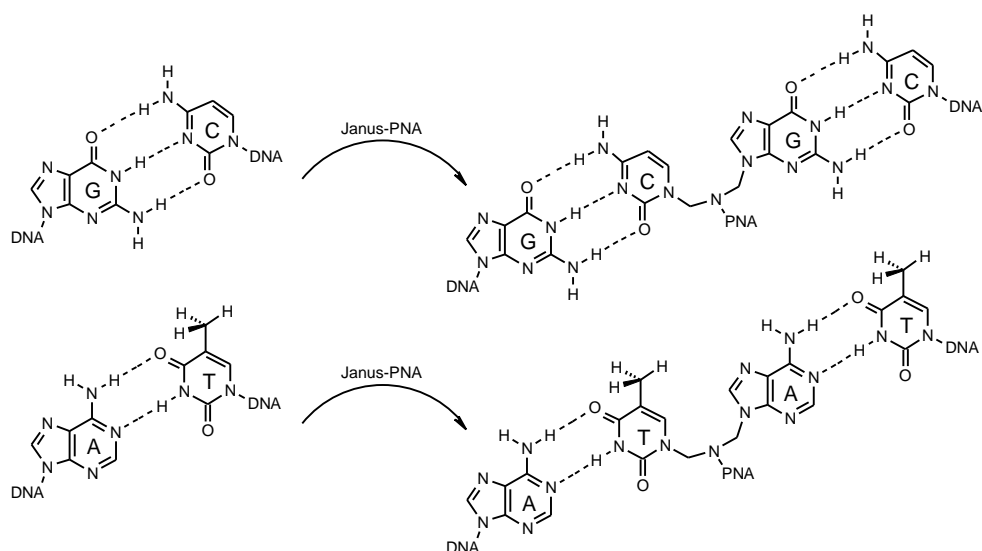


**Figure 4:** H-bonds in the proposed tertiary structure.

Free rotation of the two bases and the backbone allows recognition of the respective base-pair regardless if the purine base is placed in the encoding strand and the pyrimidine in the complementary strand or the other way around (Fig.5). Since it recognises base-pairs and not the single bases, just two different building blocks are enough to recognise a sequence (Fig.6). In other words, the target sequence, which contains four characters, gets “translated” into a binary like code which just makes a difference if there are two or three H-bonds but does not care about which base is on which strand.

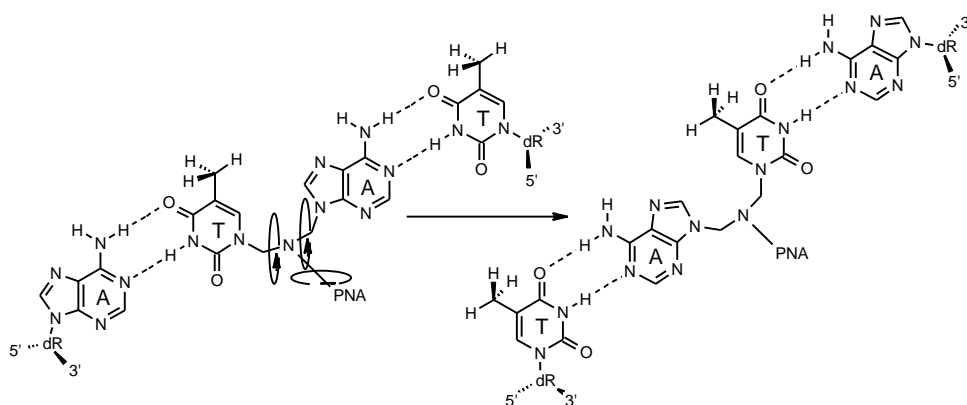


**Figure 5:** Desired 180° rotations of bases and branch to recognise a TA-bp instead of an AT-bp with the same Janus molecule.

For this reason a coincidentally sequence of our Janus building blocks would not recognise just one DNA sequence but  $2^{n+1}$  sequences (if  $n$  corresponds to the number of building blocks and is diff. from one). Assuming that the human genome contains  $5 \times 10^9$  bp, according to probability, a conventionally antigen agent must consist of 17 bases, in our case, 33 building blocks are needed to find a single target in the genome. For this calculation, we assumed that the probability for a specific sequence ( $(1/4)^n$  respectively  $(1/2)^n$ ) multiplied by the number of possible fragments with  $n$  bases in the genome ( $2 \times (5 \times 10^9)^{-n}$ ) has to be smaller than two. This will give us, the minimal probe length for a unique target.

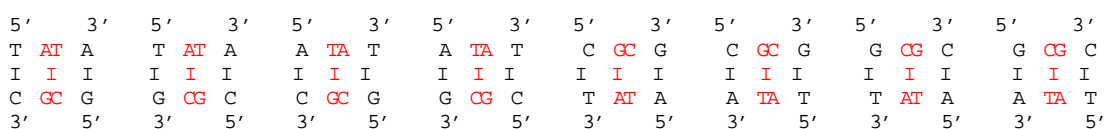


**Figure 6:** Sequence recognition for a Janus dimer. ( $n = 2$ ) → eight possible target sequences.

The Janus base branches are connected to a peptide backbone which is used quite often in PNA-Synthesis (Peptide Nucleic Acid)<sup>4-11</sup>. This PNA-backbone, in which the entire sugar-phosphate backbone is replaced by an *N*-(2-aminoethyl)glycine-based polyamide structure (Fig.7), was used first by the Danish group of Buchardt, Nielsen, Egholm and Berg<sup>12-15</sup>. The astonishing discovery that these PNAs bind with higher affinity to complementary nucleic acids than their natural counterparts<sup>16</sup> and that they obey the Watson-Crick base-pairing rules, led to the rapid establishment of a new branch of research on diagnostic and therapeutic applications<sup>17,18</sup>.

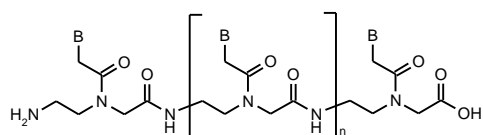


**Figure 7:** Structure of usual PNA. B = nucleobase.

The higher affinity in a PNA-DNA hybrid compared to the DNA-DNA duplex of the same sequence is based on backbone-backbone interactions. In a pure DNA duplex both backbones carry negative charges of the phosphodiester groups and due to that repel each other. However a PNA backbone contains amino groups which can be protonated, causing attraction of the backbones in a PNA-DNA hybrid. We expect a similar effect in our DNA-PNA-DNA hybrid,

where the positively charged PNA backbone is located sandwich like between the two negatively charged DNA backbones.

## Synthesis

Our synthetic propose considers experiences concerning the protection and activation of the monomers made by E. Uhlmann et al. in Hoechst AG<sup>11</sup>. The mono-methoxy-trityl protection group in the N-terminus shows advantages in the automated PNA synthesis.

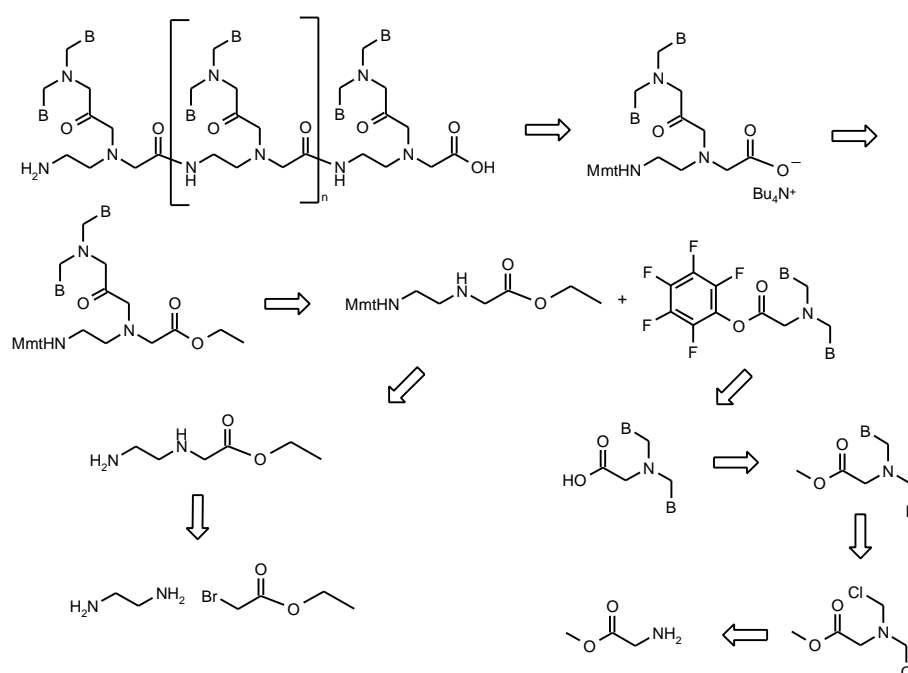


**Figure 8:** Retro synthesis of the PNA backbone.

By using an acid labile protection group (Mmt) in the N-terminus the choice to protect the nucleobases is reduced to acid stable amid protection. It showed that it is advantageous to use different protection groups to protect the amines of C, A and G.

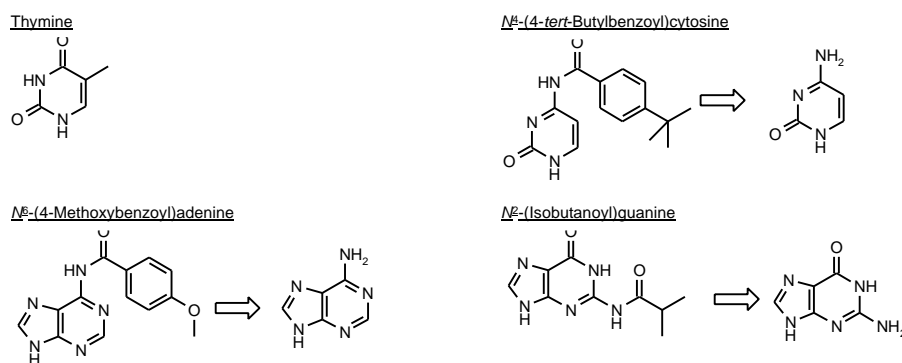


**Figure 9:** Retrosynthesis of the protected bases.

In our proposed synthesis, we start with the protection of the nucleobases C, A and G to avoid side reactions with their primary amines later on the synthesis. Uhlmann et al.<sup>5</sup> reached good results with the following protection groups: Cytosine was acylated with *tert*-butylbenzoyl chloride in DMF in the presence of triethylamine. Originally, they synthesized a benzoyl protected cytosine monomer but changed because of its tendency to precipitate during PNA synthesis to the more lipophilic *tert*-butylbenzoyl protecting group. Adenine was protected by heating with anisoyl chloride in pyridine and, for guanine, the protection with isobutanoyl chloride by heating in DMF in the presence of triethylamine turned out to be useful (Fig.10).

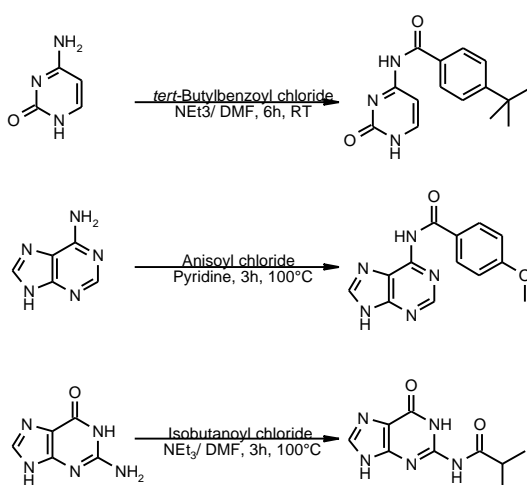


**Figure 10:** Protection of the primary amino groups of the nucleobases Cytosine, Adenine and Guanine.

We propose a separate synthesis of branches and backbone followed by coupling and finally activation of the acid (Fig.11). In the first step of branch synthesis, the primary amine of glycine methyl ester undergoes a chloromethylation upon treatment with paraformaldehyde followed by  $\text{SOCl}_2$ <sup>18</sup>. In a next step a one to one mixture of the corresponding protected nucleobases will be activated with sodium hydride in DMF followed by reaction with the dichloride at reflux temperature<sup>19</sup>. Hydrolysis of the methylester with hydrogenchloride and 1,4-dioxane in dichloromethane<sup>8</sup> followed by acetylation with DCC and pentafluorophenol in DMF<sup>6</sup> terminate branch synthesis.

Backbone synthesis starts by alkylation of ethylenediamine with ethyl bromoacetate in dichloromethane<sup>8</sup>. In the next step, the primary amine will be protected with Mmt-Cl in dichloromethane<sup>6</sup>.

Coupling of the branch and the Mmt protected backbone in the presence of triethylamine in acetonitril<sup>6</sup> and subsequent saponification and conversion to tetra-n-butylammonium salt will lead up to the desired PNA monomers<sup>6</sup>.

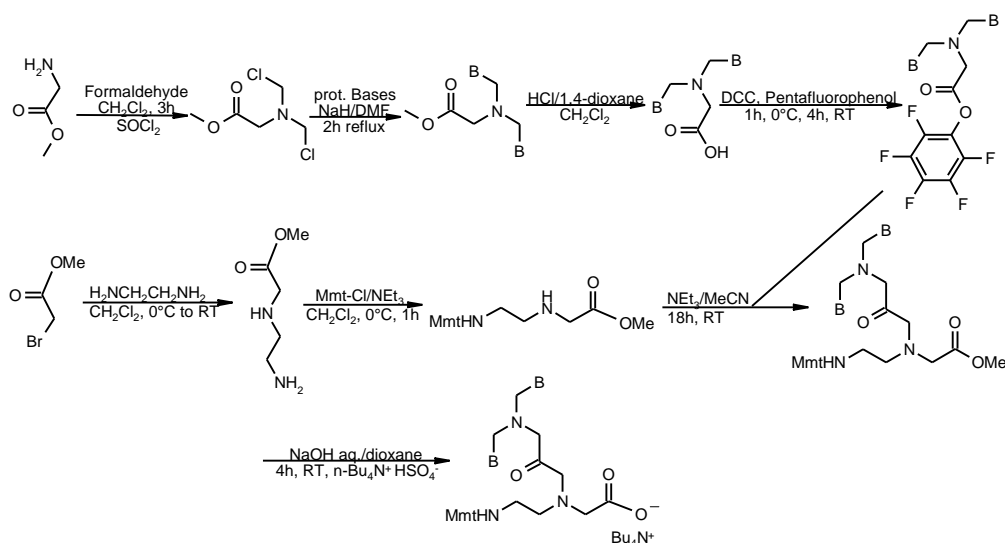


**Figure 11:** Synthesis of the protected Janus-PNA monomers for automated PNA synthesis. B = protected nucleobases.

Compared with automated DNA synthesis, where an oxidation step takes place in every cycle, the PNA synthesis cycle consists just of three steps (Fig.12): Coupling, capping and detritylation. The use of a base-labile aminohexylsuccinyl linker between the solid-support and glycine allows the simultaneous cleavage of the desired PNA oligomer from the support and deprotection of its nucleobases with concentrated aqueous ammonia.

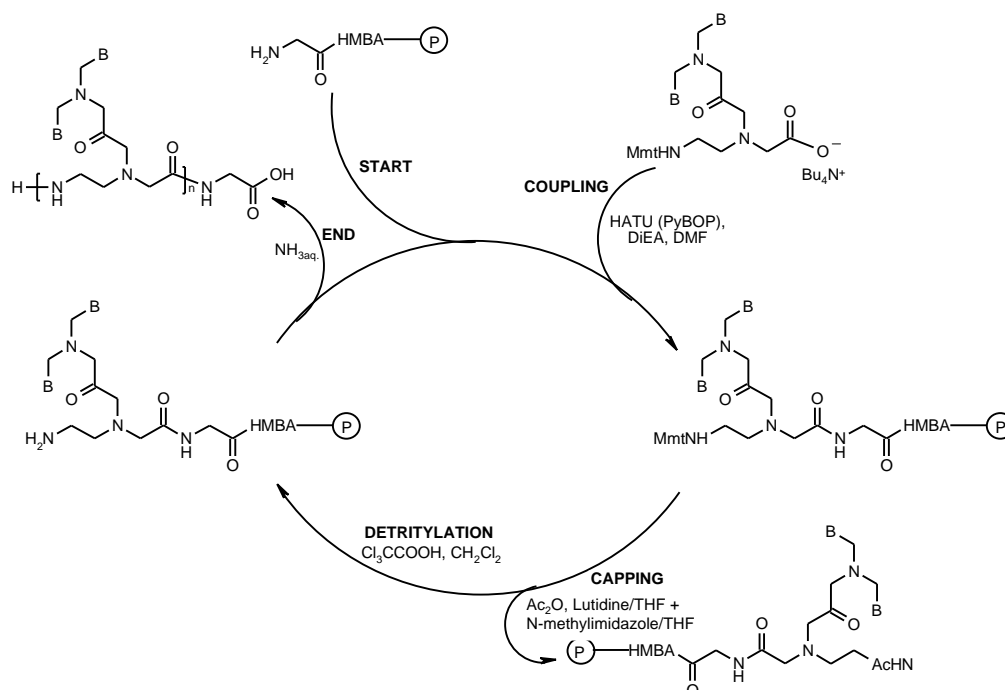


**Figure 12:** Cycle used in automated PNA synthesis using Monomethoxytrityl-protected monomers.

The temporary protecting group Mmt can be cleaved under very mild conditions with 3% trichloroacetic acid in dichloromethane and the coupling efficiency can be determined easily by measurement of the coloured Mmt cations released. The coupling step takes part in DMF by preactivation with HATU (O-(7-Azabenzotriazol-1-yl)-N,N,N',N'-tetramethyluronium hexafluorophosphate) or PyBOP (Benzotriazol-1-yloxy)tripyrrolidinophosphonium hexafluorophosphate) in the presence of DIEA. Capping, in an analogous manner to DNA synthesis, can be done with acetic anhydride/lutidine/N-methylimidazole in THF.

Pure Janus PNA should be retrieved by purification of the cleaved and deprotected oligomer with reversed phase HPLC.

## Characterisation

After confirmation of the expected mass of the purified Janus PNA, several melting experiments can be done to characterise this new oligomers. In a melting experiment one observes the change of absorbance, at a certain wavelength, as a function of the temperature. Usually, a big change is observed in the moment of denaturation - the breaking up of the base-pairing - which is a highly cooperative process. By heating up a buffered solution just containing a Janus PNA strand we could get some important informations about dimerisation, since the strands are complementary to each other. As a next experiment, melting of the PNA with a DNA single strand would allow to compare the results with those from conventional PNA-DNA hybrids. Since we expect higher stability in our complex, one should observe a higher melting temperature by heating up a DNA duplex in the presence of the corresponding PNA. To control the selectivity of our PNA, the same experiments would have to be done with different not fully complementary sequences (mismatches, insertions and deletions). By comparing the melting curves the thermodynamic parameters enthalpy and entropy can be determined and the influence of electrolyte concentration on the melting temperature would allow to calculate the number of ions used to stabilize the triplex. More difficult than characterising the pairing properties could be the determination of the DNA-PNA-DNA triplex structure. NMR studies and X-ray crystallography could solve this challenge.

## Final Remarks

The project proposed above could revolutionize classical triplex research and our Janus PNA, or a optimised version of it, might become a new important tool in gene diagnostics and antigene therapy. We tried to combine the advantages of a PNA-backbone with the recognition of both bases in a base-pair by our Janus molecules. The synthesis of the monomers consists of twelve steps to receive the two monomers. Synthesis of the Janus PNA monomers and first oligomers could be a project for a diploma in organic synthesis followed by a post doc to do the characterisation. The entire project could also serve for a PhD-thesis. The principle of Janus PNA does not necessarily depend on the building blocks we introduced in this proposal, different backbones and linkers could be used. There is also the possibility to work with four different building blocks, for example by linking the branches with a double bound to the backbone, which would not allow any further rotation. Moreover, different combinations of nucleobases are conceivable, allowing recognition of mismatches.

---

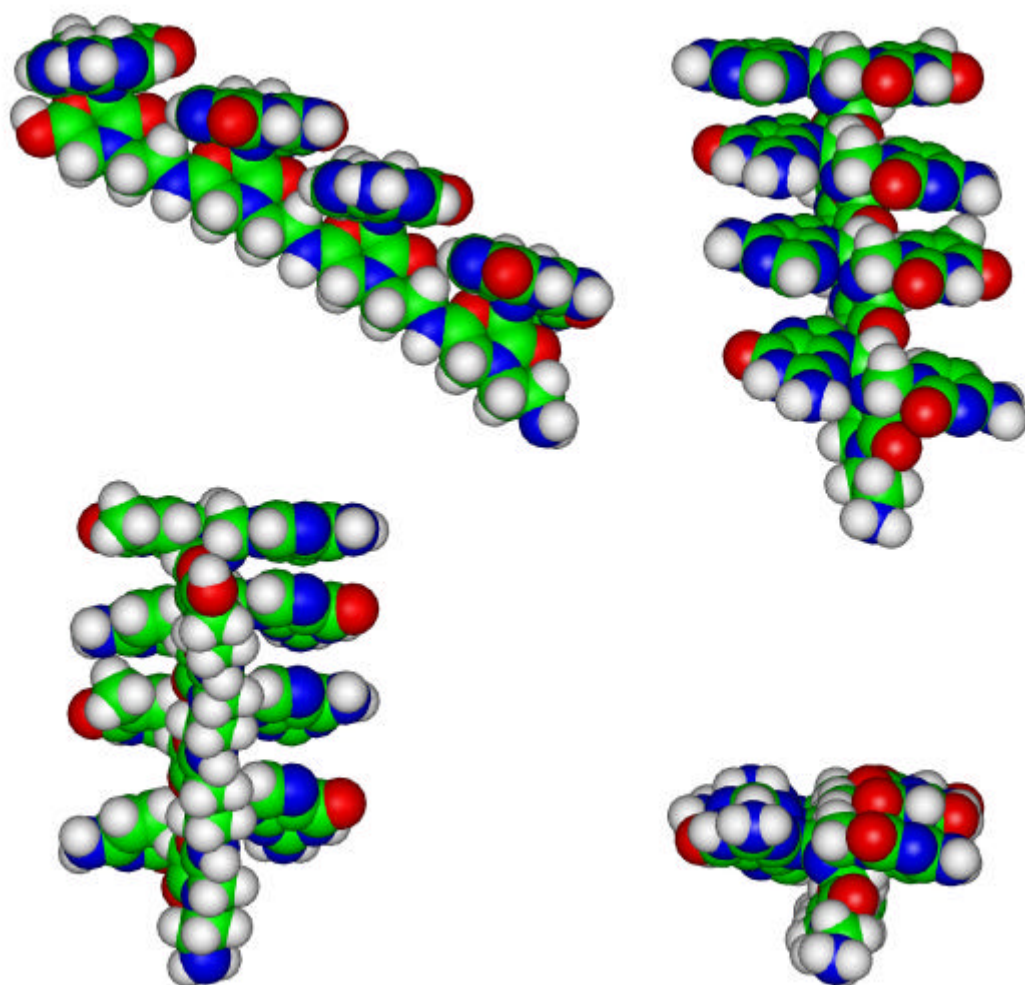


**Figure 13:** Views on H<sub>2</sub>N-AT-CG-AT-CG-OH Janus PNA tetramer from different perspectives.



---

## Literature

1. - Stanley J. Cristol, David C. Lewis; *JACS*; **1967**; 89; 6; 1476-1483
2. - Andrew Marsh, Ernest G. Nolen, Kevin M. Gardinier, Jean-Marie Lehn; *Tetrahedron Letters*; **1994**; 34; 3; 397-400
3. - Neil Branda, Guido Kurz, Jean-Marie Lehn; *Chem. Commun.*; **1996**; 2443-2444
4. - Györgyi Kovács, Zoltán Timár, Zoltán Kele, Lajos Kovács; *Nucleic Acids Lab.*; Dep. of Med. Chem.; University of Szeged; Hungary; **2000**
5. - David W. Will, Gerhard Breipohl, Dietrich Langner, Jochen Knille and Eugen Uhlmann; *Tetrahedron*; **1995**; 51; 44; 12069-12082
6. - Dmitry A. Stetsenko, Elena N. Lubyako, Viktor K. Potapov, Tatyana L. Azhikina and Evgeny D. Sverdlov; *Tetrahedron Letters*; **1996**; 37; 20; 3571-3574
7. - G. Breipohl, J. Knolle, D. Langner, G O'Malley and E. Uhlmann; *Bioorg. & Med. Chem. Letters*; **1996**; 6; 6; 665-670
8. - Stephen A. Thomson, John A. Josey, Rodolpho Cadilla, Michael D. Gaule, C. Fred Hassmann; *Tetrahedron*; **1995**; 51; 22; 6179-6194
9. - Gerhard Breipohl, David W. Will, Anusch Peyman and Eugen Uhlmann; *Tetrahedron*; **1997**; 53; 43; 14671-14686
10. - Alexander C. van der Laan, Rick Brill, Robert G. Kuimelis, Esther Kuyl- Yeheskiely; *Tetrahedron Letters*; **1997**; 38; 13; 2249-2252
11. - Eugen Uhlmann, Anusch Peyman, Gerhard Breipohl and David W. Will; Review; *Angew. Chem. Int. Ed.*; **1998**; 37; 2796-2823
12. - P. E. Nielsen, M. Egholm, R. H. Berg, O. Buchardt; *Science*; **1991**; 1497-1500
13. - M. Egholm, O. Buchardt, R. H. Berg; *J. Am. Chem. Soc.*; **1992**; 114; 9677-9678
14. - M. Egholm, O. Buchardt, P. E. Nielsen, R. H. Berg; *J. Am. Chem. Soc.*; **1992**; 114; 1895-1897
15. - M. Egholm, C. Behrens, L. Christensen, R. H. Berg, P. E. Nielsen, O. Buchardt; *J. Chem. Soc. Chem. Commun.*; **1993**; 800-801
16. - P. E. Nielsen, M. Egholm, R. H. Berg, O. Buchardt; *Anti-Cancer Drug Des.*; **1993**; 8; 53-63
17. - B. Hyrup, P. E. Nielsen; *Bioorg. Med. Chem.*; **1996**; 4; 5-23
18. - Joshua D. Lawrence, Hongxiang Li, Thomas B. Rauchfuss; *Chem. Commun.*; **2001**; 16; 1482-1483
19. - Gorczyca et al.; *Acta Pharm. Jugosl.*; **1978**; 28; 173

## 5.2 Poster - SCS Fall Meeting 2003



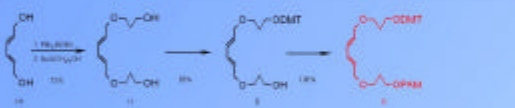
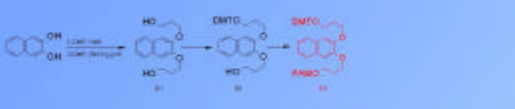
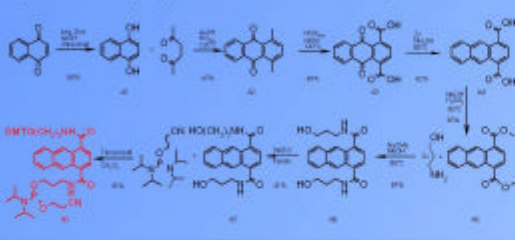
### Melting Studies on Diene Modified Oligonucleotides and their Diels-Alder Bioconjugates

Rolf Tona and Robert Haner  
Department of Chemistry and Biochemistry, University of Bern, Freiestrasse 3, CH-3012 Bern, Switzerland

#### Introduction

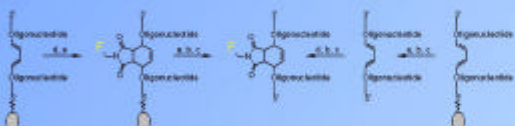
Electron rich dienes are known to undergo [2 + 4] cycloaddition with electron poor enes. We have used the Diels-Alder reaction for the preparation of bioconjugates by reacting diene-modified oligonucleotides with fluorescein maleimide. For this purpose, different diene phosphoramidites were prepared and used for the synthesis of the corresponding oligonucleotides. The reactivity of the obtained oligonucleotides towards fluorescence labeling with fluorescein maleimide was investigated. The [2 + 4] cycloaddition was performed just after automated synthesis while the diene-containing oligonucleotide was still bound on the solid support. We compared the stability of natural, diene-modified and fluorescein-labeled oligonucleotides by thermal denaturation experiments. PAGE was used to observe labeling efficiency.

#### Synthesis of the phosphoramidites and modified oligonucleotides



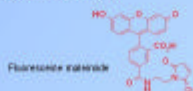
In the automated DNA synthesis, 1.0 M solutions of the building blocks were used. The coupling time for our phosphoramidites was extended from 25 seconds to 5 minutes to reach highest coupling efficiency.

#### Fluorescence labeling by bioconjugation via Diels-Alder Reaction



(Conditions: a) 25% aq ammonia, 60°C; b) HPLC; c) desalting; d) labeling; e) H<sub>2</sub>O, CH<sub>3</sub>CN washing)

After cleaving from the solid support and deprotection of the nucleobases in aqueous ammonia at 50°C, the modified oligonucleotides have been purified with HPLC and a SepPak desalting procedure. The modified oligonucleotides were reacted in 10mM phosphate buffer at pH 5.5 and with 10 equivalents of fluorescein maleimide at 20 to 30°C within 24 hours. While another HPLC purification was needed for the free labeled oligonucleotides, surplus of fluorescein maleimide can be washed away easy from solid support bound oligonucleotides. The label is stable under the deprotection conditions; just one purification is necessary.



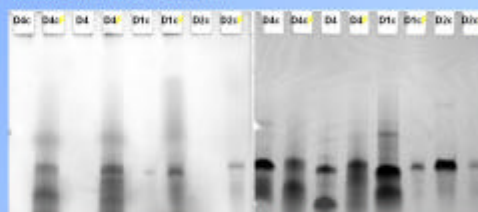
#### Conclusion

We demonstrated that bioconjugation of our diene modified oligonucleotides with a maleimide is possible in solution as well as bound on solid support under the same mild conditions. For the labeling the position of the diene in the oligonucleotide is of no relevance and intramolecular duplex formation does not inhibit the labeling. In double stranded parts we observe destabilisation while the building block used as loop replacement can favour hairpin formation. Bioconjugation with any maleimide containing molecule an also linkage of two modified oligonucleotides with a disulfide linker should be possible.

K. W. Hill, J. Tammes, R. Haner, *J. Org. Chem.*, 2005, 70, 5352-5358  
Sequence Calculator <http://pubs.chem.bern.unibe.ch/seqcalc.html>  
T. P. Liu, *J. Pol. Sci. Lett. Chem. Commun.*, 1996, 34, 15-2318

#### Gelelectrophoresis

(Conditions: 12% polyacrylamide gel, 10M urea, formamide loading buffer 1X TBE, urea-saturated, 340 V, 12 mA, 4 W, 20 minutes)



D1a : 5'-ACG-GCT-GCC-GAG-GTG-GCC-TAC-GCA-CGC-GTC-CGG-T  
D1b : 5'-TAC-CGA-CGG-CTC-GC-CGG-ACC-CGT-GCC-GAG-CGC-T  
D1c : 5'-ACG-GCT-GCC-GAG-GAG-ACC-TGC-GCA-CGC-GTC-CGG-T  
D1d : 5'-ACG-GCT-GCC-GAG-GAG-GCC-TGC-GCA-CGC-GTC-CGG-T

With fluorescence detection just fluorescein labeled oligonucleotides are visible [left] while all oligonucleotides can be observed after treating the gel with stains all reagent.

#### Melting experiments

(Conditions: 10mM phosphate pH 7.0, 10mM / 200mM NaCl, 0.5-1.0 μM DNA duplex)

Duplex	Tm 10mM NaCl	ΔT	Tm 200mM NaCl	ΔT
N1 : 5'-TGC CGA CCG CTC CCG ACC CGT GCG CAG GGC-3'	71°C		88°C	
N2 : 5'-ACG GCT GCC GAG GAG GCG TGC GCA CGC GTC CCG-3'	70°C	-1°C	84°C	-2°C
N3 : 5'-TGC CGA CCG CTC CCG ACC CGT GCG CAG GGC-3'	67°C	-4°C	83°C	-3°C
N4 : 5'-ACG GCT GCC GAG GAG GCG TGC GCA CGC GTC CCG-3'	67°C	-4°C	83°C	-3°C
N5 : 5'-TGC CGA CCG CTC CCG ACC CGT GCG CAG GGC-3'	62°C	-9°C	77°C	-8°C
N6 : 5'-ACG GCT GCC GAG GAG GCG TGC GCA CGC GTC CCG-3'	62°C	-9°C	77°C	-8°C
N7 : 5'-TGC CGA CCG CTC CCG ACC CGT GCG CAG GGC-3'	62°C	-9°C	87°C	-16°C
N8 : 5'-ACG GCT GCC GAG GAG GCG TGC GCA CGC GTC CCG-3'	60°C	-10°C		
N9 : 5'-TGC CGA CCG CTC CCG ACC CGT GCG CAG GGC-3'	60°C	-10°C		
N10 : 5'-ACG GCT GCC GAG GAG GCG TGC GCA CGC GTC CCG-3'	61°C	-10°C	87°C	-16°C
N11 : 5'-TGC CGA CCG CTC CCG ACC CGT GCG CAG GGC-3'	61°C	-10°C	87°C	-16°C
N12 : 5'-ACG GCT GCC GAG GAG GCG TGC GCA CGC GTC CCG-3'	61°C	-10°C	87°C	-16°C

While the insertion of a (unpaired) T in a natural duplex does not have a big influence on duplex stability, the diene building block leads to a significant reduction of the Tm. The lower melting point with a additional T in complementary position and the giant destabilisation after labeling could point out that the diene takes intercalator like part of the π-stacking.


Duplex	Tm 10mM NaCl	ΔT	Tm 200mM NaCl	ΔT
N13 : 5'-CGG TAC CTG CTT TTA TCA GGA CCG-3'	58°C		89°C	
N14 : 5'-CGG TAC CTG ACT TTT GTC AGT ACC GA-3'	51°C	-7°C	84°C	-5°C
N15 : 5'-CGG TAC CTG ACT TTT GTC AATG TAC CG-3'	47°C	-11°C	95°C	-14°C
N16 : 5'-CGG TAC CTG ACT TTT GTC A-3'	47°C	-12°C	99°C	-11°C

The melting temperatures are in agreement with hairpin formation. Insertion of an extra base (C) is destabilising, as expected. Introduction of a diene opposite to the bulged base leads to a further strong decrease in duplex stability. Much to our surprise, the duplex resulting after Diels-Alder bioconjugation is considerably more stable than the diene-modified analogous duplex.

Loop	Tm 10mM NaCl	ΔT	Tm 200mM NaCl	ΔT
N17 : 5'-TGA CTG CAG AAT TTT CTC TGC AGT GA-3'	69°C		73°C	
N18 : 5'-TGA CTG CAG AAGG CTC TGC AGT GA-3'	71°C (73°C) <sup>a</sup>	+4°C	81°C (84°C) <sup>a</sup>	+11°C
N19 : 5'-TGA CTG CAG AAG-3'	80°C	+9°C	81°C (79°C) <sup>a</sup>	-1°C

As can be seen, replacement of the T4-loop by the diene building block leads to a considerable stabilisation of the hairpin structure. In addition, a second weak transition can be observed at lower temperature, most likely resulting from melting of the corresponding intermolecular duplex. Thus, the diene building block seems to be a good substitute for a T4-loop in a hairpin structure. Subsequent Diels-Alder reaction with the fluorescein derived maleimide, leads to a considerable destabilisation at low salt conditions, however. More studies are ongoing to further investigate this observation.

### 5.3 Poster - SCS Fall Meeting 2004



## Templated Cross-Linkage of Modified Oligodeoxyribonucleotides


Rolf Tona and Robert Haner  
 Department of Chemistry and Biochemistry, University of Bern, Freiestrasse 3, CH-3012 Bern, Switzerland

---

#### Introduction

Electron rich dienes are known to undergo [2 + 4] cycloaddition with electron poor enes. We have used the Diels-Alder reaction for the preparation of covalently cross-linked oligodeoxyribonucleotide duplexes. Diene modified complementary strands were bridged over with dimaleimides. For this purpose, diene phosphoramidites with different carbonyl spacers were prepared and used for the synthesis of the corresponding oligonucleotides. To link the complementary strands, different dimaleimides were synthesized. The reactivity of the obtained oligonucleotides towards templated cross-linkage with dimaleimides was investigated. The [2 + 4] cycloaddition was performed in aqueous solution at room temperature. We compared the stability of natural, diene-modified and cross-linked oligonucleotides by thermal denaturation experiments. The oligomers were identified via ESI-MS. PAGE was used to observe cross-linking efficiency.

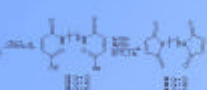
#### Phosphoramidite Synthesis



Phosphoramidites for automated DNA synthesis were synthesized in four steps. Spacers of different length were used to determine the best 2,4-hexadiene derivative for the respective experiment.

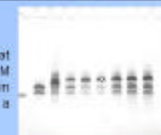
#### Dimaleimide Synthesis

To bridge over the diene building blocks, dimaleimides with different long carbonyl linkers were synthesized in two steps.




#### Automated DNA Synthesis

The respective duplexes were incubated for four days at room temperature in 10 mM Tris-HCl (pH 5.2) and 100 mM NaCl with the dimaleimides. While the control duplex in line two shows just two bands, the other samples show a third band, caused by the cross-linked duplexes.



#### Mass Spectra


Mass spectra of a modified duplex after incubation with a dimaleimide shows the mass of the two single-strands and the mass of the cross-linked duplex. No adduct of a single-strand with a dimaleimide was observed (Above).



oligonucleotide	mass - H <sup>+</sup> calc.	mass - H <sup>+</sup> found	Δ mass
D0-14-D00	11439	11433	-6
D0-13-D00	11442	11439	-3
D0-16-D00	11490	11490	0
D0-14-D06	11490	11488	-2
D0-14-D09	11490	11487	-3
D0-15-D06	11518	11515	-3
D0-16-D06	11546	11542	-4
D0-14-D10	11546	11542	-4
D0-15-D10	11574	11570	-4
D0-16-D10	11602	11599	-3

#### Mass Spectra

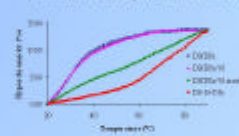
Mass spectra of the cross-linked duplexes showed all the expected mass, within the tolerance of 5%. The mass of cross-linked non complementary strands was not observed (Right side).



oligonucleotide	mass - H <sup>+</sup> calc.	mass - H <sup>+</sup> found	Δ mass
D0-14-D00	11439	11433	-6
D0-13-D00	11442	11439	-3
D0-16-D00	11490	11490	0
D0-14-D06	11490	11488	-2
D0-14-D09	11490	11487	-3
D0-15-D06	11518	11515	-3
D0-16-D06	11546	11542	-4
D0-14-D10	11546	11542	-4
D0-15-D10	11574	11570	-4
D0-16-D10	11602	11599	-3

#### Melting Experiments

Comparison of the melting-curves without dimaleimide, after addition of dimaleimide, after incubation and finally after isolation of the cross-linked product show the impressive change of denaturation.



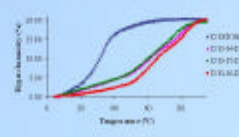
#### Melting Experiments

While all modified duplexes are about 20 °C less stable than the unmodified duplex, the cross-linked duplexes have significant higher melting temperatures than the unmodified duplex NHC.

oligonucleotide	sp.	-4-	-5-	-6-
NHC	40.5	—	—	—
D0-10	36.5	59.5	75.5	67.5(8.5)
D0-10c	32.0	68.5(7.5)	68.5(7.5)	65.5(8.5)
D0-10(NHC)	31.0	58.5(8.5)	58.5(7.5)	65.5(8.5)
D0-10(N)	27.5	58.5(7.5)	—	—

#### Melting Experiments

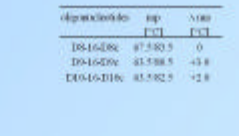
While the duplexes showed just one melting temperature, the cross-linked duplexes behave like two linked 'hairpin mimics' and denature in two steps. Comparison of the melting temperatures that cross-linked duplexes with longer dienes and longer dimaleimides are tendential more stable than the shorter combinations.



oligonucleotide	sp.	N100
D0-14-D06	67.5(8.5)	0
D0-16-D09	65.5(8.5)	-3.8
D0-16-D10	65.5(8.5)	-2.8

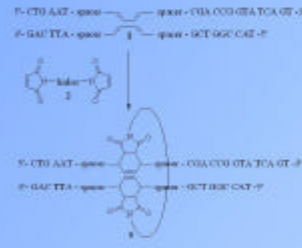
#### Melting Experiments

While the duplexes showed just one melting temperature, the cross-linked duplexes behave like two linked 'hairpin mimics' and denature in two steps. Comparison of the melting temperatures that cross-linked duplexes with longer dienes and longer dimaleimides are tendential more stable than the shorter combinations.



oligonucleotide	sp.	N100
D0-14-D06	67.5(8.5)	0
D0-16-D09	65.5(8.5)	-3.8
D0-16-D10	65.5(8.5)	-2.8

#### Templated Oligodeoxyribonucleotide Cross-Linkage



Cross-linkage of diene modified oligodeoxyribonucleotides was carried out by incubation of the diene modified strands, one equivalent of each, and the dimaleimide, one to four equivalent. A modified duplex (1) was incubated with a dimaleimide (2), in 10 mM Tris-HCl, pH 5.2 and 100 mM NaCl, at room temperature, to result in the cross-linked duplex (3). The cross-linked duplex (3) could also be considered as two linked hairpin mimics.

#### Conclusions

We demonstrated that cross-linkage of our diene modified oligonucleotides with dimaleimides is possible in aqueous solution under mild conditions. The absence of adducts between single-strands and dimaleimides show that linkage of the dimaleimide to the first strand is slow, while linkage of the second, templated, strand is fast. The cross-linked duplexes behave similar to two linked hairpin mimics and show two transitions. The cross-linked duplexes are tendential more stable when building blocks with longer spacers and dimaleimides with longer linkers were used. To identify the most stable combination of diene modified duplexes and dimaleimides, the experiments have to be repeated in consideration of some longer diene phosphoramidites and dimaleimides.

Rolf Tona and Robert Haner, Chem. Commun., Published on the web: 28th July 2004  
 Biopolymer Calculator: <http://biochem.chem.uzh.ch/edna/index.html>  
 Kenneth W. Hill, Joe Taurino-Rigby, Jeffrey D. Comer, Eric Kropp, Karl Vogls, Wolfgang Pfenke, Stanley P. C. McGeer, Gregory W. Hoar, Michael Lock, Dennis J. Azelino, and David P. Roberts, J. Org. Chem., 2001, 66(16), 5352 - 5358

239

## 5.4 Curriculum Vitae

### Rolf Tona

Untersteckholzstasse 44  
CH-4900 Langenthal  
Phone: 076 565 93 66  
Email: [tona@ioc.unibe.ch](mailto:tona@ioc.unibe.ch)  
Citizenship: Switzerland  
Date of birth: 01.12.1973  
Marital status: unmarried



### Education:

1993 Matura type C, Gymnasium Langenthal  
2000 lic. phil. nat., Chemistry, University of Berne

### Research Experience:

2000 Apr.- 2004 Nov. Ph.D. theses with Professor R. Häner  
University of Berne  
Bioconjugation and Cross-Linkage of Diene-Modified  
Oligodeoxyribonucleotides via the Diels-Alder Reaction.

2002-2004 Collaboration with Comet AG, Flamatt  
Sample preparation and method evaluation for MALDI TOF MS prototype,  
based on cryogenic STJ (Superconductive Tunneling Junction) detector.

1999 Mar.- 2000 Jan. Diploma work with Professor Ch. Leumann  
University of Berne  
Synthesis and Binding-Properties of Aminoglycoside-Modified  
Oligonucleotides.

### Personal Skills:

Mother tongue: German

Other languages: English: Writing excellent    Verbal excellent  
French: Writing good                    Verbal good

Social skills: Working in an international research group.  
Sailing in a team in the Atlantic and Mediterranean.

**Organisational skills:**

- Teaching: Organisation and leading of practical courses for chemistry and medical students.  
Examiner in oral exams for medical students.
- Military: 1994-2002: Platoon leader in infantry.  
2002-2005: ABC Schutzoff. ai Inf. Bat.  
2005: presumably last serve.

**Technical skills:**

- Chemistry: General organic synthesis.  
Oligonucleotide synthesis.  
Analytics: HPLC, MALDI TOF MS, NMR.  
Maintenance of technical infrastructure (DNA-Synthesizers, HPLC-Systems).
- Other experiences: Worked in semester holidays as:  
Sanitarily mechanic, former Klein AG, Aarwangen  
Metal construction, Schneeberger AG, Kirchberg  
Metal construction, MEBA, Kirchberg  
Assembly, Bystronic LaserAG, Niderönz  
Construction Diver, PROfessional Diving Service, Hergiswil

**Publications:**

- Synthesis of Aminoglycoside-Modified Oligonucleotides. Rolf Tona, Reto Bertolini, and Jürg Hunziker. *Organic Letters*, **2000**, 2, 12, 1693-1696.
- Functionalisation of Diene-Modified Hairpin Mimics *via* the *Diels-Alder* Reaction. Rolf Tona and Robert Häner. *Chem. Commun.*, **2004**, 17, 1908-1909.
- Templated Cross Linkage of Modified Oligodeoxyribonucleotides. Rolf Tona and Robert Häner; in preparation.

**References:**

Professor  
Dr. Robert Häner  
University of Bern  
Freiestrasse 3  
CH-3012 Bern

Dr. Urs Matter  
COMET AG  
Herrengasse 10  
CH-3175 Flamatt

Professor  
Dr. Christian Leumann  
University of Bern  
Freiestrasse 3  
CH-3012 Bern